Distribution Agreement

In presenting this thesis or dissertation as a partial fulfillment of the requirements for an advanced degree from Emory University, I hereby grant to Emory University and its agents the non-exclusive license to archive, make accessible, and display my thesis or dissertation in whole or in part in all forms of media, now or hereafter known, including display on the world wide web. I understand that I may select some access restrictions as part of the online submission of this thesis or dissertation. I retain all ownership rights to the copyright of the thesis or dissertation. I also retain the right to use in future works (such as articles or books) all or part of this thesis or dissertation.

Signature: _____ Date: _____

A furin/MMP-14 proteolytic cascade generates Vasculostatin-40 from extracellular BAI1: Implications for angiogenesis and tumorigenesis

By

Sarah M. Cork, B.S.

Graduate Program in Neuroscience

_____ Advisor: Erwin G. Van Meir, PhD.

Committee Members

_____ Randy A. Hall, Ph.D.

_____ Robert McKeon, Ph.D.

_____ Paula Vertino, Ph.D.

_____ Wei Zhou, Ph.D.

Accepted:

_____

Lisa A. Tedesco, Ph.D., Dean of the James T. Laney School of Graduate Studies

_____ Date

A furin/MMP-14 proteolytic cascade generates Vasculostatin-40 from extracellular BAI1: Implications for angiogenesis and tumorigenesis

By

Sarah M. Cork, B.S.

Advisor: Erwin G. Van Meir, Ph.D.

An abstract of

A dissertation submitted to the Faculty of the

James T. Laney School of Graduate Studies of Emory University

in partial fulfillment of the requirements for the degree of

Doctor of Philosophy

Graduate Division of Biological and Biomedical Sciences

Program in Neuroscience

2011

Abstract

A furin/MMP-14 proteolytic cascade generates Vasculostatin-40 from extracellular BAI1: Implications for angiogenesis and tumorigenesis

By Sarah M. Cork, B.S.

Vascular integrity or function is compromised in many neurological diseases, underscoring the importance of elucidating fundamental mechanisms of brain angioregulation. Notably, the exuberant vascular proliferation of glioblastoma multiforme (GBM), the most common brain malignancy in adults, significantly contributes to its rapid, aggressive growth and dismal prognosis. Improved understanding of brain-specific angiogenesis may thus prove a source of therapeutic potential for GBM, and the seven-transmembrane receptor Brain angiogenesis inhibitor 1 (BAI1) presents a promising target for such investigation. A potent anti-tumor agent in *in vivo* models, we show that expression of BAI1 is reduced in human gliomas in proportion to tumor severity, and higher levels of BAI1 are significantly associated with prolonged survival in astrocytoma but not GBM patients. While the forces driving BAI1 loss in gliomas are incompletely understood, *BAI1* mRNA expression is inversely correlated with levels of pathological GBM vasculature, implicating an anti-angiogenic mechanism. Previous work has shown that the anti-tumor effect of BAI1 derives from the proteolysis and secretion of its large extracellular domain, named Vasculostatin-120 (Vstat120), a potent angiogenesis inhibitor. Here we show that extracellular BAI1 is proteolytically cleaved to generate an abundant 40-kilodalton product named Vasculostatin-40 (Vstat40), and identify the site of processing. We demonstrate that cleavage of Vstat40 from BAI1 depends on a two-step process of activation. In the final step of the cascade, Vstat40 is directly processed from extracellular BAI1 by matrix metalloproteinase 14 (MMP-14), and this proteolytic event is greatly facilitated by the upstream activity of proprotein convertases, particularly furin. Vstat40 is observed to inhibit endothelial cell migration and cord formation in a CD36-dependent manner, and interferes with vascularization *in vivo*. While expression of Vstat40 in an LN229-derived inducible orthotopic xenograft mouse model does not significantly increase subject survival, tumors expressing Vstat40 show significantly inhibited vascularization as well as altered tumor cell morphology and reduced levels of apoptosis markers. Taken together, these findings represent an important advance in our understanding of BAI1 as both a therapeutic molecule and a receptor with diverse roles in neurobiology.

A furin/MMP-14 proteolytic cascade generates Vasculostatin-40 from extracellular BAI1: Implications for angiogenesis and tumorigenesis

By

Sarah M. Cork, B.S.

Advisor: Erwin G. Van Meir, Ph.D.

A dissertation submitted to the Faculty of the

James T. Laney School of Graduate Studies of Emory University

in partial fulfillment of the requirements for the degree of

Doctor of Philosophy

Graduate Division of Biological and Biomedical Sciences

Program in Neuroscience

2011

Acknowledgements

Nothing is harder, yet nothing is more necessary, than to speak of certain things whose existence is neither demonstrable nor probable. The very fact that serious and conscientious men treat them as existing things brings them a step closer to existence and to the possibility of being born.

Hermann Hesse

I am deeply indebted to the individuals whose support kept me going during my time at Emory. Many thanks are due to the wonderful members of the Laboratory of Molecular Neuro-Oncology who shared reagents, offered advice on experiments and never failed to cheer me up when things were rough, in particular (but in no particular order): Saroja Devi, Stefan Kaluz, Adnan Jabbar, Juliya Kalinina, Milota Kaluzova, Sok-Hyong Lee, Carol Tucker-Burden, Lucy Petrova, Gena Marie Mastrogianakis, and Daniel Brat. Special thanks are owed to Vladimir Belozerov, whose initial assistance was critical for getting my project off the ground. I am also very grateful to my thesis committee: Randy Hall, Robert McKeon, Paula Vertino and Wei Zhou, for their insight and guidance throughout the development of my project, and to the members of the Emory Neuroscience Program for their support of my training, particularly Leonard Howell and Sonia Hayden. I have also been fortunate enough to have a great group of friends, whose encouragement was essential to get me through the adventure that was graduate school, and who will be sorely missed.

The final thank-you must go to my parents, Charles and Victoria Cork, who were there from the beginning and are somehow still my biggest fans.

CONTENTS

LIST OF FIGURES

ABBREVIATIONS

7TM seven transmembrane
ADAM/TS a disintegrin and metalloproteinase / with thrombospondin repeats
BAI brain angiogenesis inhibitor
BAP BAI1-associated protein
bFGF basic fibroblast growth factor
CDK cyclin-dependent kinase
CIRL Ca2+-independent receptor for α-latrotoxin
CLESH CD36 LIMP-II Emp sequence homology
CM conditioned medium
DIVAA directed *in vivo* angiogenenesis assay
Dox doxycycline
DREG developmentally regulated GPCR
ECD extracellular domain
ECM extracellular matrix
EGF(R) epidermal growth factor (receptor)
ELMO engulfment and cell motility
EMR EGF-like module-containing mucin-like hormone receptor
GBM glioblastoma multiforme
GPCR G protein-coupled receptor
GPS GPCR proteolysis site
GST glutathione S-transferase
HBD hormone-binding domain
HIF hypoxia inducible factor
HRGP histidine-rich glycoprotein
IDH isocitrate dehydrogenase
IFP interstitial fluid pressure
ISBTRC *In Silico* Brain Tumor Research Center
IPTG isopropyl β-D-1-thiogalactopyranoside
JNK jun N-terminal kinase
MAGI MAGUK, inverted
MAGUK membrane guanylate kinase
MCA middle cerebral artery
MMP matrix metalloproteinase
mTOR mammalian target of rapamycin
NFAT nuclear factor activating T cells
NF1 neurofibromin 1
PBD PDZ-binding domain
PDGF(R) platelet-derived growth factor (receptor)
PEDF pigment endothelium-derived factor

PI3K phosphoinositide 3 kinase
PRR proline rich region
PSD post-synaptic density
PtdSer phosphatidylserine
PTEN phosphatase and tensin homolog
PTX pentraxin
RB retinoblastoma
REMBRANDT Repository for Molecular Brain Neoplasia Data
RGD arginine-glycine-aspartate
SDS-PAGE sodium dodecyl sulfate polyacrylamide gel electrophoresis
SH Src homology
SNP single nucleotide polymorphism
TIMP tissue inhibitor of metalloproteinases
TCGA The Cancer Genome Atlas
TSP thrombospondin
TSR thrombospondin type 1 repeat
VEGF(R) vascular endothelial growth factor (receptor)
VHL Von Hippel-Lindau
VPF vascular permeability factor
Vstat Vasculostatin
WCE whole cell extract

CHAPTER 1.

INTRODUCTION

The figures and some portions of the text of this chapter are currently in press in the *Journal of Molecular Medicine* as a review by Cork SM and Van Meir EG, entitled: Emerging roles for the Brain Angiogenesis Inhibitor family in the regulation of phagocytosis, synaptogenesis, neurovasculature and tumor development. DOI: 10.1007/s00109-011-0759-x

1.1. An overview of glioma molecular biology

Gliomas, the most common type of primary brain tumor in adults, are also the most deadly. The World Health Organization identifies multiple grades of malignant glioma: II, III, also known as anaplastic astrocytoma, and IV, more commonly known as glioblastoma multiforme (GBM). GBM represents half of all adult primary brain tumor diagnoses, and has a dismal prognosis of a median survival of twelve months, despite advances in chemotherapy and radiotherapy. Fortunately, gliomas are a relatively rare type of tumor, with a diagnosis of more than 22,000 new cases in 2010 (National Cancer Institute). The Surveillence Epidemiology and End Results (SEER) study indicates an incidence of nearly seven new cases annually per every 100,000 persons, with a slightly higher incidence rate in whites (http://seer.cancer.gov). While the cell of origin is unknown for gliomas, they are hypothesized to derive from either dedifferentiated glia or neural stem cell progenitors (Van Meir et al., 2010).

Historically, gliomas are characterized by a well-known set of genetic and pathological features. Prominent histopathological features of GBM include the occurrence of "pseudopalisading" cells around micro-areas of tumor necrosis in conjunction with microvascular proliferation and incidence of intravascular thrombosis (Brat and Van Meir, 2004). Aberrant cellular signaling and specific genetic alterations are also characteristic of aggressive gliomas. Of these, perhaps the best-documented alterations involve the epidermal growth factor receptor (EGFR) and phosphatase and tensin homolog (PTEN). Amplification of the EGFR locus on chromosome 7, leading to upregulation of EGFR signaling, is frequently observed in gliomas (Diedrich et al., 1995; Liu et al., 1997; Schober et al., 1995; Smith et al., 2001). Also, EGFRvIII, a ligand-independent, constitutively-active mutated form of the EGFR, is observed in the majority of aggressive gliomas, with one report finding

its expression in astrocytoma specimens to be approximately 50% and up to 75% in glioblastomas (Wikstrand et al., 1997). The other most common genetic alteration in glioblastoma is mutation and loss of heterozygosity of the phosphatase and tensin homolog (PTEN), a phosphatase that inhibits the activity of the phosphoinositide 3 kinase (PI3K). PTEN acts as a tumor suppressor in gliomas, (Cloughesy et al., 2008; Ishii et al., 1999; Rasheed et al., 1997; Steck et al., 1997), and the vast majority of glioma specimens are observed to have loss of heterozygosity as well as numerous distinct mutations in the PTEN gene (Wang et al., 1997). Other genetic alterations that are common in glioblastoma tissue specimens and cell lines are often found in transcription factors and regulators of the cell cycle, most notably p53 (Sidransky et al., 1992), a transcription factor that promotes G1 cell cycle arrest and apoptosis in response to genotoxic stressors. Mutations in the p53 gene, *TP53*, and EGFR were shown to be exclusive in gliomas (Rasheed et al., 1994). In addition to p53, gliomas are characterized by the presence of mutations in the genes encoding CDK2NA/p16, p14ARF, and retinoblastoma (RB) (Ishii et al., 1999; Ueki et al., 1996), reflecting the deregulation in molecular mechanisms of cellular quiescence in glioma.

In recent years, efforts of pan-institutional collaborations have yielded many novel insights into the big picture of glioma molecular biology. In particular, analyses of tumor specimen and associated clinical data from the Repository for Molecular Brain Neoplasia Data (REMBRANDT) and The Cancer Genome Atlas (TCGA) have succeeded at both confirming and elaborating on the previous understanding of glioma genetics as well as identifying new tumor-specific genetic alterations and opening novel lines of investigation (2008; Bredel et al., 2009; Brennan et al., 2009; Cerami et al., 2010; Freire et al., 2008; Ovaska et al., 2010; Purow and Schiff, 2009). Using the TCGA resources, nearly 90 percent of glioblastoma specimens were identified to contain mutations in genes comprising the PI3K

pathway, 75 percent had concomitant mutations in the PI3K, p53 and RB pathways, and 20 percent contained mutations in the neurofibromin 1 gene (*NF1*). This investigation also found hypermethylation of the promoter of DNA repair gene *MGMT* in treated glioma specimens, suggesting that chemotherapy may increase the frequency of genetic mutation in recurrent glioma (McLendon and Network, 2008). Another study has identified a robust signature pattern of chromosomal alterations in gliomas, affecting genes with significant impact on patient survival, such as *MYC* (Bredel et al., 2009). Other research has provided evidence for the signaling pathways most frequently dysregulated in gliomas, including upregulation of the EGFR and PDGFR signaling pathways and the downregulation of NF1 signaling (Brennan et al., 2009).

Importantly, novel genetic alterations continue to be discovered in glioblastoma as methods to study their biology become increasingly sophisticated. These include the recent discovery of glioma-associated mutations in isocitrate dehydrogenases (*IDH1* and *IDH2*) resulting in loss of enzymatic activity (Parsons et al., 2008; Yan et al., 2009) and ultimately acting to increase the level of the transcription factor HIF-1α (Zhao et al., 2009). Analyses of TCGA data have also found the EGFR inhibitor *ERRFI1* and the Aurora kinase *TACC3* as novel genes respectively deleted and overexpressed in glioma specimens (Duncan et al., 2010). Finally, these databases have also been used to identify characteristic methylation patterns associated with survival outcome (Noushmehr et al., 2010), and provide evidence for the role of certain gene-associated SNPs with glioma susceptibility (Wrensch et al., 2009).

These *in silico* resources also permit analyses of glioma molecular biology of a scale previously unattainable with more limited datasets. To this end, recent work utilizing the TCGA database has shown that gliomas may be divided into at least four classifications based on molecular subtyping (Verhaak et al., 2010). In this analysis, gliomas were classified as

proneural, neural, classical or mesenchymal based on specific patterns of gene alteration. Proneural gliomas were characterized by mutations in *PDGFRA* and *IDH1* concomitant with the majority of mutations in the p53 gene, *TP53*. The classical subtype of gliomas was defined by the presence of EGFR amplification and deletions of chromosome 10 and *CDKN2A*. Mesenchymal gliomas displayed consistant mutation or loss of *NF1*. Gliomas classified as neural lacked the genetic mutation signatures found in the other subtypes, but demonstrated upregulation of neuron markers. Interestingly, an association was observed between the transcriptome signature of the glioma subtypes and that of specific brain cell populations, suggesting that gliomas may arise from distinct subtypes of progenitor populations. In this analysis, proneural, neural, classical and mesynchymal signatures resembled those of oligodendrocytes, neurons/glia, astrocytes, and astro/microglia, respectively. Notably, patients with gliomas classified as proneural tended to be younger and have longer survival than any of the other glioma subtypes, a result also found for oligodendroglioma (Cooper et al., 2010). Collectively, these research findings indicate the importance of determining specific glioma subtype when considering the most appropriate therapeutics.

1.2 Clinical development of novel glioma therapies

Despite decades of research into potential glioma therapies, the prevailing course for treatment for glioma patients remains surgical resection with radiotherapy and chemotherapy. High-throughput screens of small-molecule inhibitors have yielded many drugs targeting specific signaling pathways or oncogenes activated in gliomas and that have demonstrated significant promise in preclinical trials. While administration of these drugs is generally well-tolerated, little beneficial effect on progression-free survival has been

demonstrated. For examples, initial results with the EGFR tyrosine kinase inhibitors gefitinib and erlotinib suggest relatively low patient response rates (Doherty et al., 2006; Franceschi et al., 2007; Preusser et al., 2008; Raizer et al., 2010). The PDGFR inhibitor imatinib has been shown to inhibit glioma growth in animal models but this benefit has not translated to the clinic (Desjardins et al., 2007; Raymond et al., 2008). Rapamycin, a potent inhibitor of mammalian target of rapamycin (mTOR) signaling, has also failed to promote progression-free survival in clinical trials (Akhavan et al., 2010). Finally, pan-spectrum tyrosine kinase inhibitor cediranib (AZD2171) showed only modest benefit in a phase III clinical trial (Batchelor et al., 2007). Overall, the failure of many of these drugs upon transition to clinical trials has constituted a major disappointment for researchers seeking to improve glioma progression-free survival, but much has been learned for the development of further therapies (Omuro et al., 2007).

Different theories could explain why so many of these agents have been unsuccessful. The most apparent explanation is that while rodents share many biological features with humans, there are distinct physiological differences that are likely to contribute to a differential response to some therapies (Rangarajan and Weinberg, 2003). While this concern is inevitable for any model organism and alternatives are limited, one possibility is the use of subjects such as dogs which can naturally develop a variety of cancers including gliomas (Kimmelman and Nalbantoglu, 2007). The artificial nature of the xenograft tumor model itself presents a challenge when extrapolating efficacy of a drug to clinical studies. Typically, xenografts are made from tumor cell lines or, more recently, tumor-derived neurospheres, which are less likely to recapitulate the response that a heterogeneous glioma can incur. In animal models, tumors are not always grown at the orthotopic site, yielding an incomplete picture of what factors may combine to modify a drug's effect. Further, brain tumors are

heterogeneous, so that targeting of a single molecule might yield initial success but due to the buildup of resistance mechanisms in the tumor ultimately not lead to a significant difference in patient survival (McCarty et al., 2003).

Finally, no matter how promising inhibitors may appear in preclinical studies, they are likely to be unsuccessful if they are not directed to the most appropriate recipients. For example, the anti-tumor activity of rapamycin appears to be stronger when administered to patients with a specific PTEN-deficient tumor molecular profile (Cloughesy et al., 2008). As for other cancers (Mullan and Millikan, 2007; Webster et al., 2008), glioma molecular profiling will ultimately play a crucial role in determining the most suitable course of treatment for patients (Mischel et al., 2004; Phillips et al., 2006; Vitucci et al., 2010).

Alternatively, glioma therapies may be directed against other features of the tumor besides the cancer cells. Targeting tumor-associated angiogenesis, for example, divests the tumor of the resources it requires to proliferate with significantly fewer harmful side effects compared with traditional therapies.

1.3. Overview of angiogenesis and pathology of tumor-associated vasculature

Angiogenesis, the formation of new vessels from pre-existing vasculature, is characterized by a series of discrete, well-characterized steps (Adams and Alitalo, 2007; Bergers and Benjamin, 2003; Pettersson et al., 2000; Plate, 1999; Plate et al., 1994). In adults, pro-angiogenic signals are first released from a source, either in conjunction with a physiological program such as menses, or in response to the biological changes associated with region of hypoxia, such as a wound or solid tumor. Of these signals, vascular endothelial growth factor (VEGF, particularly VEGF-A) is the most important for angiogenesis, but other cytokines such as platelet-derived growth factor (PDGF), basic fibroblast growth factor

(bFGF), interleukin-8 (IL-8), hepatocyte growth factor (HGF), and angiopoietin-2 (Ang-2) are also implicated in this process, particularly in tumor-associated angiogenesis. These pro-angiogenic stimuli are recognized by their respective receptors on quiescent vasculature, of which perhaps the most important association is the interaction of VEGF with VEGF receptor 2 (VEGFR2, also known as Flk-1). Subsequent signaling pathway activation (Gavard and Gutkind, 2006) leads to the breakdown of intercellular contacts between endothelial cells (Dejana, 1996). This permeability promotes the extravasation of plasma proteins, which supply a provisional matrix for the attachment of migrating endothelial cells. Typically, blood vessels in the brain are surrounded by a basement membrane containing a variety of extracellular matrix (ECM) proteins including type-IV and type-V collagens, fibronectin, laminin, vitronectin and heparin-sulfate proteoglycans (HSPGs) (Rao, 2003). Pro-angiogenic cytokines upregulate the secretion of proteases important for degradation of this basement membrane. Integrins that mediate endothelial cell attachment to the ECM are upregulated during this time, particularly the vitronectin receptor $\alpha_V\beta3$ and the fibronectin receptor $\alpha5\beta1$, and act to promote cytokine receptor signaling (Ramjaun and Hodivala-Dilke, 2009). Finally, endothelial cells proliferate and migrate in the direction of the source of angiogenic stimulus, leading to the formation of capillary tubes and the recruitment of pericytes which promote vascular maturation (Gerhardt and Betsholtz, 2003).

As the adult vascular endothelium is generally quiescent (Fraser & Lunn, 2000), adult angiogenesis is typically a pathological condition and contributes to the progression of other diseases, particularly solid malignancies such as GBM. As with other tissues, tumors require oxygen, nutrients and a system of waste removal, and it is believed that tumors require angiogenesis to grow beyond the range of passive diffusion, approximately 2-3 mm (Folkman, 1995), and it is well known that many solid tumors, including gliomas, display high levels of

neovascularization, contributing to accelerated tumor growth and malignancy (Folkman, 1971; Folkman et al., 1989). Aggressive gliomas are thus characterized by the upregulation and secretion of a plethora of soluble cytokines that regulate endothelial cell proliferation and migration (Adams and Alitalo, 2007; Bergers and Benjamin, 2003; Machein and Plate, 2004; Plate, 1999), including those described above. Gliomas also upregulate a variety of proteases including urokinase-type plasminogen activator (uPA), cathepsin B, and matrix metalloproteinases which activate growth factors, break down the extracellular matrix, and promote tumor cell invasion (Fillmore et al., 2001; Hotary et al., 2002; Itoh, 2006; Itoh and Seiki, 2006; Itoh et al., 2001; Rao, 2003). However, this upregulation alone is thought to be insufficient for tumors to induce vascularization (Folkman, 1995), and that downregulation of angiogenesis inhibitors, such as thrombospondin-1 (TSP-1) or the collagen XVIII fragment endostatin, is also required. Successful induction of angiogenesis is hypothesized to result from this imbalance in the ratio of pro- to anti-angiogenic molecules, termed the "angiogenic switch" (Hanahan and Folkman, 1996). Furthermore, recent work has shown that gliomas may recruit vasculature by other means than the sprouting angiogenesis described above. These observations include the recruitment by gliomas of Tie2-expressing proangiogenic monocytes or stromal-derived mesenchymal progenitors to the tumor-associated vasculature (De Palma et al., 2005), or formation of endothelial cells by glioma stem cells themselves (Ricci-Vitiani et al., 2010; Wang et al., 2010).

Tumor-associated neovascularization is highly pathological and contributes to poor prognosis in multiple respects (Fukumura et al., 2010; Fukumura and Jain, 2007; Fukumura and Jain, 2008; Gerstner et al., 2009; Gerstner et al., 2008; Jain, 2005). Unlike normal vessels, where the rate of endothelial cell turnover often exceeds 1000 days, tumor vasculature does not become quiescent and may turn over within 5 days (Folkman, 1995).

Tumor vessels are characterized by multiple abnormalities including irregular diameter and branching pattern, incomplete basement membrane formation and abnormal coat of pericytes and smooth muscle cells (Hashizume et al., 2000). Glioma vasculature is leaky due to the heterogenous overexpression of proangiogenic factors, particularly VEGF, from the tumor (Machein and Plate, 2000; Machein and Plate, 2004). Originally identified as vascular permeability factor (VPF), VEGF is a powerful regulator of vascular permeability. VEGF exerts its permeability-inducing effects in concert with its pro-angiogenic activity upon endothelial cells via interaction with VEFGR2 (Brekken et al., 2000; Shibuya and Claesson-Welsh, 2006). Ultimately, VEGF-VEGFR2 signaling destabilizes both adherens (AJ) and tight junctions between endothelial cells, leading to extravasation of erythrocytes and plasma (Dejana, 1996; Gavard and Gutkind, 2006; Weis and Cheresh, 2005). As a result, glioma patients suffer from the increased intracranial pressure resulting from tumor-associated edema, which contributes significantly to neurological symptoms and preoperative mortality (Jain et al., 2007; Saba and Magolan, 1991). While corticosteroid administration reduces the side effects of tumor-associated edema, steroid treatment has undesirable side effects including immunosuppression.

Further, vascular abnormalities create a pathological tumor microenvironment, increasing tumor aggressivity and resistance to treatment. It is thought that high levels of tumor interstitial fluid pressure (IFP) resulting from both leaky vessels and a lack of a functional lymphatic system ultimately causes vascular compression and subsequent necrosis in the core of the tumor (Folkman, 1995; Jain and Baxter, 1988). IFP also is observed to increase vascular endothelial cell proliferation and constitute a barrier to drug delivery (Hofmann et al., 2007; Jain and Baxter, 1988). Stabilization of vasculature is thought to increase efficacious delivery of standard chemotherapeutic agents by reducing IFP (Jain et al.,

2007; Tong et al., 2004). Also, increased tumor mass from cellular proliferation generates regions of hypoxia, which selects for more malignant cells in addition to decreasing effectiveness of drug and radiation therapies (Jain et al., 2007). Hypoxia leads to the upregulation of hypoxia-regulated genes, most notably the transcriptional regulator hypoxia inducible factor 1 alpha (HIF-1α). HIF-1α upregulates many genes implicated in cancer biology and progression, notably pro-angiogenic molecules like VEGF-A (Belozerov and Van Meir, 2005). Overall, the diversity of complications resulting from tumor-associated angiogenesis highlights this system as an important therapeutic target.

In addition to glioblastoma multiforme, many neurological diseases are characterized by pathology of the vasculature, including stroke (Hayashi et al., 2003; Lin et al., 2003; Sun et al., 2003), Alzheimer's Disease (Deane and Zlokovic, 2007; Paris et al., 2010; Tarkowski et al., 2002; Vagnucci and Li, 2003), vascular dementia (Tarkowski et al., 2002), glaucoma (Yazdani et al., 2009), and amyotrophic lateral sclerosis (Azzouz et al., 2004; Lambrechts et al., 2006). Advances in the overall understanding of the regulation of vascular maintenance or angiogenesis are likely to lead to improved therapeutics or better strategies of preventative medicine for many of these diseases (Greenberg and Jin, 2005; Zlokovic, 2008).

1.4. Anti-angiogenic therapy in the clinic: promise and pitfalls

Anti-angiogenic therapies have many desirable features, including low mutagenic potential due to slow replication and stable genomic background of endothelial cells (ECs), specific targeting to angiogenic blood vessels, and a lack of the cytotoxic effects characteristic of traditional chemotherapy (Eskens and Verweij, 2006). There are a variety of types of clinically-relevant angiogenesis inhibitors, ranging from small molecule inhibitors to humanized antibodies and modified versions of endogenous proteins, some of which have

already demonstrated significant promise in clinical trials. Most significantly, treatment with the VEGF blocking antibody bevacizumab has improved progression-free survival in a variety of cancers including gliomas (Van Meir et al., 2010), pancreatic cancer (Van Cutsem et al., 2009), lung cancer (Sandler et al., 2006), breast cancer (Miller et al., 2007; Yamauchi et al., 2009), sarcoma (D'Adamo et al., 2005), renal cell carcinoma (Escudier et al., 2007), and colorectal cancer (Tol et al., 2009). Other angiogenesis inhibitors, including the thrombospondin mimetic ABT-510 (Hoekstra et al., 2005; Rusk et al., 2006; Yang et al., 2007), endostatin (Herbst et al., 2002), and the integrin-blocking peptide cilengitide (Desgrosellier and Cheresh, 2010), have also yielded promising results in clinical trials for a variety of solid tumors including glioblastoma. Cediranib, a potent small-molecule inhibitor of VEGFR2 and other receptor tyrosine kinase activity, been observed to induce vascular stabilization and block tumor-associated edema (Batchelor et al., 2007). It has long been thought that a combination of antiangiogenic and cytotoxic therapy may be more effective than either type alone (Folkman, 1995), and many studies are presently making use of such an approach. Overall, there is a clear need for the continued development and study of novel angiogenesis inhibitors for the treatment of tumors as well as other diseases characterized by vascular pathology, and a variety of anti-angiogenic compounds are currently in clinical trials (National Cancer Institute).

It should be noted that the previously-described work on glioma molecular profiling has relevance for studies of anti-angiogenic therapy. For example, tumors with wild-type p53 appear to be more responsive to anti-angiogenic therapy than p53-null tumors (Yu et al., 2002), possibly because the p53-null tumors are better able to adapt to the hypoxia induced by the therapy. Further, patients with VHL mutations tend to develop more vascularized tumors, making them particularly good therapeutic targets (Yang and Kaelin, 2001). In

considering the glioma molecular classification data, it may be hypothesized that neural, classical, or mesenchymal gliomas may prove the most responsive tumor types for anti-angiogenic therapy. In addition, new explorations might reveal specific molecular pathology of angiogenesis in different tumor types that would better direct therapy.

The use of anti-angiogenic therapies has not been without its problems. While studies involving anti-VEGF therapeutics have identified little toxicity as a result of taking the treatment, multiple side effects have been observed. These side effects include hypertension, pulmonary hemorrhage and thrombo-embolic events (McCarty et al., 2003). The latter is thought to result from endothelial cell apoptosis specifically due to VEGF inhibition, as low levels of VEGF are required to maintain the health of quiescent endothelial cells. Also, as with traditional chemotherapeutics, tumors are hypothesized to be able to develop resistance to anti-angiogenic therapy (Bergers and Hanahan, 2008). Such resistance is thought to be indirect, as while a specific target remains inhibited, but other ways to stimulate tumor growth are activated. For examples, alternative pro-angiogenic signaling pathways may be upregulated, or endothelial cells may be formed from tumor- or stromal-derived progenitors. In the case of glioblastoma, a notoriously invasive tumor, cancer cells may disperse and migrate into the brain along existing vasculature or otherwise independently of the recruitment of new vessels. Alternatively, tumors may be indifferent to angiogenesis inhibition, particularly if redundant pro-angiogenic signals or vasculoprotective mechanisms are already in place.

As with other glioma therapies described previously, clinical trials of angiogenesis inhibitors may be unsuccessful for a variety of reasons. Therapies may be administered to animal subjects when their tumor burden is relatively small, often directly after tumor cell implantation, and when little vascular response has been generated. In clinical trials,

however, angiogenesis inhibitors are typically administered to patients whose tumors are already characterized by extensive vascular proliferation. Another important factor is that the vasculature of a human tumor at diagnosis is significantly older than the vasculature of that of a mouse newly implanted with tumor cells, and this difference in age and maturity of the vasculature should be taken into account when designing therapeutics. For example, vascular age may have functional consequences, as more mature vasculature is coated with pericytes, which may prove a barrier to anti-angiogenic treatments (McCarty et al., 2003).

A better understanding of the most effective ways to target angiogenesis may lead to improvements in the approach to the development of anti-angiogenic therapy. As described above, there are a variety of types of angiogenesis inhibitors for clinical use, including modified versions of endogenous proteins. In particular, this group directly mimics the body's own natural strategies of regulating its vascular biology, which may confer advantages of greater efficacy and fewer attendant side effects.

1.5. Endogenous angiogenesis inhibitors: generation and significance

Endogenous inhibitors of angiogenesis are often generated from the proteolysis of larger parent molecules that are not themselves angioregulators, typically extracellular matrix proteins (Albini et al., 2010; Mundel and Kalluri, 2007; Rege et al., 2005). These cryptic inhibitors derive from such diverse ECM molecules as collagen IV (arresten, canstatin, and tumstatin) (Colorado et al., 2000; Hamano et al., 2003; Kamphaus et al., 2000), collagen XVIII (endostatin) (Abdollahi et al., 2004; Felbor et al., 2000), perlecan (endorepellin) (Mongiat et al., 2003), and fibronectin (anastellin) (Yi and Ruoslahti, 2001). Other non-ECM parent molecules are processed into inhibitors of angiogenesis, such as reduced plasmin

(angiostatin) (Morikawa et al., 2000) and matrix metalloproteinase 2 (PEX) (Bello et al., 2001; Brooks et al., 1998).

In contrast, other angiogenesis inhibitors are not derived from parent molecules. This group includes the thrombospondins TSP1 and TSP2 (de Fraipont et al., 2001), the tissue inhibitors of metalloproteinases (TIMPs) (Handsley and Edwards, 2005; Stetler-Stevenson and Seo, 2005), PEDF (Broadhead et al., 2009; Guan et al., 2004), long pentraxin 3 (PTX3), which specifically inhibits FGF-induced angiogenesis (Rusnati et al., 2004), and the vasohibin family (Sato and Sonoda, 2007; Watanabe et al., 2004) which are upregulated by proangiogenic factors. In sum, endogenous inhibitors of angiogenesis may be expressed through a diversity of mechanisms, and production of angiogenesis inhibitors is likely to be under tight physiological control, whether by regulation of transcription of the inhibitor or of the protease that generates it.

The existence of these multiple means of inhibiting angiogenesis has long invited speculation concerning their significance (Hanahan and Folkman, 1996). Release of cryptic angiogenesis inhibitors may maintain normal vascular quiescence or terminate non-pathological angiogenesis events such as ovulation or wound healing. Alternatively, it has been suggested that the endothelium may be able to sense when revascularization may be premature. In the example of an infected wound, inhibition of angiogenesis would prevent the spread of the infection to other tissues (Albini et al., 2010). In this case, rapid generation of anti-angiogenic fragments would be an efficient way for the endothelium to regulate its biological response. By contrast, angioregulators that are generated via transcriptional regulation may contribute to persistence of either angiogenesis or its inhibition.

This wide array of endogenous angiogenesis inhibitors and their varied means of generation attests to the complexity underlying the physiological regulation of angiogenesis. It

is not yet clearly understood how the diversity of available pro- and anti-angiogenic signals are interpreted and integrated by endothelial cells to control the balance of quiescence, angiogenesis and differentiation of either normal or pathological vasculature in many different tissue types. In considering the optimal development of anti-angiogenic therapeutics, however, it is entirely plausible that the efficacy of specific angiogenesis inhibitors may be dependent on specific characteristics of their target endothelium, whether by stage of the angiogenesis process targeted or tissue-specific markers. In the latter case, brain-specific endogenous angiogenesis inhibitors may prove most effective as therapeutics for brain diseases characterized by vascular pathology, particularly gliomas. The brain angiogenesis inhibitor (BAI) family proteins provide an intriguing avenue for this study.

1.6. An overview of the BAI family proteins

The three members of the brain angiogenesis inhibitor (BAI1-3, Figure 1.1) family of molecules are putative G protein coupled receptors (GPCRs), a diverse group of seven-transmembrane receptors that are phylogenetically distributed into five primary families (Bjarnadottir et al., 2004; Bjarnadottir et al., 2006). While not known to couple to a GTPase, the BAI family of molecules are classified into the class B subtype of GPCRs, also known as the adhesion family. These are a group of 33 known members characterized by the presence of large N-terminal extracellular domains (ECDs) which typically contain multiple subdomains and are believed to be highly glycosylated, rendering their putative adhesive properties. Due to their complicated genetic structure, however, study of the class B GPCRs has proven challenging and many are orphan receptors with unknown ligands.

BAIs are large molecules of approximately 200 kilodaltons in size and contain a number of functional domains in both their extra- and intracellular regions, summarized in

Figures 1.1-3. The 7-transmembrane domain of all three BAIs is highly conserved and forms the basis for their phylogenetic association (Bjarnadottir et al., 2007). All three BAI ECDs contain an evolutionarily conserved GPCR proteolysis site (GPS), a putative hormone-binding domain, and multiple N-glycosylation sites. They also contain thrombospondin type 1 repeats (TSRs), domains first discovered to regulate the anti-angiogenic activity of thrombospondin-1. BAI1 contains five TSRs and BAIs 2 and 3 each contain four TSRs. An integrin-binding Arg-Gly-Asp (RGD) motif is unique to the BAI1 extracellular domain. The C-terminal intracellular portion of the BAIs terminates in a conserved Gln-Thr-Glu-Val (QTEV) motif known to interact with PDZ domain-containing molecules, which are implicated in such functions as cytoskeletal architecture and protein trafficking and localization. Finally, only BAI1 contains a proline-rich region in its intracellular domain, a feature known to interact with SH3- and WW domain-containing proteins and regulate signal transduction (Oda et al., 1999).

1.7. BAI family gene regulation and expression in development

Little is known regarding the mechanisms of BAI family transcriptional regulation and expression. BAI1 was initially identified in a screen for genes regulated by the tumor suppressor p53 (Nishimori et al., 1997) as a result of a putative p53 binding site located in its 9th intron on chromosome 8q24 (Figure 1.2A), and was suggested to be a candidate paracrine effector for the anti-angiogenic effects of p53 (Van Meir et al., 1994). Some studies have found that restoration of p53 expression in p53 mutant glioma cells can upregulate BAI1 mRNA (Shiratsuchi et al., 1997), while others have not (Kaur et al., 2003), suggesting this needs further study. The BAI1 promoter has predicted binding sites for a wide variety of transcription factors but their involvement has not been confirmed experimentally. Recently,

studies of the mouse BAI1 gene have identified a second promoter located downstream of the GPS site, generating a variant of BAI1 lacking its extracellular domain and expressed in the hippocampus (Valen et al., 2009). Further work is warranted to establish the expression pattern of these two independent promoters and their importance in different tissues.

The BAI 2 and 3 genes were discovered as a result of their homology with *BAI1*, and are localized at chromosomes 1p35 and 6q12 respectively. In contrast to *BAI1*, *BAI2* and *BAI3* are not known to contain p53-binding sites and p53 has not been demonstrated to regulate mRNA levels of either (Shiratsuchi et al., 1997). The promoters regulating the expression of these two genes have not been studied to date.

All BAI family members are expressed in fetal and adult human brain tissue (Shiratsuchi et al., 1997). Expression of *BAI1* mRNA is highly enriched in the brain compared with other tissues and specifically localized in neurons (Mori et al., 2002), glia and macrophages (Park et al., 2007). The expression of *BAI2* and *BAI3* mRNA is more widely distributed; in addition to brain expression, both *BAI2* and *BAI3* mRNA are expressed in adult human heart tissue, and *BAI2* mRNA is also detected in skeletal muscle and thymus, while *BAI3* mRNA is found in testis and small intestine tissue specimens. Little is known about the expression of the BAI proteins themselves, however, and further research is necessary to determine their localization at the cellular level and gain insight into these proteins' function in normal brain or elsewhere.

Studies of expression of BAI family members in mouse brain development have generally mirrored the findings in human tissue. Murine *Bai1* mRNA expression, like that of human *BAI1*, is primarily brain-specific and increases after birth to reach the highest level of expression at approximately P10. *mBai1*, which shares a 94% sequence identity with *hBAI1*, is expressed at high levels in cortical neurons, the pyramidal neurons of the hippocampus, the

granular cell layer of the olfactory bulb, cerebellar Purkinje neurons, and in the craniofacial nerve nuclei (Koh et al., 2001). As for hBAI1, further work is necessary to determine localization of the mBAI1 protein and what role it is likely to play in these cell types.

In contrast, *mBai2* and *mBai3* are expressed ubiquitously during embryonic development but largely restricted to the brain after birth. In the brain, the localization pattern of *mBai2* is highly similar to that of *mBai1*. Notably, anti-*mBai2* mRNA probes detected seven mRNA splice variants, some lacking such important functional features as the third cytoplasmic loop of the seven-transmembrane domain (Kee et al., 2002). More recent work has determined that *mBai3* continues to be expressed in the muscle-myenteric nerve layer of the adult mouse gastrointestinal tract (Ito et al., 2009). Given their wide-ranging distribution, these proteins may serve biological functions in a wide range of tissue types.

1.8. Proteolysis of BAI proteins and functional implications

Many extracellular proteolysis events have been identified for the cell adhesion GPCRs, including the BAIs. The majority of cell adhesion GPCRs are known to be proteolytically processed at the G-protein proteolysis site (GPS), a highly conserved, cysteine-rich domain located proximal to the seven-transmembrane domain. The GPS contains a site for autoproteolytic cleavage, resulting from a nucleophilic attack of a conserved arginine or histidine on a serine (Deyev and Petrenko, 2010; Perler, 1998; Perler et al., 1997; Wei et al., 2007), and recent work suggests that N-glycosylation may regulate this processing (Hsiao et al., 2009). Following autoproteolysis, the cleaved N-terminal piece is believed to remain noncovalently associated with its transmembrane region, as detectable under nonreducing conditions (Krasnoperov et al., 2002). Proteolytic GPS cleavage at the GPS has been experimentally demonstrated for Ig-Hepta/GPR116 (Fukuzawa and Hirose, 2006), CIRL

(Krasnoperov et al., 2009; Krasnoperov et al., 2002; Sugita et al., 1998), EMR2 (Chang et al., 2003; Lin et al., 2004), GPR56 (Huang et al., 2008) and CD97 (Gray et al., 1996; Hsiao et al., 2009), and implicated for polycystin-1(Wei et al., 2007), Flamingo (Usui et al., 1999), and HE6 (Obermann et al., 2003). The significance of GPS processing remains incompletely understood, but mutations in the GPS site impair the ability of these receptors to traffic properly out of the endoplasmic reticulum (Deyev and Petrenko, 2010; Jin et al., 2007; Sugita et al., 1998; Volynski et al., 2004).

BAI1 and BAI2 undergo processing at the GPS (Kaur et al., 2005; Okajima et al., 2010). In BAI1, this proteolytic event generates a 120 kDa secreted fragment, known as Vasculostatin-120 (Vstat120) (Kaur et al., 2005; Kaur et al., 2009). Vstat120 is secreted into the conditioned media of BAI1-expressing cells, suggesting that it may incompletely associate with the transmembrane part of BAI1 in culture. Also, full-length BAI1 is detectable under reducing conditions of SDS-PAGE, indicating that GPS processing may not be automatic and thus is likely a tightly regulated event.

Other recent work has identified a proteolytic cascade regulating a second processing event in the BAI1 extracellular domain (Chapter 2). In this two-step cascade, pro-protein convertase furin activates matrix metalloproteinase 14 (MMP-14), which directly cleaves extracellular BAI1 at a previously uncharacterized processing site to generate a 40 kDa fragment, named Vasculostatin-40 (Vstat40). Vstat40 contains the RGD motif and one TSR (Figure 1.1) and has been determined to have significant anti-angiogenic activity in culture and *in vivo*. As shown for Vstat120, Vstst40-mediated angiogenesis inhibition appears to depend on the presence of the CD36 receptor on target endothelial cells. Vstat40 is more abundantly expressed than Vstat120 under culture conditions and is hypothesized to be the primary effector of the paracrine anti-angiogenic activity of BAI1. It should be noted,

however, that as for Vstat120, Vstat40 is not always cleaved from the full-length molecule and thus its processing is also likely to be under significant regulatory control.

These proteolyses of extracellular BAI1 are predicted to serve or mediate multiple functions either of the parent receptor or its cryptic derivatives, and these activities may depend on cell type. In particular, the anti-angiogenic properties of Vstat120 and Vstat40 have received significant investigation due to their thrombospondin type-1 repeats, (TSRs, Figure 1.4), domains which are responsible for the angioinhibitory activity of thrombospondin 1 (TSP-1). The TSRs' activity is best characterized by their interaction with the CD36 scavenger receptor, a heavily-glycosylated 53 kDa transmembrane receptor expressed on microvascular but not large vessel epithelium as well as adipocytes, retinal epithelium and hematopoietic cells, platelets, and macrophages (Febbraio and Silverstein, 2007). Notably, the Val-Thr-Cys-Gly (VTCG) motif in TSRs binds a highly conserved CLESH (CD36 LIMP-II Emp sequence homology) domain (Febbraio et al., 2001; Febbraio and Silverstein, 2007). TSP1-CD36 binding activates p59fyn kinase and p38, ultimately leading to caspase-3-dependent apoptosis, and Jun N-terminal kinase, which induces the gene encoding the ligand for the Fas death receptor (Jimenez et al., 2000; Jimenez et al., 2001). TSRs also inhibit angiogenesis through their heparin-binding Trp-Ser-Pro-Trp (WSPW) motifs by competing for VEGF attachment to heparin sulfate on the surface of endothelial cells (Gupta et al., 1999) and interfering with heparin's growth factor-stabilizing activity (Vogel et al., 1993). Another significant angio-regulatory feature of TSRs is a GXXXRXR motif, which strongly inhibits endothelial proliferation and serves the basis for the therapeutic peptide ABT-510 (Zhang and Lawler, 2007).

A variety of evidence suggests that the BAI1 TSRs are potent regulators of angiogenesis. Early work demonstrated that synthetic peptides containing BAI1 TSRs 2-4

and 3-5 could inhibit rabbit corneal angiogenesis when administered exogenously (Nishimori et al., 1997). Subsequently, the secreted 120 kDa extracellular domain resulting from GPS cleavage (Vstat120) was shown to inhibit angiogenesis in culture and tumor-associated angiogenesis in xenografts (Kaur et al., 2005; Kaur et al., 2009; Klenotic et al., 2010). More recently, the most N-terminal TSR was also shown to exhibit CD36-dependent anti-angiogenic activity as part of the 40 kDa Vstat40 fragment (Chapter 3). Recent work has also shown that histidine-rich glycoprotein (HRPG) modulates the anti-angiogenic effect of Vstat120 in culture via competing for binding to CD36 (Klenotic et al., 2010).

However, the role of the TSRs of full-length BAI1 or the other BAI proteins in normal brain and in other tissues is incompletely understood, and accumulating evidence implicates them in a diversity of functions. Recently, the TSRs of BAI3 have been shown to recognize C1q-like (C1ql) proteins, and the presence of these TSRs interferes with the loss of synapse density mediated by C1ql proteins (Bolliger et al., 2011). Another study in macrophages has shown that extracellular BAI1 specifically recognizes phosphatidylserine (PtdSer) on the surface of apoptotic cells via binding with its TSRs (Park et al., 2007). This binding subsequently triggers the BAI1 C-terminal-mediated activation of the Dock180-ELMO complex and Rac, promoting actin cytoskeleton remodeling and ultimately engulfment of the apoptotic target by the macrophage. Processing of the BAI1 extracellular domain is likely to interfere with phagocytic activity, suggesting that this portion of the molecule may have different functions in different microenvironments (Figure 1.5), and that these cleavage events are likely tightly regulated and may vary in different cell types.

Other class B GPCRs undergo proteolysis at sites in their extracellular domains beyond the GPS. Recent work has demonstrated that extracellular BAI2 is processed by furin (Okajima et al., 2010). Furin preferentially processes its target substrates after a highly-

conserved dibasic motif, preferentially Arg-X-Arg-X-(Lys/Arg)-Arg, with arginines in the P1, P4 and P6 positions (Duckert et al., 2004). BAI2 appears to be cleaved by furin *in vitro* after a noncanonical Gln-Trp-Pro-Arg (QWPR) sequence. However, the existence and biological significance of this processing event *in vivo* remains to be determined, and no extracellular proteolysis event has yet been shown for BAI3. Similar findings have been determined for the extracellular domains of other class B GPCRs. Of note, the receptor Ig-Hepta contains a prohormone processing site (RPKR) which is cleaved by the serine endoprotease furin to release EGF2 domain-containing fragments (Fukuzawa and Hirose, 2006). The developmentally regulated GPCR (DREG) receptor also contains a furin cleavage motif (KVKR) and may be activated by this protease (Moriguchi et al., 2004). In sum, proteolysis of the extracellular portion of these class B GPCRs is a common event, and the significance of these proteolysis events either with regard to the activity of the fragments generated or that of the parent molecule is expected to be wide-ranging.

1.9. Intracellular signaling and C-terminal binding partners

The signaling cascades regulated by BAI family proteins are poorly characterized to date, and the majority of known interactions have been identified for BAI1 only. The intracellular C-terminal domain of BAI1 contains multiple features of interest, including a proline-rich region (PRR) and PDZ-binding domain (PBD) (Figures 1.1-2). While BAI1 has not been determined to associate with a specific GTPase, early studies have identified at least five molecules capable of physically interacting with the C-terminal domain of BAI1.

BAP-1. BAI1-associated protein 1 (BAP-1) is a PDZ domain-containing scaffolding protein that directly associates with the QTEV motif located at the most C-terminal portion of BAI1. Later determined to be MAGI-1, a member of the membrane guanylate kinase

(MAGUK) inverted family of scaffolding proteins commonly found in the post-synaptic density, BAP-1 was observed to co-localize with BAI1 at intercellular contacts (Shiratsuchi et al., 1998a). BAP-1 may thus play a role in regulating the localization of BAI1 at neuronal synapses, but this relationship is yet to be conclusively determined.

BAP-2. Another binding partner of C-terminal BAI1 is BAP-2/IRSp53, a Src homology 3 (SH3) domain-containing molecule. BAP-2 interacts with a regulator of the actin cytoskeleton, mDia, in the presence of active RhoA, a process believed to mediate stress fiber formation and cytokinesis (Fujiwara et al., 2000), and hypothesized to regulate signal transduction during neuronal growth. Taken in conjunction with the ability of C-terminal BAI1 to bind the ELMO/Dock180 complex and regulate Rac signaling, these studies provide strong support for the hypothesis that intracellular BAI1 plays an important role in regulating cytoskeletal activity.

BAP-3. BAP-3, an 1187 amino acid protein expressed predominately in the brain, contains two C2 domains and has sequence homology to Munc13, as well as to synaptotagmin. BAP-3 was discovered in a yeast-two-hybrid screen for molecules interacting with C-terminal BAI1 (Shiratsuchi et al., 1998b). The interaction between BAI1 and BAP3 is mediated by BAP-3 amino acids 569-882, a region which has homology to a functional domain of Munc13 but is not a C2 domain. C2 domains are implicated in fusion of presynaptic vesicles to membranes, again suggesting a role for BAI1 in the regulation of multiple features of neuronal activity.

BAP-4. Little is known concerning the significance of the interaction between BAI1 and the BAI1 associated protein 4 (BAP-4), alternatively known as phytanoyl-CoA alpha-hydroxylase-associated protein 1 (PAHX-AP1) (Koh et al., 2001). This molecule is specifically expressed in mouse brain, where it associates with the Refsum disease product PAHX.

Immunoprecipitation experiments have shown that BAP4 specifically interacts with the 1254-1516 C-terminal amino acids of BAI1, but not with BAI2 or BAI3.

PSD-95. Further immunoprecipitation experiments have demonstrated that BAI1 binds to another PDZ domain-containing scaffolding protein, PSD-95 (Lim et al., 2002). PSD-95 is a key molecular component of synapses and regulates the localization of many receptors in neurons. Together this work shows that BAI1 localization is mediated by PDZ-containing proteins and is likely to be tightly regulated. These associations are also likely to govern BAI1's potential functions either as a cell adhesion molecule or as a receptor. Its localization at the cell surface is also believed to factor into the processing of its extracellular domain, as BAI1 lacking a C-terminus is not efficiently processed into Vstat40 (Chapter 2).

In sum, the features of intracellular BAI1 and its interacting partners suggest that BAI1 may serve disparate functions in the normal adult brain beyond angioregulation, including the regulation of signal transduction, cell adhesion, growth cone guidance and neurotransmitter release (Mori et al., 2002). Continued investigation into the role of BAI1 in the brain will be necessary to demonstrate existence of these activities and their significance for brain function.

The intracellular signaling cascades regulated by the other BAI family proteins are poorly studied. One report suggests BAI2 represses VEGF expression via an association of its C-terminal region with the GA-binding protein gamma through mechanisms that are not well characterized (Jeong et al., 2006). The significance of these associations has not yet been demonstrated *in vivo*, but may contribute to the observed anti-tumor activity of BAI2.

1.10. A role for BAIs in neurovascular function and disease

Many neurological diseases are characterized by compromise or pathology of the vasculature, notably stroke (Hayashi et al., 2003; Lin et al., 2003; Sun et al., 2003) and the lethal brain tumor glioblastoma multiforme (GBM). Advances in the overall understanding of the regulation of vascular maintenance or brain angiogenesis are likely to lead to improved therapeutics or better strategies of preventative medicine for many of these diseases (Greenberg and Jin, 2005; Zlokovic, 2008), and the BAI family proteins provide a novel and intriguing avenue for such inquiry. As described below, emerging evidence already implicates the BAI proteins in multiple neurovascular diseases.

Cancer. BAI1 has been implicated in the biology of many cancers. *BAI1* mRNA levels are consistently downregulated in primary glioma specimens and cell lines (Kaur et al., 2003) as well as brain metastases from lung adenocarcinoma (Hatanaka et al., 2000). Loss of *BAI1* expression was recently shown to occur via epigenetic silencing in glioblastoma (Zhu D et al., in submission). Pulmonary adenocarcinomas, gastric and colorectal cancers also show reduced BAI1 expression compared with normal tissue (Fukushima et al., 1998; Hatanaka et al., 2000; Miyamoto et al., 2007; Yoshida et al., 1999), suggesting that successful tumor formation selects for the loss of BAI1 expression, an interpretation recently borne out with the finding of multiple somatic point mutations in the *BAI*s in several cancers (Kan et al., 2010) (Figure 1.1). BAI1 expression in glioblastoma patients correlates with a positive clinical outcome (Nam et al., 2004). Further, exogenous restoration of BAI1 expression reduces growth and vascularization of tumors derived from gliomas, pancreatic cancers and renal cell carcinomas (Berger et al., 2010; Fukushima et al., 1998; Kudo et al., 2007; Xiao et al., 2006; Yoon et al., 2005). While the precise mechanisms of its anti-tumor activity are not clearly defined, BAI1 is hypothesized to impede the growth and progression of a variety of cancers

via interfering with tumor-associated angiogenesis. In support of this theory, Vstat120 is demonstrated to interfere with the migration of cultured endothelial cells and block vascularization and tumor growth in an orthotopic xenograft mouse model (Kaur et al., 2005; Kaur et al., 2009). Vstat40 is also a potent angiogenesis inhibitor, although its anti-tumor activity remains to be conclusively determined (Chapters 3-4). Thus, BAI1 fulfills the criteria for a *bona fide* tumor suppressor and there is significant potential for BAI1 and its extracellular derivatives as therapies for the treatment of human cancers.

While less well understood than BAI1, the role of BAIs 2 and 3 in tumor suppression and angioregulation is gaining appreciation. Expression of *BAI3* mRNA is lost in approximately 50% of assayed glioblastoma cell lines (Shiratsuchi et al., 1997). Importantly, somatic mutations of *BAI3* have been detected in 13% of squamous lung carcinoma and 5% of lung adenocarcinoma (Kan et al., 2010). Other somatic mutations in lung, breast and ovarian cancers have been identified for *BAIs* 1 and 2 (Figures 1.1 and 1.3). The functional relevance of these mutations for tumor biology and progression remains to be determined.

Ischemia. The potent angioregulatory activity of the BAI proteins is likely to be modulated in response to neurovascular injury. In support of this hypothesis, one experiment observed that expression of *mBai1* decreases by 24 hours post-ischemia induction in a mouse middle cerebral artery (MCA) occlusion model of stroke (Koh et al., 2001). This finding suggests that the anti-angiogenic activity of BAI1 may be preferentially suppressed in order to allow revascularization of the damaged brain tissue. BAI2 is also implicated in the biology of ischemic stroke. In the MCA model, *mBai2* expression is observed to decrease prior to the decrease of mBAI1 mRNA expression after induction of ischemia (Kee et al., 2002). While the significance of the post-ischemic loss of BAI2 remains to be determined, these findings suggest that it may play a role in the regulation of brain vascular homeostasis and that its

downregulation likely reflects the response of hypoxic brain tissue to favor the regrowth of new vasculature.

Schizophrenia. Given the BAIs' expression pattern and synaptic association, it is anticipated they may function in many aspects of neurological development or activity. In one such recent example, an analysis of SNPs associated with schizophrenia focused on a region of 6q encoding *BAI3* and previously associated with disorganized symptoms (DeRosse et al., 2008). The study determined that the SNPs rs1415031 and rs9446083 located in the intronic region 5' to the 9th exon of *BAI3* were significantly associated with lifetime severity of disorganized symptoms. Other *BAI3*-associated SNPs were investigated for their relationship to symptomology of the disease, and of these, 20% yielded a statistically significant association with disorganized symptoms. While it is yet unclear how a SNP in the *BAI3* intron may yield such a biological effect, it highlights the importance of considering BAI family protein function in other neurovascular diseases beyond tumor biology.

1.11. Conclusions

Aggressive gliomas represent a significant health problem due to their high mortality rates and resistance to standard avenues of treatment. Continued investigation into their molecular biology is necessary for the development of more effective therapeutics. Preliminary research into the BAI family proteins, particularly BAI1, has already yielded important insights into their promise as anti-cancer agents, and further work on the BAIs may improve our ability to treat other neurological or vascular diseases. While we are only beginning to learn the roles that the BAI family proteins play in physiology and disease, continued study of their biology is ultimately essential for a complete understanding of GPCR biology and pharmacology as well as improvements in the development of biomedical therapeutics.

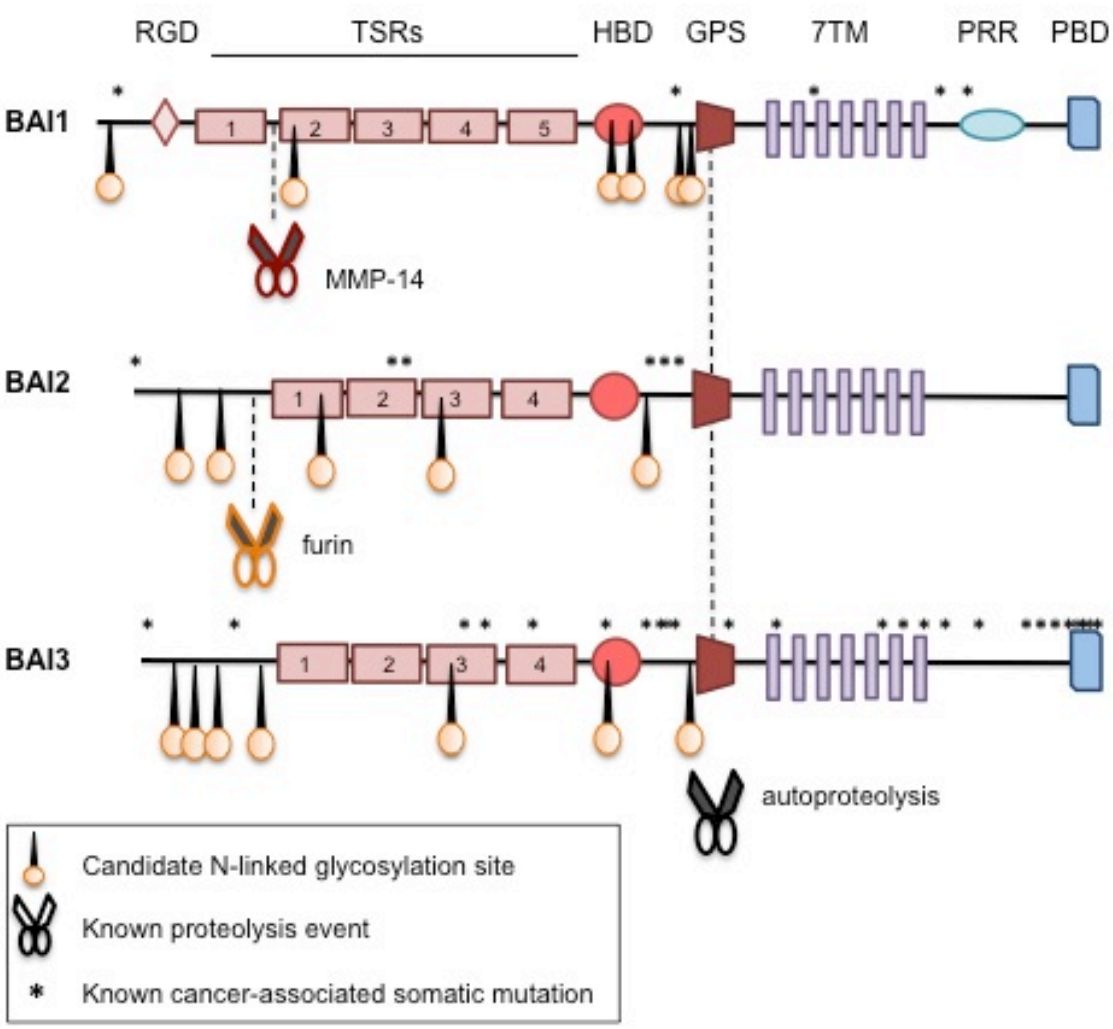

Figure 1.1. Schematic of the three BAI family proteins, representing the major known structural and functional features as well as known proteolysis events and cancer-associated somatic mutations. *Abbreviations*: RGD: Arg-Gly-Asp integrin-binding motif; TSR: thrombospondin type 1 repeat; HBD: hormone-binding domain; 7TM: seven-transmembrane region; PRR: proline-rich region; PBD: PDZ-binding domain.

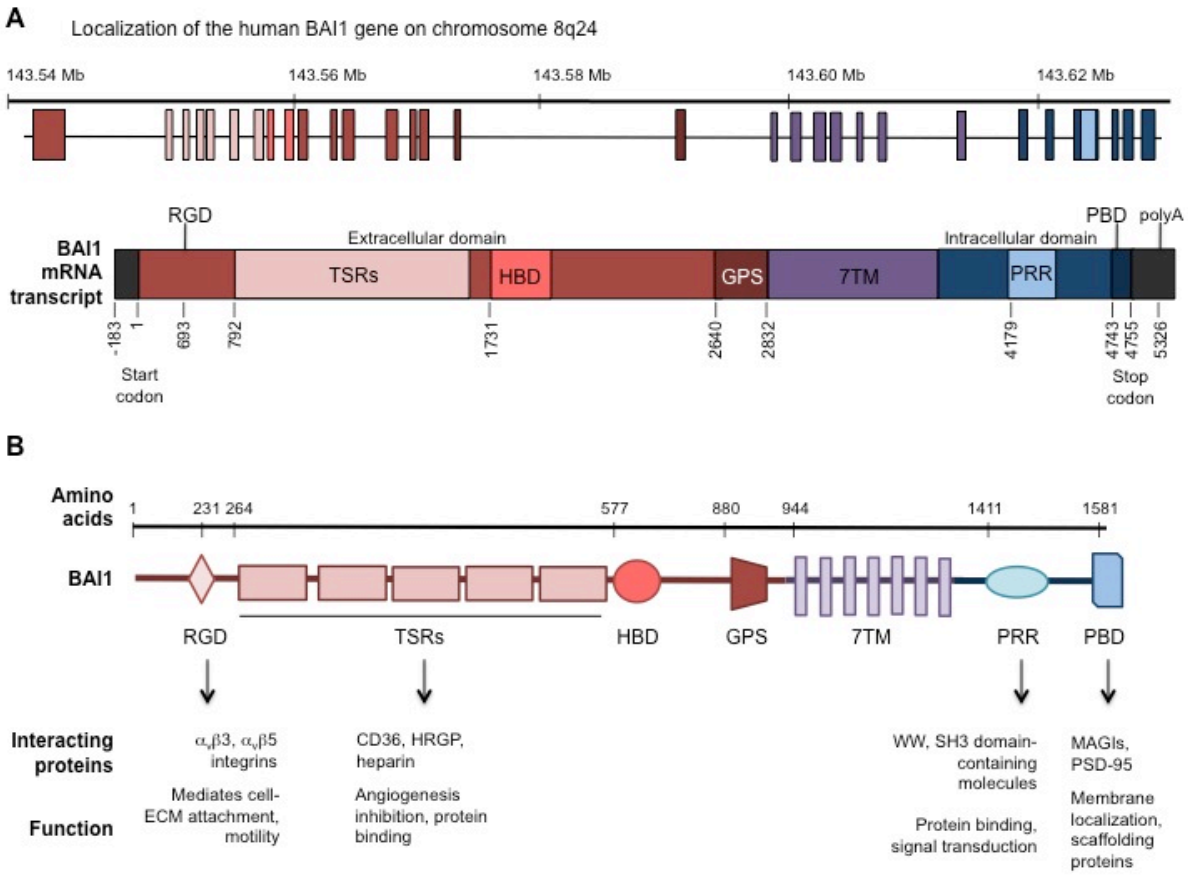

Figure 1.2. Genomic, mRNA and protein structure of BAI1. (**A**) Genomic structure of BAI1 localized on human chromosome 8q24. Exons are colored to indicate position in the resulting mRNA transcript (NCBI Reference Sequence NM_001702.2). (**B**) Structure of the BAI1 protein including a summary of known functional information for selected domains.

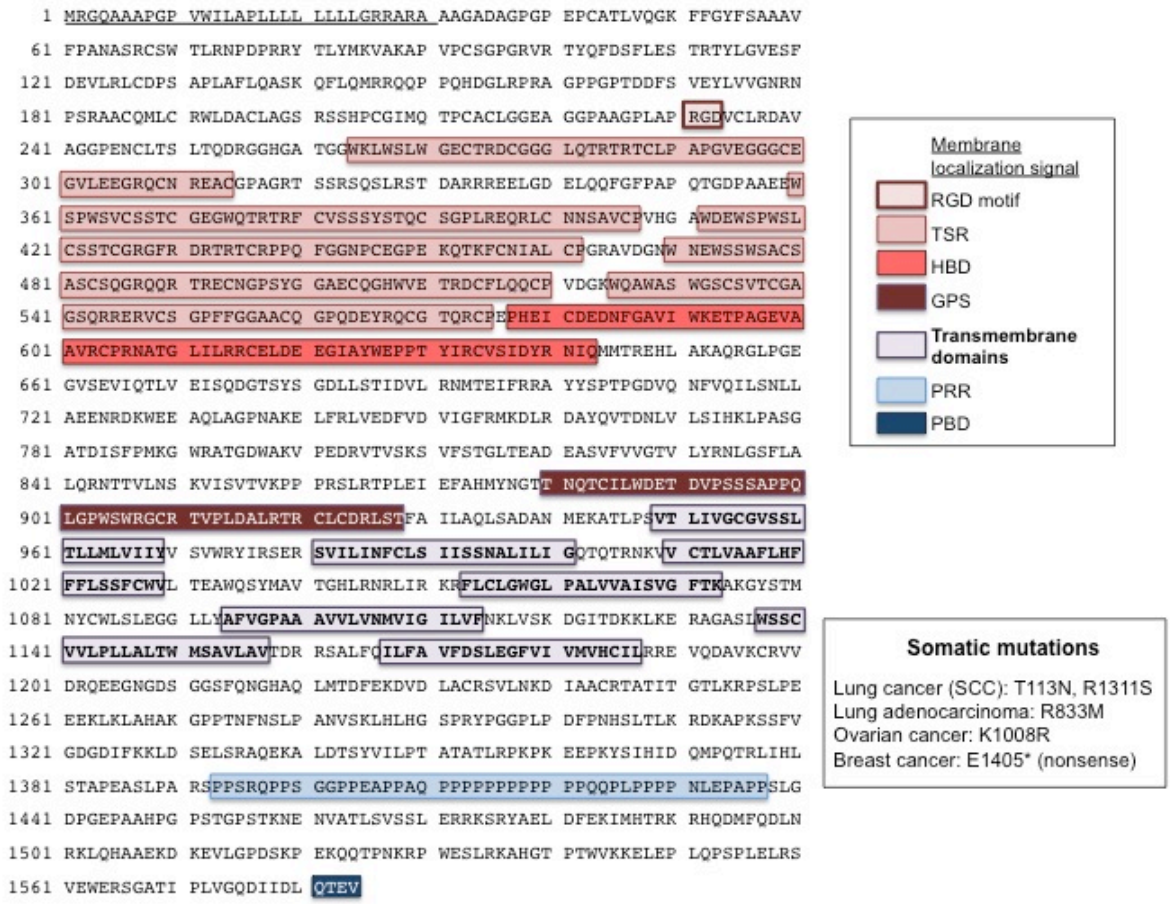

Figure 1.3. Amino acid structure of BAI1, detailing the composition of indicated domains and their precise location within the protein. Known cancer-associated somatic mutation information provided at right.

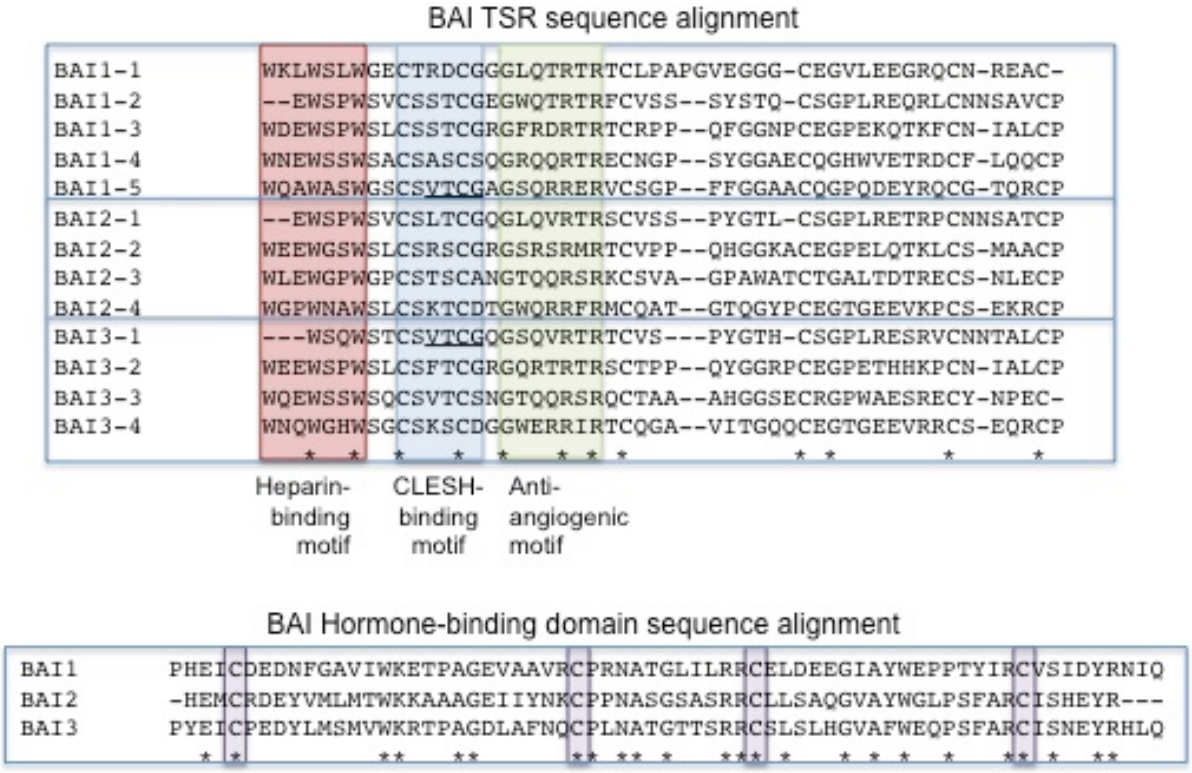

Figure 1.4. Alignment of the BAI family thrombospondin type 1 repeats and hormone-binding domains. While variable, the TSRs are characterized by features including heparin- (indicated in red) and CD36-binding (blue) motifs and other regions known to interfere with angiogenesis (green). The BAI hormone-binding domains are characterized by four conserved cysteine residues (purple). Conserved residues are indicated by asterices.

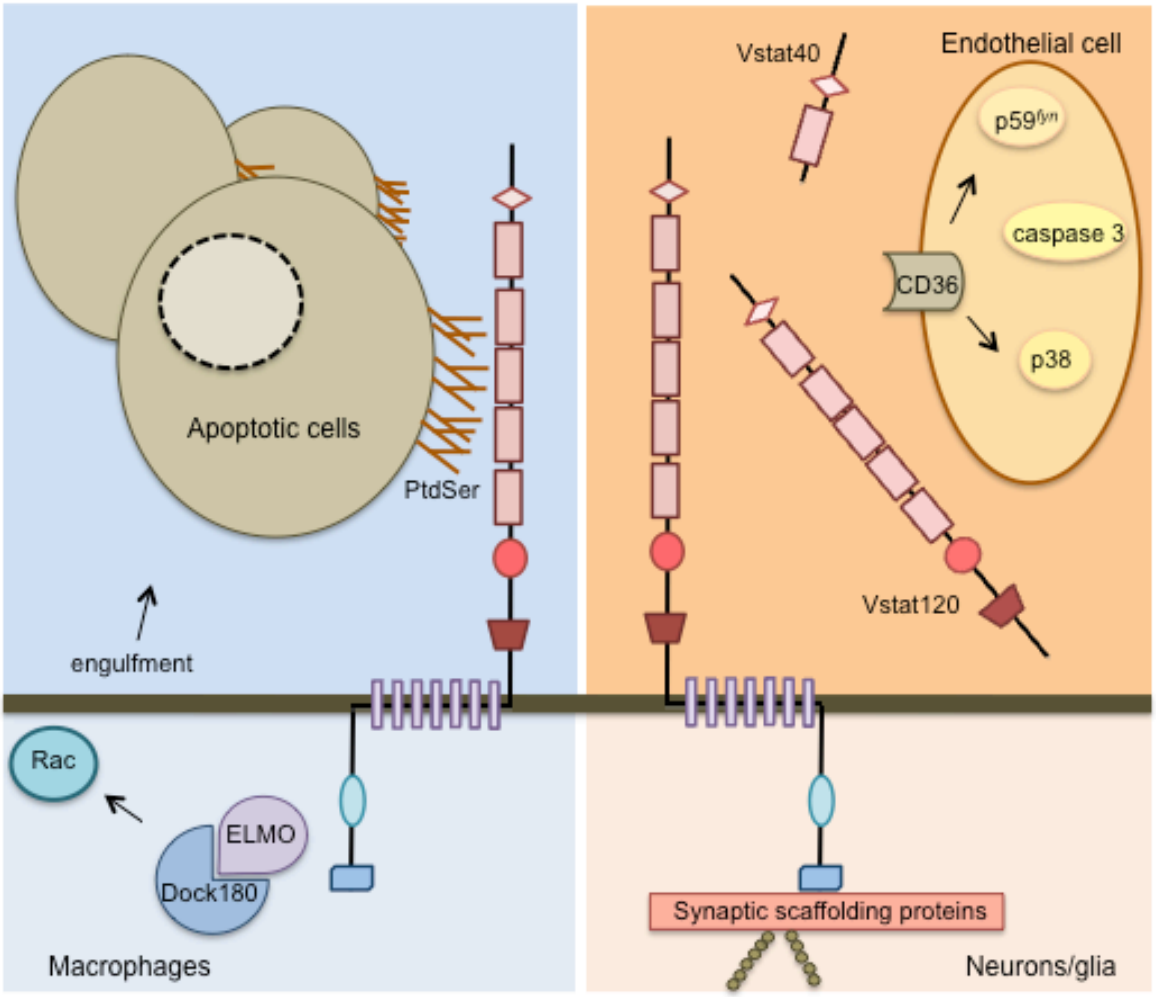

Figure 1.5. Illustration of the multiple identified functional roles for BAI1. *Left*: expressed on macrophages, the TSRs of extracellular BAI1 interact with phosphatidylserine (PtdSer) on the surface of apoptotic cells leading to activation of the ELMO/Dock180 complex and Rac by intracellular BAI1 and engulfment of the apoptotic cell by the macrophage. *Right*: expressed in brain tissue, BAI1 is proteolytically processed to generate at least two secreted molecules, Vstat120 and Vstat40, which inhibit angiogenesis in a CD36-dependent manner.

CHAPTER 2.

MECHANISMS OF VSTAT40 PROTEOLYSIS.

This chapter includes the majority of the research for publication by: Cork SM, Kaur B, Cooper L, Saltz JH, Sandberg EM, and EG Van Meir, entitled A furin/MMP-14 proteolytic cascade releases a novel 40 kDa vasculostatin from tumor suppressor BAI1, currently in submission.

Introduction

Many neurological diseases are characterized by pathology of the vasculature, including stroke, particularly the aggressive and highly vascularized glioblastoma multiforme (GBM). For many of these diseases, a better understanding of regulation of vascular maintenance or angiogenesis in the nervous system could lead to improved therapies or better strategies of preventative medicine (Greenberg and Jin, 2005). Previous work has illustrated the diversity of molecules that participate in regulating vascular system function, typically functionaing as either angiogenesis stimulators or inhibitors (Plate, 1999; Rege et al., 2005; Somanath et al., 2009; Stupack and Cheresh, 2003; Zhang and Lawler, 2007), but the larger picture of the individual roles of these molecules and their complex interplay *in vivo* remains poorly understood.

Brain-specific angiogenesis inhibitor 1 (BAI1) is so named for its ability to inhibit angiogenesis *in vivo* (Nishimori et al., 1997), and exogenous expression of its extracellular domain in gliomas interferes with tumor-associated angiogenesis (Kaur et al., 2009). BAI1 is the first GPCR known to undergo proteolysis to generate secreted angiogenesis inhibitors. The Van Meir lab first determined that BAI1 undergoes endogenous processing at its conserved GPCR processing site (Kaur et al., 2005) to generate a 120 kDa secreted fragment called Vasculostatin-120 (Vstat120) and demonstrated that upon overexpression it had significant anti-angiogenic and anti-tumor activity in an orthotopic xenograft model (Kaur et al., 2009), but the significance of this observation for spontaneous brain tumor formation is unclear as under physiological conditions Vstat120 is a low abundance fragment in human brain extracts. While the physiological function of BAI1 in normal brain remains poorly defined, these findings support the hypothesis that BAI1 and its N-terminal cleavage products

play an important role in the inhibition of neuro-oncogenesis via maintenance of vascular homeostasis in the brain.

In the present study we demonstrate the existence of a novel secreted 40 kDa fragment derived from extracellular BAI1, which is present in human cortical tissue. We identify the location of the cleavage site and show that this fragment retains the RGD motif and the first TSR of BAI1, and named it Vasculostatin-40 (Vstat40) for its ability to inhibit angiogenesis in a battery of culture-based assays described in Chapter 3. We identified the proteolytic cascade that results in Vstat40 cleavage and determined whether it was an extracellular processing event. We investigated the relationship of Vstat40 to Vstat120 to determine whether Vstat120 is an intermediate in the processing of Vstat40, or whether Vstat40 processing may serve as a mechanism to inactivate Vstat120. The findings advance our understanding of BAI1 by highlighting the importance of its extracellular proteolysis and indicate the importance of further research into the functional significance of these processing events.

Materials and Methods

Cell culture. HEK 293 cells and human glioma cell lines U87MG, LN229 (Beck-Sickinger et al., 1992; Ishii et al., 1999), and U251-BAI1 (Clone B12 (Kaur et al., 2003)) were cultured in DMEM with 10% fetal bovine serum (FBS) and antibiotics and passaged every 2-4 days. LoVo cells and furin-transfected derivatives were the kind gift of the C. Dubois lab (Université de Sherbrooke).

Conditioned medium (CM) used in experiments was prepared from either indicated cell lines for inhibitor or *in vitro* cleavage assays. For the collection of CM, indicated cells were plated in 15 cm cell culture dishes (Corning) and allowed to achieve approximately 80% confluence. For all experiments, CM was harvested under sterile conditions after 48 hours unless otherwise indicated and centrifuged at 6000xg for 15' to remove floating cells prior to analysis. CM was concentrated using an Amicon Ultra concentrator (5 kDa MW cut-off) approximately 30x to a final volume of 500 μL. Levels of Vstat proteins present in the CM were characterized exclusively using Western blot.

Transfection of cDNA and siRNA. For transfection, cells were grown to 60-80% confluency. Transfection using the GenePorter (Genlantis) reagent was carried out according to the manufacturer's instructions. Briefly, GenePorter (20 μL/mL) and plasmid DNA (0.5-1 μg/mL) were each separately incubated in half the total transfection volume of serum-free medium for 10 minutes, then combined and incubated for 10 minutes and briefly centrifuged. Cells were washed thoroughly with PBS and transfection medium added and plates were swirled gently to cover. Transfection proceeded for 4-6 hours, after which time medium containing 20% FBS was added in a 1:1 ratio and transfected cells were allowed to recover overnight. Cells were washed with PBS and incubated for 24 hours in serum-free medium for all CM collections. For the furin knockdown assay, a proprietary mix of anti-

furin siRNAs (NE Biolabs ShortCut siRNA mix, N2026S) was used at indicated concentrations. Anti-MMP-14 siRNA was purchased from Ambion (Silencer Select Validated siRNA, ID# s8877).

Generation of constructs. All truncation constructs were generated by polymerase chain reaction (PCR) using *Bai1* cDNA as a template (Nishimori et al., 1997). PCR-derived inserts were cloned into the directional cloning vector pcDNA3.1D/V5-His (Invitrogen) using the forward primer 5' CACCCTTAAGCTTCGAGCTAGG containing the HindIII cloning site and N-terminal BAI1 sequence. Reverse primers for untagged contructs (Figure 2.3A) were (1) 5' CTATCAGTCCCGCGTGCATTCGCC, (2) 5' CTATCAGCCCTCCACGCCCGG, (3) 5' CTATCAGGGGCTGGGAACCCAAAC, (4) 5' CTATCACCAGCCCTCGCCGCAGGTG. Reverse primers for tagged constructs (Figure 2.3B) were (1) 5' GCTGGTGCGCCCAGCGGG and (2) 5' TGTGGACCGCAGGGACTG. Reverse primers for point mutant constructs were (Figure 2.3C): (1) 5' GGACCGCAGGGACTGGCTCGCGGAGCTGGTGCGCCCAGC, (2) 5' ATCTGTGGACCGCAGGGACACGCTCCGGGAGCTGGTGCG, (3) 5' GGCATCTGTGGACCGCAGGGCCTGGCTCCGGGAGCTGGT, (4) 5' GCGCCGCCGGGCATCGTGTGGACGCCAGGGACTGGCTCCGGAG, (5) 5' GCGCCGCCGGGCATCTGTGGCCCGCAGGGACTGGCTCCGG.

Constructs were generated in full-length BAI1 in pcDNA 3.1, with the XhoI site in the MCS removed using restriction digest of flanking sites XbaI and EcoRI and treatment with the Klenow fragment. Mutagenesis was performed using a primer overlap extension method and two unique sites (XhoI and AgeI) flanking the region of Vstat40 cleavage. Mutagenic primer sequences were constructed as follows and obtained commercially (IDTDna): QSL foward: 5' CAGGCAGCAGCATCCACAGATGCCCGGCG; QSL

reverse: 5' GGATGCTGCTGCCTGGCTCCGGGAGCTGT; RSQ forward: 5' TCCGCAGCAGCATCCCTGCGGTCCACAGAT; RSQ reverse: 5' GGATGCTGCTGCGGAGCTGGTGCGCCCAG. The secondary PCR reaction was allowed to proceed 5 cycles without primers to promote amplification of the desired template. Restriction enzymes and buffers were obtained from NE Biolabs. Presence of the mutation was confirmed by sequencing the constructs (Macrogen USA).

Inhibitor assays. Indicated cells were plated at a density of $1x10^5$ in 6-well plates and allowed to recover overnight or until approximately 70% confluence. Cells were washed with PBS and incubated in serum-free medium with decanoyl-RVKR-cmk (Calbiochem 344930), GM6001 (Calbiochem 364205), MMP-3, MMP-8 or MMP-2/9 (Calbiochem) inhibitors reconstituted in dimethyl sulfoxide (DMSO) at indicated concentrations. Caspase inhibitor II cmk (Anaspec, Catalog # 60861) was used as a negative control, and α1-PDX (Thermo Scientific, Catalog # RP-070) was used as a positive control as indicated. For every experiment, each condition received an equal amount of DMSO, and no sample received more than 1% DMSO in the final treatment volume. CM was collected after 12 hours and immediately precipitated with 50% trichloroacetic acid (TCA) on ice for at least one hour prior to Western blot analysis.

Western blots. Western blots were performed on both CM and WCE samples as indicated. Serum-free CM was collected after 12-24 hours as indicated and either precipitated with 50% TCA or 4 volumes of ice-cold acetone. Precipitated CM pellets were resuspended by extensively washing collection tubes in 100-150 μL 1x sample buffer. Following CM collection, cells were washed 2x with PBS and WCE was collected in 150-250 μL 1x sample buffer containing SDS and β-mercaptoethanol, sonicated and boiled 2 minutes. Samples

were immediately loaded on 10% Criterion precast gels (BioRad) and electrophoresed for 2 hours at 100 volts at room temperature. Separated proteins were transferred to nitrocellulose membranes at 47 volts for 3.5 hours at 4°C. Membranes were blocked for at least 1 hour in fresh 5% PBST-milk solution and incubated with primary antibody overnight at 4°C. Antibodies used include: the BAI1 N-terminal antibody N-Ab (Kaur et al., 2003), 1:1000); MMP-14 (ab38971) and TIMP-3 (ab66022) (Abcam, 1:1000); monoclonal antibodies to TIMP-1 and -2 (Calbiochem Cat# IM32 and IM11, 1:1000); p53 and actin (Santa Cruz; 1:2500); furin (MON-152 monoclonal antibody, Fisher; 1:500).

***In vitro* cleavage reactions**. Serum-free conditioned medium from U87MG-Vstat120 cells was collected after 72 hours and filtered by 8000xg centrifugation for 20 minutes at 4°C under sterile conditions. Purified CM was divided into two equal portions and concentrated 60x using Amicon Ultra centrifugal filter devices (5 kDa MW cut-off) to a final volume of 250 μL each. Samples were buffer-exchanged by adding 15 mL of either furin or MMP-14 reaction buffer (described below) to the respective concentrates, gently mixed and concentrated as before to a final volume of 500 μL each. Buffer-exchanged concentrates were kept on ice and portioned into input and treatment samples. Input samples were immediately precipitated with four volumes of ice-cold acetone and stored at -20°C. 0.2 μg of indicated enzymes were added to their respective treatment samples, and control and enzyme-containing samples were incubated at 37°C for the indicated time intervals, after which all samples were precipitated with ice-cold acetone. Precipitates were reconstituted in 1x sample buffer for Western blot analysis. Human furin recombinant catalytic domain was purchased from New England Biolabs (Cat. # 8077S). Furin hydrolysis reaction buffer: 1mM $CaCl_2$, 100 mM HEPES, 0.5% Triton X-100, 1 mM β-mercaptoethanol. Human MMP-14 recombinant catalytic domain was purchased from Calbiochem (Cat. # 475935). MMP-14

hydrolysis reaction buffer: 50 mM Tris-HCl, pH 7.5, 150 mM NaCl, 5 mM $CaCl_2$, 0.025% Brij35 detergent, made fresh prior to experiment and stored at 4°C. Catalytic activity of rhFurin was verified by incubation with the fluorogenic furin substrate peptide Boc-RVRR-AMC (Alexis Biochemicals, Cat. # ALX-260-040). Fluorescence of the substrate peptide in buffer-exchanged concentrated CM either with or without rhFurin (1U/mL) was measured at 380 excitation and 460 emission wavelengths at indicated time points and normalized to the baseline fluorescence of the substrate peptide in furin hydrolysis buffer alone.

Immunofluorescence. Cells were washed and fixed with ice-cold methanol for 15 minutes, blocked in 5% PBST-BSA for an hour at room temperature and incubated with BAI1 C-terminal antibody (1:200) and a anti-rabbit IgG conjugated to Alexa Fluor 555 (1:1000, Invitrogen), and anti-myc tag antibody 9e10 conjugated to Alexa Fluor 488 (1:200, SCBT). Confocal imaging was performed at 63x magnification using oil drop immersion (Zeiss IX-50).

Brain/tumor samples used. Samples of human cortex NHB1 (95-268) and NHB2 (95-308) and GBM samples 1-4 (06-23, 06-19, 05-64, and 05-96, respectively) were obtained from the Emory University Brain Tumor bank.

Results

N-terminal BAI1 is processed to yield a major 40-kilodalton secreted fragment. Following our prior discovery that cleavage of the BAI1 N-terminus produced a secreted angiogenesis inhibitor (Kaur et al., 2005), we sought to determine whether it was present in the normal human brain (NHB). As expected, we detected the previously-identified 120 kDa fragment, and also discovered another novel major fragment in the 40 kDa size range (Figure 2.1A, NHB(2)). Importantly, these fragments and full-length BAI1 were not detected in four randomly chosen glioblastoma tissues, suggesting a potential role in antagonizing glioma growth (Figure 2.1A, GBM(1-4)). To investigate whether this fragment could be generated through processing of the extracellular domain of BAI1, we transfected 293 cells with an expression vector for wild-type BAI1 (BAI1) and harvested the serum-free conditioned medium (CM). Analysis of the CM by Western blot using an antibody recognizing N-terminal amino acids 103-118 (N-Ab; Figure 2.1B) showed a very prominent band approximately 40 kilodaltons in size, clearly representing the major secreted product of BAI1 (Figure 2.1C). Upon longer exposure, the previously identified, 120-kDa fragment (Vstat120) (Kaur et al., 2005) was also detected (Figure 2.1C, long exposure panel). Processing of BAI1 into this 40 kDa fragment was not unique to 293 cells and also occurred constitutively in tumor and non-tumor cell lines, including the immortalized human fibroblast cell line HFF-1 and LN229, U87MG and U251MG cell lines (not shown). This experiment demonstrated that a very important secretion product of BAI1 had been overlooked in prior studies, and we wished to evaluate its function.

We first questioned whether the 40 kDa fragment was processed independently of Vstat120 or whether the processing of Vstat120 represented an intermediary step in the

generation of the 40 kDa fragment. To this purpose, we transfected 293 cells with a Vstat120 expression vector (Figure 2.1C, lane 3) and determined that the 40 kDa fragment is processed from Vstat120 albeit at significantly lower efficiency compared with its processing from the full-length BAI1 protein, suggesting that the generation of Vstat120 is unlikely to be a required step for production of the 40 kDa fragment. To follow up on this observation, we investigated processing of Vstat120 and the 40 kDa fragment using a BAI1 mutant containing a point mutation in the GPS region ($S_{927}D$). We observed that the mutant yielded increased levels of Vstat120 production and a corresponding decrease in the secretion of the 40 kDa fragment (Figure 2.1D), suggesting that secretion of Vstat120 interferes with rather than promotes the generation of the 40 kDa fragment. To investigate the role of C-terminal BAI1 in its extracellular processing, we generated a truncated form of BAI1 containing its extracellular domain and three transmembrane domains (BAI1-3TM). We observed that this truncation interferes with secretion of both Vstat120 and the 40 kDa fragment (Figure 2.1E), suggesting that a complete transmembrane domain or the intracellular portion of BAI1 are required for efficient generation of the 40 kDa fragment.

Identification of the site of Vstat40 processing. Based on the observation that BAI1 N-terminal constructs containing the Vstat40 cleavage site are processed to some extent into true Vstat40 (e.g., Figure 2.1C), we reasoned that we would be able to narrow down the location of the processing site by examining the cleavage of progressively shorter N-terminal fragments. Accordingly, we generated serial truncations of N-terminal *Bai1* cDNA flanking the likely region of Vstat40 cleavage based on its predicted size, and transfected cDNA constructs containing these truncations into 293 cells. Processing of the resulting secreted peptides narrowed the location of Vstat40 cleavage to between amino acids 297 and 351

(Figure 2.2A). Use of the Western blot technique does not permit the distinction of cleaved and uncleaved fragments differing in only a few amino acids' size. To overcome this limitation, we generated expression vectors that added 3 kDa V5/His tags to the uncleaved N-terminal fragments. Using this approach we were able to demonstrate that Vstat40 is processed between amino acids 322 and 330 (Figure 2.2B). Finally, to determine the relative contribution of selected amino acids to Vstat40 processing, we used an alanine scanning approach to introduce point mutations in the prospective region of cleavage (Figure 2.2C). Peptides containing point mutations N-terminal to Arg_{328} were inefficiently processed into Vstat40 (lanes 1-3), and the Arg_{328}Ala mutation appears to abrogate processing entirely. In contrast, the Ser_{329}Ala mutation appears to facilitate Vstat40 processing by comparison (Figure 2.2C, lane 5). To confirm the importance of this region for Vstat40 processing, the site was mutated in the full-length BAI1 protein in two locations (Figure 2.2D). Mutation of the QSL_{327} motif led to virtually complete abrogation of Vstat40 processing, confirming that this site is essential for protease recognition and the production of Vstat40. The reason for the difference in levels of Vstat40 processing from the membrane-inserted BAI1 molecule and secreted extracellular constructs such as Vstat120 is yet incompletely understood. We observe at least partial intracellular colocalization of these molecules when co-expressed in cells, however (Figure 2.2E), and hypothesize the mechanism underlying Vstat40 proteolysis is most likely to occur extracellularly.

Inhibition of furin activity reduces Vstat40 processing. We next investigated the composition of the region of processing to identify candidate proteases cleaving Vstat40. We observed that the region of Vstat40 cleavage contains multiple basic amino acids, suggesting the potential involvement of proprotein convertases (PCs) in Vstat40 processing. PCs cleave their targets after dibasic motifs, preferentially Arg/Lys-X_n-Arg where n=0,2,4 (Duckert et

al., 2004; Rockwell et al., 2002; Thomas, 2002), and the region of Vstat40 cleavage contains an Arg-X-X-X-X-Arg sequence potentially recognized by PCs. We used PC cleavage site prediction software ProP v1.0 (Duckert et al., 2004) to predict whether extracellular BAI1 was likely to be cleaved by PCs. The ProP software does not predict any PC cleavage sites in extracellular BAI1 above a generally accepted specificity cutoff of 0.5 (Roebroek et al., 2004); however, the site of highest probability (0.304) occurs between Arg_{328} and Ser_{329}.

To specifically investigate the ability of proprotein convertases, particularly the ubiquitously-expressed endoprotease furin, to process Vstat40, we treated BAI1-transfected 293 cells with PC inhibitors and evaluated the resulting Vstat40 levels in the CM. Treatment with the irreversible PC inhibitor dec-RVKR-cmk significantly abrogated Vstat40 processing in a dose-dependent manner (Figure 2.3A). Transient expression of BAI1 in furin-deficient human colon adenocarcinoma LoVo cells (Takahashi et al., 1995) yielded reduced processing of Vstat40 compared with that found in the CM of LN229 cells transfected with an equivalent amount of *Bai1* cDNA (Figure 2.3B). This reduction was accompanied by a corresponding increase in Vstat120 levels. Processing of Vstat40 was largely restored in LoVo cells with stable transfection with wild-type *fur* cDNA. We verified that LoVo cells express very little furin protein (Takahashi et al., 1995) and that wild-type furin levels were restored upon stable *fur* transfection to levels comparable to those found in LN229 cells (Figure 2.3C). Functional status of furin in these cells could be assessed by the level of processing of the known furin target MMP-14 (Sato et al., 1996) from its pro-peptide (63 kDa) to its active (60 kDa) form. Together these results suggest that activity of PCs, particularly that of furin, are involved in Vstat40 processing.

To further confirm the association of furin activity and Vstat40 levels, we knocked down furin protein expression with siRNA in U251-BAI1 cells. Furin levels were strongly

reduced at all time points and treatments under consideration (Figure 2.3D). The secreted (active) form of MMP-2 was used as a positive control for furin activity, as MMP-2 is activated by furin target MMP-14, and is cleaved by furin as well (Cao et al., 2005). As expected, no cleaved MMP-2 was observed in the CM of cells subjected to furin knockdown while levels of pro-MMP-2 in the whole cell extract (WCE) were relatively unchanged. Vstat40 processing was strongly inhibited 48 hours after furin siRNA transfection, and a corresponding increase in Vstat120 levels was observed. Unexpectedly, levels of secreted Vstat40 reverted to baseline 72 hours post-transfection, even though furin levels remained reduced, suggesting involvement of a compensatory mechanism.

Finally, we performed an *in vitro* cleavage experiment to determine whether furin can directly process extracellular BAI1 into Vstat40 (Figure 2.3E). We incubated CM containing Vstat120 with recombinant human furin, but levels of Vstat40 and Vstat120 remained constant after 18.5 hours of incubation (Figure 2.3E, left panel), indicating that furin is not able to directly process Vstat40. Activity of the recombinant furin in these reaction conditions was confirmed by incubation with the fluorogenic furin substrate peptide Boc-RVRR-AMC (Figure 2.3E, right panel). Overall, these results show that proprotein convertase activity is important for Vstat40 processing, possibly by indirect activation of an enzyme able to cleave extracellular BAI1 directly.

A furin-activated metalloproteinase processes extracellular BAI1 into Vstat40. Furin processes over a hundred known targets into their bioactive forms (Thomas, 2002), including multiple subclasses of metalloproteinases, extracellular proteases which often process cell-adhesion molecules and are therefore prime candidate molecules to cleave BAI1. Treatment of U251-BAI1 cells with the general metalloproteinase inhibitor GM6001 inhibited Vstat40 processing at a level comparable to equimolar inhibition with irreversible PC inhibitor dec-

RVKR-cmk, while a control molecule containing chloromethylketone had no effect (Figure 2.4A). We also treated BAI1-expressing cells with α1-PDX, a peptide-based inhibitor of proprotein convertases, to demonstrate that interference with Vstat40 processing was not due to some unforeseen toxicity of the inhibitors (Figure 2.4B). To examine whether the activity of other PCs or metalloproteinases accounts for the majority of the proteolytic cleavage in the absence of furin, we treated BAI1-transfected LoVo cells with equimolar dec-RVKR-cmk and GM6001 singly or in combination (Figure 2.4C). For both inhibitors, single treatments reduced the levels of secreted Vstat40 in the CM compared with levels from vehicle-treated cells, while combined treatment largely abolished Vstat40 processing. These results are compatible with the interpretation that dec-RVKR-cmk inhibits residual PC activity in LoVo cells, and that these PCs may activate one or more metalloproteinases responsible for the residual Vstat40 processing in the absence of furin.

To confirm the involvement of metalloproteinases in Vstat40 cleavage, we wished to determine whether tissue inhibitors of metalloproteinases (TIMPs) regulate this processing event. Overexpression of TIMPs 1-3 in 293 cells transiently co-transfected with *Bai1* cDNA showed a clear inhibitory effect of TIMP-3 on Vstat40 processing (Figure 2.4D), a result which was replicated in U251-BAI1 cells (not shown). Levels of pro- and active forms of MMP-14, an endogenous TIMP-3 target, were not affected by this manipulation. We conclude that PC and metalloproteinase activities are responsible for Vstat40 processing, either independently or in a sequential fashion.

MMP-14 directly processes extracellular BAI1 into Vstat40. In our search for the metalloproteinase cleaving BAI1, we focused first on MMP-14 for its role in glioma biology and activation of other MMPs (Fillmore et al., 2001; Holopainen et al., 2003; Hotary et al., 2002; Itoh et al., 2001). SiRNA-mediated knockdown of MMP-14 expression yielded

virtually complete abrogation of Vstat40 processing by 72 hours post-transfection even in the presence of furin (Figure 2.5A), suggesting that MMP-14 is essential for Vstat40 generation and acts downstream of furin. As expected, this was accompanied by an accumulation of uncleaved full-length BAI1. Since MMP-14 is known to activate other matrix metalloproteinases, including MMP-2 and MMP-8, we wished to determine whether Vstat40 processing was directly mediated by MMP-14 or involved its target MMPs. Treatment of BAI1-transfected 293 cells with specific inhibitors of the stromelysin MMP-3, the gelatinases MMP-2/9, and the collagenase MMP-8 did not yield a substantial inhibition of Vstat40 processing (Figure 2.5B), a result also observed after identical treatment of U251-BAI1 cells (data not shown).

To verify that MMP-14 is the primary enzyme cleaving Vstat40, we performed an *in vitro* cleavage experiment, incubating the recombinant active catalytic domain of human MMP-14 with CM containing Vstat120 (Figure 2.5C). After 1.5 and 18.5 hours of incubation, Vstat120 levels decreased strongly and Vstat40 levels showed a corresponding increase. We conclude that MMP-14 is sufficient to process Vstat40 from BAI1 and is likely a primary mediator of this process in culture and *in vivo*, as we observed that pro and active forms of MMP-14 are abundantly expressed in normal brain tissue in addition to the Vstat40 fragment (Figure 2.5D). While MMP cleavage sites are poorly defined compared with furin cleavage sites, *in vitro* studies have demonstrated that the position and composition of certain amino acids mediates efficiency of MMP-14 proteolytic activity (Turk et al., 2001). In this work, MMP-14 is found to prefer a P1-P1'-P2' motif of Ser-Leu-Arg, where P1 indicates the amino acid directly N-terminal to the cleavage and P1' is the amino acid directly C-terminal to the cleavage. Based on these studies, we predict that MMP-14 cleaves BAI1 into Vstat40 between S_{326} and L_{327}.

Discussion

In the present work we demonstrate that extracellular BAI1 is proteolytically processed to yield at least two secreted fragments of 120 and 40 kDa, respectively named Vstat120 and Vstat40. Expression of wild-type BAI1 in cultured cancer and non-cancer cell lines results in almost exclusive release of Vstat40 into the conditioned medium, showing that Vstat40 production is the predominant default cleavage pathway and the enzymatic machinery for cleavage is constitutively activated in culture conditions. The mechanisms of Vstat40 proteolysis appear to occur independently of Vstat120 processing, and our findings indicate the importance of association of extracellular BAI1 with the cell membrane for Vstat40 cleavage to occur. We have also shown that Vstat40, like Vstat120 and BAI1, is detected in non-tumor human cortical brain tissue and was not observed in randomly-selected specimens of glioblastoma multiforme. Vasculostatin processing and expression is therefore likely to be a physiologically relevant event that is lost during brain tumor formation.

Our findings suggest that Vstat40 generation is the result of a proteolytic signaling cascade, of which the ultimate step is the direct processing of extracellular BAI1 into Vstat40 by MMP-14, and that this proteolysis is facilitated by localization of extracellular BAI1 on the cell membrane. While MMP-14 is expressed on a variety of cell types and tissues, it is strongly upregulated on the surface of glioma cells, where it promotes cancer invasion and progression by degrading multiple components of the extracellular matrix (ECM) and glioma basal lamina (Belkin et al., 2001; Fillmore et al., 2001), and its activity is inhibited by TIMPs 2-4 but not TIMP-1 (Woessner and Nagase, 2000). MMP-14 also activates other MMPs such as MMP-2 and MMP-8 (Holopainen et al., 2003; Itoh et al., 2001). In the present study, we demonstrate that Vstat40 processing decreases concordantly with siRNA-mediated MMP-14

knockdown, and recombinant MMP-14 directly processes Vstat120 into Vstat40 *in vitro*. Small-molecule inhibitors of other MMPs had little effect on this process, suggesting that MMP-14 is the major enzyme cleaving BAI1 into Vstat40. Finally, the MMP-14 inhibitor TIMP-3 appears to play a specific role in inhibiting Vstat40 processing. Furthermore, any tumor- or stromal-derived BAI1 is likely to be processed into Vstat40, given the expression of furin and MMP-14 in normal human brain and that furin and MMP-14 activity is upregulated in aggressive cancers including gliomas (Bassi et al., 2001; McMahon et al., 2005; Mercapide et al., 2002; Sato et al., 1996; Sato et al., 1994).

We further show that proprotein convertase activity is an important mediator of this process through the synergistic inhibition of Vstat40 processing in furin-deficient LoVo cells with PC and MMP inhibitors, although furin does not directly process BAI1 into Vstat40 *in vitro*. Furin activates many proteases including many of the members of the three major metalloproteinase families: the matrix metalloproteinases (MMPs), and the a disintegrin and metalloproteinases/ with thrombospondin motifs (ADAMs/ADAMTSs). Nearly all metalloproteinases of these families contain a minimal consensus Arg-X-X-Arg or Lys-X-X-Arg PC recognition site in their propeptide sequence (Yana and Weiss, 2000). These metalloproteinases are widely implicated in cancer biology and regulation of angiogenesis, often via cleavage of the extracellular domains of cell adhesion molecules (Held-Feindt et al., 2006; Sato et al., 1994). PCs have been shown to directly activate a variety of MMPs, including MMP-14 (Sato et al., 1996; Stawowy et al., 2005; Yana and Weiss, 2000) and regulate the processing of others such as MMP-2 (Cao et al., 2005). Of special relevance, the furin target MMP-14 is still activated in LoVo cells (Deryugina et al., 2004), possibly as a result of autocatalysis, a property which has been demonstrated for this molecule (Rozanov and Strongin, 2003), thus providing an explanation for why Vstat40 processing is not

completely abrogated in this cell type. Alternatively, the members of the PC family have a highly conserved catalytic domain and some overlapping cleavage specificity (Bergeron et al., 2000) and processing of furin target molecules in these cells may result from the activity of other PCs such as PC5A, as has been observed for such furin targets as integrin alpha subunits (Lissitzky et al., 2000) or the gp160 of HIV-1 (Ohnishi et al., 1994).

Vstat40 and likely Vstat120 thus belong to the large group of endogenous angiogenesis inhibitors that are the proteolytic products of parent molecules though as yet, BAI1 is the only GPCR known to undergo proteolysis to release such angioregulatory molecules. Typically, these cleavage fragments derive from a plethora of extracellular matrix proteins (Albini et al., 2010; Mundel and Kalluri, 2007; Rege et al., 2005) notably collagen IV, which is the source of several derivatives including arresten, canstatin, and tumstatin (Colorado et al., 2000; Hamano et al., 2003; Kamphaus et al., 2000). Cryptic inhibitors of angiogenesis may be generated from a variety of non-ECM parent molecules, however, and still more angiogenesis inhibitors are produced via transcription (Bello et al., 2001; Brooks et al., 1998; Morikawa et al., 2000; Rege et al., 2005). This variety of inhibitors and their production mechanisms indicates that maintenance and growth of blood vessels in the body may be regulated in many ways. Production of these potent angiogenesis inhibitors is thus likely to be under tight physiological control, either through the regulation of transcription of the inhibitor itself or of the protease that generates it. Future research will illustrate the significance of Vstat40 proteolysis by MMP-14 with regard both to its function as an angioregulator in the human brain and a mechanism of regulating the activity of BAI1 itself as a cell surface receptor.

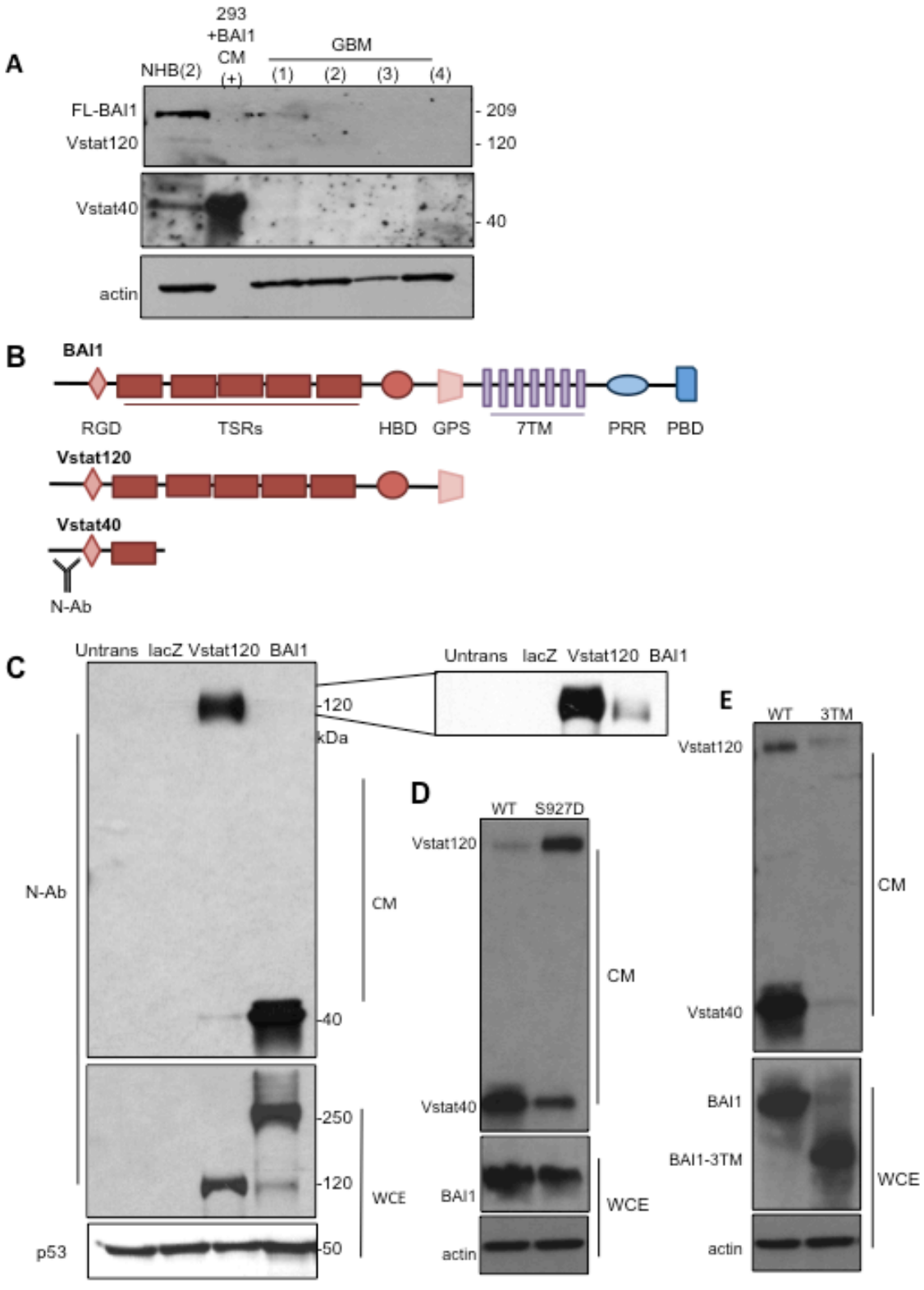
A
293
+BAI1
CM
(+)
NHB(2)
GBM
(1)
(2)
(3)
(4)
FL-BAI1
Vstat120
Vstat40
actin
209
120
40
B
BAI1
RGD
TSRs
HBD
GPS
7TM
PRR
PBD
Vstat120
Vstat40
N-Ab
C
Untrans
lacZ
Vstat120
BAI1
120
kDa
N-Ab
CM
40
250
120
WCE
p53
50
D
WT
S927D
Vstat120
Vstat40
CM
BAI1
WCE
actin
E
WT
3TM
Vstat120
Vstat40
CM
BAI1
BAI1-3TM
WCE
actin

Figure 2.1. Extracellular BAI1 is processed into two secreted fragments, Vstat120 and the 40 kDa fragment (Vstat40).

(**A**) Western blot showing expression of full-length BAI1 and extracellular derivatives in normal human brain cortex (NHB2) and in four randomly-selected specimens of glioblastoma multiforme (GBM) probed with N-Ab. CM from 293 cells transfected with BAI1 used as a positive control for the 40 kDa fragment.

(**B**) Schematic of BAI1 indicating the sizes and pertinent features of the Vasculostatins, and the region of the molecule recognized by the BAI1 N-terminal antibody (N-Ab).

(**C**) Secreted (CM) and intracellular (WCE) BAI1-derived fragments observed by Western blot with N-Ab in 293 cells 24 hours after transfection with plasmids expressing BAI1, Vstat120 alone, or a control vector (lacZ). UT: untransfected control. The inset shows that upon overexposure of the blot low levels of Vstat120 are detected in lane 4.

(**D**) Levels of secreted 120 and 40 kDa fragments following transfection with wild type or Ser927Asp ($S_{927}D$)-mutant BAI1.

(**E**) Levels of secreted 120 and 40 kDa fragments following transfection with wild-type BAI1 or BAI1 expressing the extracellular domain and 3 transmembrane repeats (BAI1-3TM).

Abbreviations: RGD: Arginine(Arg)- Glycine(Gly)- Aspartate(Asp); TSR: thrombospondin type-1 repeat; HBD: hormone-binding domain; GPS: GPCR processing site; 7TM: seven-transmembrane region; PRR: proline-rich region; PBD: PDZ-binding domain. N-Ab: BAI1 N-terminal antibody.

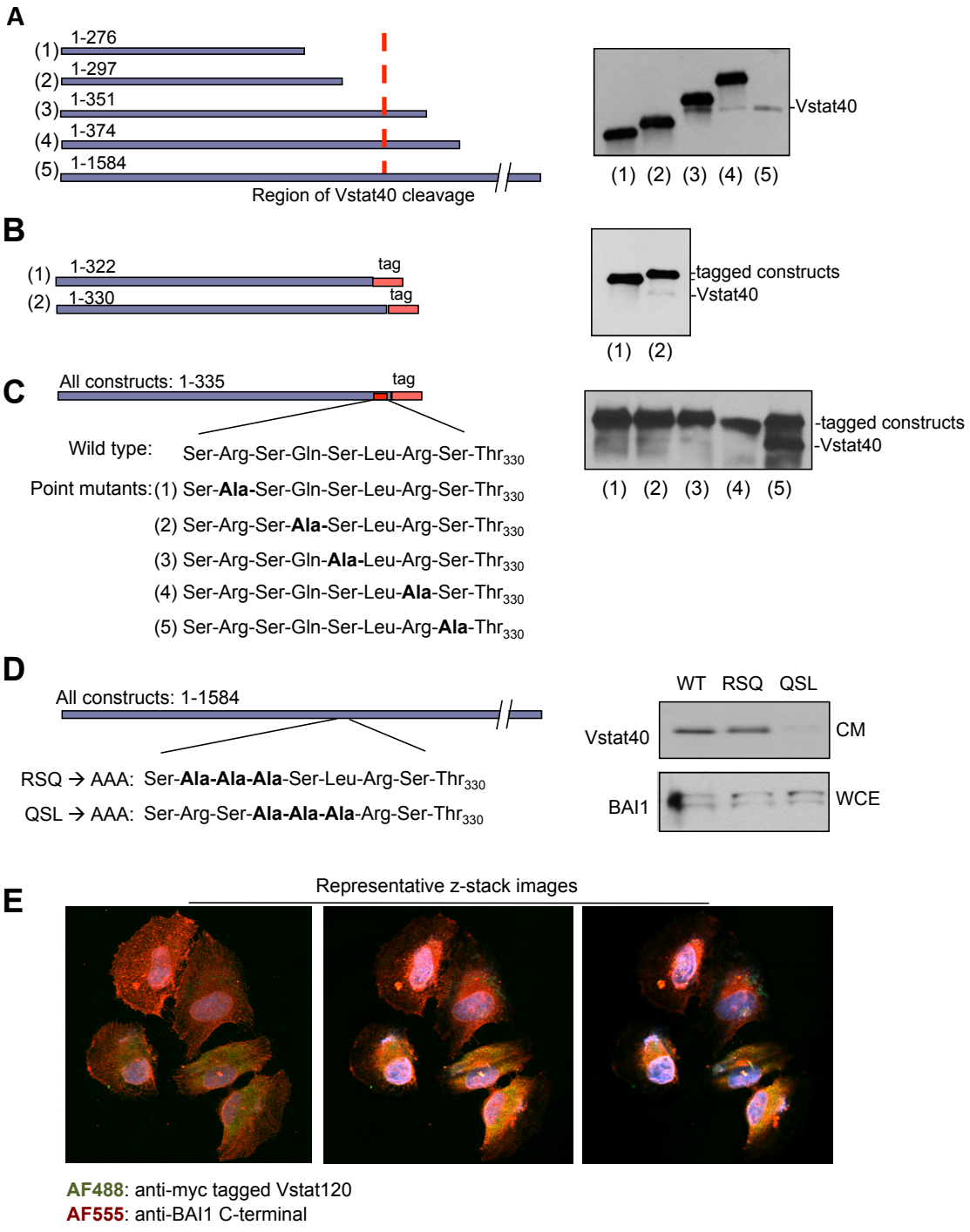
A
(1) 1-276
(2) 1-297
(3) 1-351
(4) 1-374
(5) 1-1584
Region of Vstat40 cleavage
-Vstat40
(1) (2) (3) (4) (5)
B
(1) 1-322 tag
(2) 1-330 tag
-tagged constructs
-Vstat40
(1) (2)
C
All constructs: 1-335 tag
Wild type: Ser-Arg-Ser-Gln-Ser-Leu-Arg-Ser-Thr330
Point mutants: (1) Ser-Ala-Ser-Gln-Ser-Leu-Arg-Ser-Thr330
(2) Ser-Arg-Ser-Ala-Ser-Leu-Arg-Ser-Thr330
(3) Ser-Arg-Ser-Gln-Ala-Leu-Arg-Ser-Thr330
(4) Ser-Arg-Ser-Gln-Ser-Leu-Ala-Ser-Thr330
(5) Ser-Arg-Ser-Gln-Ser-Leu-Arg-Ala-Thr330
-tagged constructs
-Vstat40
(1) (2) (3) (4) (5)
D
All constructs: 1-1584
RSQ → AAA: Ser-Ala-Ala-Ala-Ser-Leu-Arg-Ser-Thr330
QSL → AAA: Ser-Arg-Ser-Ala-Ala-Ala-Arg-Ser-Thr330
WT RSQ QSL
Vstat40
CM
BAI1
WCE
E
Representative z-stack images
AF488: anti-myc tagged Vstat120
AF555: anti-BAI1 C-terminal

Figure 2.2. Identification of the site of Vstat40 processing in extracellular BAI1.

(**A**) Truncated constructs of N-terminal BAI1 cDNA encompassing the indicated amino acids (lanes 1-4) were transfected into 293 cells and the resulting CM harvested after 48 hours for Western blot analysis with N-Ab. CM from cells transfected with BAI1 cDNA was used as a marker for Vstat40 size (lane 5).

(**B**) Additional truncation constructs differing from each other by a few amino acids and expressing a 3-kDa V5/His tag were generated and analyzed to detect Vstat40 processing.

(**C**) An alanine scanning approach using additional tagged constructs was used to identify the relative contribution of selected amino acids in the region of processing to Vstat40 cleavage.

(**D**) Indicated point mutations were introduced into the region of Vstat40 proteolysis in the full-length BAI1 molecule using primer overlap extension. Western blot was used to detect relative levels of Vstat40 processing in wild-type and mutant BAI1 constructs following transient transfection in LN229 glioma cells.

(**E**) Immunofluoresence of LN229-L16-ecb glioma cells expressing myc-tagged Vstat120 following doxycycline administration and transiently transfected with full-length BAI1. Expression of respective proteins was visualized using confocal microscopy, with representative z-stack images shown. Immuofluorescence was performed using anti-myc tag antibody conjugated to AF488 and anti-BAI1 C-terminal with anti-rabbit IgG conjugated to AF555.

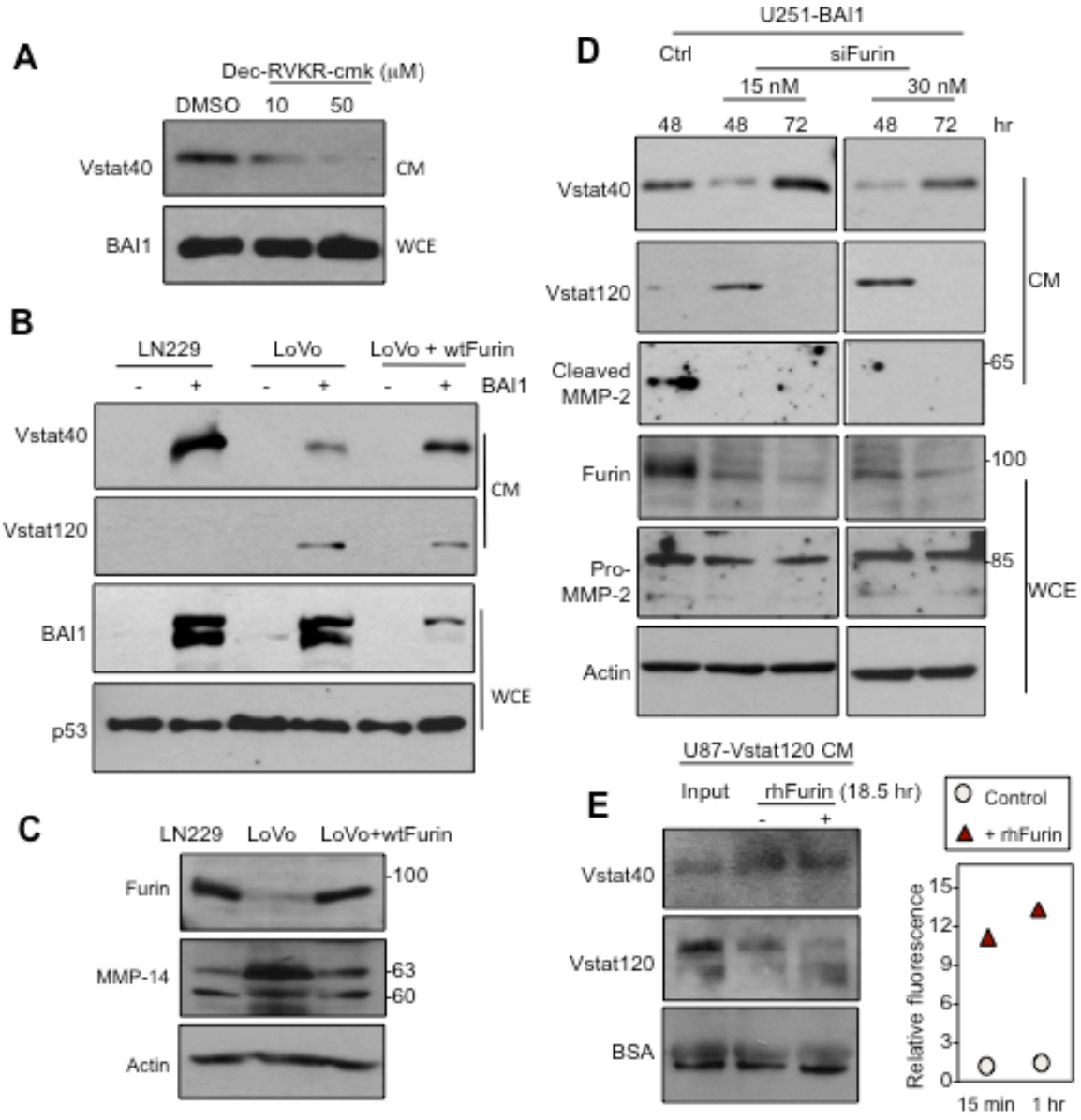
A
Dec-RVKR-cmk (μM)
DMSO 10 50
Vstat40
CM
BAI1
WCE
B
LN229 LoVo LoVo + wtFurin
- + - + - + BAI1
Vstat40
Vstat120
CM
BAI1
p53
WCE
C
LN229 LoVo LoVo+wtFurin
Furin
100
MMP-14
63
60
Actin
D
U251-BAI1
Ctrl siFurin
15 nM 30 nM
48 48 72 48 72 hr
Vstat40
Vstat120
CM
Cleaved MMP-2
65
Furin
100
Pro-MMP-2
85
WCE
Actin
U87-Vstat120 CM
E
Input rhFurin (18.5 hr)
- +
Vstat40
Vstat120
BSA
Control
+ rhFurin
Relative fluorescence
15
12
9
6
3
0
15 min 1 hr

Figure 2.3. Proprotein convertase activity indirectly regulates Vstat40 processing.

(**A**) Western blot showing the dose-dependent inhibition of Vstat40 secretion with the irreversible PC inhibitor dec-RVKR-cmk in the CM of U251 glioma cells stably expressing BAI1 (U251-BAI1: clone B12). Expression levels of BAI1 in the WCE were used as a control.

(**B**) Levels of Vstat40 and Vstat120 in the CM of control LN229 glioma cells, furin-deficient LoVo cells, and LoVo cells stably transfected with wild-type furin cDNA in the presence (+) or absence (-) of transient transfection with a BAI1 expression vector.

(**C**) Western blot showing the levels of furin and pro (63 kDa) and active (60 kDa) MMP-14 expression in the WCE of LN229 and LoVo cells.

(**D**) Levels of secreted Vstats observed in the CM of U251-BAI1 cells after indicated time points following transfection of anti-furin siRNA at a concentration of either 15 or 30 nM. Note that furin levels are strongly downregulated at 48 and 72 hours post-transfection. Levels of secreted cleaved MMP-2 and cellular MMP-2 are used as a control for furin activity.

(**E**) *In vitro* cleavage assay of Vstat120 with rhFurin. Left panel: Western blot with N-Ab was used for detection of peptides processed from Vstat120 by recombinant human furin. Concentrated and buffer-exchanged CM from U87MG cells stably transfected with Vstat120 (U87MG-Vstat120) cells was treated with the catalytically active domain of recombinant human furin for 18.5 hours at 37 ^{o}C. Right panel: To verify the activity of the rhFurin in the CM-buffer solution, the fluorogenic furin substrate was added to the solution -/+ furin and we examined the levels of fluorescence from the cleaved peptide after 15 minutes and 1 hour incubation. The relative fluorescence was calculated by normalizing against background fluorescence of the substrate peptide in furin reaction buffer alone.

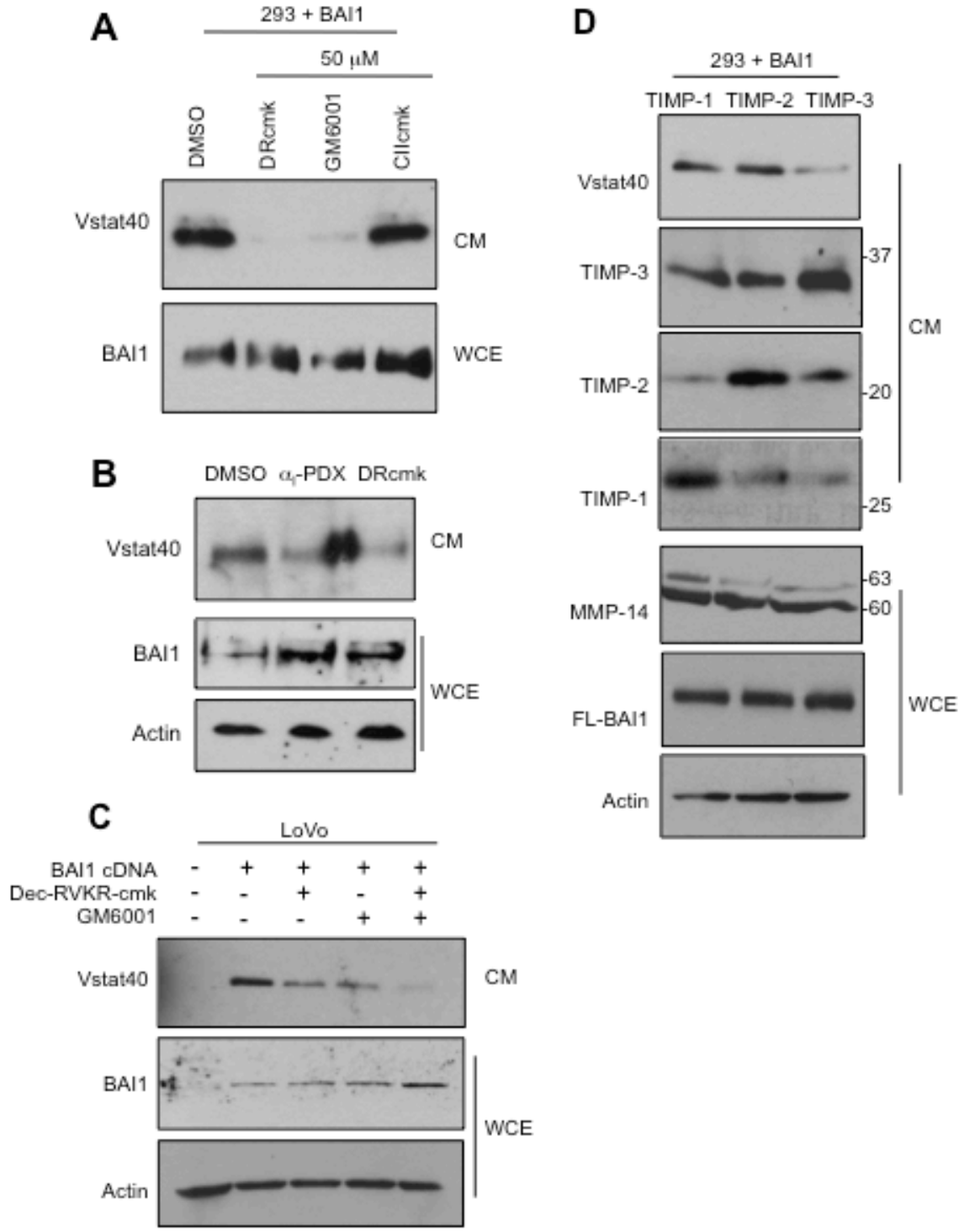
A
293 + BAI1
50 μM
DMSO
DRcmk
GM6001
CIIcmk
Vstat40
CM
BAI1
WCE
B
DMSO
α1-PDX
DRcmk
Vstat40
CM
BAI1
WCE
Actin
C
LoVo
BAI1 cDNA - + + + +
Dec-RVKR-cmk - - + - +
GM6001 - - - + +
Vstat40
CM
BAI1
WCE
Actin
D
293 + BAI1
TIMP-1 TIMP-2 TIMP-3
Vstat40
TIMP-3
TIMP-2
TIMP-1
37
20
25
CM
63
60
MMP-14
FL-BAI1
WCE
Actin

Figure 2.4. Vstat40 is processed from the extracellular domain of BAI1 by a furin-activated metalloproteinase.

(**A**) Levels of secreted Vstat40 in the CM of U251-B12 cells after 12 hours incubation with equimolar (50 μM) dec-RVKR-cmk (DRc) and the general metalloproteinase inhibitor GM6001. Equimolar caspase inhibitor II cmk (CIIcmk) was used as a negative control.

(**B**) Levels of Vstat40 in the CM were analyzed by Western blot following treatment with α1-PDX (20 μM) and dec-RVKR-cmk (50 μM).

(**C**) Expression of Vstat40 in the CM of LoVo cells transiently transfected with BAI1 cDNA and treated with dec-RVKR-cmk and GM6001 (50 μM each) as indicated. All conditions received equal amounts of DMSO.

(**D**) Overexpression of tissue inhibitors of metalloproteinases (TIMPs) 1-3 by transient transfection in BAI1-transfected 293 cells specifically implicates TIMP-3 in the inhibition of Vstat40 processing.

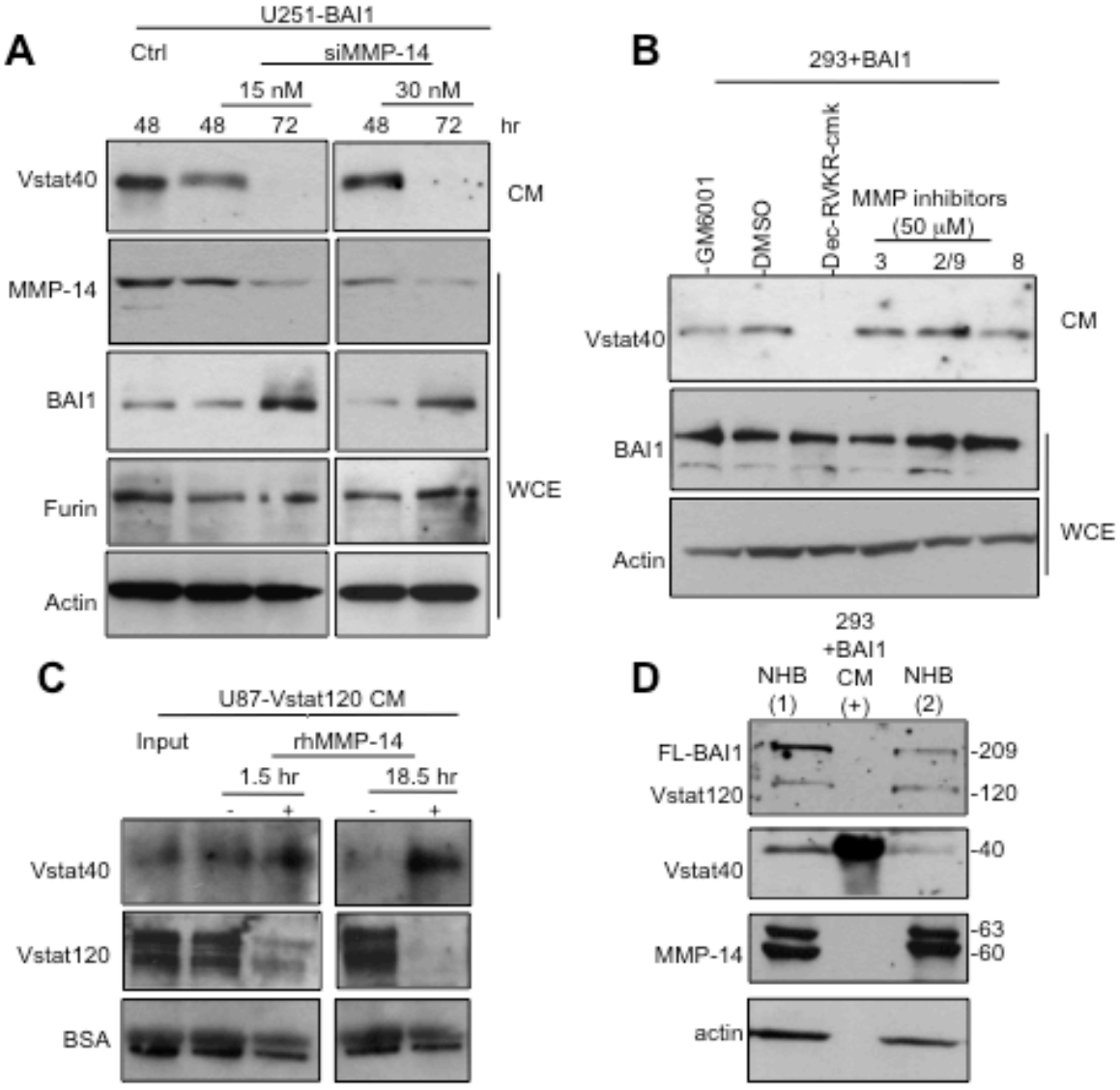
A
U251-BAI1
Ctrl
siMMP-14
15 nM
30 nM
48
48
72
48
72
hr
Vstat40
MMP-14
BAI1
Furin
Actin
CM
WCE
B
293+BAI1
GM6001
DMSO
Dec-RVKR-cmk
MMP inhibitors
(50 μM)
3
2/9
8
Vstat40
BAI1
Actin
CM
WCE
C
U87-Vstat120 CM
Input
rhMMP-14
1.5 hr
18.5 hr
-
+
-
+
Vstat40
Vstat120
BSA
D
293
+BAI1
NHB
(1)
CM
(+)
NHB
(2)
FL-BAI1
Vstat120
Vstat40
MMP-14
actin
-209
-120
-40
-63
-60

Figure 2.5. MMP-14 is the primary enzyme processing BAI1 into Vstat40.

(**A**) Evaluation of secreted Vstat40 and cellular BAI1 levels in response to treatment of U251-BAI1 cells with siRNA against MMP-14 at indicated concentrations, for indicated time intervals.

B) Levels of Vstat40 following treatment of U251-BAI1 cells with specific protease inhibitors against MMP-3, MMP-8 or MMP-2/9 (50 μM).

(**C**) *In vitro* cleavage assay of Vstat120 with rhMMP-14. Concentrated CM of U87MG-Vstat120 cells was buffer-exchanged and incubated with recombinant catalytically active human MMP-14 at 37°C for 1.5 and 18.5 hours. Western blot with N-Ab evidences the relative levels of Vstat40 and 120 peptides following incubation. Note the decrease of Vstat120 levels and the concomitant increase of Vstat40 with rhMMP-14 treatment.

(**D**) Western blot demonstrating expression of BAI1, Vstat120 and Vstat40 along with pro- (63 kDa) and active MMP-14 (60 kDa) in two independent samples of human non-tumor cortical brain tissue (NHB1 & 2), with CM of BAI1-transfected 293 cells used as a positive control for Vstat40 expression.

CHAPTER 3.

VSTAT40 IS A POTENT REGULATOR OF ANGIOGENESIS.

This chapter includes portions of the research for publication by: Cork SM, Kaur B, Cooper L, Saltz JH, Sandberg EM, and EG Van Meir, entitled A furin/MMP-14 proteolytic cascade releases a novel 40 kDa vasculostatin from tumor suppressor BAI1, currently in submission. Some figures from this chapter are here reproduced with permission from the journal from: Kaur B, **Cork SM** et al. (2009). Vasculostatin inhibits intracranial glioma growth and negatively regulates *in vivo* angiogenesis through a CD36-dependent mechanism. *Cancer Research*. **69**(3):1212-20.

Introduction

An improved understanding of the mechanisms by which vascular integrity is compromised remains an important therapeutic goal for many neuropathological diseases, particularly the aggressive brain tumor glioblastoma multiforme (GBM). GBM is characterized by its exuberant vascular proliferation, which is believed to play a major role in its aggressive growth, rapid progression and disease symptoms such as seizures (Brat and Van Meir, 2004). Much interest is accordingly directed at inhibiting GBM-associated angiogenesis, whether via interference with pro-angiogenic signaling or the induction of apoptosis of the endothelial cells comprising the vasculature.

The biology of the angiogenic process is relatively well understood (Adams and Alitalo, 2007). Unlike normal angiogenesis, however, the neovascularization associated with gliomas is highly pathological and interferes with patient progression-free survival in several ways (Fukumura et al., 2010; Gerstner et al., 2009; Jain, 2005). Tumor-associated vasculature delivers oxygen and nutrients to the growing tumor and contributes to malignancy as described in the Introduction. Tumor vessels are also characterized by physiological irregularities which exacerbate glioma patient symptoms, including fenestrations between endothelial cells, which together cause the vasculature to become leaky (Hashizume et al., 2000), ultimately leading to patient edema and seizures or other neurological complications, and also prevents drug delivery to the tumor (Jain, 2005). Stabilization of these angiogenic vessels is thus an important therapeutic goal, in addition to inhibiting their growth.

These abnormalities are due to heterogenous overexpression of pro-angiogenic factors, particularly vascular endothelial growth factor (VEGF) (Machein and Plate, 2000; Machein and Plate, 2004), a powerful regulator of both angiogenesis and vascular permeability. In binding VEGFR2, VEGF destabilizes adherens junctions (AJ) between

endothelial cells (Gavard and Gutkind, 2006; Weis and Cheresh, 2005), leading to extravasation of erythrocytes, plasma, and subsequent edema. AJ are intracellular junctions linking endothelial cells together via homodimeric binding of vascular endothelial (VE) cadherins, which are maintained at the cell membrane by a complex of molecules including p120 and β-catenin (Dejana, 1996; Dejana et al., 1995; Dejana and Del Maschio, 1995; Lampugnani and Dejana, 2007). Disruption of cadherin-cadherin interactions is further shown to promote a proliferative cellular phenotype (Cavallaro et al., 2006; Gottardi et al., 2001), and permits the endothelial cells to migrate in the direction of the pro-angiogenic stimulus. Thus, stabilization of vasculature primarily occurs through the maintenance of AJ at the endothelial cell surface.

Importantly, heterodimeric integrin receptors function as important mediators of AJ stability via direct association with the VEGFR2 (Somanath et al., 2009). Certain integrins, particularly $\alpha_v\beta_3$ and $\alpha_v\beta_5$, are upregulated on certain malignant tumor cells and angiogenic blood vessels and act to regulate the ability of ECs to proliferate and invade into surrounding tissues by binding an Arg-Gly-Asp (RGD) motif on extracellular matrix proteins including vitronectin, laminin and fibronectin. Antagonists of these integrins, including soluble RGD-containing peptides, are known to inhibit tumor-associated angiogenesis and promote survival (Brooks et al., 1994; Brooks et al., 1995; Eliceiri and Cheresh, 2000; Varner and Cheresh, 1996a; Varner and Cheresh, 1996b).

As described previously, BAI1 is classified in the cell adhesion subtype of the class B G protein-coupled receptors (GPCRs), a group of seven-transmembrane proteins characterized by large multidomain N-terminal extracellular domains (ECDs) (Bjarnadottir et al., 2007). The anti-tumor properties of BAI1 are thought to derive from its ECD, which contains five thrombospondin-type 1 repeats (TSRs) in addition to an RGD motif recognized by the $\alpha_v\beta_3$

and $\alpha_v\beta_5$ integrins. Among the best-understood properties of TSRs is their ability to inhibit angiogenesis, a mechanism demonstrated for thrombospondin-1 (TSP-1) in which a Cys-Ser-Val-Thr-Cys-Gly (CSVTCG) sequence in certain TSRs engages the CLESH domain of the CD36 receptor on endothelial cells and initiates a caspase 3-mediated pro-apoptotic signaling cascade (Jimenez et al., 2000). TSRs also inhibit angiogenesis through their heparin-binding Trp-Ser-Pro-Trp (WSPW) motifs by competing for VEGF attachment to heparin sulfate on the surface of endothelial cells (Gupta et al., 1999) and interfering with heparin's growth factor-stabilizing activity (Vogel et al., 1993). Another significant angio-regulatory feature of TSRs is a Gly-Val-Ile-Thr-Arg-Ile-Arg (GVITRIR) motif, which strongly inhibits endothelial proliferation and serves the basis for the therapeutic peptide ABT-510 (Zhang and Lawler, 2007). However, not all TSRs have anti-angiogenic activity (Tolsma et al., 1993), and not all TSR-containing proteins regulate angiogenesis (Nicholson et al., 2005).

The TSRs in BAI1 appear to serve different functions which may depend on cell type. In full-length BAI1, they act as binding motifs for phosphatidylserine (PtdSer) on the surface of apoptotic cells and mediate their engulfment by macrophages (Park et al., 2007). Other research suggests that at least some BAI1 TSRs can regulate angiogenesis. Early work demonstrated that exogenous synthetic peptides containing BAI1 TSRs 2-4 and 3-5 could inhibit rabbit corneal angiogenesis (Nishimori et al., 1997), but the activity of the first BAI1 TSR is unknown. Notably, the first BAI1 TSR lacks a VTCG sequence, but contains WSXW and GXXTRXR motifs.

Vasculostatin-40 (Vstat40), the primary known secreted fragment of the BAI1 extracellular domain, contains both the RGD motif and one TSR. The presence of the TSR suggests that Vstat40 might function to inhibit angiogenesis via the induction of endothelial cell apoptosis. The presence of the RGD motif indicates that Vstat40 may act to inhibit

angiogenesis either by competing with mechanisms of EC-ECM attachment or promote vascular quiescence by interfering with integrin-VEGFR2 interaction and subsequently inhibit vascular permeability. In the following series of experiments, we investigate the anti-angiogenic activity of Vstat40 with respect to these questions to determine its potential as a therapeutic.

Materials and Methods

Cell culture. HDMECs and HUVECs were obtained from the Emory University Dermatology Core facility and cultured in EBM-2 medium (Lonza) supplemented with growth factors, and used between passages 2-6. LN229 glioma cells (Ishii et al., 1999) and derivatives were cultured in DMEM with 10% fetal bovine serum (FBS) and antibiotics and passaged every 2-4 days. To maintain selection of stably transfected constructs, LN229-L16 cells were maintained with 2 μg/mL puromycin and clone LN229-L16-ecb and clone LN229-L16-17 were maintained with 2 μg/mL puromycin and 400 μg/mL geneticin (G418; Invitrogen).

Conditioned medium used in experiments was prepared from indicated cell lines for angiogenesis assays as described in Chapter 2 and the Appendix. Briefly, CM used in angiogenesis assay experiments was prepared from parental LN229-L16 (control), LN229-L16-ecb (Vstat120) and LN229-L16-17 (Vstat40) cells. Both parental and clone cell lines were washed and incubated with serum-free culture medium containing doxycycline (2 μg/mL) for 48 hours to collect CM. For all experiments, CM was harvested under sterile conditions after 48 hours unless otherwise indicated and centrifuged at 6000xg for 15' to remove floating cells. CM was concentrated using an Amicon Ultra concentrator (5 kDa MWCO) approximately 30x to a final volume of 500 μL and used at approximately 1x in experiments.

Angiogenesis assays: In the modified Boyden chamber migration assays (Kaur et al., 2009), HDMECs and HUVECs were serum-starved overnight, then trypsinized and counted. Cell suspensions in serum-free endothelial culture medium were divided and combined with concentrated control CM or CM containing Vstat40 or Vstat120. Cells were plated in triplicate at a density of 50,000 cells/chamber in the top well of Transwell chambers (Becton

Dickinson Labware # 353097) with a pore size of 8 μm. Complete medium containing 10% serum was used as a chemo-attractant in the bottom chamber, and cells were allowed to migrate for 10 hours, after which time unmigrated cells on the top side of the membrane were removed with a Q-tip and migrated cells were fixed and stained (Diff-Quik, Dade Behring). Migrated cells were quantified by counting six 20x microscopic views/condition and the data presented as the means of counts from three membranes.

In the scratch wound assay (Kaur et al., 2009), confluent HDMECs were serum-starved overnight, then wounded with a 10 μL pipet tip and detached cells washed off with PBS. Cells were then treated with control or Vstat-containing CM at a final concentration of 1x in endothelial culture medium with or without an anti-CD36 function-blocking antibody at a concentration of 10 μg/mL (FA6-152, Cell Sciences) or equimolar treatment with a control antibody (mAb against p53, Santa Cruz). Cells were allowed to recover in 10% serum and migrate for 8 hours, followed by fixation, staining and analysis of scratch wound closure.

In the matrigel assay, HDMECs and HUVECs were serum-starved overnight, then seeded into 24-well plates at a density of 50,000 cells/well in complete endothelial medium containing 1x control or Vstat-containing CM. Wells were precoated with 250 μL of Matrigel and cells were plated in triplicate for each condition. HDMECs were allowed to recover overnight, then imaged to determine the formation of endothelial tubes. Formation of endothelial cords and enclosed structures was quantified with three views per well at 10x magnification.

The quantitative directed *in vivo* angiogenesis assay (DIVAA; Trevigen, Catalog # 3450-048-K) was performed according to the manufacturer's instructions. Briefly, basement membrane extract was thawed and prepared with VEGF (0.5 ng/ mL), bFGF (1.5 ng/mL) and heparin (100 ng/mL). The extract was then divided and mixed with concentrated CM

(20 μL CM per 200 μL of extract). Provided "angioreactor" tubes were filled with 20 μL of extract, with care taken to avoid air bubbles in the gel and the formation of a meniscus at the open end. Tubes were inverted and incubated at 37°C for an hour to promote solidification of the gel. 9-week old female nude mice (Harlan) were anesthetized with intraperitoneal injection of ketamine/xylazine and subcutaneously implanted with prepared tubes. Mice were sacrificed with CO_2 after twelve days and tubes excised and photographed. Gel was removed from the tubes and a single-cell suspension formed. Suspensions were incubated in 10% FBS-containing culture medium for 1 hour at 37°C to promote recovery of cell-surface molecules including glycoproteins. The kit provides FITC-lectin, *Griffonia simplicifolia* (Bandeiraea) isolectin B4 (IB4), which recognizes terminal α-galactosyl residues on endothelial glycoproteins. Cells were washed, pelleted and incubated overnight at 4°C with the prepared FITC-lectin solution. After incubation, cells were washed extensively and resuspended in provided wash buffer. FITC fluorescence was quantified using a fluorometer at 485 nm excitation and 538 nm emission. Graphed data derive from two independent experiments.

Statistical analysis: Two-tailed Student's t-test (assuming equal variance) for all angiogenesis assays was conducted using Excel software (Microsoft).

In vitro vascular permeability. To ascertain the effects of Vstat40 on VEGF-induced changes in VE-cadherin, indicated endothelial cells were obtained from the Emory Core and plated in 6-well plates (Corning) to achieve complete confluence. Cells were starved overnight prior to pretreatment with 1x control or VEGF-containing CM for 30 minutes, followed by treatment with rhVEGF-165 (Cell Signaling Technology, Catalog #8065), used at 10 ng/mL. Cells were lysed after indicated time points and centrifuged at 4 degrees to obtain a pellet of

cellular membrane material. Pellets were resuspended in 1x sample buffer, sonicated and boiled for Western blot analysis.

For an assay of Vstat40's effects on functional vascular permeability, a transwell kit was used (Millipore). Briefly, HDMEC were trypsinized at passage 3 and seeded in transwell inserts (50,000 cells/well). Cells were allowed to become confluent over 48 hours. Cells were pretreated with control or Vstat40-containing CM for 30 min and VEGF (10 ng/mL) for 18 hr per manufacturer's instructions. Conditions were performed in triplicate. After the incubation period, medium was removed and a FITC-dextran solution placed in the upper well of the chamber. Medium containing FITC-dextran that permeated the monolayer and insert was collected from the bottom part of the chamber after 5 minutes and its fluorescence analyzed at 485 nm excitation / 538 nm emission values.

In vivo vascular permeability. 9-week old female nude mice were intracranially implanted with 10^6 LN229-L16-17 cells as part of a larger tumorigenesis experiment (please see Chapter 4). Three mice in the *in vivo* vascular permeability substudy received doxycycline (2 mg/mL) in drinking water with 4% sucrose to induce expression of Vstat40, while three control mice received water and sucrose. After approximately two months of tumor growth under these conditions, the mice were weighed to confirm equivalent subject weight and overall health levels in the two conditions, then anesthetized with ketamine/xylazine and injected in the tail vein with an Evans blue dye solution (Sigma; used at 30 mg/kg). Subjects were kept warm on a heating pad and monitored for recovery. After 24 hours, subjects were humanely sacrificed with CO2 asphyxiation and their brains immediately dissected and photographed. Brains were homogenized and suspended in dimethylformamide to extract the EBD leached through the permeabilized tumor vasculature. After 24 hours at room temperature, extracts

were centrifuged and fluorescence of the supernatant analyzed using a fluorometer at 540 nm excitation and 680 nm emission.

Western blot. Western blot was performed on both CM and WCE samples as indicated. Serum-free CM was collected after 12-24 hours as indicated and either precipitated with 50% TCA or 4 volumes of ice-cold acetone. Precipitated CM pellets were resuspended by extensively washing collection tubes in 100-150 μL 1x sample buffer. Following CM collection, cells were washed 2x with PBS and WCE was collected in 150-250 μL 1x sample buffer containing SDS and b-mercaptoethanol, sonicated and boiled 2 minutes. Samples were immediately loaded on 10% Criterion precast gels (BioRad) and electrophoresed for 2 hours at 100 volts at room temperature. Separated proteins were transferred to nitrocellulose membranes at 47 volts for 3.5 hours at 4 degrees Celsius. Membranes were blocked for at least 1 hour in fresh 5% PBST-milk solution and incubated with primary antibody overnight at 4 degrees. Antibodies used include: the BAI1 N-terminal antibody N-Ab (#14933 (Kaur et al., 2003), 1:1000); MMP-14 (ab38971) and TIMP-3 (ab66022) (Abcam, 1:1000); monoclonal antibodies to TIMP-1 and -2 (Calbiochem Cat No.s IM32 and IM11, 1:1000); p53 and actin (Santa Cruz; 1:2500); furin (MON-152 monoclonal antibody; 1:500).

Immunohistochemistry. For each tissue type, specimens were snap-frozen and sectioned at 7 microns on a cryostat. Briefly, sections were blocked for 10 min with a universal serum blocking solution (Dako #X0909), then incubated with primary antibodies either at room temperature for 2 hours or at 4 degrees overnight. Primary antibodies were diluted to 1:20 in an antibody diluent (Dako #S3022); anti-CD36 (mouse monoclonal FA6-152, Santa Cruz #sc-52645) and anti-Factor VIII (rabbit polyclonal Labvision/ThermoFisher, #RB281A) were used. Between incubations, sections were washed 3x 3 min with 1% BSA in PBS. Specimens were incubated with respective secondary

antibodies diluted 1:200 (anti-mouse IgG conjugated to Alexa fluor 488, Invitrogen #A31620; anti-rabbit IgG conjugated to Alexa fluor 594, Invitrogen #A31632) at RT for 1 hr. Specimens were mounted with Prolong Gold antifade reagent with DAPI (Invitrogen #P36931) and imaged at 20x magnification.

Results

Vstat40 inhibits endothelial cell migration in culture in a CD36-dependent manner. We wished to determine whether, like Vstat120, Vstat40 is a bioactive molecule able to inhibit angiogenesis in standard culture assays. We first collected and concentrated Vstat40 and Vstat120 from the CM of stably transfected inducible LN229-L16 glioma cell lines to verify selective expression of desired peptides (Figure 3.1A). Concentrated CM from untransfected parental LN229 cells was used as a control. Next, we verified relative expression levels of the CD36 receptor on the endothelial cell lines under study, human dermal microvascular endothelial cells (HDMECs) and human umbilical vein endothelial cells (HUVECs) (Figure 3.1B). We verified that this receptor is expressed at much higher levels on HDMECs than on HUVECs, as previously reported. In contrast to previous reports, however, a minimal level of CD36 was detected in HUVEC lysate. While these results prevent an ideal comparison of HDMECs and HUVECs as CD36-expressing and CD36-null cells, we hypothesize that any effect of TSR-CD36 interaction will be amplified in cells expressing higher levels of the receptor. We previously showed that Vstat120 was a potent inhibitor of the migration of human endothelial cells, specifically human brain-derived microvascular endothelial cells, in a modified Boyden chamber assay (Kaur et al., 2009).

We thus investigated whether CD36 expression on endothelial cells is necessary for the anti-angiogenic activity of Vstat40 by testing to see if an anti-CD36 function-blocking antibody would rescue migration of HDMECs in the presence of Vstat40. The migration of wounded confluent HDMECs was significantly inhibited in the presence of Vstat40 or Vstat120-containing CM, compared with migration of HDMECs incubated in control medium (Figure 3.1C). The antibody completely neutralized the inhibitory effect of Vstat40 and Vstat120 on EC migration, while an isotypic control antibody had no effect. These

results indicate that the Vstat40 and Vstat120 TSRs are interacting with the CD36 receptor to inhibit angiogenesis. We subsequently performed a Boyden chamber assay to determine whether Vstat40 was similarly able to inhibit the migration of endothelial cells, using CD36+ human dermal microvascular endothelial cells (HDMECs) and CD36-deficient human umbilical vein endothelial cells (HUVECs) (Kaur et al., 2009) (Figure 3.1D). Treatment of cells with Vstat-containing CM significantly inhibited the serum-induced migration of the HDMECs but not the migration of HUVECs. These results support the hypothesis that CD36 acts as a primary mediator of the Vstats' anti-angiogenic activity, but do not preclude a role for other differentially-expressed receptors on these cells as targets of Vstat40.

As mentioned previously, the TSR-CD36 association is believed to promote apoptosis in endothelial cells. We thus wished to determine whether Vstat40 treatment would lead to HDMEC apoptosis, particularly through the upregulation of cleaved caspase 3. To this end, lysates of cells treated for 72 hours with control or Vstat40-containing CM or recombinant thrombospondin-1 (2 μM) were analyzed for their levels of cleaved caspase 3 and the pro-apoptotic protein Bax (Figure 3.1E). Lysates of HDMEC treated with staurosporine were used as a positive control for cleaved caspase 3 induction. We observed that, while levels of the pro-caspase 3 protein were decreased slightly in the Vstat40 and TSP1 treatment conditions, no bands corresponding to the 19 and 17-kDa cleaved fragments were observed under either condition. However, a modest increase was observed in the levels of Bax, a mitochondrial protein regulating the release of cytochrome c. It should be noted that these results do not conclusively show that Vstat40 does not promote apoptosis in any type of endothelial cells or at any concentration of the peptide. Further experiments are necessary to more conclusively elucidate the Vstats' pro-apoptotic capabilities.

The Vstats interfere with endothelial cord formation. We next used an endothelial cord formation assay to determine whether Vstat40 interferes with events in the process of angiogenesis in addition to the migration of endothelial cells. The endothelial cord formation assay recapitulates the 3-dimensional formation of blood vessels in a Matrigel matrix. HDMECs formed tube-like structures when plated on matrigel in control medium, which were observed to attach to nodes of endothelial cells, frequently leading to the formation of enclosed ring-like structures (Figure 3.2A). Incubation with Vstat40 yielded significantly fewer cords and enclosed structures, while few cords and no enclosed structures were observed in HDMECs incubated with Vstat120. In contrast, the presence of Vstats in the CM did not have a significant effect on cord or enclosed structure formation of HUVECs plated under the same conditions. However, it is unclear whether this effect is dependent on CD36 or some other biological difference across the cell types.

Vstat40 inhibits angiogenesis *in vivo*. We investigated whether Vstat40 interfered with biological angiogenesis using a quantitative *in vivo* angiogenesis model (Guedez et al., 2003). We observed differential levels of hematocyte-containing vascularization in angioreactors filled with basement membrane extract prepared with CM containing Vstat40 compared to vascularization in extracts containing control CM (Figure 3.2B, left panel). Vessels were extracted and incubated with FITC-lectin as described for a more quantitative analysis of vascularization. We observed that angiogenesis was decreased in vessels extracted from Vstat40- or Vstat120-containing angioreactors versus control ($p=0.011$ and 0.008, respectively) (Figure 3.2B, right panel). These data support the hypothesis that, like Vstat120, Vstat40 is a biologically active inhibitor of angiogenesis *in vivo* and may be useful as a therapeutic for diseases characterized by a pathological overabunance of vasculature.

To investigate the potential of Vstats to regulate angiogenesis in the brain, we wished to determine whether the CD36 receptor was indeed present in the brain vasculature of both mice and humans. Immunohistochemistry was performed to demonstrate co-localization of CD36 and Factor VIII in wild-type adult mouse brain (Figure 3.3A), non-tumor human brain (Figure 3.3B, specimen #01-89) and human glioblastoma (Figure 3.3C, specimen #04-20). These results show that CD36 is expressed in the normal brain vasculature of both mice and humans, as well as human tumor-associated blood vessels, and thus the biological activity of the Vstats mediated by the C36 receptor is likely to affect these vessels. As a result, the use of Vstats as anti-angiogenic agents in either system is biologically founded.

Vstat40 interferes with VEGF-induced vascular permeability. As described previously, a significant early step in the induction of angiogenesis is the VEGF-induced breakdown of adherens junctions between endothelial cells. This process is complex and mediated by VEGFR2-integrin coactivation and upregulation of specific signaling pathways (summarized in Figure 3.4), most notably activation of Src and Rac leading to recruitment of β-arrestin and displacement of β-catenin at adherens junctions, leading to increased vascular permeability. We wished to determine whether Vstat40 could function as an anti-permeability agent, most likely through the prevention of VEGF-induced destabilization of adherens junctions. We observed that treatment of HUVEC with VEGF led to a prolonged decrease in expression of VE-cadherin by 6 hours after treatment (Figure 3.5A, left panel). A similar finding was observed for HDMEC (data not shown). Pretreatment with Vstat40-containing but not control CM somewhat rescued VE-cadherin expression after 18 hours (Figure 3.5A, right panel). In keeping with these findings, we observed that VE-cadherin was maintained at intercellular contacts between endothelial cells in response to VEGF treatment only when cells were pretreated with CM containing Vstat40 (Figure 3.5B). To test whether

maintenance of VE-cadherin corresponded to a decrease in vascular permeability, we performed a similar experiment using confluent HDMECs in a modified Boyden chamber apparatus. Significantly less FITC-conjugated dextran was observed to leak through VEGF-stimulated cells that had been pretreated with Vstat40 (Figure 3.5C). We conclude that Vstat40 inhibits VEGF-induced vascular permeability via the maintenance of adherens junctions.

To determine whether Vstat40 might interfere with vascular permeability *in vivo*, a limited sample of subjects bearing control and Vstat40-expressing xenografts (n=3 per group; clone 17 tumors, described in Chapter 4) received tail-vein injections of an Evans blue dye (EBD) solution. Analysis of EBD extravasation in subjects' brain tissue subsequently showed significantly reduced levels of dye in Vstat40-expressing tumors (Figure 3.6A-B). However, other followup analysis shows that overall tumor vascularization is reduced in these Vstat40-expressing tumors, while subject weight did not differ significantly between the two groups (Chapter 4). In tumorigenesis experiments, subject weight may be used as a rough proxy for subject health, which is affected by tumor burden. We tentatively conclude that Vstat40 inhibits permeability *in vivo*, but until tumor size is definitively quantified, these preliminary results cannot be disentangled from the overall reduced tumor vascularization resulting from Vstat40 overexpression.

Discussion

In the present work, we show that Vstat40, like BAI1 and Vstat120, is a potent inhibitor of angiogenesis and that its activity is mediated by the CD36 receptor. Previous work identified that the anti-angiogenic mechanism of Vstat120 derived from its interaction with the CD36 receptor, presumably via binding its TSRs as has been shown for thrombospondin-1 (TSP1). Vstat40 contains a single TSR with features similar to those known to regulate angiogenesis in other molecules that contain TSRs, and it also contains an RGD integrin-binding motif, which has been shown to inhibit angiogenesis under certain conditions (Brooks et al., 1994; Gutheil et al., 2000). Our results indicate that the TSR of Vstat40 is responsible for at least a significant portion of its anti-angiogenic activity.

Many secreted endogenous angiogenesis inhibitors are the proteolytic products of parent molecules, typically cleavage fragments of extracellular matrix proteins. BAI1 is unique in that it is the only class B GPCR known to release such potent anti-angiogenic fragments. Vstat40 processing and the regulation thereof are very likely to have implications both for angiogenesis and the function of the full-length BAI1 molecule including the intracellular signaling cascades mediated by its C-terminal domain. For example, macrophage-expressed BAI1 recognizes phosphatidylserine (PtdSer) on the surface of apoptotic cells via TSR binding and promotes target engulfment by the macrophage via Rac activation by its C-terminal domain (Park et al., 2007), and it is likely that BAI1 ECD proteolysis would affect such functionality. The observation that the BAI1 ECD is processed into secreted fragments with anti-angiogenic activity suggests that this portion of the molecule may have different functions in different cell types and environments and thus its processing is likely to be a complex and tightly-regulated event. While the present research demonstrates

the anti-angiogenic activity of Vstat40, further studies will more completely elucidate the functional significance of its generation, particularly in tumorigenesis.

One important direction for future research is characterizing the association between the Vstat40 RGD motif and integrins. Integrins are well-known to activate diverse pro-survival intracellular signaling pathways, but can promote apoptosis if not bound to immobilized ligands (Stromblad and Cheresh, 1996; Stupack and Cheresh, 2002; Stupack et al., 2001). As mentioned previously, these integrins bind ECM proteins containing an exposed Arg-Gly-Asp (RGD) sequence to promote EC attachment. Soluble RGD-containing peptides and RGD-blocking antibodies compete with integrin-ECM interaction to induce EC detachment and apoptosis and inhibit tumor-associated angiogenesis (Brooks et al., 1995; Buerkle et al., 2002; MacDonald et al., 2001; Maubant et al., 2006; Sudhakar et al., 2003), and notable anti-tumor therapeutics such as Cilengitide and Vitaxin are designed around this concept (Gutheil et al., 2000; Nabors et al., 2007).

Notably, integrins mediate VEGF-induced Src activation, leading to AJ destabilization in ECs (Wang et al., 2006). Significant recent attention has been given to the role of integrins, particularly $\alpha_v\beta_3$, as critical regulators of VEGFR2 signaling. The interaction is complex and bidirectional, as growth factor signaling also potentiates integrin activation (Byzova et al., 2000; Kuwada and Li, 2000). Other growth factor-integrin relationships have been indentified, as $\alpha_5\beta_1$ mediates EC proliferation via EGFR activation (Kuwada and Li, 2000), indicating the prevalence and importance of these interactions in the regulation of cellular activity. AJ destabilization remains one of the best-characterized events leading to vascular permeability and angiogenesis, and has many important consequences, including the release of the transcriptional coactivator β-catenin into the cytosol (Ilan et al., 2003). VEGF-mediated dysregulation of cadherin function is observed to lead to subsequent

transcriptional upregulation of β-catenin targets (Behrens et al., 1993; Gottardi et al., 2001; Reiss et al., 2005) and upregulation of the angiogenic switch and metastatic progression in non-small cell lung cancer (Ceteci et al., 2007). Of note, VEGF activates multiple pathways to regulate vascular permeability, including upregulation of endothelial NOS and inflammatory mediators such as platelet activating factor (PAF) (Bernatchez et al., 1999; Brkovic and Sirois, 2007; Gelinas et al., 2002), and disruption of tight junction stability via PKC-mediated phosphorylation of occludin (Harhaj et al., 2006).

These previous experiments provide many possible avenues for the exploration of Vstat40 function as both an anti-angiogenic and an anti-permeability agent, though distinguishing between these functions may prove a challenge, particularly in *in vivo* tumorigenesis assays. To disentangle anti-angiogenic and anti-permeability effects of Vstat40, future research may wish to consider molecular analyses of adherens junction stability on the surface of tumor vasculature, indicating the stability of VE-cadherin/β-catenin complexes in response to Vstat expression.

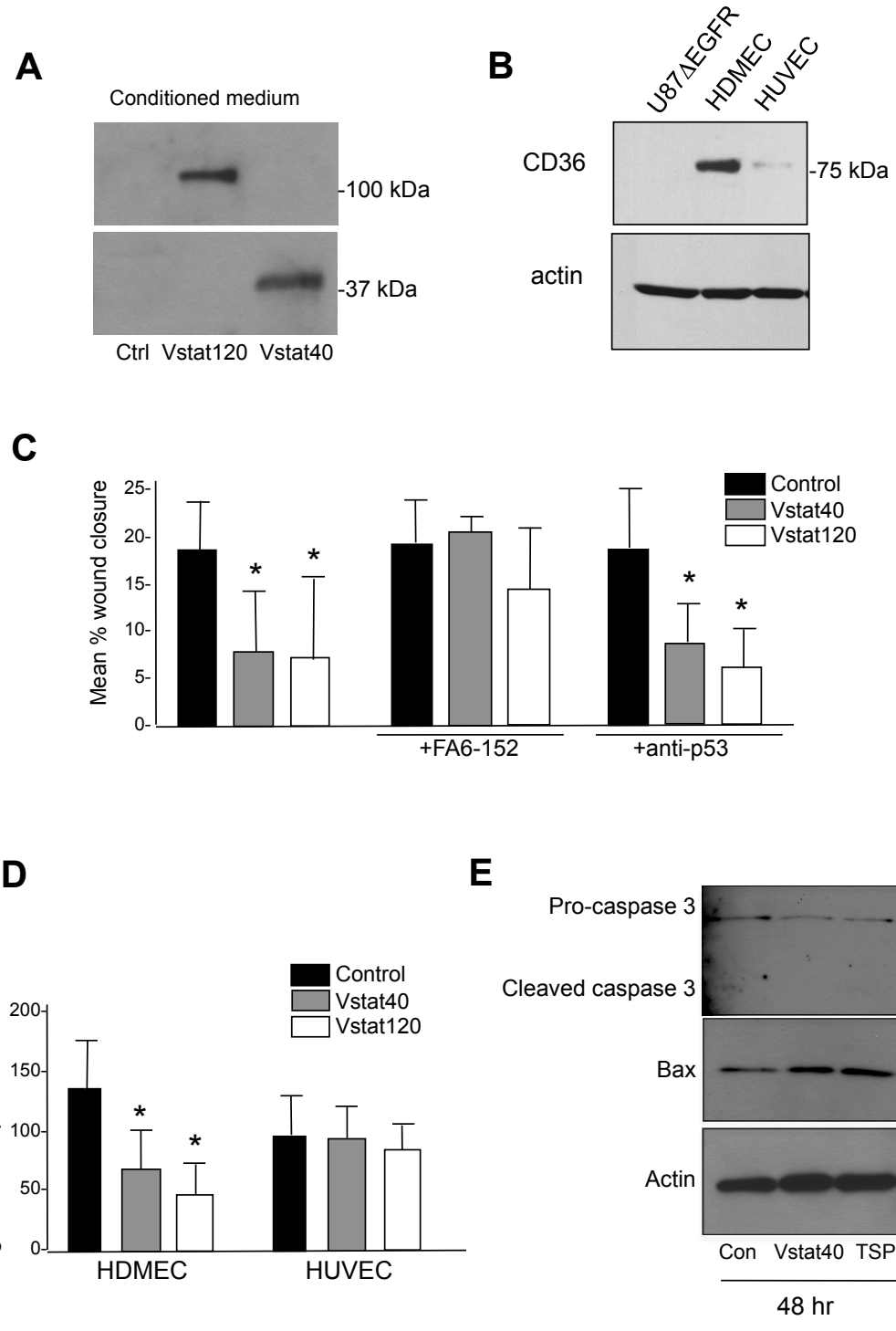
A
Conditioned medium
-100 kDa
-37 kDa
Ctrl Vstat120 Vstat40
B
U87ΔEGFR
HDMEC
HUVEC
CD36
-75 kDa
actin
C
Mean % wound closure
25-
20-
15-
10-
5-
0-
Control
Vstat40
Vstat120
*
+FA6-152
+anti-p53
D
Migrated cells per view field
200-
150-
100-
50-
0-
Control
Vstat40
Vstat120
HDMEC
HUVEC
E
Pro-caspase 3
Cleaved caspase 3
Bax
Actin
Con Vstat40 TSP1 Ssprn
48 hr
8 hr

Figure 3.1. Vstat40 is anti-angiogenic in culture.

(**A**) Representative Western blot of concentrated conditioned media (CM) demonstrating relative levels of the Vstats used in angiogenesis experiments. CMs prepared from parental LN229-L16 glioma cells (control) or LN229-16 cells stably transfected with respective inducible Vstat vectors.

(**B**) Verification of CD36 expression in selected cell types. Western blot demonstrating the relative levels of CD36 on HDMECs and HUVECs as well as a tumor cell type (U87MG derivative).

(**C**) Endothelial migration scratch wound assay. The ability of an HDMEC monolayer to close a scratch wound after 10 hours was measured in the presence of control or 1x Vstat-containing CM. The role of CD36 was tested by pretreating HDMEC scratches with anti-human CD36 function-blocking antibody (clone FA6-152; 10 μg/mL) or an isotypic control antibody (p53; 10 μg/mL) for 30 minutes prior to incubation with control or Vstat-containing CM.

(**D**) Boyden chamber migration assay. The relative migration of CD36-expressing HDMECs and CD36-deficient HUVECs towards serum-containing medium in a Boyden chamber assay was quantified following 10 hours of incubation with control or Vstat-containing CM in the top compartment of the chamber.

(**E**) Western blot illustrating the ability of Vstat40 to promote apoptosis. Western blot representing HDMEC lysate following treatment with control or Vstat40-containing CM or TSP-1 (2 μM) for 48 hours or staurosporine (500 nM) for 8 hours, demonstrating relative levels of pro-apoptotic proteins cleaved caspase 3 and Bax.

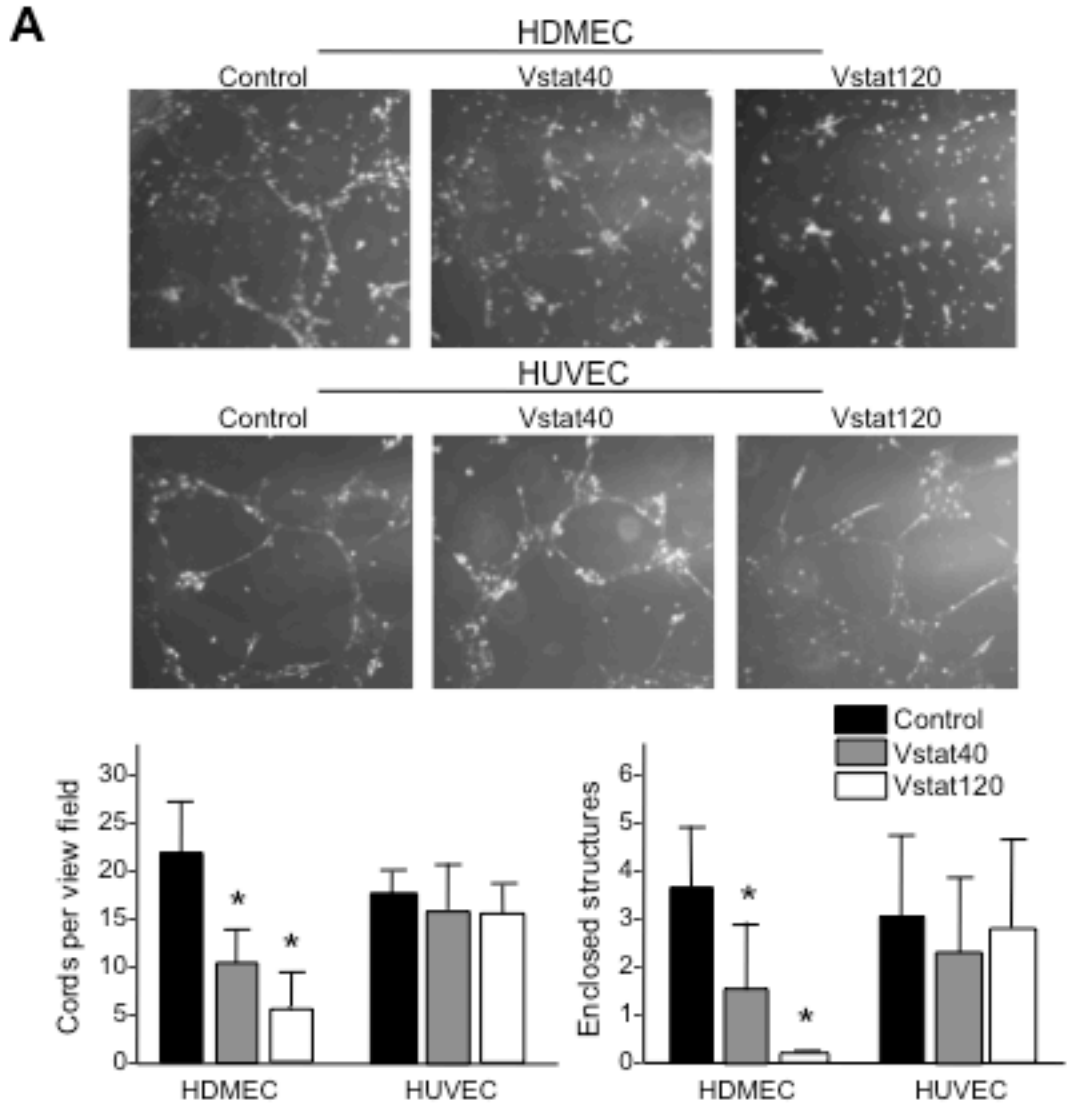
A
HDMEC
Control
Vstat40
Vstat120
HUVEC
Control
Vstat40
Vstat120
Cords per view field
30
25
20
15
10
5
0
HDMEC
HUVEC
Enclosed structures
6
5
4
3
2
1
0
HDMEC
HUVEC
Control
Vstat40
Vstat120
B
Control
Vstat40
Relative fluorescence
20
18
16
14
12
10
8
0
Control
Vstat40
Vstat120

Figure 3.2. Vstat40 inhibits cord formation and neovascularization *in vivo*.

(**A**) *In vitro* vascular tube formation assay. The formation of endothelial cords and enclosed tube-like structures by HDMECs or HUVECs at passage 3 plated in matrigel with either control CM or CM containing either Vstat40 or Vstat120 was quantified.

(**B**) Quantitative *in vivo* angiogenesis assay using angioreactors containing control or Vstat40 CM, implanted subcutaneously in nu/nu mice. (Left) Images are shown representing vascularization of angioreactors containing either control or Vstat40-containing CM excised twelve days after implantation. (Right) The graph shows fluorescence of cell pellets derived from angioreactors and stained with FITC-lectin. Significance using Student's t-test was determined using statistical software. Error bars indicate standard deviation from the mean. * = $p < 0.05$.

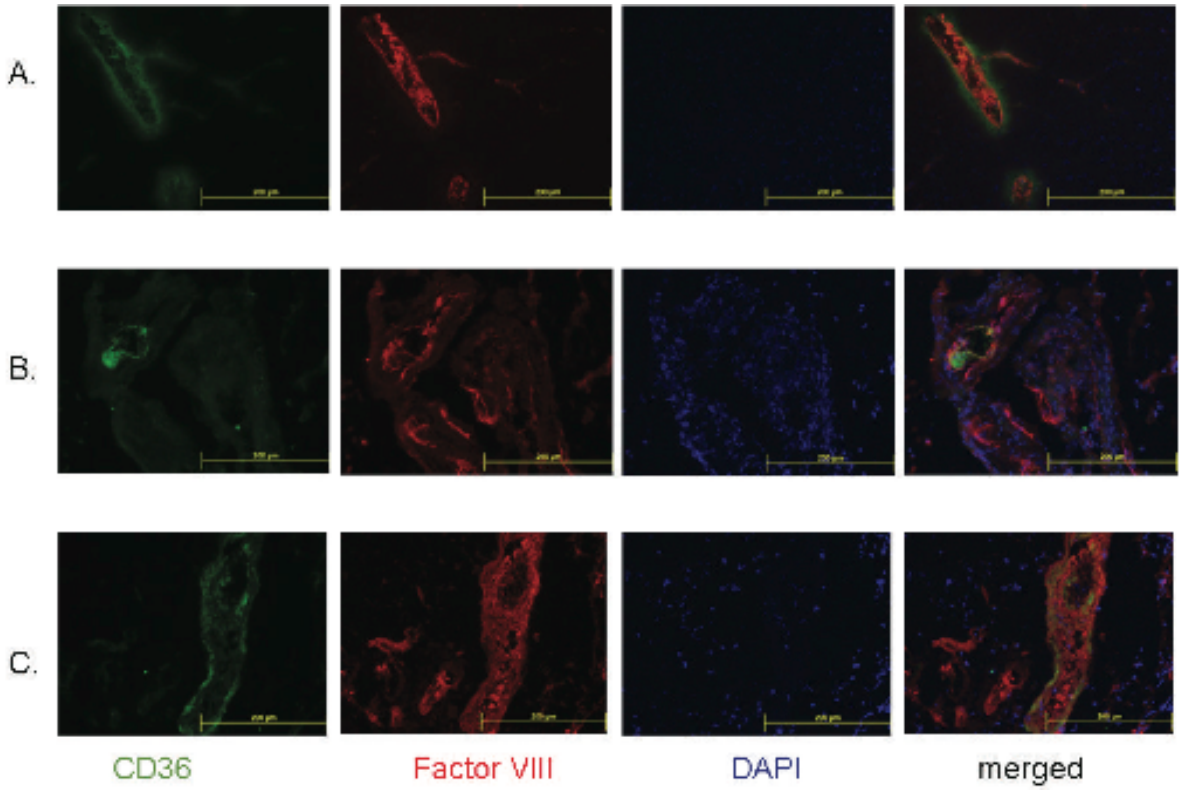

Figure 3.3. Immunohistochemistry was performed to demonstrate co-localization of CD36 and vascular marker Factor VIII in wild-type adult mouse brain (**A**), non-tumor human brain (**B**, Emory Brain Tumor bank specimen #01-89) and human glioblastoma (**C**, Emory Brain Tumor bank specimen #04-20).

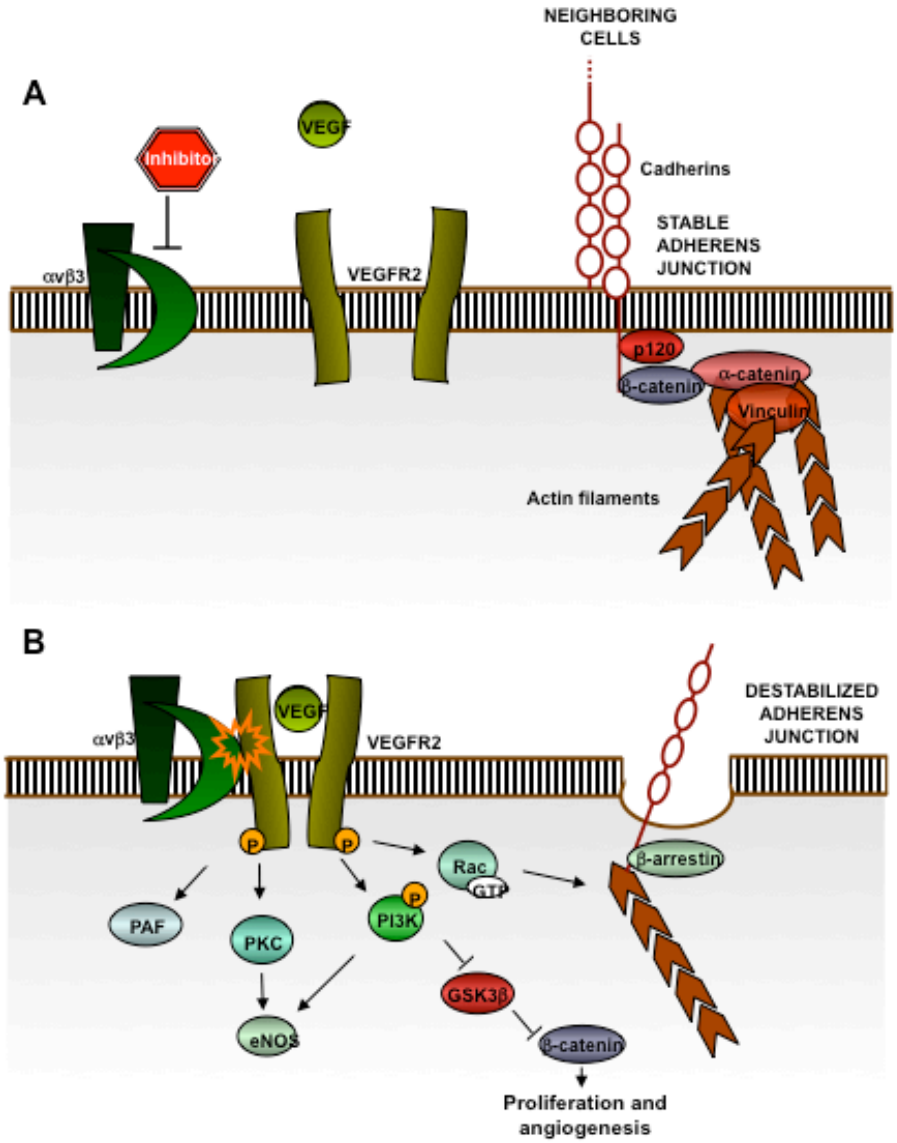

Figure 3.4. Schematic of cell signaling events underlying vascular permeability. (**A**) In the absence of stimulation by pro-permeability cytokines, a complex of molecules including beta-catenin maintains VE-cadherin at the surface of endothelial cells, forming a stable adherens junction. (**B**) VEGF-VEGFR2 activation recruits integrins to promote co-activation of intracellular pro-permeability signaling pathways. This activation promotes destabilization of VE-cadherin at the cell surface and release of beta-catenin from the adherens junction.

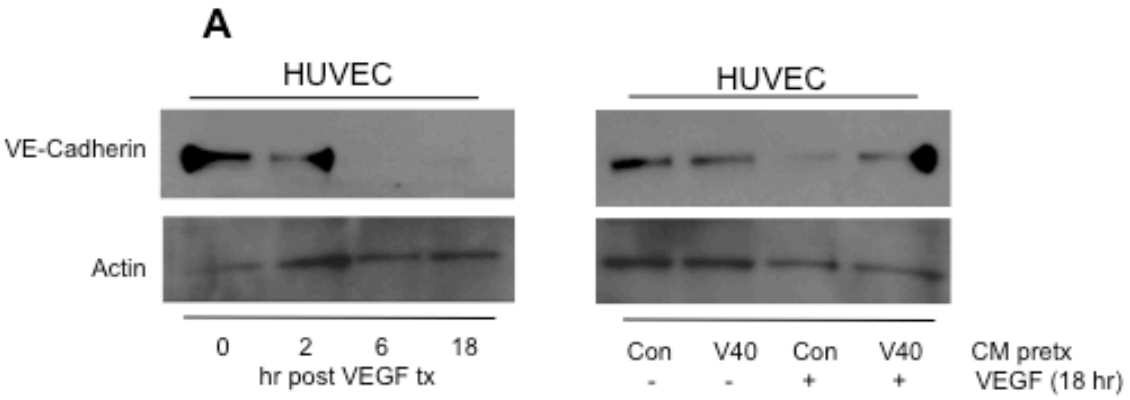
A
HUVEC
HUVEC
VE-Cadherin
Actin
0
2
6
18
hr post VEGF tx
Con
V40
Con
V40
CM pretx
VEGF (18 hr)
-
-
+
+

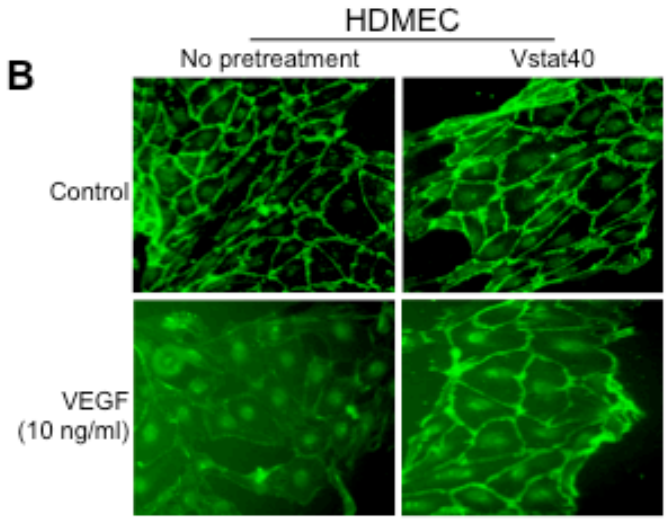
HDMEC
B
No pretreatment
Vstat40
Control
VEGF
(10 ng/ml)

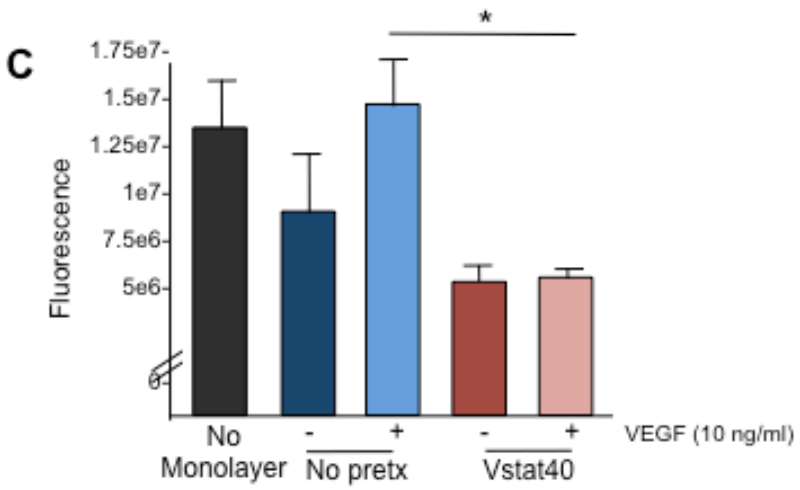
C
*
1.75e7
1.5e7
1.25e7
1e7
7.5e6
5e6
Fluorescence
No
Monolayer
-
+
No pretx
-
+
Vstat40
VEGF (10 ng/ml)

Figure 3.5. Vstat40 inhibits VEGF-induced vascular permeability in culture.

(**A**) Left panel: Treatment with VEGF (10 ng/mL) promotes endocytosis of VE-cadherin from the cell surface of HUVEC and subsequent degradation over a period of 18 hours. Right panel: comparison of levels of VE-cadherin in HUVEC following stimulation with VEGF, after pretreatment with either control CM or CM containing Vstat40.

(**B**) Immunocytochemistry demonstrating effect of Vstat40 pretreatment on localization of VE-cadherin at the cell surface and intercellular contacts of confluent HDMEC following 18 hours of stimulation with VEGF (10 ng/mL).

(**C**) Culture-based assay to assess functional vascular permeability, performed in triplicate. Quantification of fluorescent FITC-dextran following VEGF stimulation (10 ng/mL) for 18 hours illustrates effect of Vstat40 pretreatment on intercellular contact integrity of confluent HDMEC. Student's t-test, * = $p<0.05$.

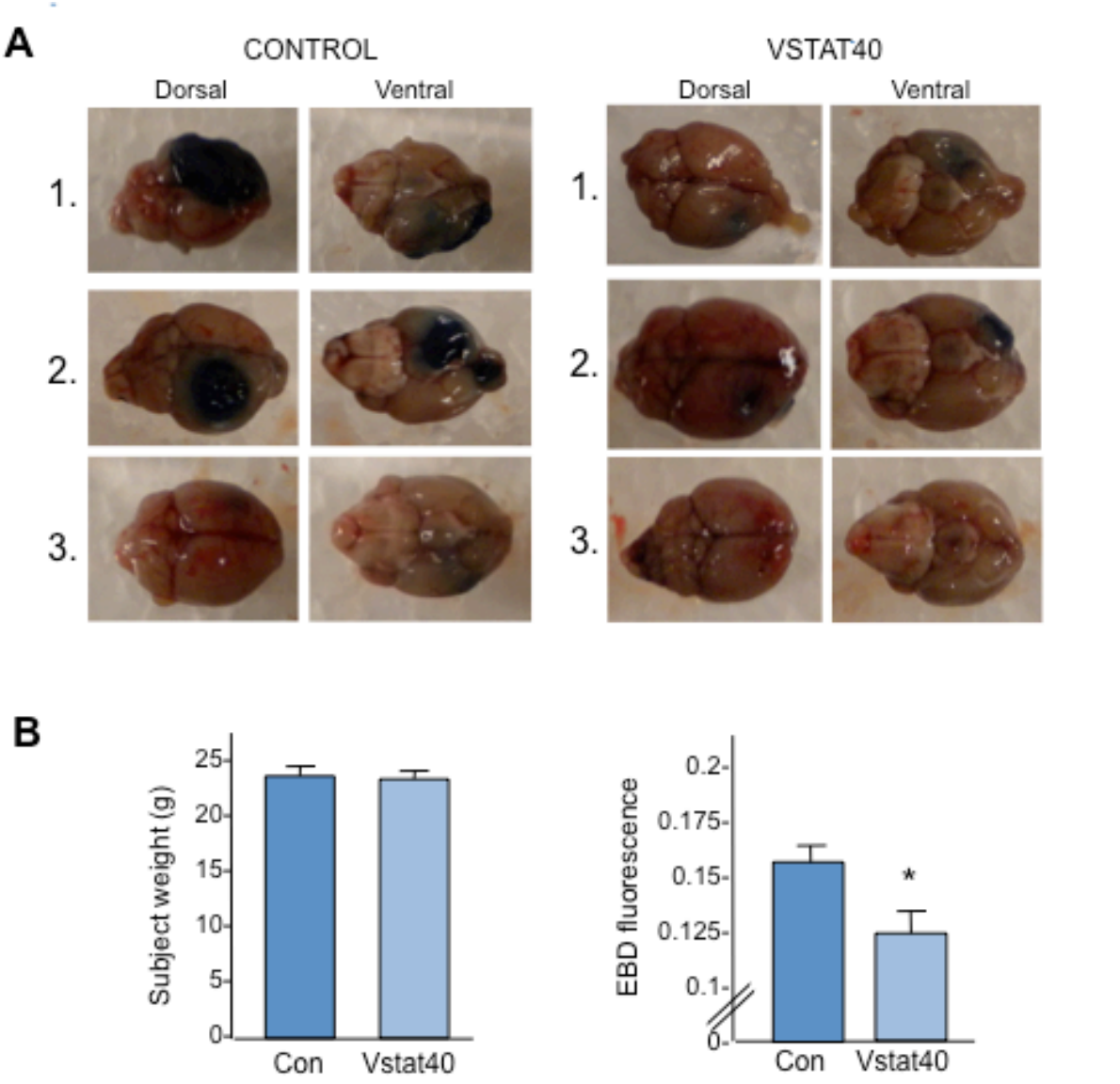

Figure 3.6. Vstat40 and vascular permeability *in vivo*. (**A)** Images of the dorsal and ventral surfaces of mouse brains with control or Vstat40-expressing tumors (n = 3/group) 24 hours after intravascular injection of Evans blue dye (EBD, 30 mg/kg). (**B**) Left panel: subject weight indicating equivalent health of subjects at the time of EBD administration. Right panel: EBD fluorescence following brain homogenization and dye extraction in dimethylformamide.

CHAPTER 4.

VSTAT40 AND BAI1 IN GLIOMAGENESIS.

Some figures from this chapter are here reproduced with permission from the journal from: Kaur B, **Cork SM** et al. (2009). Vasculostatin inhibits intracranial glioma growth and negatively regulates *in vivo* angiogenesis through a CD36-dependent mechanism. *Cancer Research*. **69**(3):1212-20.

Introduction

Brain-specific angiogenesis inhibitor 1 (BAI1) is implicated in the biology of a variety of tumors, particularly gliomas. BAI1 was initially discovered due to the presence of a potential binding site for the tumor suppressor p53 in its 9th intron (Nishimori et al., 1997), and its expression is lost in the development of brain tumors (Kaur et al., 2003) through unknown mechanisms. Overexpression of full-length exogenous BAI1 has been demonstrated to slow the growth of GBM and other cancer types in tumor xenografts through stable transfection studies and gene therapy (Duda et al., 2002; Kudo et al., 2007; Yoon et al., 2005). Conversely, BAI1 loss may correlate with poor survival in glioblastoma patients (Nam et al., 2004), and loss of BAI1 expression has also been shown to correlate with negative clinical outcome in gastric (Hatanaka et al., 2000) and colorectal cancers (Fukushima et al., 1998; Yoshida et al., 1999). The full-length BAI1 protein has also been observed to inhibit tumor growth and angiogenesis when expressed in *in vivo* mouse models, and is a candidate effector for the anti-angiogenic activity regulated by p53 (Nishizaki et al., 1999; Van Meir et al., 1994). In sum, BAI1 has gained significant attention as a tumor suppressor and potential therapeutic agent for aggressive gliomas. While the precise mechanisms of its anti-tumor activity have not been completely elucidated, it is hypothesized to interfere with tumorigenesis via the inhibition of formation of tumor-associated vasculature.

Prior work from our lab has shown that the extracellular domain is responsible for much of the observed anti-tumor activity of BAI1, and which has several features implicated in the regulation of angiogenesis. Specifically, the BAI1 extracellular portion contains an Arg-Gly-Asp (RGD) integrin-binding motif and five thrombospondin type 1 repeats (TSRs). Our lab first determined that BAI1 undergoes endogenous processing at its GPS (Kaur et al., 2005) to generate a 120 kDa secreted fragment called Vasculostatin-120 (Vstat120) and

demonstrated that upon overexpression it had significant anti-angiogenic and anti-tumor activity in an orthotopic xenograft model (Kaur et al., 2009). Thus, the precise mechanisms whereby BAI1 exerts its tumor-suppressive activity in the human body have not been clearly established, but the structure of BAI1 supports an anti-angiogenic role.

In the previous chapters, we have shown that the primary detectable secreted fragment from the BAI1 extracellular domain is a 40-kDa peptide containing the RGD motif and one TSR, named Vasculostatin-40 (Vstat40) (Cork et al. in submission). We have also demonstrated that, like Vstat120, Vstat40 is a potent inhibitor of angiogenesis both in culture-based assays and *in vivo*, and may also inhibit vascular permeability. The anti-angiogenic activity of both Vstat peptides appears to depend in a large part upon the CD36 receptor, which is expressed on microvascular endothelial cells in the brain and in brain tumors. In the present work we wished to determine whether, like Vstat120, Vstat40 could act to suppress tumor growth via the inhibition of tumor-associated angiogenesis.

We also wished to consider the role of BAI1 in the larger picture of glioma biology. The recent development of large repositories of tumor genetic and clinical data has made possible sophisticated analyses of the relationship of individual genes to aspects of tumor biology (Bredel et al., 2009; Cooper et al., 2010; Madhavan et al., 2009; McLendon and Network, 2008; Noushmehr et al., 2010), including survival and angiogenesis. We have analyzed these databanks to determine whether there is a detectable relationship between levels of angiogenesis in human gliomas and BAI1 expression in these tumors, as well as other clinically relevant associations.

Materials and Methods

Cell culture. Human glioma cell lines U87MG, LN229 (Ishii et al., 1999), and U251-BAI1 (Clone B12 (Kaur et al., 2003)) were cultured in DMEM with 10% fetal bovine serum (FBS) and antibiotics and passaged every 2-4 days.

Microarray databases. Affymetrix microarray data from the Repository of Molecular Brain Neoplasia Data (REMBRANDT) and The Cancer Genome Atlas (TCGA) databases were used to investigate collectively gene expression in non-tumor and glioma tissue specimens. Diagnostic data for the REMBRANDT dataset were accessed prior to January 2010. Histopathological necrosis and angiogenesis data were independently scored by a trained neuropathologist (DJ Brat) prior to analysis of association with BAI1 gene expression levels.

Annotations: Affymetrix microarray probe annotations are available on the Affymetrix website. Specific probes used to generate the data described in the figures include: BAI1: 206083_at, BAI2: 204966_at, BAI3: 205638_at, N-cadherin: 203440_at, E-cadherin: 201130_s_at, VE-cadherin: 204677_at, GPR56: 212070_at, EMR-2: 207610_s_at, p53: 201746_at, TSP-1: 201110_s_at, collagen XVIII: 209081_s_at, VEGF-A: 210512_s_at, HIF-1a: 200989_at, IL-6: 205207_at, IL-8: 211506_s_at, TNF-a: 207113_s_at.

Generating clones for tumor experiments. To generate a tetracycline-inducible Vstat40 vector construct, we used PCR to generate a Vstat40-encoding insert (comprising BAI1 amino acids 1-328) flanked by HindIII and XbaI sites. This insert was cloned into pTRE2 (Invitrogen) vector backbone with T4 ligase (Invitrogen) using standard cloning techniques and verified by restriction digest. The pTRE-Vstat40 construct was co-transfected into previously described tet-on LN229-L16 glioma cells (Kaur et al.) with pEGFP-N2 containing the neomycin resistance marker at a ratio of 10:1, using the GenePorter transfection system.

After 24 hours' recovery, cells were passaged to very low density in complete medium containing 800 μg/mL G418 (Invitrogen) and 0.5 μg /mL puromycin. Selection was maintained for approximately two weeks, after which time clones were carefully selected using cloning disks. Clones were expanded and treated with doxycycline (2 μg /mL) to test for Vstat40 induction by Western blot. Several clones with tight dox-induced gene regulation (#5, #14, #17) were selected for further investigation.

Implantation of tumor cells. Cells were implanted intracranially as described (Kaur et al., 2009), using 9-week old female nude mice (Harlan). Briefly, indiciated cells were trypsinized, counted with a hemocytometer and resuspended in a volume of serum-free culture medium to achieve a desired cell concentration of $1x10^6$ cells in 4 μL. Under sterile conditions, subjects were anesthetized with a mixture of ketamine/xylazine as previously described (Kaur et al., 2009) and immobilized in a stereotactic frame. 4 μL of cells were implanted per subject. Care was taken to prevent leakage of cells through the site of implantation, and the site sealed with bone wax and sutures. Following implantation, the remainder of the cell suspension was plated in culture to verify cell viability. Subjects were randomly distributed into two groups for the purposes of the experiment. Dox-treated subjects received doxycycline (2 mg/mL) in 4% sucrose in drinking water; control subjects received sucrose/water alone. Drinking water was changed 2-3 times each week. Subject weight was monitored by weekly weighings and subject health was visually monitored to insure compliance with IACUC guidelines. When health of subjects was observed to decline after 2.5 months, tumor growth was ascertained using T1-weighted magnetic resonance imaging (MRI) as previously described (Kaur et al., 2009). Subjects were weighed at time of MRI. Tumor volume was quantified using ImageJ software (NIH). When tumor burden exceeded

IACUC specifications as determined by more than 20% weight loss, subjects were sacrificed with CO_2 and their brains immediately dissected out for further study.

Sulforhodamine B (SRB) assay. Briefly, tumor cells from the post-injection plating were trypsinized and plated in a 24-well plate at a density of 2.5 $x10^4$ cells per well. Doxycycline was administered to indicated cells (2 μg/mL) and cells were fixed at 4 degrees with cold 10% TCA in PBS after the indicated time intervals. Cells were washed 3x with dH2O and air-dried prior to staining with 0.4% SRB in 1% acetic acid solution (Vichai and Kirtikara, 2006). After staining 1 hr, cells were washed with 1% acetic acid 5x and air-dried. The SRB dye was solubilized with 10 mM Tris buffer and absorbance quantified at 564 nm.

Immunohistochemistry. Brains were excised and fixed in 10% formalin/PBS, then embedded in paraffin, sectioned and stained by the Emory Pathology Core. Antibodies used in these experiments include anti-human cleaved caspase 3 (1:100 dilution) and anti-human Ki67 (1:100 dilution), which were provided by the Core. Specimens were imaged at 10x magnification using an Olympus IX50 Inverted microscope.

Results

BAI1 expression is lost in gliomas in proportion to tumor severity. We investigated levels of *BAI* family mRNA expression in non-tumor, astrocytoma, glioblastoma multiforme (GBM) and oligodendroglioma (ODG) tissue samples in the REMBRANDT database. For all BAIs, we observed that mean levels of mRNA expression were significantly decreased in astrocytomas relative to levels in non-tumor brain tissue (Figure 4.1A). Expression levels were further decreased in GBM specimens, indicating an association with glioma severity. When astrocytoma specimens were subdivided into grade II and III, the negative correlation between tumor grade and BAI1 mRNA expression was maintained (Figure 4.1B). Of note, a negative correlation for expression in ODG specimens was also detected for BAI2 and BAI3 but not BAI1. While the significance of these associations is unknown, this observation highlights the importance of BAI1 loss in astrocytoma and GBM specifically. Notably, BAI1 expression does not vary significantly across the four previously-identified subtypes of GBM (Figure 4.1C).

BAI1 expression is associated with a survival benefit to astrocytoma but not GBM patients. The relationship of BAI1 expression to patient survival was investigated separately for astrocytoma and GBM specimens from the REMBRANDT dataset. For both subtypes, samples were identified as either "low" or high" BAI1 expressors depending on whether BAI1 expression fell above or below the median value for that subgroup. Samples were then matched to respective patient survival data to generate Kaplan-Meier survival curves (left panels) and average survival (right panels). We observed that expression of BAI1 was associated with a statistically significant increase in survival for astrocytoma patients (grades II and III combined; Figure 4.2A), with a survival increase of approximately two months

(p=0.0186) for the high-expressing group. We observed that elevated BAI1 did not confer a statistically significant survival benefit (p=0.636) to GBM patients (Figure 4.2B), however.

Elevated BAI1 is associated with reduced angiogenesis and necrosis. Previous research has linked BAI1 expression to a positive clinical outcome for cancer patients (Lee et al., 2001; Zohrabian et al., 2007). While the survival benefit has been hypothesized to derive from BAI1's angioregulatory capabilities, no research to date has demonstrated that BAI1 inhibits angiogenesis in human gliomas. To determine whether the pro-survival benefit of elevated BAI1 could be explained by its effects on tumor-associated angiogenesis, we compared BAI1 expression to levels of angiogenesis in GBM specimens. First, a trained neuropathologist (DJ Brat) independently scored selected histological specimens from the TCGA to determine the percentage of tissue necrosis and analyze certain features of pathological tumor vasculature, including endothelial hyperplasia, endothelial hypertrophy, and endothelial complexity, indicated by the presence of branching vessels. These three features of angiogenesis were then combined to generate a single composite score of angiogenesis (scale of 0-3) for the tumor specimen. Samples were subsequently ordered by increasing BAI1 expression, and samples at both ends of the spectrum were matched to available pathological data. After obtaining 20 specimens for both "low" and "high"-expressing groups of tumor tissues, we verified a significant difference in levels of BAI1 expression in low versus high groups (Figure 4.3A). Importantly, we detected a significant difference in levels of tumor angiogenesis and necrosis when comparing their levels in low versus high-BAI1 expressing tumors. To determine whether pro-angiogenic hypoxia might be responsible for downregulating BAI1, we incubated primary glial cultures under hypoxic conditions (1% O_2). This treatment was not observed to alter BAI1 protein expression levels in these cultures after 48 hours (Figure 4.3B).

Patterns of angioregulator expression in brain tumors. In analyzing the TCGA Affymetrix microarray data, we observed two distinct patterns of angioregulator expression in relation to BAI1 expression. The first pattern indicated gene expression independent of BAI1 expression, and was demonstrated by genes known to regulate both the inhibition and promotion of angiogenesis (Figure 4.4A). Pro-angiogenic genes that demonstrated this pattern of expression included both the hypoxia inducible factor (HIF)-1alpha subunit and its target gene VEGF-A, and tumor necrosis factor (TNF). Anti-angiogenic genes that demonstrated this pattern of expression included the tumor suppressor p53, which is known to regulate the secretion of other anti-angiogenic stimuli, and both alpha and beta subunits of interleukin-12 (IL-12). By contrast, expression levels of other angioregulators were markedly elevated when BAI1 expression was low and decreased as BAI1 expression increased (Figure 4.4B). Pro-angiogenic molecules under study in this group were interleukins 6 and 8 (IL-6 and IL-8) and angiogenesis inhibitors were thrombospondin-1 (TSP-1) and collagen XVIII, a rare form of collagen that serves as a precursor to endostatin. Together these findings indicate at least two specific patterns of angioregulator regulation relative to BAI1 expression in GBM.

To follow up on these observations, we investigated expression of TSP-1 and collagen XVIII in the REMBRANDT databank. We observed that, for all specimens regardless of tissue type, the pattern of regulation was similar to that noted for the TCGA dataset (Figure 4.5A), demonstrating the robustness of association across different tumor datasets. We followed up on this observation by subdividing the REMBRANDT specimens by tissue type to evaluate whether the association was specific to tumors or a general relationship also observable in non-tumor brain. We observed that, for both TSP-1 and collagen XVIII, the inverse relationship with BAI1 expression was preserved only in tumor specimens, and most strongly in astrocytomas (Figure 4.5B). In non-tumor brain tissue, the relationship between

both molecules and BAI1 expression appears to be positively correlated. Thus, the inverse relationship likely reflects tumor control over specific transcriptional pathways.

Association of BAI1 expression with that of other cell adhesion molecules. While the majority of research on BAI1 has focused on its angioregulatory activity, it is classified as a potential cell adhesion molecule based on its structure. We followed up on the findings of the angioregulator molecules by investigating whether BAI1 expression resembled patterns of expression of other cell adhesion molecules using the TCGA Affymetrix microarray data (Figure 4.6A-B). We considered the other cell adhesion GPCRs EMR-2 and GPR56 as well as BAI2 and BAI3, and the cell adhesion molecules E-cadherin, N-cadherin and VE-cadherin, which are typically expressed on epithelial, neural and vascular tissues, respectively. We observed that expression of BAI2 and BAI3 correlated strongly with that of BAI1, suggesting that these genes are regulated by similar mechanisms or are co-regulated. We observed that expression of E-cadherin and N-cadherin did not change in relation to BAI1 expression, but that expression of VE-cadherin decreased in relation to BAI1.

Validation of the *in vivo* tumor model. In performing tumor experiments it is of great importance to demonstrate how the *in vivo* model corresponds to the biology of human gliomas. In Chapter 3 we demonstrated the presence of the CD36 receptor in the brain vasculature of both mouse brain and adult human tumor and non-tumor brain specimens. Our lab has also previously constructed stably-transfected glioma cell lines expressing Vstat120 for use in tumorigenesis experiments, specifically the U87ΔEGFR parental cell line, and clones Δ19 and Δ22 constitutively expressing Vstat120 (Kaur et al., 2009). Expression of Vstat120 in tumors formed from these clones as compared to control cells was verified using Western blot (Figure 4.7A). Use of these cell lines showed the ability of Vstat120 to significantly inhibit tumor growth via the inhibition of tumor-associated angiogenesis.

We modified this approach for a study of the effects of Vstat40 on tumorigenesis. For the Vstat40 tumorigenesis experiment, Vstat40-inducible clones were generated by stably transfecting LN229 human glioma cells with an inducible Vstat40 expression vector (LN229-L16-Vstat40-tet on). We screened 25 clones generated via selection with geneticin by dividing each clone into two cell populations and treating one with doxycycline. We selected three clones: LN229-L16-#5, LN229-L16-#14, and LN229-L16-#17 (Figure 4.7B). Selection was based on the strength of Vstat40 induction in the conditioned medium (CM) in response to doxycycline treatment and the specificity of the induction, such that no Vstat40 was observed in the CM of untreated clone cells, and no additional bands besides Vstat40 were generated in response to induction.

We wished to account for the possibility of potentially confounding effects that this model might incur. Specifically, we wanted to verify that doxycycline administration would not have a significant anti-proliferatory effect upon the tumor cells themselves. We also sought to determine whether Vstat40 could affect tumor cell proliferation in a manner independent of angiogenesis. Treatment of the Vstat40-expressing clone 17 cells and parental LN229-L16 cells with doxycycline was not observed to exert a significant effect on proliferation of these cell lines in culture (Figure 4.7C). While this experiment does not account for complicating *in vivo* factors that could affect these issues, it provides foundation for using these cell lines in tumorigenesis studies.

Vstat40 does not promote survival in an *in vivo* tumorigenesis experiment. We hypothesized that, like Vstat120, Vstat40 may act as a tumor suppressor in the brain via the inhibition of angiogenesis (Kaur et al., 2005; Kaur et al., 2009). To address this hypothesis, cells from the three previously-described clones were implanted intracranially in nu/nu mice (10 subjects used for each clone). Half of the subjects (5 per clone) received doxycycline in

drinking water to induce Vstat40 expression. While subjects bearing tumors of clones 5 and 14 reached endpoint by 100 days post injection, three dox-treated subjects were healthy more than 120 days afterward (Figure 4.8A). Kaplan-Meier analysis of survival of clone 5 and clone 14 control and treatment subjects showed no statistically significant difference of doxycycline administration ($p=0.704$ and $p=0.585$, respectively), while treatment yielded a significant survival benefit for clone 17 ($p=0.002$). The survival of mice implanted with LN229-L16 cells was unaffected by doxycyline (not shown). MRI imaging of control and dox-treated subjects 60 days after injection demonstrates the relative difference in tumor size between these groups at this time (Figure 4.8B-C). Quantitative analysis of the MRI data for clone 17 demonstrates a significant difference in mean tumor volume between control and dox-treated subjects (Figure 4.8C) with no significant difference in subject weight. As it was unclear why Vstat40 expression would affect tumorigenesis for clone #17 but not clones #5 or #14, we followed up on the observation by repeating the experiment for this clone and using an increased number of subjects ($n=12$ per condition). We observed that survival did not differ between the two groups in this repeat experiment ($p=0.45$, Figure 4.9A), indicating that some unknown confounding factor was responsible for the survival and tumor size differences observed for this clone in Figure 4.8B-C.

Several controls were used to verify the function of Vstat40 in the tumorigenesis model. We attempted to verify that Vstat40 was only produced in clones in response to doxycycline induction. However, using cell pellets formed from clone 17 cells (Figure 4.9B), we observed that the BAI1 N-terminal antibody recognized the untreated as well as dox-treated cells. An antibody dilution of 1:8000 yielded the optimal contrast in cell staining. This observation in cell pellets corresponds to results of BAI1 staining of control and treatment tumors, which detects the presence of Vstat40 in control tumor tissue. Staining of other

pellets of 293 cells untransfected or stably transfected with BAI1 shows that the BNT antibody recognizes BAI1 specifically without a high level of background staining (not shown). We followed up on these results by analyzing WCE and CM of clone #17 cells prior to implantation, showing that while Vstat40 is only secreted in response to induction, low levels of Vstat40 are produced in the WCE of both treated and untreated cells (Figure 4.9C). We conclude that there is some background level of Vstat40 production in cells stably transfected with the inducible vector, but that cells only secrete Vstat40 at detectable levels under conditions of induction. We conclude that effects on either tumor or endothelial cells in these *in vivo* tumorigenesis experiments are due to Vstat40 expressed only in response to doxycycline. Unfortunately, the observation of background Vstat40 expressed in control tumor cells precludes an assessment of the specificity of Vstat40 secretion *in vivo* in response to doxycycline, as with the current setup we are not able to detect whether some other mechanism may be inducing Vstat40 release in the growing tumor.

Vstat40-expressing tumors have reduced angiogenesis and differential levels of cleaved caspase 3. While no difference in overall subject survival was identified between the control and Vstat40-expressing tumors, we wished to follow up on these findings in the clone 17 tumors by investigating differences in the biology of the tumor specimens. Of particular importance was the question of whether Vstat40 expression in tumors inhibited tumor-associated angiogenesis. Importantly, control tumors were characterized by the presence of many vascular structures, while tumors of dox-treated subjects showed significantly less vascularization (Figure 4.10A). In this model, however, the inhbition of angiogenesis was not sufficient to improve subject survival.

To better understand the reason for this discrepancy, the tumors were subjected to further examination. A trained neuropathologist (DJ Brat) observed that the cells of the

control tumors were less adherent, causing the tissue to separate during fixation, and that control tumor cells also had a stellate shape. In contrast, cells in the dox-treated tumors were rounder and more tightly adherent, with clearly evident cytoplasm and prominent nucleoli. Immunohistochemistry was used to investigate selected cellular markers of interest in the clone 17 tumors. Control and Vstat40-expressing clone 17 tumor sections were stained for the cell proliferation marker Ki67 and cleaved caspase 3, an important indicator of apoptosis. We observed no difference in Ki67 staining between the two conditions, as tumors stained for Ki67 showed expression in virtually all tumor cells (not shown). This finding indicates that Vstat40 does not inhibit tumor cell proliferation *in vivo*. However, the number of cells positively stained for cleaved caspase 3 was increased in tumors obtained from subjects not receiving doxycycline (Figure 4.10B), suggesting that Vstat40 may interfere with apoptosis via undetermined mechanisms. The significance of this finding is not clear, but it suggests the possibility that Vstat40 may exert biologically relevant activity on the tumor cells themselves without interfering with overall tumor cell proliferation.

Discussion

A thorough understanding of the bioactivity of the Vasculostatin peptides is vital for any future development of anti-tumor therapeutics based on the extracellular domain of BAI1. Earlier work from our lab has convincingly shown the anti-tumor efficacy of the entire BAI1 ECD, otherwise known as Vstat120 (Kaur et al., 2005; Kaur et al., 2009). In the present work we investigated whether Vstat40 could also act to suppress tumor growth via the inhibition of tumor-associated angiogenesis, as it is the predominately-expressed known secreted BAI1 fragment. While we have demonstrated that Vstat40 regulates tumor-associated angiogenesis, its expression was not able to significantly promote subject survival in one model (LN229) of *in vivo* glioma tumorigenesis.

The result that, unlike Vstat120, Vstat40 is not able to inhibit *in vivo* tumor growth in this study may reflect one of several possibilities. First, it may be the case that the biological properties of Vstat40 do not enable it to inhibit tumor-associated angiogenesis to the point of preventing tumorigenesis, whereas Vstat120 may be a more potent molecule, likely due to the activity of its four other TSRs. However, another possibility is that the model under study is too limited to determine the true anti-tumor activity of Vstat40. With this model, we opted to improve upon the previous model of Vstat120 studies (Kaur et al., 2009) by making Vstat40 inducible in response to doxycycline administration. This approach improves upon the previous model of tumorigenesis in several respects. First, it ensures that the cellular genomic background of both controls and treatment cells are identical, because the previous experiments use clones and parental cells that may differ significantly as a consequence of selection. Further, it permits control over when Vstat40 is expressed during the period of tumor growth. However, a different cell line (LN229) was utilized instead of U87MG derivatives used in the previous studies. If LN229-derived tumors are less vascularized than

U87MG tumors, the biological effects of Vasculostatin treatment may be muted. Indeed, unpublished subcutaneous tumorigenesis studies of doxycycline-inducible Vstat120 using LN229 cells showed a more moderate growth inhibition than the U87MG studies (E.G. Van Meir, pers. comm.). A final alternative is that Vstat40 may be a less effective therapeutic as a result of unforeseeable confounding influences of *in vivo* expression. These confounds could range from a shorter half-life of Vstat40 or competition of some unknown substrate with the active portions of Vstat40. Future research on the utility of Vstat40 as an anti-tumor agent should consider the use of other cell lines and any possible controls to better interpret these issues, and should further explore the potential effects of Vstat peptides upon the tumor cells themselves.

The *in silico* analyses described in this chapter both bolster the rationale for continued experimentation on BAI1 as an anti-tumor therapeutic and provide new directions for these studies. This recent wealth of microarray and clinical data have allowed us to confirm previous findings that BAI1 expression is frequently lost in aggressive gliomas, and to investigate the specific role of BAI1 as an important inhibitor of human glioma angiogenesis. For the first time, we show that BAI1 expression in human gliomas is negatively correlated with levels of tumor angiogenesis. While no underlying hypothesis yet explains the association with necrosis, this phenomenon warrants further study. One hypothesis is that hypoxia-regulated genes such as HIF-1alpha and its target VEGF, which are upregulated around the necrotic core tissue of solid tumors and are well understood to promote angiogenesis, might contribute to the downregulation of BAI1 expression in cells. However, no change in BAI1 protein expression levels was detected in primary human astrocyte cultures incubated under hypoxic conditions up to 48 hours. While this experiment does not preclude the possibility of

hypoxia- or necrosis-mediated BAI1 regulation, particularly under conditions of tumor necrosis, it appears that hypoxia itself is insufficient to regulate BAI1 expression.

In conjunction with clinical data on patient survival, our findings suggest that elevated levels of BAI1 may improve survival of astrocytoma grade II-III patients, but the aggressive nature of GBM may overwhelm any pro-survival advantage that would otherwise be associated with BAI1. These observations do not rule out the possibility that BAI1 may be beneficial to GBM patients in a manner not associated with survival *per se*. For example, increased BAI1 could maintain a reduced, less-permeable tumor-associated vasculature, leading to reduced edema and associated symptomology. While this latter possibility remains to be verified, overall these results suggest that BAI1 may prove an appropriate therapeutic mechanism for lower-grade glioma patients.

These results also suggest further avenues for study. A prevailing doctrine in glioma biology is the existence of an "angiogenic switch," in which pro-angiogenic molecules are upregulated and anti-angiogenic molecules are downregulated, to facilitate growth of the tumor. Many pro-angiogenic molecules are known to be upregulated in gliomas, such as VEGF, bFGF, HGF, IL-8 and angiopoietin-2 (Ang-2). As previously described, expression of the BAIs and other anti-angiogenic molecules is often lost in gliomas, but the specific means by which successful tumors co-opt angiogenic processes is not well understood. It may be that certain groups of angioregulators may undergo specific patterns of regulation to achieve a glioma's vascularization requirements. In considering whether such might be the case for BAI1, we compared expression of selected genes with that of BAI1 to investigate whether other angioregulator molecules are specifically regulated in relation to BAI1.

As shown, we observed that certain angioregulators do not appear to be correlated with BAI1, whereas others have a strong inverse relationship, and that this association

appears to be tumor-specific. Regarding the association of BAI1 with specific genes, more research will be necessary to confirm the existence of such associations and determine the cellular mechanisms responsible. These studies may also provide important insight into the forces that drive BAI1 expression or its loss in tumors. For example, the observation that VE-cadherin expression is reduced when BAI1 levels are elevated is of particular interest because VE-cadherin is a major component of adherens junctions and Vstat40 is thought to inhibit vascular permeability (Chapter 3). These findings from the TCGA microarray are consistent with the hypothesis that Vstat40 inhibits vascular permeability, as VE-cadherin transcription is upregulated in angiogenic tumors (Prandini et al., 2005) and the stability of adherens junctions is likely to suppress transcription of VE-cadherin.

Ultimately, the significance of these associations cannot be completely elucidated from correlation data. The observation that different genes demonstrate consistent patterns of expression in relationship to BAI1 indicates that they may be co-regulated or that they may act to influence the expression of the other, whether directly or indirectly. Further work should be undertaken to determine whether these molecules have similar patterns of transcriptional regulation. Such research will be quite valuable as it will shed light on patterns of angioregulator expression in gliomas, which may prove of significant therapeutic benefit by identifying which angiogenic pathways are the most appropriate targets for a given tumor.

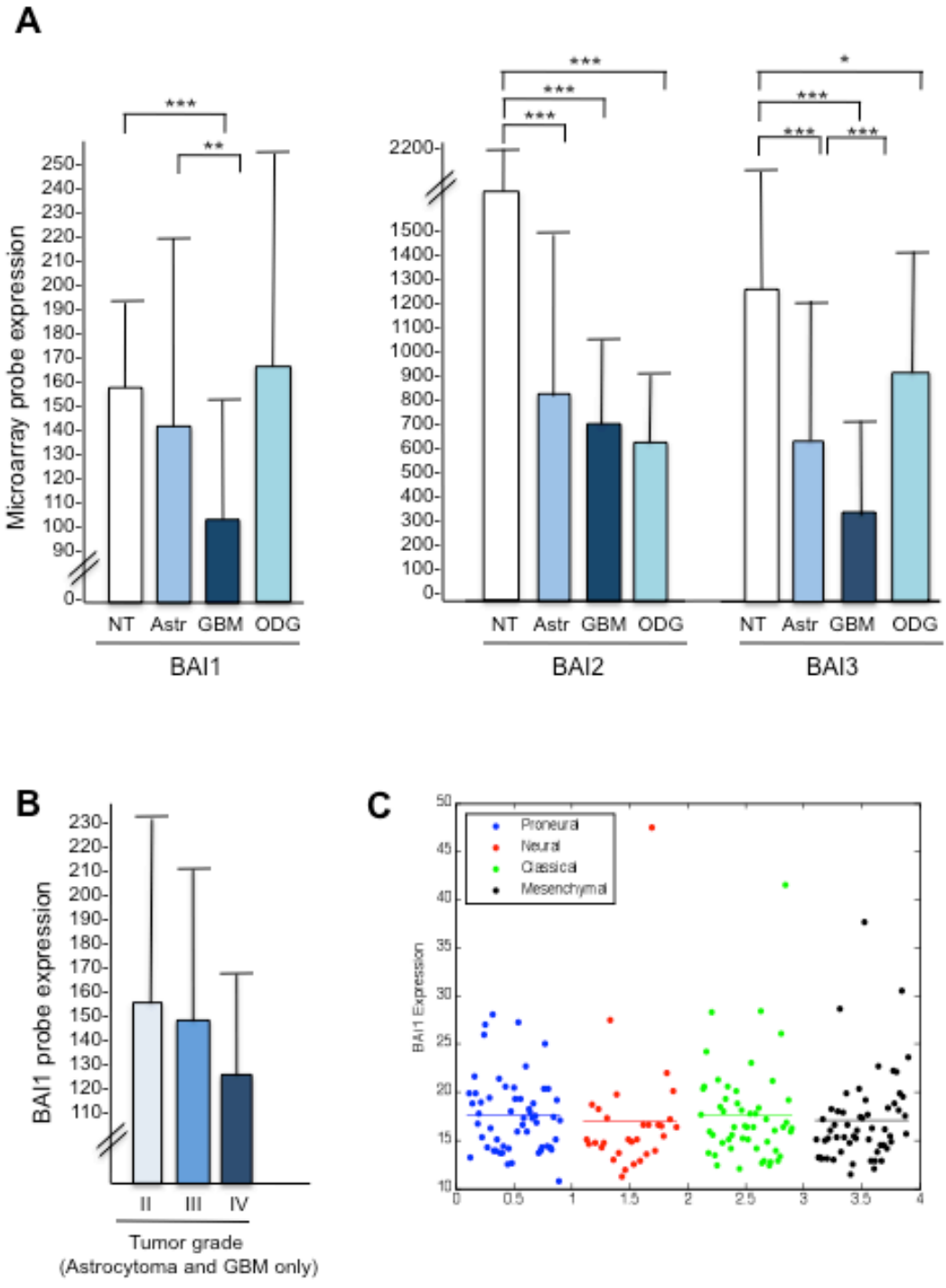
A
Microarray probe expression
NT Astr GBM ODG
BAI1
BAI2
BAI3
B
BAI1 probe expression
II III IV
Tumor grade
(Astrocytoma and GBM only)
C
Proneural
Neural
Classical
Mesenchymal
BAI1 Expression

Figure 4.1. BAI1 expression is lost in gliomas in proportion to tumor severity. From REMBRANDT.

(**A**) We investigated levels of BAI family expression in non-tumor brain (NT), astrocytoma (AST), glioblastoma multiforme (GBM) and oligodendroglioma (ODG) tissue samples in the REMBRANDT databank. Asterices represent statistical significance of indicated t-tests (* $p < 0.05$, ** $p < 0.01$, *** $p < 0.001$).

(**B**) BAI1 expression evaluated as a function of astrocytoma grade (II, III, IV) using available clinical data.

(**C**) Levels of expression of BAI1 in TCGA samples, subdivided by the four primary subtypes of GBM identified by Verhaak et al. (2010): proneural, neural, mesenchymal, and classical.

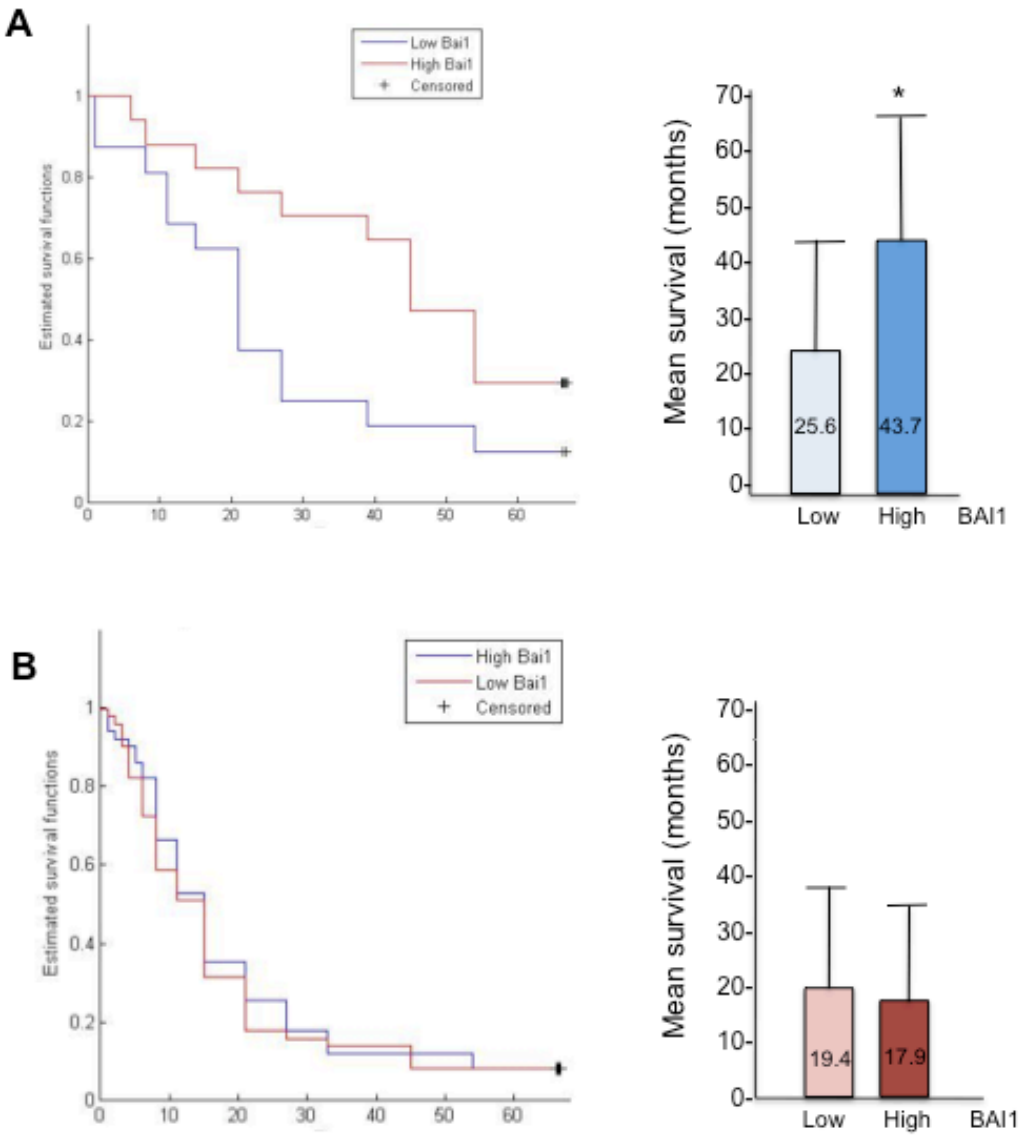

Figure 4.2. BAI1 expression is associated with survival benefit for astrocytoma but not GBM patients. From REMBRANDT. (**A**) Left: Kaplan-Meier curve demonstrating significant survival benefit of elevated BAI1 expression for astrocytoma patients ($p = 0.034$). Right: Comparison of average survival in months for astrocytoma patients with high (above median) BAI1 levels versus low (below median) BAI1 levels ($p = 0.019$). (**B**) Left: Kaplan-Meier curve demonstrating survival benefit of elevated BAI1 expression for GBM patients ($p = 0.36$). Right: Comparison of average survival in months for GBM patients with high versus low BAI1 levels ($p = 0.636$).

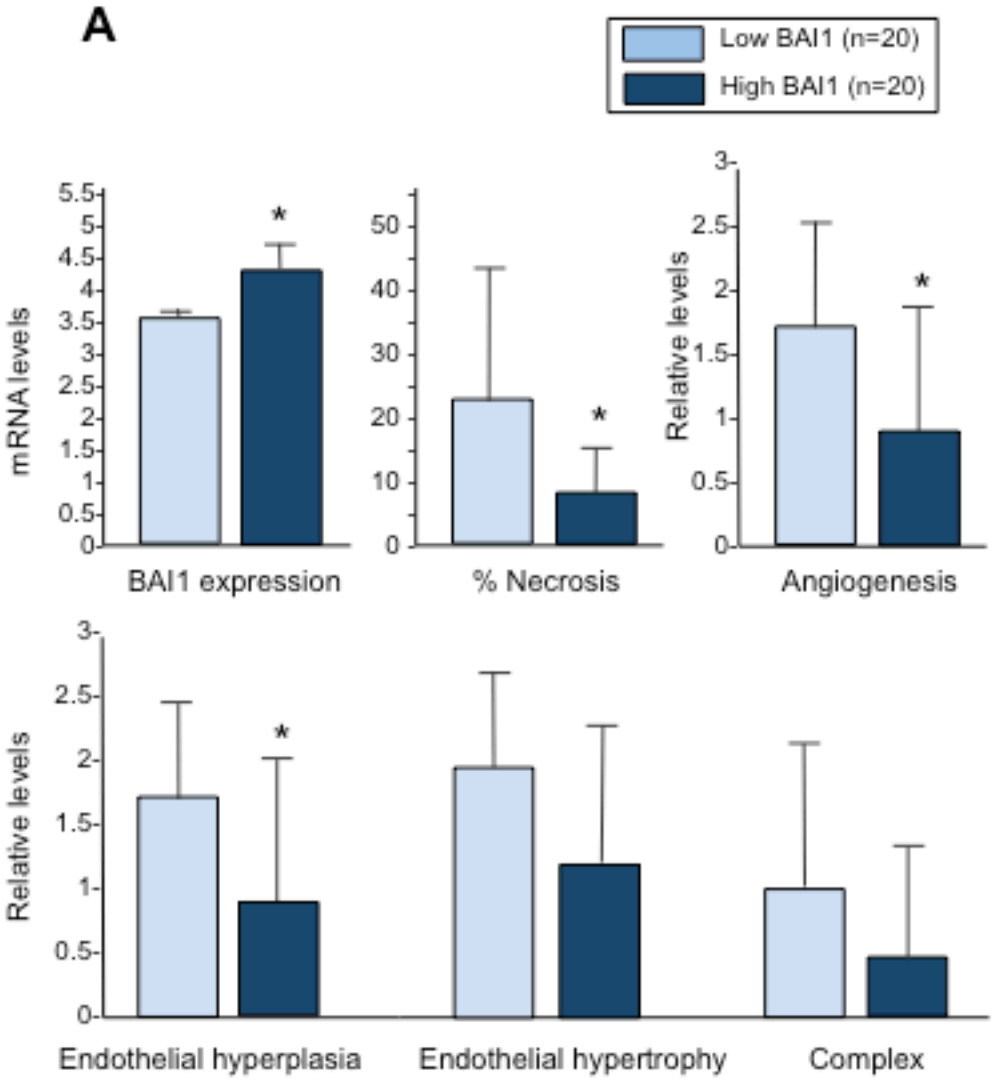
A
Low BAI1 (n=20)
High BAI1 (n=20)
mRNA levels
BAI1 expression
% Necrosis
Relative levels
Angiogenesis
Relative levels
Endothelial hyperplasia
Endothelial hypertrophy
Complex

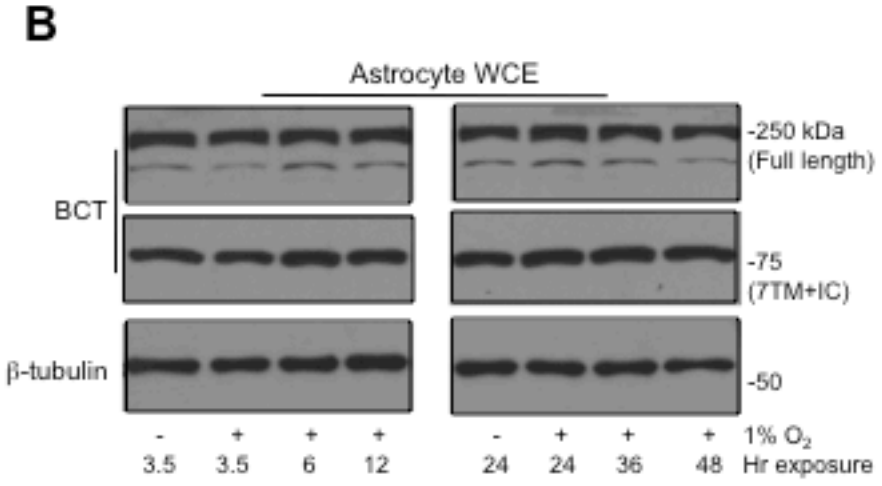
B
Astrocyte WCE
-250 kDa
(Full length)
BCT
-75
(7TM+IC)
β-tubulin
-50
1% O2
3.5 3.5 6 12 24 24 36 48 Hr exposure

Figure 4.3. Elevated BAI1 is associated with reduced angiogenesis and necrosis. From TCGA and ISBRTC annotations.

(**A**) BAI1 is positively correlated with reduced angiogenesis and reduced necrosis in human glioma specimens (n = 20 TCGA specimens/group). Expression of BAI1 mRNA in "low" versus "high" expressing samples is significantly different (p = 3.72e-19). Individual statistical significance values for associations with BAI1 expression: necrosis (p = 0.009), angiogenesis (p = 0.024), endothelial hyperplasia (p = 0.019), endothelial hypertrophy (p = 0.058), complexity (p = 0.109).

(**B**) Western blot demonstrating that hypoxia does not regulate BAI1 expression in primary human astrocyte cultures (passage 3), when probed with the BAI1 C-terminal antibody (BCT).

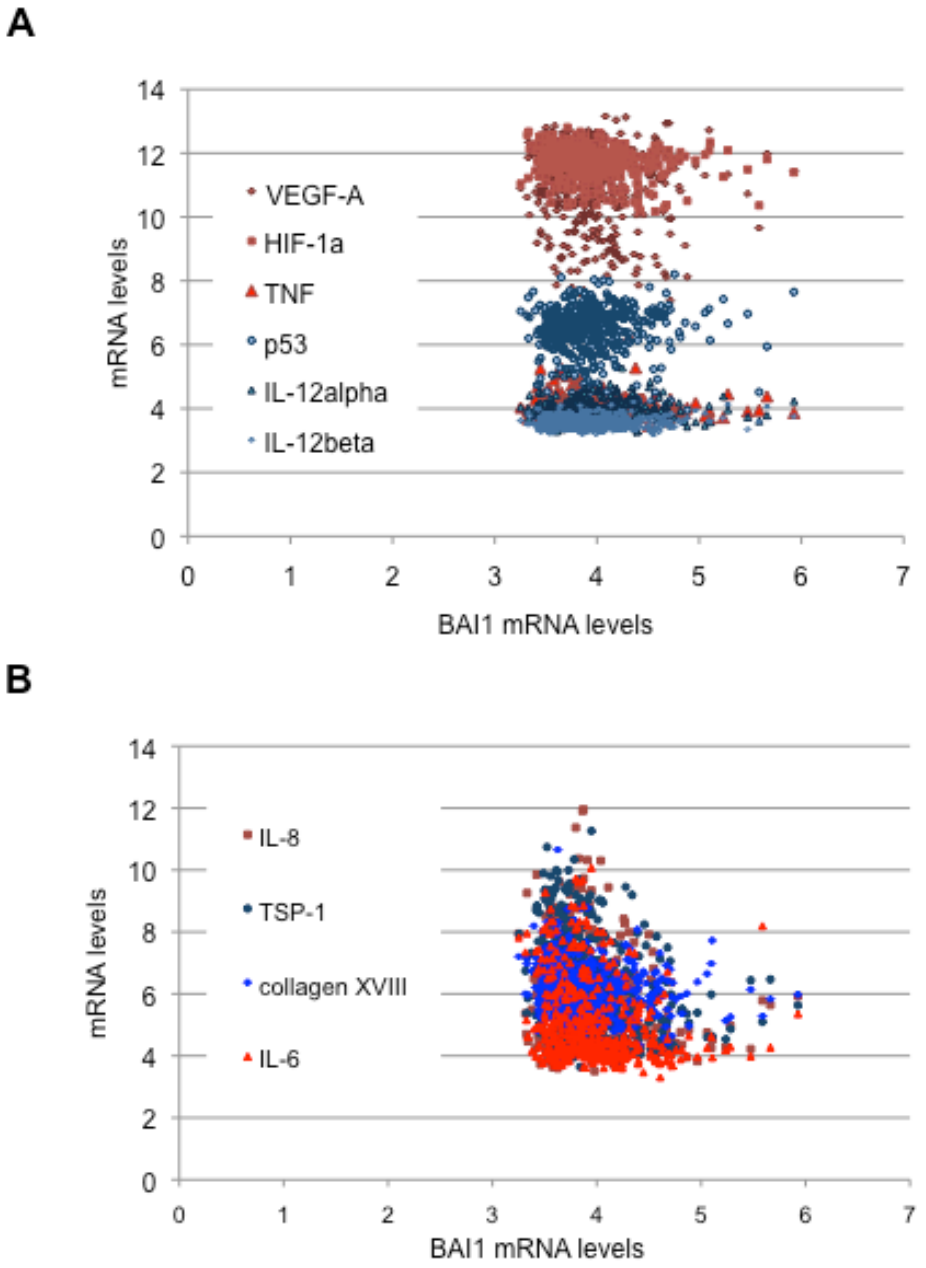

Figure 4.4. BAI1 expression compared with other angioregulators in GBM. From TCGA. (**A**) Expression of selected angioregulator molecules in available GBM tissue samples demonstrating no observable association when plotted as a function of BAI1 expression. (**B**) Expression of angioregulators observed to be inversely associated with BAI1 expression. Figures plotted using Excel software.

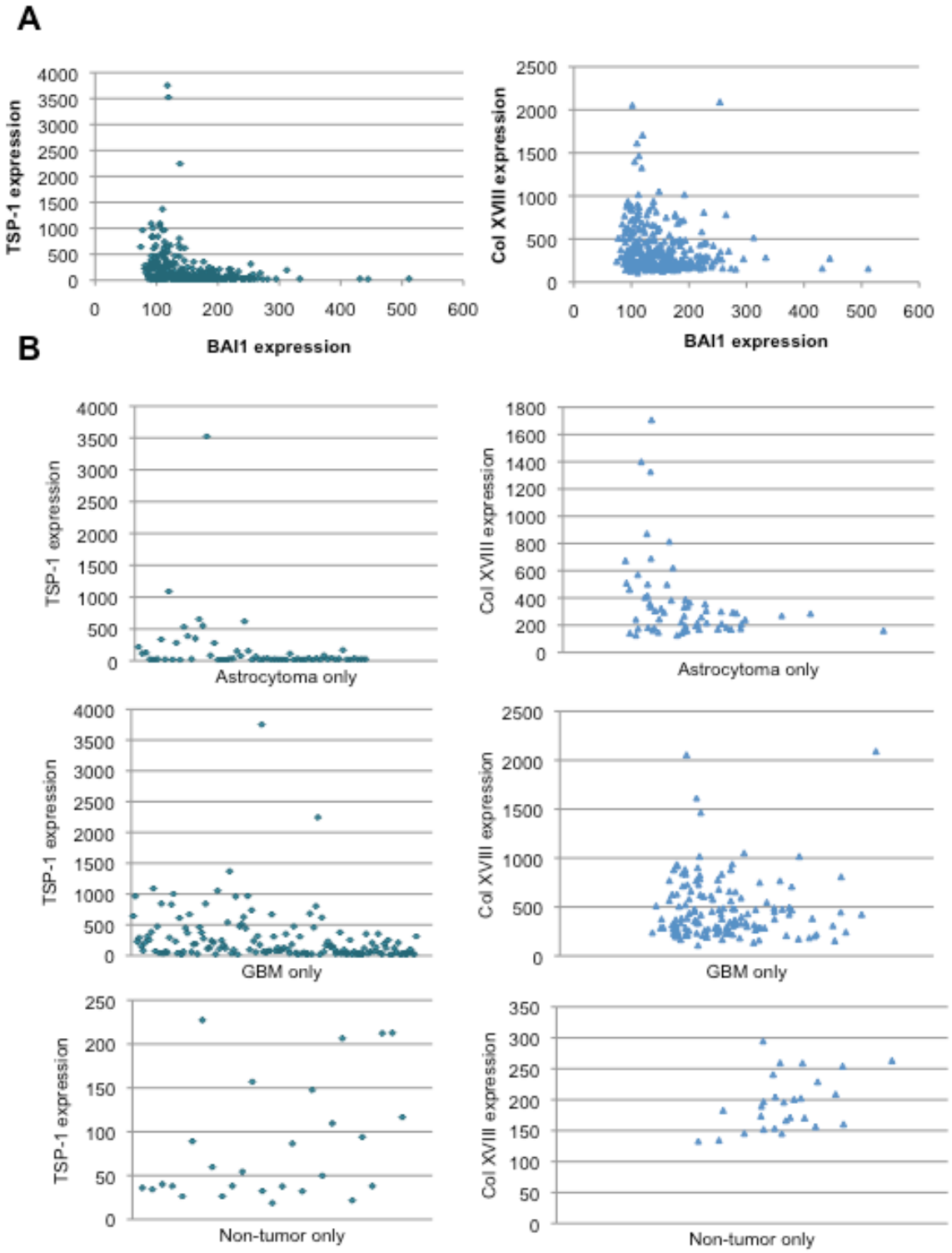
A
TSP-1 expression
BAI1 expression
Col XVIII expression
BAI1 expression
B
TSP-1 expression
Astrocytoma only
Col XVIII expression
Astrocytoma only
TSP-1 expression
GBM only
Col XVIII expression
GBM only
TSP-1 expression
Non-tumor only
Col XVIII expression
Non-tumor only

Figure 4.5. Tumor-specific regulation of BAI1 and other angioregulators. From REMBRANDT.

(**A**) Pattern of thrombospondin-1 (TSP-1) and collagen XVIII (Col XVIII) expression versus BAI1 expression in all samples.

(**B**) Patterns of TSP-1 and collagen XVIII expression when subdivided by tissue type: astrocytoma, glioblastoma multiforme (GBM), or non-tumor brain specimens.

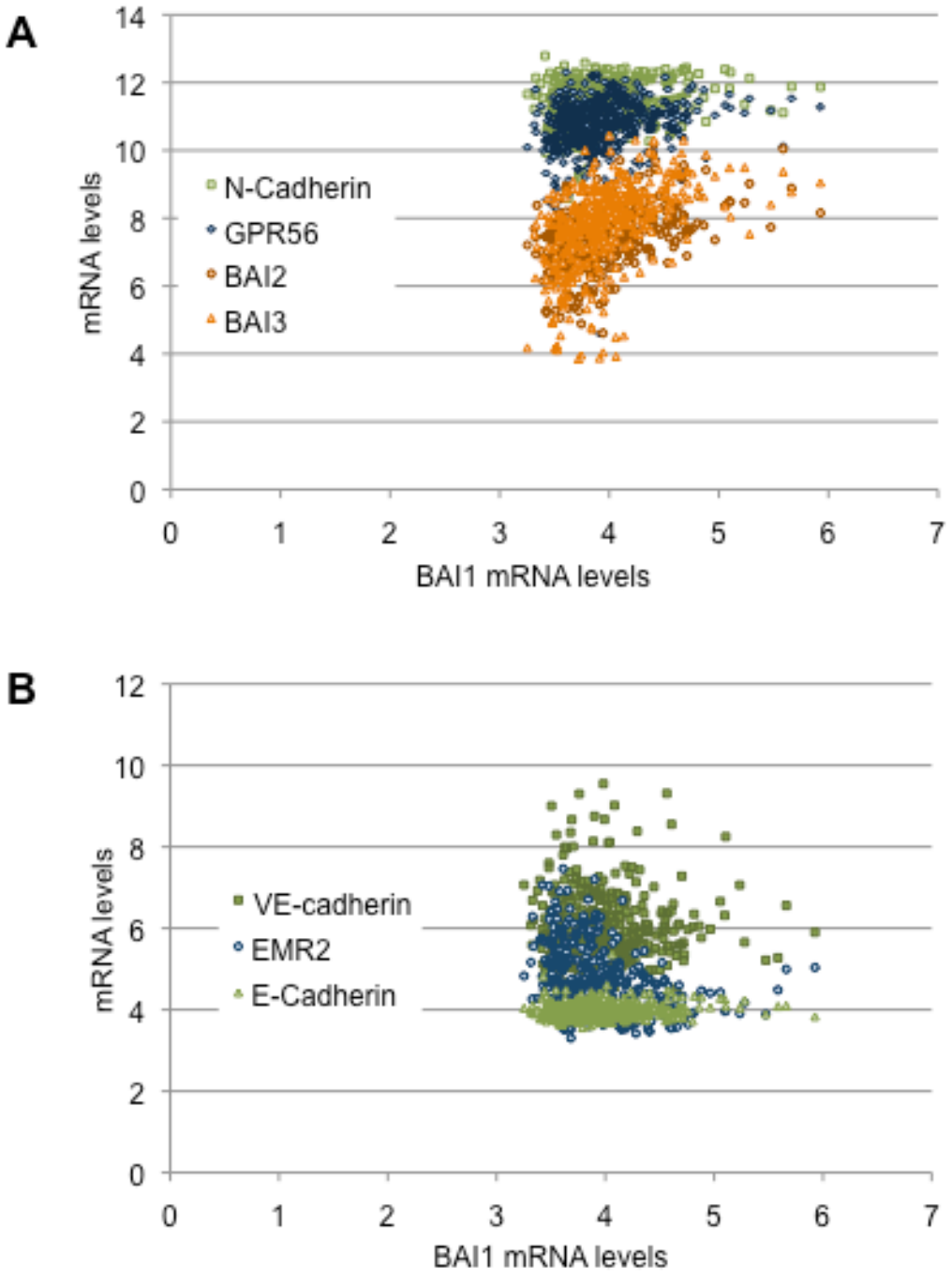

Figure 4.6. BAI1 expression compared with other cell adhesion molecules and GPCRs in GBM. From TCGA. (**A-B**). Association of BAI1 mRNA expression with expression of other cell adhesion molecules (N-, E- and VE-cadherin) and class B GPCRs (BAI2-3, EMR2, GPR56) in GBM tissue samples. Figures plotted using Excel.

A

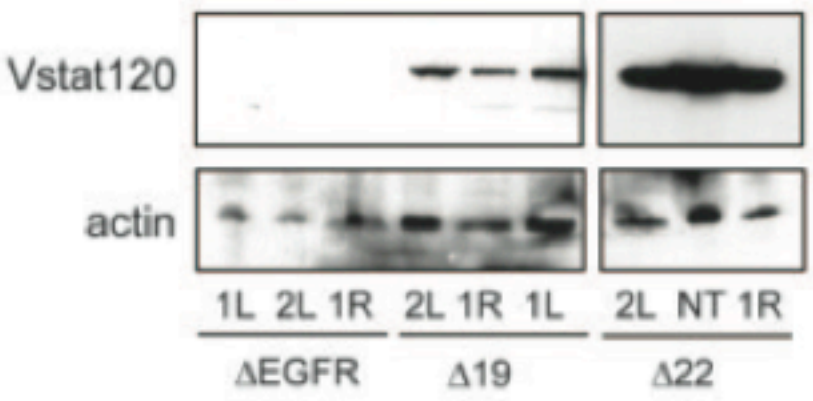
Vstat120
actin
1L 2L 1R 2L 1R 1L 2L NT 1R
ΔEGFR
Δ19
Δ22

B

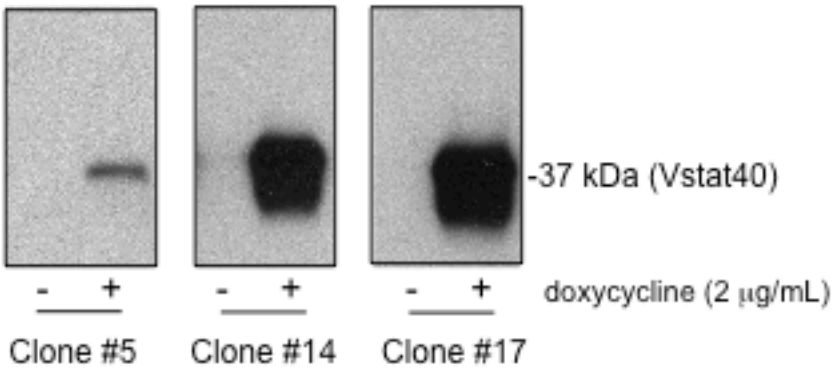
-37 kDa (Vstat40)
- + - + - +
doxycycline (2 μg/mL)
Clone #5
Clone #14
Clone #17

C

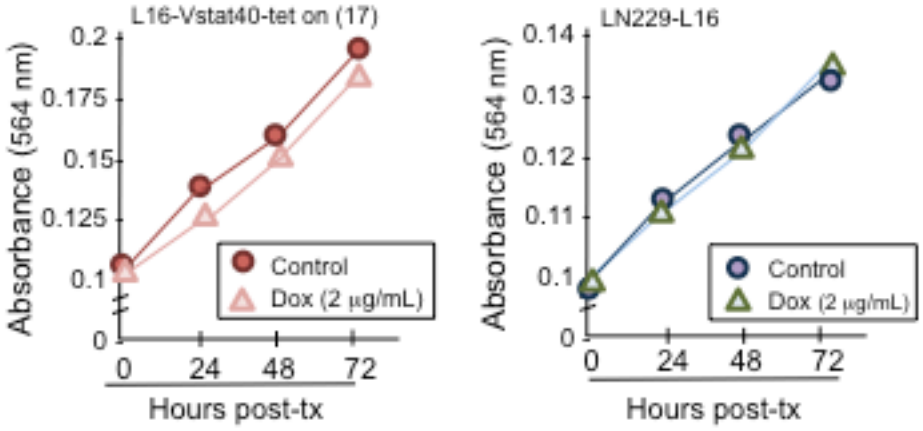
L16-Vstat40-tet on (17)
Absorbance (564 nm)
0.2
0.175
0.15
0.125
0.1
0
Control
Dox (2 μg/mL)
0 24 48 72
Hours post-tx
LN229-L16
Absorbance (564 nm)
0.14
0.13
0.12
0.11
0.1
0
Control
Dox (2 μg/mL)
0 24 48 72
Hours post-tx

Figure 4.7. An inducible model to investigate the anti-tumor activity of Vstat40 *in vivo*.

(**A**) This figure demonstrates expression of Vstat120 in lysates of 3 individual tumors (labeled 1L, 2L, etc.) for each cell line (U87ΔEGFR parental cells, and clones Δ19 and Δ22) grown subcutaneously in *nu/nu* mice.

(**B**) CM from prepared inducible Vstat40-expressing clones cultured in 6-well plates untreated (-) or treated with doxycycline (+) for 48 hours was precipitated and subjected to Western blot to determine levels and cleanliness of Vstat40 induction.

(**C**) Comparison of proliferation of LN229-L16-#17 cells (left) and parental LN229-16 cells (right) in response to doxycycline treatment (2 μg/mL) for up to 72 hours using the SRB assay.

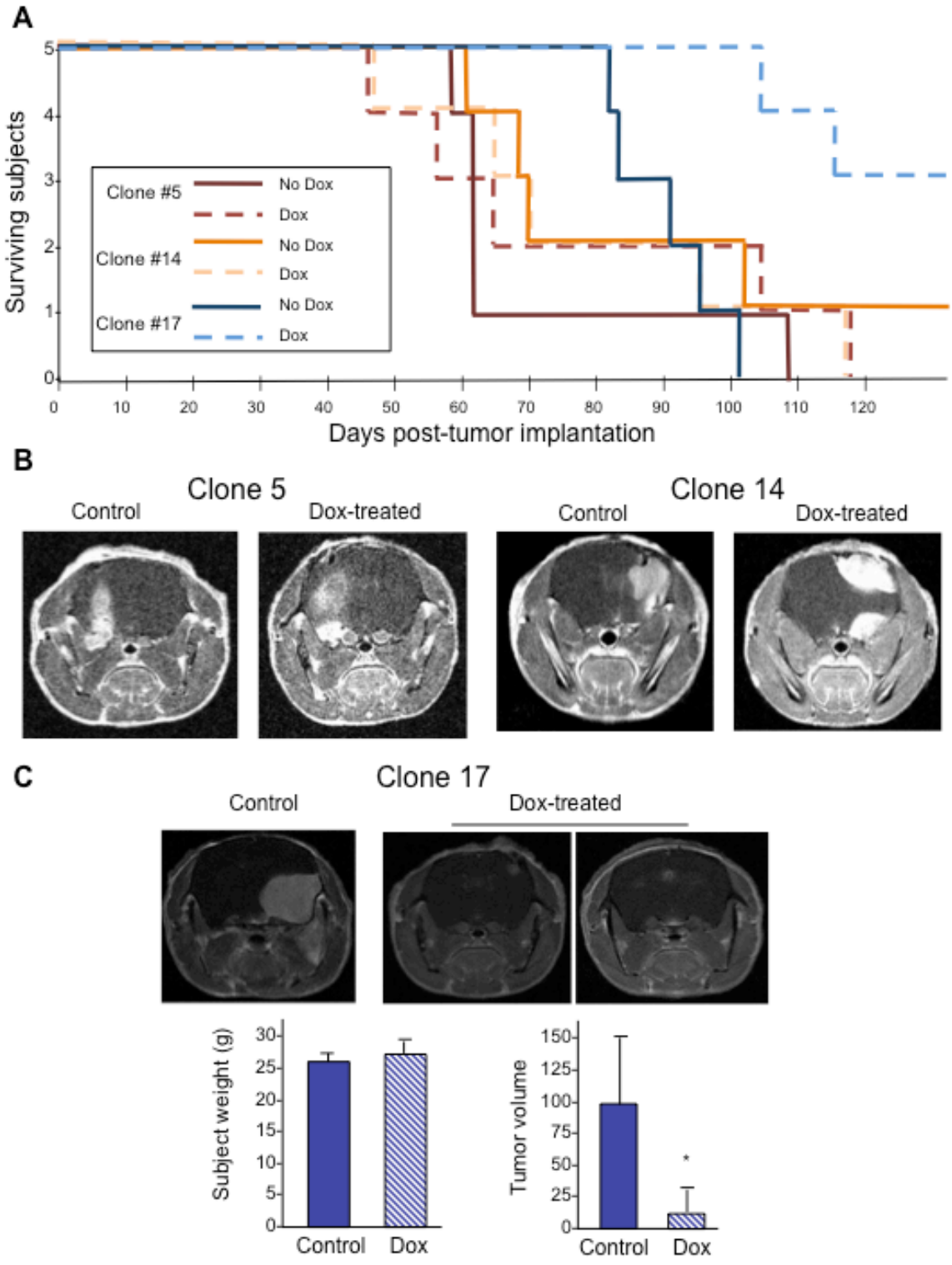
A
Surviving subjects
Days post-tumor implantation
Clone #5
No Dox
Dox
Clone #14
No Dox
Dox
Clone #17
No Dox
Dox
B
Clone 5
Control
Dox-treated
Clone 14
Control
Dox-treated
C
Clone 17
Control
Dox-treated
Subject weight (g)
Control
Dox
Tumor volume
Control
Dox
*

Figure 4.8. Survival and MRI followup of inducible tumor cell clones.

(**A**) Survival curve of control or doxycycline-treated mice (n=5/condition) bearing intracranial tumors for each of the three clones under study. Subjects were implanted intracranially with 10^6 cells and followed for up to 4 months. Subjects received 4% sucrose (control, solid line) or 4% sucrose with 2 mg/mL doxycycline (dashed line) to induce Vstat40 expression 3 days after tumor cell implantation. Kaplan-Meier analysis of statistical significance for the survival of clone-bearing subjects under study as a function of doxycycline administration: clone 5 ($p = 0.704$), clone 14 ($p = 0.585$), clone 17 ($p = 0.002$).

(B) Intracranial observation of tumor growth using MRI. Representative images from T_2-weighted MRI detection of intracranial tumors in mice bearing tumors from clone #5 and clone #14, demonstrating relative tumor burden in control and dox-treated subjects.

(**C**). T_2-weighted MRI detection of intracranial tumors derived from clone #17 cells. Left bottom panel: mean subject weight of subjects bearing clone 17 tumors at time of MRI . Right bottom panel: volumetric reconstruction of clone 17 tumors following MRI using ImageJ (NIH) analytical software.

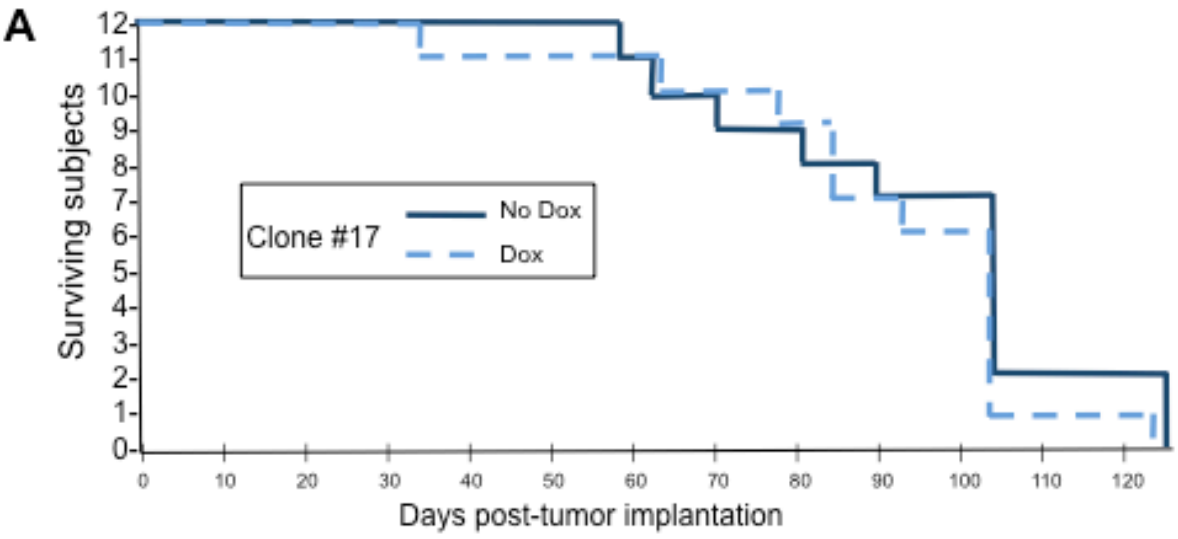
A
Surviving subjects
Clone #17
No Dox
Dox
Days post-tumor implantation

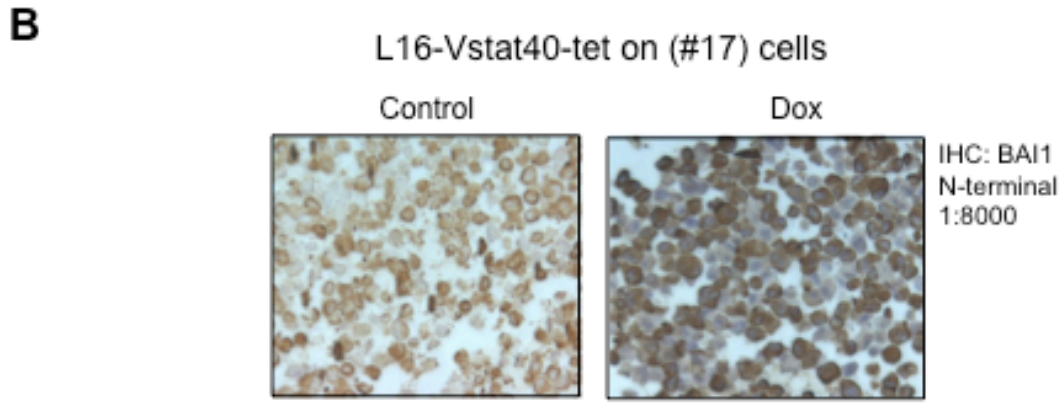
B
L16-Vstat40-tet on (#17) cells
Control
Dox
IHC: BAI1
N-terminal
1:8000

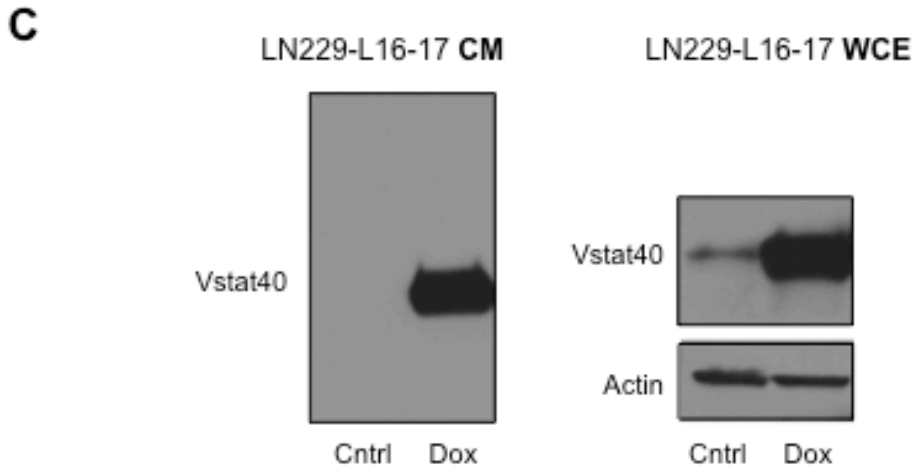
C
LN229-L16-17 CM
LN229-L16-17 WCE
Vstat40
Vstat40
Actin
Cntrl
Dox
Cntrl
Dox

Figure 4.9. Vstat40 does not promote survival in a repeat *in vivo* tumorigenesis experiment.

(**A**) Follow-up study of survival of subjects (n=12 per condition) was performed as previously described for the LN229-L16-17 clone (Kaplan-Meier analysis: $p = 0.45$).

(**B**) Immunohistochemical analysis of Vstat40 expression in LN229-L16-17 cell pellets untreated or treated with doxycycline, using the BAI1 N-terminal antibody (1:8000).

(**C**) Expression of Vstat40 in the CM and WCE of LN229-L16-17 cells used in tumorigenesis experiments to verify specific induction in the presence of doxycycline.

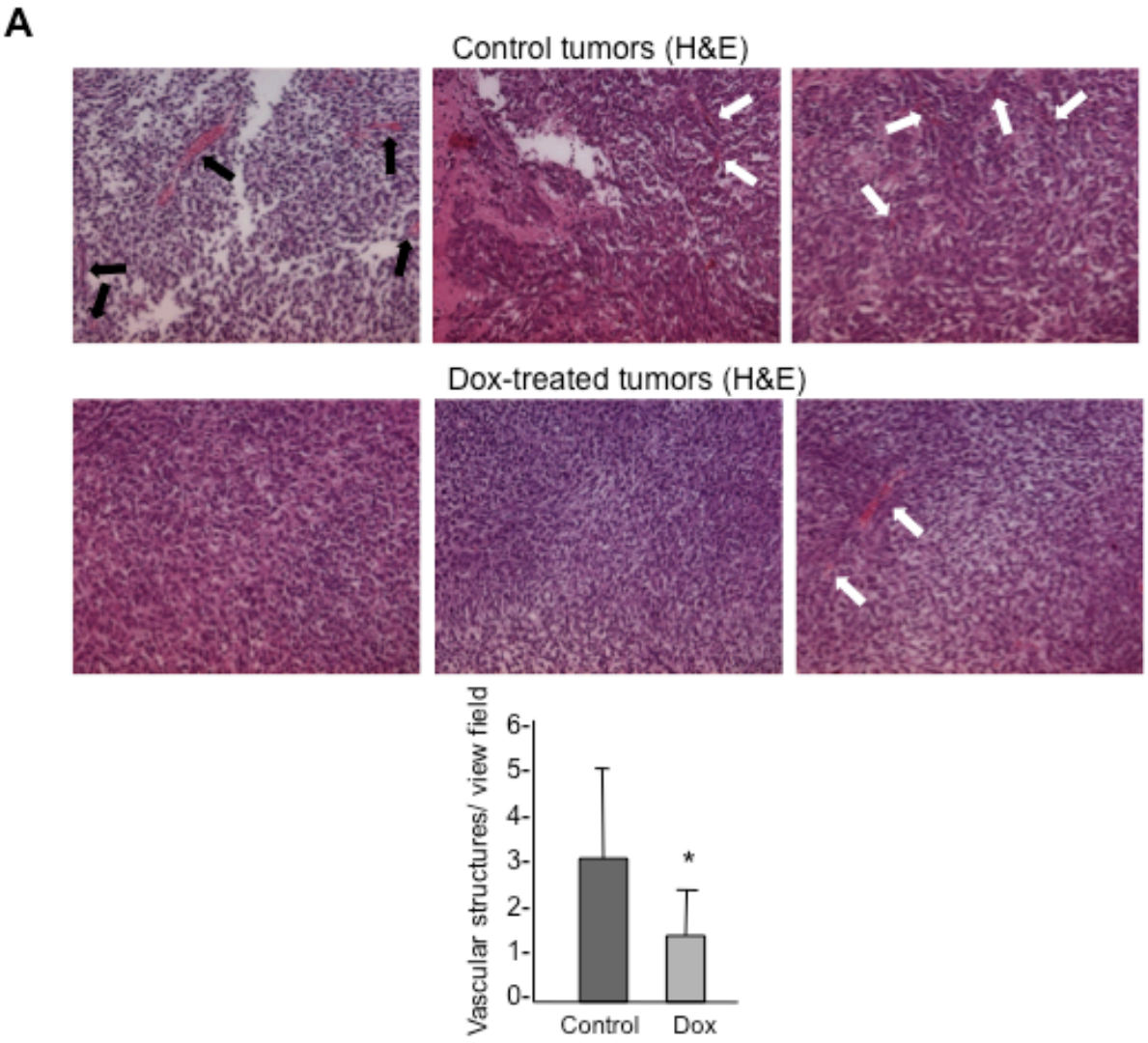
A
Control tumors (H&E)
Dox-treated tumors (H&E)
Vascular structures/ view field
6
5
4
3
2
1
0
*
Control
Dox
B
No dox
Dox (Vstat40)
Cells per view field
30
25
20
15
10
5
0
*
Cntrl
Dox

Figure 4.10. Dox-treated tumors demonstrate reduced tumor-associated vascular structures, altered tumor cell morphology, and a reduction in cleaved caspase 3.

(**A**) Tumor-associated vessels (indicated by arrows) were counted and quantified in clone 17 tumors from subjects receiving control or doxycycline treatment (n=3 tumors/group) in the repeated experiment. Tumors were stained with H&E. Three views were obtained per tumor. Differences in the shape and adhesion properties of control and dox-treated tumors may also be detected. 10x magnification.

(**B**) Immunohistochemistry was utilized to ascertain levels of cleaved caspase 3 in multiple specimens of formalin-fixed control and doxycycline-treated clone 17 tumors. Positively-stained cells were counted in three independent views for each tumor.

CHAPTER 5.

TOWARDS THE FURTHER CHARACTERIZATION OF EXTRACELLULAR BAI1.

Introduction

The experiments described in Chapters 2-4 represent a significant advance in our understanding of the proteolysis and function of extracellular BAI1, particularly the portion identified as Vstat40. As with any system, however, the procedures and reagents used in these previous studies have certain limitations. If these limitations were overcome, future work on BAI1 would be greatly refined and improved.

Specifically, a major limitation of many of the experiments described previously is that they rely on the use of bioactive Vstat peptides secreted into the conditioned medium (CM) from transfected or stable cell lines of variable background. The primary problem with this approach is that it does not account for uncontrolled expression of indeterminate proteins and cytokines into the experimental CM. Expression of these other molecules may be undesirable in cell culture-based experiments for a variety of reasons, not least because of their possible effects on or interference with Vstat activity itself. Under these conditions, the best possible control for these experiments is the use of control CM derived from cells of the same background and concurrent passage. Even with this control, however, strong potential still exists for significant variability in the background composition between control and experimental CM samples.

A more advantageous system would utilize purified recombinant human Vstat (rhVstat) proteins. First, this approach would minimize the presence of contaminating elements in experiments aimed at elucidating the specific bioactivity of the Vstats, enabling greater confidence in the functional characterization data found in Chapter 3 and elsewhere (Kaur et al., 2005; Kaur et al., 2009). This approach would also have other important benefits such as enabling the precise quantification of Vstat activity via the determination of an IC_{50} value in functional assays, such as the angiogenesis assays described in Chapter 3.

Ultimately, the use of purified recombinant Vstats would enable meaningful comparisons of the activities of both Vstat120 and Vstat40 with each other, as well as provide opportunity for comparisons with other angiogenesis inhibitors such as endostatin or thrombospondin-1. To this end, we attempted the generation and purification of recombinant human Vstat proteins using a bacterial expression system (Figure 5.1). Once optimized, such a system would allow the utilization of purified rhVasculostatin peptides in experiments.

Another significant limitation on studies of extracellular BAI1 concerns the dearth of antibodies suitable for its detection. While the BAI1 N-terminal antibody (BNT) used extensively in the research of Chapters 2-4 is a powerful tool to detect both Vstat40 and Vstat120, it conveys no information about the portion of extracellular BAI1 remaining after Vstat40 proteolysis occurs, tentatively referred to as Vstat80. This remaining fragment may exert important biological activity of its own or undergo further proteolysis, however, and thus its detection is critical for a complete understanding of BAI1 biology.

We selected the BAI1 hormone-binding domain (HBD), a domain characteristic of the cell adhesion GPCR subfamily, as an antigenic region for the development of another antibody against extracellular BAI1. These hormone-binding regions are comprised of 30-35 amino acids featuring four highly conserved cysteine residues, which are thought to be essential for the three-dimensional structure of the hormone-binding domain. Some of the receptors in this subfamily have known peptide hormone ligands, including parathyroid hormone (PTH) (Pioszak and Xu, 2008; Zhou et al., 1997), vasoactive intestinal peptide (VIP) (Couvineau et al., 2010) and corticotropin releasing factor (CRF) (Pioszak et al., 2008). Peptides and other agents that interact with the hormone-binding region or other parts of the receptor may thus be used to investigate GPCR function (Fortin et al., 2009; Gomes et al., 1999; Mijares et al., 2000). However, no hormone ligand has yet been identified for many of

the cell adhesion GPCRs, including the BAI family proteins. Like the other cell adhesion GPCRs, the BAI family of molecules has a HBD structure in their N-terminal domain. As described previously, the BAI1 N-terminal domain undergoes multiple known proteolysis events, and the N-terminal domain has at least one non-hormone ligand, phosphatidylserine, which regulates at least one cell signaling pathway via the BAI1 C-terminal domain (Park et al., 2007).

Ultimately, an antibody against the BAI1 hormone-binding domain would be useful for a variety of experimental purposes. One important application of this reagent could be in functional or cell signaling studies of activation or inactivation of the BAI1 receptor. Such an antibody could compete with any identified natural hormone ligand for BAI1 GPCR activity assays, or the enable the detection of other N-terminal cleavage fragments, including the previously undetectable Vstat80 fragment. To this end, we sought to develop and characterize an antibody specifically recognizing the BAI1 HBD.

Materials & Methods

Cloning of GST-Vstat vectors. Vstat40 and Vstat120 were cloned into the pGEX-2T GST expression vector (Invitrogen), which appends two tandem thrombin cleavage sites after a glutathione S-transferase (GST) tag and before the inserted gene of interest. Briefly, the inserts were generated by PCR using a primer complementary to an endogenous BamHI site at the 5' end of the gene and a primer introducing an EcoRI restriction site at the 3' end, and subsequently gel-purified (Qiagen). Inserts and vector were digested by BamHI and EcoRI enzymes (New England Biolabs) at 37 ^{o}C for 5 hours. Digested DNA was gel-purified, quantified and ligated using T4 DNA ligase (Invitrogen) according to the manufacturer's instructions. Composition of resulting constructs was verified by digestion with restriction enzymes.

Bacterial culture and induction. Bacterial strains utilized in this experiments were TOP10 (Invitrogen) and BL21.DE (Invitrogen), where indicated. E.coli were transformed with the generated pGEX-2T-Vstat constructs and an aliquot amplified at 37 ^{o}C at an agitation of 250 rpm. Induction with allolactose homolog isopropyl β-D-1-thiogalactopyranoside (IPTG) (0.1-1 mM) was carried out when the bacterial density yielded a reading of OD_{600}: ~0.7 using a spectrophotometer (approximately 3 hours). Following stimulation with IPTG, bacteria were grown with agitation at 30 ^{o}C for an additional 3 hours prior to harvest or subsequent experimental manipulation.

Western blot. For Western blot analysis, induced bacterial slurries were centrifuged at 15,000xg for 25 minutes to generate a bacterial pellet. Aliquots of sonicated bacterial pellets were resuspended in 1x denaturing sample buffer and boiled for 3-5 minutes to reduce blot smearing caused by high levels of DNA in the sample. Solubilized and dialyzed samples, in addition to the wash buffers and all supernatants, were precipitated with 4 volumes of ice-

cold acetone overnight, centrifuged 10,000xg for 15 minutes and air-dried prior to resuspension in 1x sample buffer. SDS-PAGE was performed on 10% Criterion gels (BioRad) and transferred to nitrocellulose at 87V for 1.5 hours at 4 ^{o}C, followed by blocking with fresh 5% PBST-milk for one hour and overnight incubation with the primary antibody, the anti-BAI1 N-terminal antibody described previously.

Bacterial pellet lysis. Centrifuged bacterial pellets were lysed for 25 minutes on ice using lysis buffer: 100 mM Tris-Cl, 0.1% Triton X-100, 50 mM PMSF, protease inhibitors (Calbiochem) and 1mM DTT. Lysates were centrifuged 15,000xg for 25 minutes to generate a supernatant (soluble fraction) and pellet (insoluble fraction comprised of inclusion bodies). Supernatants and pellets were precipitated with 4 volumes ice-cold acetone for Western blot analysis or subjected to further manipulation.

Inclusion body resuspension. Inclusion bodies containing the GST-Vstats were solubilized using 8M Urea buffer. A washing protocol was developed to solubilize the protein, consisting of four steps with associated buffers (Doonan, 1996). Lysis: 100 mM Tris-Cl, 50 mM EDTA, 50 mM PMSF, lysozyme (300 μg/mL), sodium deoxycholate (1 mg/mL) and DNAse (10 mg/mL). Lysates were incubated for 30 minutes on ice on rocker. Wash 1: Lysis buffer + 2M urea + 0.5% Triton X-100. Lysates were incubated for 4 hours at RT on rocker. Wash 2: Lysis buffer + 4M urea + 0.5% Triton X-100. Lysates were incubated for 2 hours at RT on rocker. Solubilization: 8M urea, 50 mM Tris, 1 mM DTT. Final incubation ran overnight at RT, on rocker.

Purification with dialysis. The dialysis was performed using ThermoScientific dialysis cassettes (Catalog #87724). A volume of 15 mL solubilized GST-Vstat solution was placed in the cassette and immersed in a covered beaker containing the indicated solutions of decreasing urea concentration for the indicated time intervals. Constant stirring occurred

during dialysis. (1) 24 hour incubation: 4M Urea, 50 mM Tris. (2) 24 hour incubation: 2M Urea, 50mM Tris. (3) 24 hour incubation: 1M Urea, 50 mM Tris. (4) 24 hour incubation: 0.5M Urea, 50 mM Tris. Aliquots of dialysate were removed during each buffer change for subsequent analysis or experimental manipulation.

Glutathione pulldown and thrombin proteolysis. Dialysate was incubated with glutathione resin (ratio 1mL dialysate to 300 uL beads) at 4 degrees Celsius overnight. Following incubation, resin was centrifuged at 1500xg for 15 minutes at 4 degrees C and washed 1x PBS. The pulldown fraction was resuspended in 300 uL PBS and incubated with 1 U catalytically active human thrombin (Sigma, Catalog #T4648) on the rocker at room temperature overnight. Samples were centrifuged as before to yield supernatant and pellet fractions for analysis with SDS-PAGE and Western blot.

Generation of the anti-HBD antisera. The rationale for the selection of the antigenic region of the BAI1 hormone-binding domain is described in the Results section. The sequence was entered into Basic Local Alignment Search Tool (BLAST, www.ncbi.nlm.nih.gov/blast/) database search engine to confirm a high degree of sequence homology specificity for the human BAI1 gene. Synthesis and keyhole limpet hemocyanin (KLH) conjugation of the chosen antigenic sequence, CELDEEGIAYWEPPT, was performed at Pocono Rabbit Farm and Laboratory, Inc. 666 Dutch Hill Road, PO Box 240, Canadensis, PA 18325. This peptide was used to immunize a chosen rabbit using the company's commercial Quick Draw (28 day protocol) procedure.

Four preimmune sera were screened by Western blot for overall background levels against a battery of cell and tissue lysates. All antisera were assessed at a dilution of 1:1000. The rabbit with the least background immunoreactivity was selected for immunization with the antigenic HBD peptide, with the understanding that low background levels could

potentially indicate a sluggish immune system and the possibility of inefficient antibody production. The immunized rabbit was boosted 4 times, with a 15 mL blood draw obtained after every immunization for analysis. A total of 120 mL of antiserum was obtained.

Results

Expression of GST-Vstat40 in inclusion bodies. In developing a protocol to optimize GST-Vstat induction, we observed that bacteria transformed with the pGEX2T-Vstat40 vector produced a protein of approximately 55 kDa detectable by the BAI1 N-terminal antibody. This band was observed when the bacterial slurry was treated with IPTG at any of the indicated dilutions for any of the durations under study (Figure 5.2A). This corresponds to the size of the expected product of the GST tag (approximately 20 kDa) coupled to the Vstat40 peptide. As this peptide appeared to be marginally increased at the highest level of IPTG tested (1 mM) when treated for 3 hours, further experiments on this construct were conducted under these conditions. Of note, the BAI1 N-terminal antibody recognizes a background bacterial protein of approximately 60 kDa, which is observed in both IPTG-treated and control bacterial slurries. We confirmed that this peptide was not due to some nonspecific effect of either the transformation itself or the introduction of a Vstat40-containing vector (Figure 5.2B), as no Vstat40 peptide was observed in extracts from *E.coli* transformed with a pcDNA3.1-Vstat40 vector.

We next wished to determine whether the GST-Vstat40 peptide was present in the supernatant of the slurry lysate or whether it was localized in insoluble inclusion bodies. If present in the supernatant, this peptide could be purified from the background with relative ease, using reduced glutathione. Analysis of supernatants and inclusion body fractions from IPTG-treated pGEX2T-transformed *E.coli* confirmed that under present induction conditions the GST-Vstat40 band is specifically localized to the inclusion body fraction, and that this band is specifically due to induction of the GST-Vstat40 peptide (Figure 5.3A). An additional protocol to wash and solubilize the inclusion fraction was developed, demonstrating that the GST-Vstat40 can be solubilized with minimal background using an

8M Urea buffer (Figure 5.3B). Ultimately, this solubilized fraction must be dialyzed into appropriate buffer conditions before proceeding with purifying the recombinant protein.

Expression of GST-Vstat120 in inclusion bodies. We next expressed the GST-Vstat120 vector in E.coli and observed that a peptide of approximately 150 kDa was induced under induction conditions similar to those previously described for GST-Vstat120 (data not shown). However, this construct yielded a significant amount of background detected by the BAI1 N-terminal antibody. We therefore elected to induce this construct with 0.1 mM IPTG in further experiments. As with GST-Vstat40, the GST-Vstat120 peptide and the majority of the background proteins were observed to localize in inclusion bodies. These peptides were solubilized only with 8M urea buffer; very little signal was observed in the wash buffer fractions (Figure 5.4A). This finding was observed in both TOP10 and BL21.DE *E.coli* transfected with the GST-Vstat120 construct (Figure 5.4B).

Initial results of purifying dialyzed GST-Vstat40 with reduced glutathione and thrombin. We wished to dialyze the solubilized inclusion body containing GST-Vstat40 in order to create buffer conditions suitable for GST pulldown and thrombin cleavage. To this end, the solubilized GST-Vstat40 was dialyzed in buffers of decreasing urea concentration using dialysis cassettes. Aliquots of the dialysate were taken with each buffer change to monitor for sample loss (Figure 5.5A). Other dialysate aliquots were also incubated with glutathione resin and subsequently with thrombin in an attempt to release purified Vstat40 into the slurry supernatant. While incubation with thrombin yielded a previously unobserved fragment corresponding in size with cleaved Vstat40, this fragment was unexpectedly observed in both the supernatant and glutathione pellet fraction (Figure 5B), suggesting that Vstat40 may interact nonspecifically with the glutathione resin. A final step to remove

thrombin from the reaction was not attempted but would be necessary to proceed with purification.

To investigate the possibility of nonspecific interaction with glutathione, nontagged Vstat40 was generated in the CM of mammalian cells and incubated with the glutathione resin or a control agarose resin. While a minimal amount of unbound Vstat40 was observed in the supernatant of the glutathione pulldown, a larger amount was observed to be retained in the bead fraction (Figure 5.5C). In contrast, no Vstat40 was observed to be pulled down by the agarose beads. In sum, these findings suggest that Vstat40 may have some previously unknown specific interaction with glutathione. More immediately, it presents a significant complication for purifying Vstat40 via this approach. Further troubleshooting will be required to generate purified recombinant human Vstat40.

Factors complicating GST-Vstat120 purification. As observed in Figure 5.4A, a significant amount of nonspecific background is initally retained in the insoluble pellet fraction when the GST-Vstat120 inclusion bodies are solubilized. In the hopes of reducing this background prior to thrombin purification, we wished to determine whether the pH of the dialysate of solubilized GST-Vstat120 could be altered to improve binding of the solubilized protein to the reduced glutathione. Following dialysis, the GST-Vstat40-containing solution was found to have a pH of approximately 9. The solution was divided into equal aliquots and pH-adjusted to the indicated values prior to incubation with reduced glutathione. We observed that solutions adjusted to a pH of 7-8 showed improved peptide binding to glutathione (Figure 5.6A). This step will be important in future studies for removing the background for GST-Vstat120.

An additional problem with the thrombin approach to purification of the recombinant Vstat120 protein is that Vstat120 itself appears to be cleaved by thrombin.

Extracellular BAI1 contains one motif that is identical to one of the two known thrombin recognition sites, Gly-Arg-Gly$_{428}$ (Figure 5.6B). This site is not found in Vstat40 but is present in the Vstat120 in the second TSR. Thus, while thrombin has not been demonstrated to process extracellular BAI1, it is possible that it may cleave Vstat120 at this site. If this is demonstrated to occur, purification with thrombin of the entire GST-Vstat120 peptide may not be a possibility. In support of this hypothesis, we observe that when dialyzed GST-Vstat120 is treated with thrombin, an additional band appears to be amplified in the subsequent supernatant (Figure 5.6C, arrow). This band corresponds to the correct size of the piece recognized by the BAI1 N-terminal antibody if Vstat120 were cleaved at the predicted thrombin cleavage site.

Identification of a desired antigenic region in the hormone-binding domain of human BAI1. In designing an appropriate antibody against the HBD of BAI1, selection of a desirable antigenic region in the BAI1 HBD was determined in consultation with R. Hall. Preferably, an antigenic sequence should be between 12-25 amino acids, as longer sequences may promote structural complications. The sequence should contain no glycosylation modification sites. Internal cysteines should be avoided due to the coupling to KLH via a cysteine. We sought to minimize certain amino acids, including cysteine, methionine, arginine, tryptophan, and glutamine, as well as the number of hydrophobic amino acids in the sequence. No glutamic acid residues were included at the N-terminal end of the sequence to prevent the formation of pyroglutamine by cyclization. Conversely, proline and tyrosine residues are optimal and promote antigenicity. In accordance with these guidelines, the human BAI1 sequence CELDEEGIAYWEPPT was ultimately chosen as the source for the HBD antibody.

It should be noted that the mouse hormone-binding domain contains a similar sequence, CELDEEGIA**F**WEPPT (Figure 5.7A), where the two species' sequences are identical except for the tyrosine substitution to a phenylalanine. As tyrosine is an antigenic residue, this substitution may interfere with the effectiveness of this antibody in any future administration to mice, or the detection of murine BAI1-derived peptides by Western blot.

Characterization of antiserum against the hormone-binding domain. The antiserum was assessed for recognition of the BAI1 N-terminal domain by Western blotting against cellular extracts lacking or expressing BAI1. Specifically, whole cell extracts were prepared from 293 cells mock-transfected or transfected with Vstat120, wild-type BAI1 or a combination of the two vectors. The benefit afforded by this approach is that it verifies both that the antiserum is specifically recognizing BAI1 and that the recognition is specific to the N-terminal domain. Compared to the background signal from identical extracts probed with the preimmune serum (Figure 5.7B, left panel), the anti-HBD antiserum specifically recognized the Vstat120 and full-length BAI1 proteins (Figure 5.7B, middle panel). Identity of the recognized proteins was verified using the BAI1 N-terminal antiserum (BNT, Figure 5.7B, right panel). Of note, Western blotting with BNT yields a stronger signal than blotting with the HBD antibody when the primary antiserum is incubated at equivalent dilutions (1:1000). This suggests that BNT has a higher affinity for the denatured BAI1 protein than HBD, though the significance of this association is unclear.

Detection of BAI1 fragments in CM. The HBD antiserum was able to detect the presence of the Vstat120 fragment in the CM of 293 cells transfected with either wild-type or S927D mutant BAI1 cDNA (arrow; Figure 5.7C). As shown by the N-terminal antibody, the S927D construct yielded much higher levels of Vstat120 peptide. No fragment corresponding to Vstat40 was detected by the HBD under these conditions, as expected. Other bands were

detected in the CM of these transfected cells (indicated by asterix), but further characterization is necessary to determine whether these bands represent other events of proteolysis of the BAI1 extracellular domain, or whether they are nonspecific CM proteins recognized by the antiserum, as has been shown for the N-terminal antiserum.

Discussion

Retention of overexpressed proteins in inclusion bodies presents a major challenge for those interested in purifying these molecules. In the present work, we have shown that we have cloned the Vstat proteins into GST vectors and that the resulting constructs yield GST-Vstats in the presence of IPTG. We have further shown that the inclusion bodies containing the Vstats may be solubilized in 8M urea, and that this solution may be dialyzed into a Tris buffer for further purification via pulldown with reduced glutathione. However, under the conditions of the system, the majority of the dialyzed GST-Vstats either did not bind to the reduced glutathione or was present in the wash buffer. Further optimization of the dialysis and glutathione binding steps will be required if any large-scale production of GST-Vstats is to be attained by this method.

Notably, we were able to precipitate GST-Vstat40 using reduced glutathione. However, we show that non-GST-tagged Vstat40 expressed in the conditioned medium of mammalian cells was also able to bind to reduced glutathione. This is likely due to the predicted glycosylation of Vstat40 or some other aspect of its three-dimensional conformation. However, it casts doubt on the assumption that the purification of GST-Vstat40 is due to a highly specific GST-glutathione interaction. Further work is necessary to determine the integrity of the GST tag and to characterize the nature of the Vstat40-glutathione interaction. If a way to avoid Vstat40-glutathione binding can be found, the preliminary data show that bead-attached GST-Vstat40 may be processed into a fragment corresponding to the size of Vstat40 following incubation with thrombin, suggesting that this approach is able to yield the desired recombinant Vstat40 peptide. Again, troubleshooting to improve the efficiency of thrombin cleavage will be useful in increasing the generation of

rhVstat40. Further characterization with HPLC and mass spectrometry will be required to verify identity and purity of this preparation.

Purification of rhVstat120 poses a larger challenge due to the high levels of background generated by construct induction and which are retained in the inclusion bodies. The origin of these fragments is not immediately apparent. If many of these fragments are due to GST-Vstat120 degradation by bacterial enzymes, purification of the desired full-length peptide is likely to pose a significant challenge. Another problem with the current approach is that thrombin appears to cleave Vstat120 at a canonical thrombin cleavage site within the molecule itself. If GST-Vstat120 is to be purified, a different method of eluting it from the glutathione slurry will have to be identified.

Further work is necessary to best elucidate how to purify the GST-Vstats from the inclusion bodies. Preliminary work with 8M urea, dialysis and alterations of system pH yielded modest success but it is likely that much of the expressed protein is lost in the process. After a more effective approach is achieved, final experiments should focus on characterizing the subsequent peptides with a combination of HPLC and mass spectrometry. Once this is achieved, future experiments can begin to more precisely elucidate the function of the Vstat proteins.

Even if this purification system were ultimately optimized and yielded the desired recombinant Vstat peptides, a major limitation of this system is that the peptide is currently expressed in bacterial cells, not mammalian cells. While this permits expression of a large amount of relatively pure protein, it raises questions about its functionality. This is particularly relevant for BAI1 as its extracellular domain is believed to be heavily glycosylated, which is very likely to contribute to its function and is a mechanism that is not present in bacteria. There are thus concerns about the three-dimensional structure of the

GST-Vstats in this system with important implications for the functionality of the resulting peptides. One potential solution to this problem would be to express the constructs in insect cells, which are able to attach modifications such as glycosylation.

Another potential alternative would avoid complications of dialysis and tag removal altogether. If the Vstats nonspecifically bind glutathione, this interaction could potentially be used to purify bioactive Vstats directly from the conditioned medium. Due to the likelihood of CM contaminants also binding to the glutathione, this approach may prove problematic. It may however be worth a serious attempt, if a cell line with minimal secretion of background peptides is identified.

In addition to the work on GST-tagged Vstat peptides, in this chapter we also demonstrate generation of antiserum that specifically recognizes the hormone-binding domain of BAI1 under the reducing conditions of gel electrophoresis. We further show that the antiserum is sufficient to recognize the BAI1 extracellular domain, both as a part of the full-length BAI1 receptor and when secreted into the CM, with high specificity and low background. The HBD antiserum is able to detect Vstat120 and replicate and confirm findings of the BNT antibody of relative Vstat120 levels when derived from either the wild-type or S927D mutant BAI1 cDNAs. As expected, the HBD antiserum does not detect Vstat40, as this fragment does not contain the HBD.

This antibody is likely to prove useful for many applications. The antibody may already be incorporated into ongoing studies of BAI1 extracellular domain proteolysis. It may also be an asset in studies of BAI1 function as either a mediator of engulfment or angiogenesis inhibitor. If the endogenous ligand for the BAI1 HBD is identified, the antibody may be able to compete for ligand-receptor binding, or function as an agonist. Such an interaction would permit finely-tuned study of BAI1 function either under cell culture conditions or *in vivo*. For

this and similar applications, it may thus be desirable to separate out the HBD antibody with an additional purification step in order to remove background contaminants.

Further characterization will be necessary to fully understand the biological activity of the HBD antibody. We have shown that it recognizes BAI1 under the denaturing conditions of Western blot, but have not tested whether the antibody recognizes the BAI1 hormone-binding domain in its native conformation, which may preclude its use in assays of that domain's functionality. More research will thus be necessary to determine whether the antibody recognizes nondenatured BAI1, preferably using functional assays such as reporter assays for the activity of Rho, Rac or β-catenin. Overall, the development of this antibody constitutes an important step for a more complete understanding of the complex interplay of proteolysis and ligand-binding activity of the BAI1 N-terminal domain.

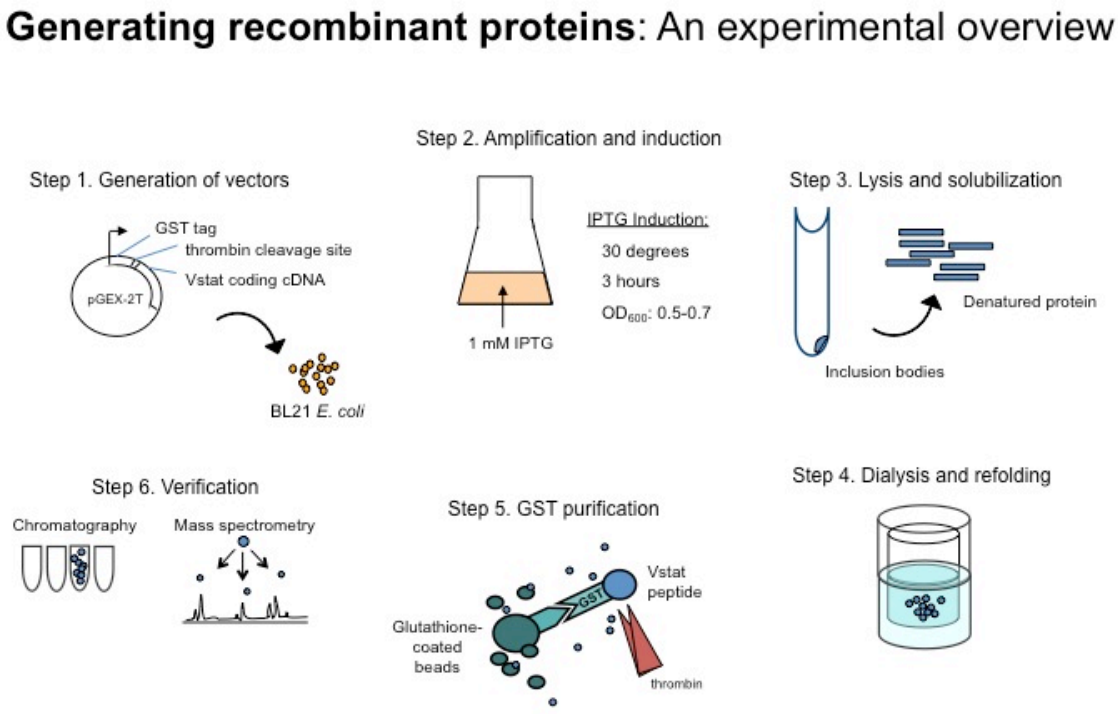

Figure 5.1. Schematic of steps involved in producing and purifying recombinant Vasculostatin peptides.

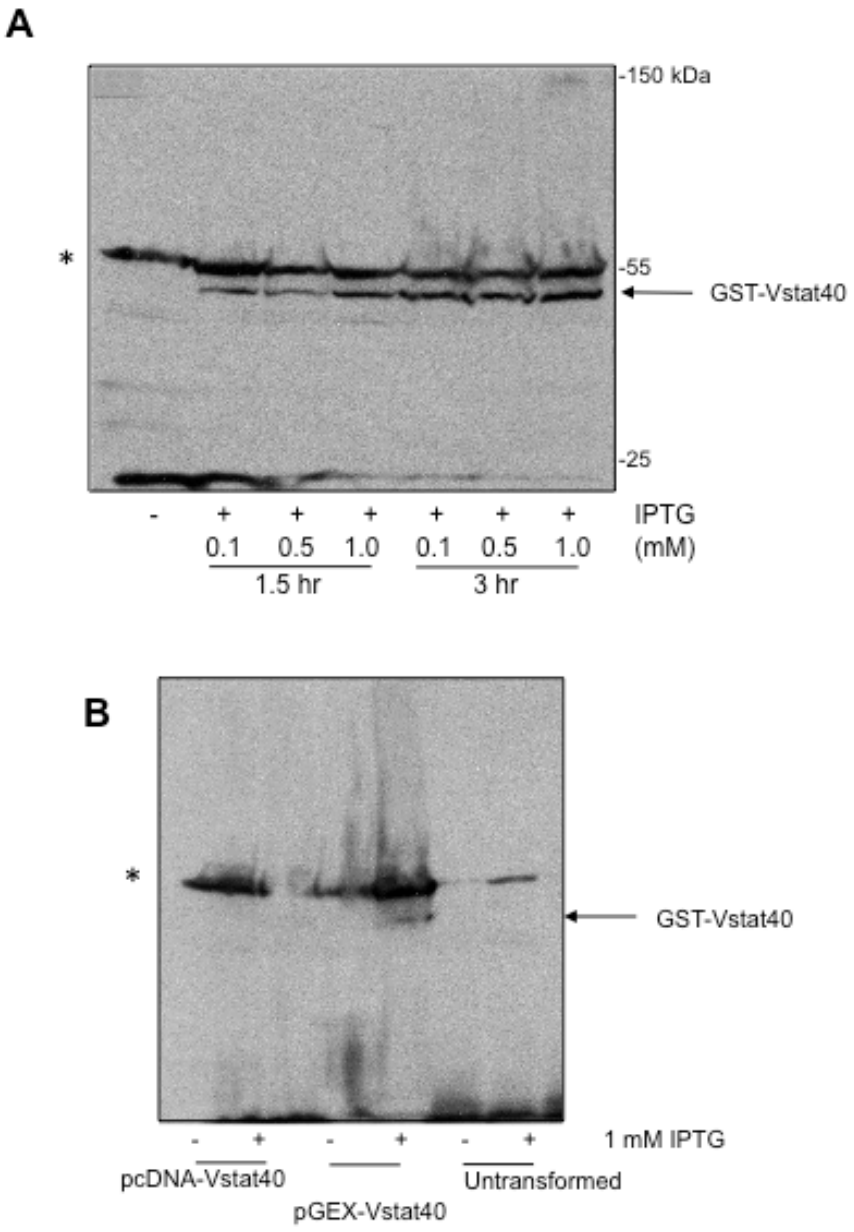

Figure 5.2. GST-Vstats are inducible following IPTG stimulation. (**A**) Results of IPTG treatment of TOP10 E. coli transformed with pGEX2T-GSTVstat40. Western blot analysis of pellet lysates with the BNT antibody. (**B**) Comparison of IPTG treatment of E.coli transformed with pGEX2T-GSTVstat40 or pcDNA-Vstat40 to confirm specificity of induction. * indicates nonspecific background.

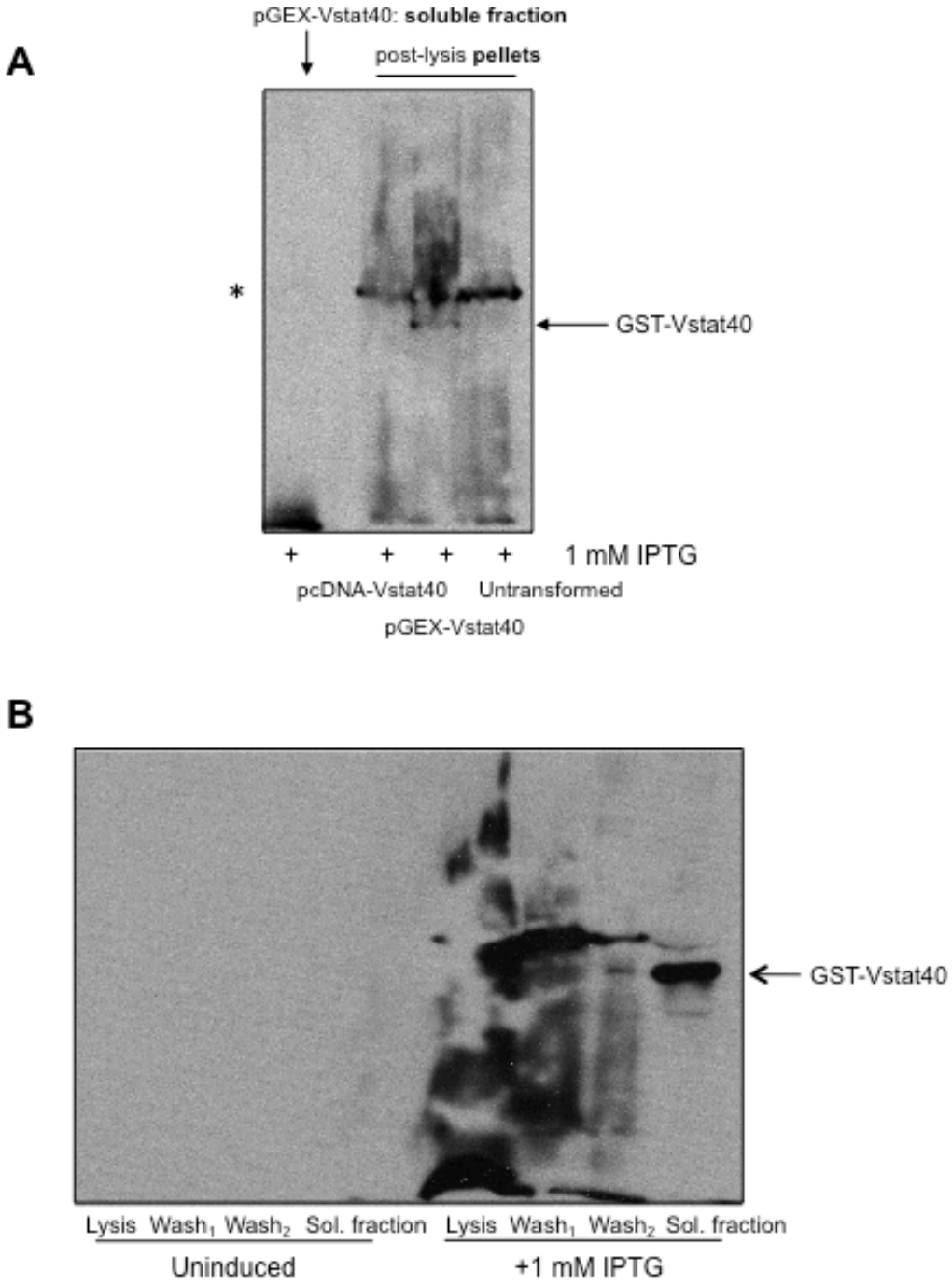

Figure 5.3. GST-Vstat40 is localized in inclusion bodies following induction and lysis. (**A**) Western blot demonstrating specific localization of GST-Vstat40 in *E.coli* inclusion bodies. (**B**) Optimization of a washing protocol to remove background from the GST-Vstat40 inclusion body pellets. * indicates nonspecific background.

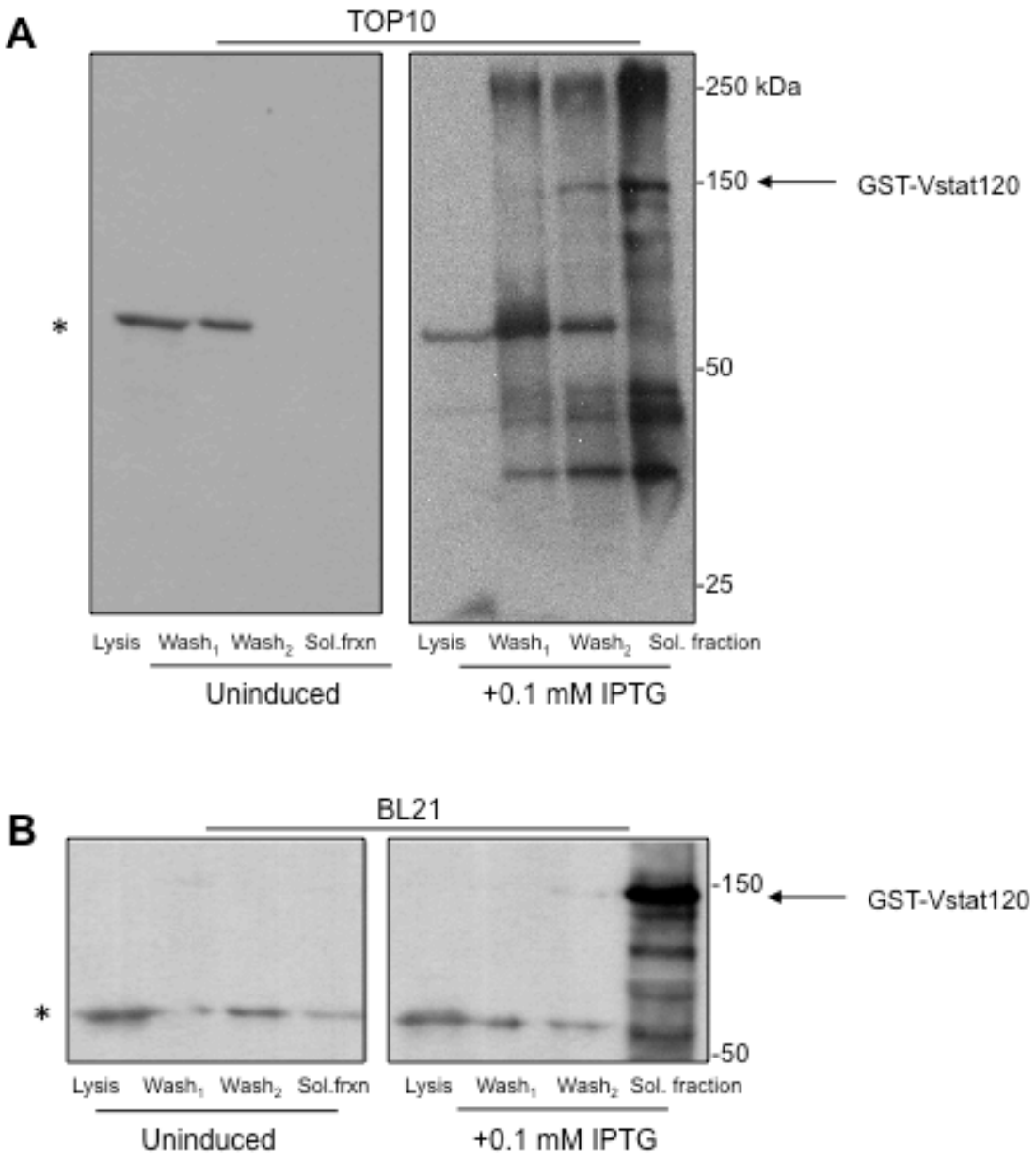

Figure 5.4. Isolation of the GST-Vstat120 inclusion body fraction. (**A**) Isolation of the GST-Vstat120 inclusion body pellet from TOP10 *E.coli* using the washing protocol. (**B**) Similar expression and isolation of GST-Vstat120 from BL21.DE *E.coli*. * indicates nonspecific background.

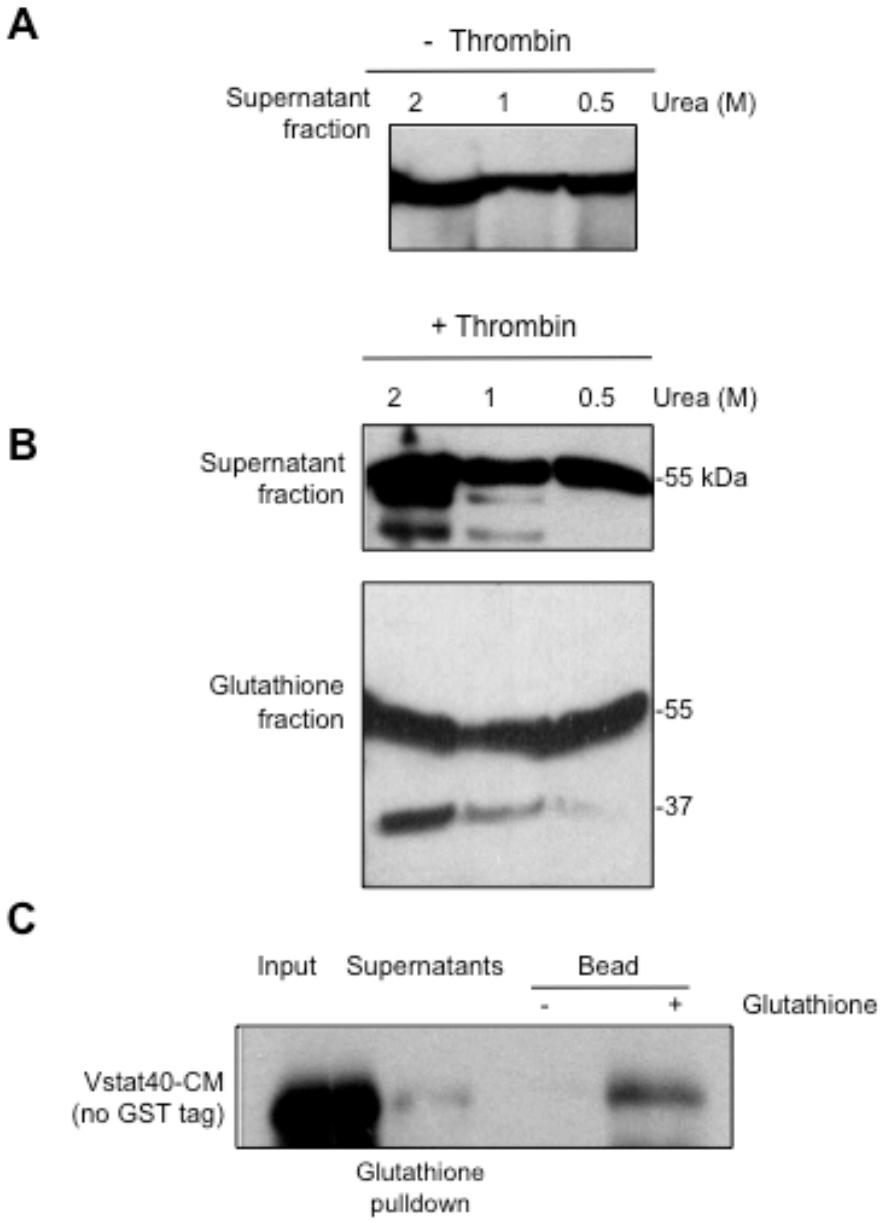

Figure 5.5. Dialysis and pulldown of GST-Vstat40. (**A**) Western blot demonstrating successful pulldown of solubilized, dialyzed GST-Vstat40 by gluthatione resin. (**B**) Western blot showing cleavage of pulled down GST-Vstat40 by recombinant human thrombin and both released into the supernatant and retained in the bead fraction. (**C**) Retention of non GST-tagged Vstat40 prepared from the CM of mammalian cells in the glutathione bead fraction.

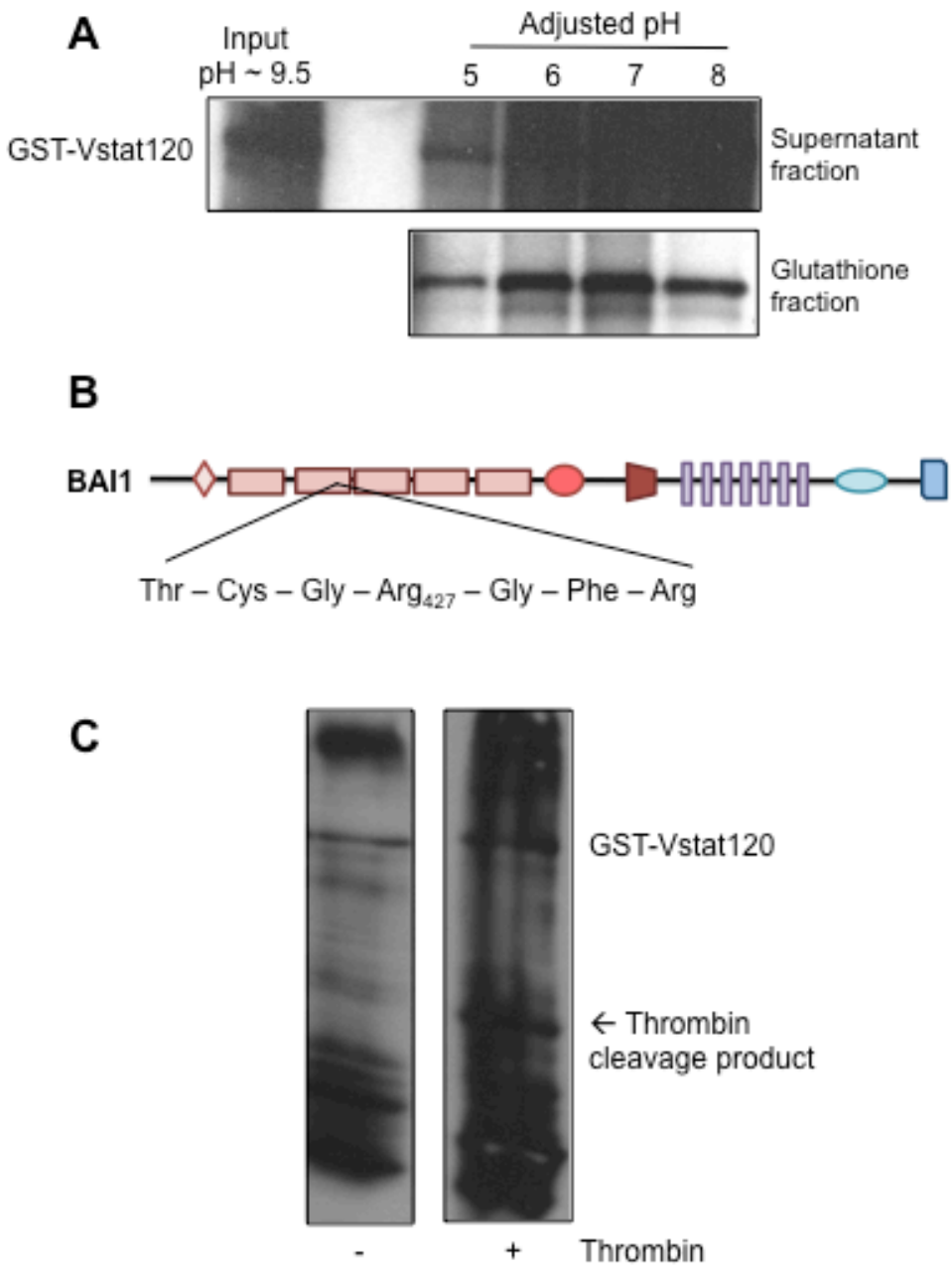

Figure 5.6. Factors affecting GST-Vstat120 purification by pulldown. **A**) Effect of modulating pH on solubilized GST-Vstat120 pulldown by gluthathione resin. (**B**) Schematic of canonical thrombin cleavage site in extracellular BAI1. (**C**) Western blot depicting increased levels of a previously unidentified fragment when GST-Vstat120 is incubated with thrombin, suggesting that thrombin may process the BAI1 extracellular domain.

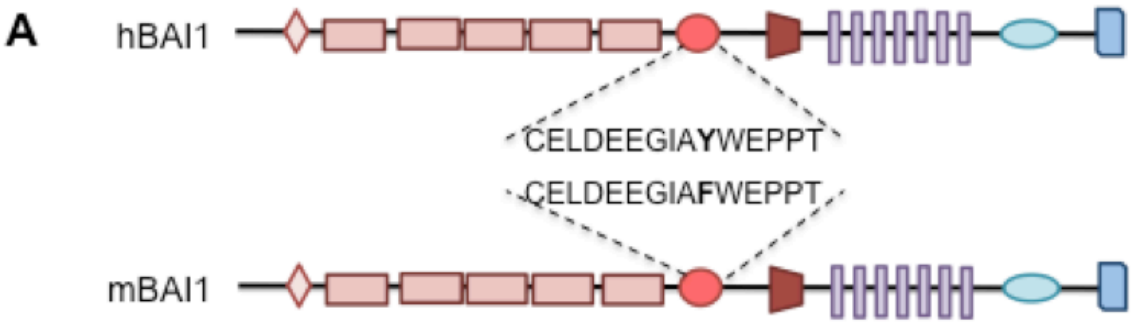
A
hBAI1
CELDEEGIAYWEPPT
CELDEEGIAFWEPPT
mBAI1

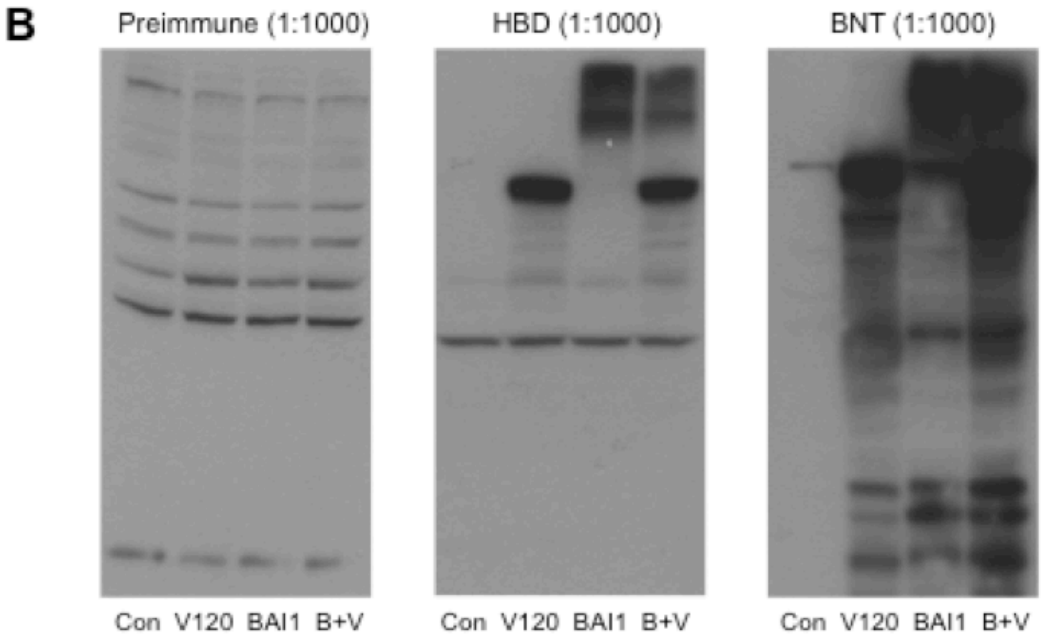
B
Preimmune (1:1000)
HBD (1:1000)
BNT (1:1000)
Con V120 BAI1 B+V
Con V120 BAI1 B+V
Con V120 BAI1 B+V

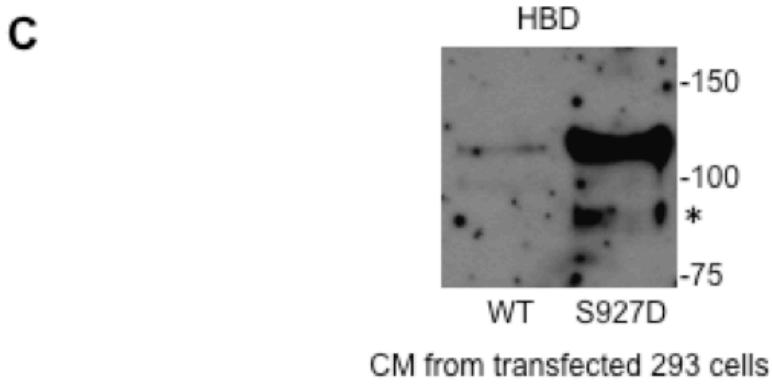
C
HBD
-150
-100
*
-75
WT S927D
CM from transfected 293 cells

Figure 5.7. Development of an antiserum against the BAI1 HBD.

(**A**) Schematic of location and composition of antigenic peptide selected to generate the HBD. Antigenic human sequence is shown in comparison to corresponding mouse sequence.

(**B**) Comparison of 293 extracts expressing indicated constructs and analyzed by Western blot. Left: Extracts probed with the HBD preimmune serum (1:1000). Middle: Extracts probed with the HBD antiserum (1:1000). Right: Extracts probed with the BAI1 N-terminal antibody (1:1000).

(**C**) CM from WT or S927D BAI1-expressing cells probed with the HBD antibody, replicating the findings of Vstat120 expression when probed with the BNT antibody.

CHAPTER 6.

DISCUSSION AND FUTURE DIRECTIONS.

As emphasized in the introduction, aggressive gliomas constitute a significant health problem for many, and the need for improved therapies is urgent. While many novel therapeutic approaches to the treatment of gliomas have been unsuccessful at promoting patient progression-free survival, much has been learned in the process to inform the continued development of treatments for this disease. The prospect of using naturally-occurring molecules such as BAI1 as anti-angiogenic therapeutics continues to be an important area for further research in this regard.

The aims underlying the work summarized in the previous chapters have been to characterize the cellular mechanisms underlying the generation of the primary known secreted product of the BAI1 extracellular domain, Vasculostatin-40, and to determine the functional significance of this processing. Despite the focus on BAI1, this research reveals novel insights about the complexity of mechanisms regulating angiostasis, particularly in the brain. Investigations of functionality indicate the significant promise of this molecule and its derivatives as an anti-cancer agent or as a treatment for other neurological diseases marked by vascular compromise. Finally, a more thorough understanding the biology of BAI1 significantly expands and improves upon our knowledge of GPCR biology and pharmacology, especially that of the class B GPCRs, a group which has historically received less attention, but whose complex structure and function play vital roles in physiology and disease. Taken together, the results of these studies paint a picture of a regulatory event with significant biological impact, both for BAI1 itself and its microenvironment.

6.1. Summary of results.

In Chapter 2, we observe that Vstat40 is a biologically relevant fragment of the BAI1 extracellular domain and that, like BAI1, its expression is lost in GBM. We show that Vstat40 is the primary known secreted fragment of the BAI1 ECD and its processing is affected by levels of Vstat120 secretion. Specifically, increases in Vstat120 generation inhibit Vstat40 proteolysis, suggesting that attachment of the ECD to the cell membrane is crucial to promote Vstat40 generation. Our data suggest that matrix metalloproteinase 14 (MMP-14) is directly responsible for cleaving the extracellular domain of BAI1 between amino acids 320 and 328 into Vasculostatin-40 (Vstat40). This proteolysis is specifically inhibited by overexpression of tissue

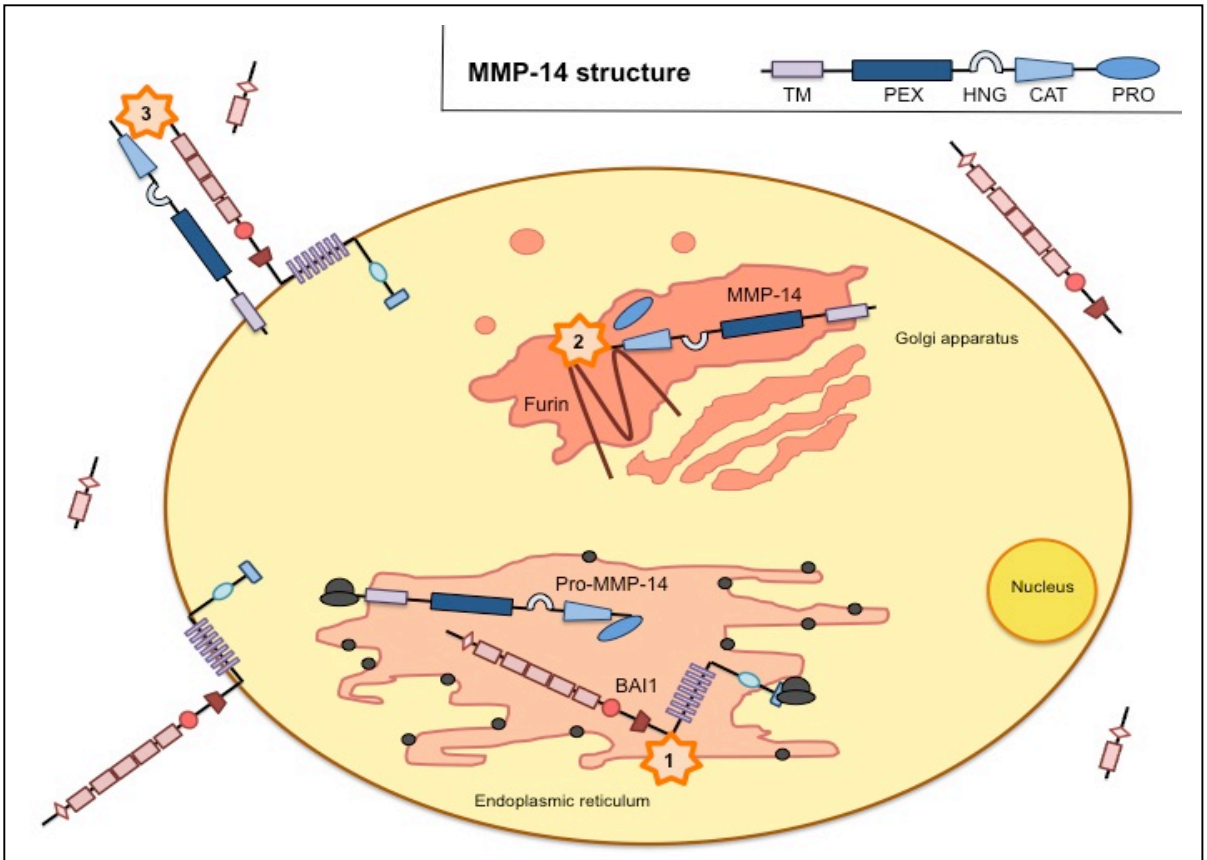

Figure 6.1 Schematic representing localization and sequence of three major events in BAI1 proteolysis and MMP-14 activation during protein maturation. *Abbreviations*: TM, transmembrane; PEX, hemopexin; HNG, hinge; CAT, catalytic domain; PRO, propeptide sequence.

inhibitor of metalloproteinases 3 (TIMP-3), a known MMP-14 inhibitor. The proprotein convertase family of enzymes, particularly furin, play an important role in MMP-14 activation, which serves to explain why Vstat40 proteolysis is reduced but incompletely inhibited when levels of active furin are experimentally modulated. The ubiquitous expression of furin and MMP-14 in the brain, and their upregulation in aggressive gliomas, supports the hypothesis that Vstat40 processing is likely a common biological event with widespread significance for the regulation of angiostasis.

We also show the association between the generation of Vstat120 and Vstat40, using the BAI1-S927D mutant, which may act as a phosphomimetic substitution, and the BAI1-3TM, which lacks the C-terminal domain and 4 of the transmembrane repeats. As discussed in the Introduction and illustrated in Figure 6.1, GPS proteolysis yielding Vstat120 is believed to occur in the endoplasmic reticulum. Because MMP-14 is believed to be inactive prior to its cleavage by furin in the trans-Golgi network, it is hypothesized that Vstat40 has not yet been cleaved from extracellular BAI1 at this stage. Once cleaved, Vstat120 may be secreted into the medium or be retained at the cell surface via non-covalent association with the transmembrane portion of BAI1. BAI1 containing the S927D mutation yields increased secreted Vstat120, due to chemical mechanisms as yet incompletely understood, and which leads to a significant decrease in the production of Vstat40. Vstat40 production is also inhibited in a BAI1 construct containing only the extracellular portion and three transmembrane repeats (BAI1-3TM). These findings strongly indicate that association of the extracellular domain of BAI1 with the transmembrane portion, or with the cell membrane, is important for Vstat40 proteolysis. Additionally, MMP-14 is a membrane-bound receptor and is likely to most efficiently cleave molecules also located at the cell surface. Localization of the BAI1 receptor, potentially via association of its PDZ-binding domain with specific scaffolding molecules, may thus be critical for this event, possibly by

aligning BAI1 in proximity to MMP-14. These hypotheses remain to be tested, possibly through co-immunoprecipitation studies that could be used to demonstrate a physical association. What becomes of the portion of extracellular BAI1 following Vstat40 proteolysis, tentatively named Vstat80, is a question that is as yet unanswered, although the HBD antibody described in Chapter 5 is now available to address this problem.

In Chapter 3, the functional significance of Vstat40 generation is examined by investigating the anti-angiogenic activity of Vstat40. Vstat40 is observed to inhibit angiogenesis in a battery of standard culture assays, indicating that its proteolysis is not necessarily a mechanism to inhibit the potent anti-angiogenic activity of Vstat120. While both Vstat40 and Vstat120 inhibit endothelial cell migration and tube formation in a CD36-dependent manner, the data do not provide a clear interpretation of their relative potency. A more precise system of experimental Vstat administration, such as the purified peptides obtained from the GST pulldown approach described in Chapter 5, is necessary to most conclusively elucidate their differential bioactivity. We further show that CD36 is expressed on the vasculature of mouse and human brains as well as human GBM, indicating that Vstats are appropriate therapies for this target *in vivo*. We include the caveat that as CD36 does appear to be broadly expressed and not limited to tumor-associated vasculature, administration of CD36-interacting peptides may have unwanted consequences in vivo, such as the induction of apoptosis in healthy vessels. Future clinical use of Vstats should factor in the goal of site-specific administration to avoid side effects of this kind. Importantly, Vstat40 is demonstrated to inhibit angiogenesis *in vivo*, supporting the rationale for further investigation of its therapeutic properties. Finally, preliminary evidence indicates that Vstat40 may act to counteract the pro-permeability effects of VEGF in culture, suggesting an alternative therapeutic application for this molecule.

In Chapter 4, we observe that, in contrast to the published reports on Vstat120, Vstat40 is not sufficient to inhibit the growth of orthotopic LN229-derived glioma xenografts when induced via doxycycline administration. The previous Vstat120 studies utilized clones of a different tumor cell line (U87MG), and which expressed Vstat120 constitutively (Kaur et al., 2009), rendering any comparison to these results imperfect. Further, previous work on LN229-derived xenografts expressing Vstat120 have previously exerted a less dramatic effect on subcutaneous tumor growth than upon the tumorigenecity of U87MG-derived clones. Thus, one cannot rule out cell line-dependent mechanisms underlying Vstat40's failure as an anti-tumor therapeutic, or the possibility that it may yet demonstrate anti-tumor efficacy. Notably, we observe that Vstat40 significantly inhibits angiogenesis in xenografts only when Vstat40 expression is induced, in keeping with observations of Vstat120 activity (Kaur et al., 2005; Kaur et al., 2009). We demonstrate other effects that may depend on Vstat40 expression, such as significant differences in tumor cell morphology and adhesive properties, and a reduction in the levels of cleaved caspase 3. Collectively these observations serve as an indication of the bioactivity of Vstat40, which may extend beyond the regulation of angiogenesis in *in vivo* models.

Also in Chapter 4, we take a step back to examine the role of BAI1 in the larger picture of glioma biology, an analysis made possible due to recent developments in microarray and clinical analysis of large numbers of tumor specimens. We confirm previous observations that BAI1 expression is lost in astrocytomas and GBM and that the loss is proportional to increase in tumor grade. In keeping with the hypothesis that BAI1 acts as a tumor suppressor, we show that higher levels of BAI1 confer a statistically significant survival benefit to astrocytoma but not GBM patients. Importantly, we demonstrate for the first time that elevated BAI1 is also associated with reduced levels of GBM angiogenesis, confirming the importance of pursuing studies of its molecular biology or therapeutic significance.

These microarray data also permit a big-picture investigation of the biology of multiple angiogenesis regulators in tumors. The prevailing hypothesis, described previously as the "angiogenic switch," is that more successful tumors generally upregulate pro-angiogenic molecules and downregulate angiogenesis inhibitors (Hanahan and Folkman, 1996). This imbalance leads to an overall gain in tumor neovascularization, subsequently promoting tumor growth and metastasis. Interestingly, we observe that tumors do not treat all angiogenesis regulators according to this simple principle. If the principle were generally correct, one would expect to see low levels of angiogenesis inhibitors and high levels of angiogenesis stimulators when BAI1 levels are low, and vice versa. When expression of other pro- and anti-angiogenic molecules, such as VEGF, TSP-1, interleukins, and the endostatin precursor collagen XVIII, is ordered by increasing BAI1 expression, several distinct patterns of regulation emerge. Specifically, the expression of molecules such as IL-6 and TSP-1 decrease as BAI1 increases, while expression of VEGF-A and HIF-1alpha does not change in relation to BAI1 and expression of BAIs 2 and 3 is positively correlated with BAI1 expression. The specificity of the observed patterns, and their robustness across databases, suggests that some angiogenesis regulators may be regulated in concert by tumor-specific mechanisms currently unknown. The significance of these observations is not yet clearly understood, but further investigation may yield important insights impacting the optimization of anti-angiogenic therapy for aggressive gliomas.

In Chapter 5, we highlight noteworthy technical advances aimed at encouraging novel and finely-tuned investigations of the biology of BAI1. First, we show development of constructs that yield GST-tagged Vstat peptides upon induction in bacteria. This system currently requires improvement in several arenas, primarily in enhancement of the specific binding of dialyzed GST-Vstats to glutathione resin. While more troubleshooting is required to perfect this

approach, however, the generation of purified recombinant Vstat peptides will be of great benefit to studies of Vstat functionality, as the current approach using Vstats expressed in conditioned medium is beset by concerns of contaminants and lack of quantifiability. Further, we demonstrate the generation of antiserum against the BAI1 hormone-binding domain. This antiserum will be useful to detect other portions of the BAI1 extracellular domain not recognized by the antibody against extracellular BAI1 used in these studies to identify Vstat40 (BNT), permitting the observation of other fragments or proteolysis events occurring in the BAI1 extracellular domain. It may also serve as an agonist or antagonist of BAI1 activity, or competing with an endogenous HBD ligand. Together, these advances set the stage for the next generation of BAI1 studies and offer new avenues for these investigations.

6.2. Conclusions.

We identify that furin-activated MMP-14 directly processes extracellular BAI1 at a previously unknown cleavage site into a secreted, highly-abundant fragment. While both furin and MMP-14 are implicated in tumorigenesis, we show that they act sequentially to generate a novel angiogenesis inhibitor, Vstat40. We show that Vstat40 generation is not merely a mechanism to inactivate Vstat120, though it is as yet difficult to draw precise comparisons of their bioactivity. While a wealth of clinical and *in silico* data demonstrates the promise of the BAIs, particularly BAI1, for cancer therapy, studies of Vstat40 represent a less promising avenue for future followup in that arena than those of full-length BAI1 or the Vstat120 peptide, due to its negligible effect on subject survival using the inducible model described in Chapter 4. However, these observations *per se* are not conclusive proof of its lack of anti-tumor activity and should not be taken as a rationale not to pursue further work on the utility of Vstat40 as an anti-tumor agent. Indeed, we observe that the LN229-derived glioma xenografts used in the *in vivo*

tumorigenesis study demonstrate significantly decreased angiogenesis when Vstat40 is induced with doxycycline. That Vstat40 expression does not exert a significant effect on subject survival under these conditions does not diminish the significance of its overall biological effect in gliomas or in the normal cellular milieu. The MMP-14 proteolysis event is clearly robust and highly conserved as Vstat40 is observed in the conditioned medium of a variety of cells transfected with BAI1 cDNA. Vstat40 cleavage may thus affect multiple aspects of BAI1 function, as angioregulator, engulfment mediator, cell adhesion molecule, or GPCR. When taken together, these results demonstrate that Vstat40 processing is an important biological event, and is ultimately likely to have important consequences for neurovascular or glioma biology.

6.3. Future directions.

One important criticism leveled at the current approach to studying the Vstats is that currently there is no conclusive method by which one can accurately compare the efficacy of the Vstat peptides in biological assays, and in so doing derive conclusions about their relative functions *in vivo*. The differential effects of Vstat40 and Vstat120 on tumor growth, among other differences, underlie the need for further exploration of these questions. To this end, production of purified recombinant human Vstat fragments will be the best and most reliable method to compare their activities, and for this reason, it will be essential for further studies on this subject to troubleshoot and improve upon the preliminary system designed for this purpose and described in Chapter 5. When optimized, this system, based on the generation of GST-tagged Vstat proteins, will represent an important advance in the study of BAI1 function. For example, preliminary work with GST-tagged Vstat120 suggests that thrombin as well as MMP-14 may act to process extracellular BAI1 into secreted fragments (Figure 5.6C). More extensive analyses should be undertaken to determine whether Vstat120 or the putative Vstat80 fragment are

cleaved into smaller fragments by thrombin or other undetermined enzymes. BAI2 is also known to be cleaved (Okajima et al., 2010), suggesting that the extracellular domains of the three BAI family members undergo proteolysis, with broad functional implications.

In any event, proteolytic cleavage is likely to affect the biological activity of the receptors themselves. To this end, further studies on BAI1 should be informed by previous work on the protease activated receptor 1 (PAR1). Extensive research has shown that thrombin's proteolysis of the extracellular domain of PAR1 exposes a tethered ligand in the cell-attached portion of the ECD, leading to both receptor and platelet activation (Andersen et al., 1999; Macfarlane et al., 2001; Vu et al., 1991). Notably, the secreted fragment generated from this PAR1 proteolysis may act as an inhibitor of angiogenesis, termed parstatin (Zania et al., 2009). The proteolysis is thus a critical means of regulating intracellular signaling of PAR1, itself a GPCR. It is possible that such a proteolysis exposes a similar peptide ligand in the ECD of BAI1, and this event could have functional consequences for intracellular BAI1 signaling. Exposure of such a tethered ligand could result either from MMP-14 processing or by thrombin processing at the canonical thrombin cleavage site, though the latter has not yet been demonstrated in culture or *in vivo*. Overall, this comparison with the biology of PAR1 opens up avenues for research into other important functional consequences of Vstat40 generation.

An important limitation of research on the function of the BAI1 extracellular domain is that the BNT antibody detects both Vstat40 and Vstat120 but not the piece of extracellular BAI1 remaining after Vstat40 processing, tentatively named Vstat80. If stable, the Vstat80 piece would contain four bioactive TSRs, and could prove to inhibit tumor growth with similar efficacy to that of Vstat120. Further research into the use of fragments of extracellular BAI1 as anti-cancer therapeutics could be designed to focus on verifying the existence of Vstat80 and evaluating its anti-tumor activity. Naturally, such studies would also further our understanding of the function

of BAI1 and its extracellular domain in particular. To this end, these experiments could utilize the newly-designed antibody against the BAI1 hormone-binding domain, described in Chapter 5, to detect the presence of Vstat80 or other BAI1-derived peptides undetectable with the N-terminal antibody.

Other research on Vstat40 may focus on its potential ability to regulate vascular permeability as well as angiogenesis, and results of preliminary experimentation in this area are described in Chapter 3. Most research on the functionality of the BAI1 extracellular domain has focused on its thrombospondin type 1 repeats, and with good reason, as they appear to exert an important influence on the angiogenic process via engaging the CD36 receptor. Another motif implicated in the regulation of angiogenesis is the RGD motif found in Vstat40 and Vstat120. Integrins containing an α_V subunit bind RGD motifs found in extracellular matrix proteins, and soluble RGD-containing proteins can be used to compete with cell attachment to the extracellular matrix. Thus, Vstats are capable of interfering with the function of integrins, which serve as essential co-regulators of VEGFR2 signaling (Byzova et al., 2000; Somanath et al., 2009). A more in-depth study, using a construct with a mutation in the RGD motif (Vstat40-RAD), would more conclusively determine the mechanisms by which Vstat40 inhibits VEGF-induced vascular permeability and any involved downstream signaling pathways (Gavard and Gutkind, 2006). A more thorough investigation of Vstat40's cell surface targets will further our understanding of Vstat40's anti-permeability activity, whether through an interaction with the VEGFR2, VEGF itself, or integrins, and determine which intracellular signaling cascades are regulated in the process.

A final important direction for future studies of BAI1 function should be its role in the brain as a cell surface molecule with important implications for synaptic function. As previously noted, BAI1 interacts with a variety of molecules associated with the post-synaptic density (Lim et

al., 2002; Shiratsuchi et al., 1998a). If expressed at synapses or associated glia, BAI1 or its Vstat derivatives could play a role in synaptic function, or the maintenance of the neurovascular niche so critical to brain function (Abbott et al., 2006; Pumiglia and Temple, 2006). Further, the TSRs of TSP-1 are known to play an important role in synaptogenesis (Christopherson et al., 2005), and it is conceivable that the TSRs of BAI1 could have similar activity. Further studies, ideally using a BAI1 knockout mouse, should investigate this interesting possibility.

REFERENCES

Abbott, N. J., Ronnback, L., and Hansson, E. (2006). Astrocyte-endothelial interactions at the blood-brain barrier. Nat Rev Neurosci *7*, 41-53.

Abdollahi, A., Hahnfeldt, P., Maercker, C., Grone, H. J., Debus, J., Ansorge, W., Folkman, J., Hlatky, L., and Huber, P. E. (2004). Endostatin's antiangiogenic signaling network. Mol Cell *13*, 649-663.

Adams, R. H., and Alitalo, K. (2007). Molecular regulation of angiogenesis and lymphangiogenesis. Nat Rev Mol Cell Biol *8*, 464-478.

Akhavan, D., Cloughesy, T. F., and Mischel, P. S. (2010). mTOR signaling in glioblastoma: lessons learned from bench to bedside. Neuro Oncol *12*, 882-889.

Albini, A., Indraccolo, S., Noonan, D. M., and Pfeffer, U. (2010). Functional genomics of endothelial cells treated with anti-angiogenic or angiopreventive drugs. Clin Exp Metastasis *27*, 419-439.

Andersen, H., Greenberg, D. L., Fujikawa, K., Xu, W., Chung, D. W., and Davie, E. W. (1999). Protease-activated receptor 1 is the primary mediator of thrombin-stimulated platelet procoagulant activity. Proc Natl Acad Sci U S A *96*, 11189-11193.

Azzouz, M., Ralph, G. S., Storkebaum, E., Walmsley, L. E., Mitrophanous, K. A., Kingsman, S. M., Carmeliet, P., and Mazarakis, N. D. (2004). VEGF delivery with retrogradely transported lentivector prolongs survival in a mouse ALS model. Nature *429*, 413-417.

Bassi, D. E., Mahloogi, H., Al-Saleem, L., Lopez De Cicco, R., Ridge, J. A., and Klein-Szanto, A. J. (2001). Elevated furin expression in aggressive human head and neck tumors and tumor cell lines. Mol Carcinog *31*, 224-232.

Batchelor, T. T., Sorensen, A. G., di Tomaso, E., Zhang, W. T., Duda, D. G., Cohen, K. S., Kozak, K. R., Cahill, D. P., Chen, P. J., Zhu, M., *et al.* (2007). AZD2171, a pan-VEGF receptor tyrosine kinase inhibitor, normalizes tumor vasculature and alleviates edema in glioblastoma patients. Cancer Cell *11*, 83-95.

Beck-Sickinger, A. G., Grouzmann, E., Hoffmann, E., Gaida, W., van Meir, E. G., Waeber, B., and Jung, G. (1992). A novel cyclic analog of neuropeptide Y specific for the Y2 receptor. Eur J Biochem *206*, 957-964.

Behrens, J., Vakaet, L., Friis, R., Winterhager, E., Van Roy, F., Mareel, M. M., and Birchmeier, W. (1993). Loss of epithelial differentiation and gain of invasiveness correlates with tyrosine phosphorylation of the E-cadherin/beta-catenin complex in cells transformed with a temperature-sensitive v-SRC gene. J Cell Biol *120*, 757-766.

Belkin, A. M., Akimov, S. S., Zaritskaya, L. S., Ratnikov, B. I., Deryugina, E. I., and Strongin, A. Y. (2001). Matrix-dependent proteolysis of surface transglutaminase by membrane-type metalloproteinase regulates cancer cell adhesion and locomotion. J Biol Chem *276*, 18415-18422.

Bello, L., Carrabba, G., Giussani, C., Lucini, V., Cerutti, F., Scaglione, F., Landre, J., Pluderi, M., Tomei, G., Villani, R., *et al.* (2001). Low-dose chemotherapy combined with an antiangiogenic drug reduces human glioma growth in vivo. Cancer Res *61*, 7501-7506.

Belozerov, V. E., and Van Meir, E. G. (2005). Hypoxia inducible factor-1: a novel target for cancer therapy. Anticancer Drugs *16*, 901-909.

Berger, B., Capper, D., Lemke, D., Pfenning, P. N., Platten, M., Weller, M., von Deimling, A., Wick, W., and Weiler, M. (2010). Defective p53 antiangiogenic signaling in glioblastoma. Neuro Oncol.

Bergeron, F., Leduc, R., and Day, R. (2000). Subtilase-like pro-protein convertases: from molecular specificity to therapeutic applications. J Mol Endocrinol *24*, 1-22.

Bergers, G., and Benjamin, L. E. (2003). Tumorigenesis and the angiogenic switch. Nat Rev Cancer *3*, 401-410.

Bergers, G., and Hanahan, D. (2008). Modes of resistance to anti-angiogenic therapy. Nat Rev Cancer *8*, 592-603.

Bernatchez, P. N., Soker, S., and Sirois, M. G. (1999). Vascular endothelial growth factor effect on endothelial cell proliferation, migration, and platelet-activating factor synthesis is Flk-1-dependent. J Biol Chem *274*, 31047-31054.

Bjarnadottir, T. K., Fredriksson, R., Hoglund, P. J., Gloriam, D. E., Lagerstrom, M. C., and Schioth, H. B. (2004). The human and mouse repertoire of the adhesion family of G-protein-coupled receptors. Genomics *84*, 23-33.

Bjarnadottir, T. K., Fredriksson, R., and Schioth, H. B. (2007). The adhesion GPCRs: a unique family of G protein-coupled receptors with important roles in both central and peripheral tissues. Cell Mol Life Sci *64*, 2104-2119.

Bjarnadottir, T. K., Gloriam, D. E., Hellstrand, S. H., Kristiansson, H., Fredriksson, R., and Schioth, H. B. (2006). Comprehensive repertoire and phylogenetic analysis of the G protein-coupled receptors in human and mouse. Genomics *88*, 263-273.

Bolliger, M. F., Martinelli, D. C., and Sudhof, T. C. (2011). The cell-adhesion G protein-coupled receptor BAI3 is a high-affinity receptor for C1q-like proteins. Proc Natl Acad Sci U S A *108*, 2534-2539.

Brat, D. J., and Van Meir, E. G. (2004). Vaso-occlusive and prothrombotic mechanisms associated with tumor hypoxia, necrosis, and accelerated growth in glioblastoma. Lab Invest *84*, 397-405.

Bredel, M., Scholtens, D. M., Harsh, G. R., Bredel, C., Chandler, J. P., Renfrow, J. J., Yadav, A. K., Vogel, H., Scheck, A. C., Tibshirani, R., and Sikic, B. I. (2009). A network model of a cooperative genetic landscape in brain tumors. JAMA *302*, 261-275.

Brekken, R. A., Overholser, J. P., Stastny, V. A., Waltenberger, J., Minna, J. D., and Thorpe, P. E. (2000). Selective inhibition of vascular endothelial growth factor (VEGF) receptor 2 (KDR/Flk-1) activity by a monoclonal anti-VEGF antibody blocks tumor growth in mice. Cancer Res *60*, 5117-5124.

Brennan, C., Momota, H., Hambardzumyan, D., Ozawa, T., Tandon, A., Pedraza, A., and Holland, E. (2009). Glioblastoma subclasses can be defined by activity among signal transduction pathways and associated genomic alterations. PLoS One *4*, e7752.

Brkovic, A., and Sirois, M. G. (2007). Vascular permeability induced by VEGF family members in vivo: role of endogenous PAF and NO synthesis. J Cell Biochem *100*, 727-737.

Broadhead, M. L., Dass, C. R., and Choong, P. F. (2009). In vitro and in vivo biological activity of PEDF against a range of tumors. Expert Opin Ther Targets *13*, 1429-1438.

Brooks, P. C., Clark, R. A., and Cheresh, D. A. (1994). Requirement of vascular integrin alpha v beta 3 for angiogenesis. Science *264*, 569-571.

Brooks, P. C., Silletti, S., von Schalscha, T. L., Friedlander, M., and Cheresh, D. A. (1998). Disruption of angiogenesis by PEX, a noncatalytic metalloproteinase fragment with integrin binding activity. Cell *92*, 391-400.

Brooks, P. C., Stromblad, S., Klemke, R., Visscher, D., Sarkar, F. H., and Cheresh, D. A. (1995). Antiintegrin alpha v beta 3 blocks human breast cancer growth and angiogenesis in human skin. J Clin Invest *96*, 1815-1822.

Buerkle, M. A., Pahernik, S. A., Sutter, A., Jonczyk, A., Messmer, K., and Dellian, M. (2002). Inhibition of the alpha-nu integrins with a cyclic RGD peptide impairs angiogenesis, growth and metastasis of solid tumours in vivo. Br J Cancer *86*, 788-795.

Byzova, T. V., Goldman, C. K., Pampori, N., Thomas, K. A., Bett, A., Shattil, S. J., and Plow, E. F. (2000). A mechanism for modulation of cellular responses to VEGF: activation of the integrins. Mol Cell *6*, 851-860.

Cao, J., Rehemtulla, A., Pavlaki, M., Kozarekar, P., and Chiarelli, C. (2005). Furin directly cleaves proMMP-2 in the trans-Golgi network resulting in a nonfunctioning proteinase. J Biol Chem *280*, 10974-10980.

Cavallaro, U., Liebner, S., and Dejana, E. (2006). Endothelial cadherins and tumor angiogenesis. Exp Cell Res *312*, 659-667.

Cerami, E., Demir, E., Schultz, N., Taylor, B. S., and Sander, C. (2010). Automated network analysis identifies core pathways in glioblastoma. PLoS One *5*, e8918.

Ceteci, F., Ceteci, S., Karreman, C., Kramer, B. W., Asan, E., Gotz, R., and Rapp, U. R. (2007). Disruption of tumor cell adhesion promotes angiogenic switch and progression to micrometastasis in RAF-driven murine lung cancer. Cancer Cell *12*, 145-159.

Chang, G. W., Stacey, M., Kwakkenbos, M. J., Hamann, J., Gordon, S., and Lin, H. H. (2003). Proteolytic cleavage of the EMR2 receptor requires both the extracellular stalk and the GPS motif. FEBS Lett *547*, 145-150.

Christopherson, K. S., Ullian, E. M., Stokes, C. C., Mullowney, C. E., Hell, J. W., Agah, A., Lawler, J., Mosher, D. F., Bornstein, P., and Barres, B. A. (2005). Thrombospondins are astrocyte-secreted proteins that promote CNS synaptogenesis. Cell *120*, 421-433.

Cloughesy, T. F., Yoshimoto, K., Nghiemphu, P., Brown, K., Dang, J., Zhu, S., Hsueh, T., Chen, Y., Wang, W., Youngkin, D., *et al.* (2008). Antitumor activity of rapamycin in a Phase I trial for patients with recurrent PTEN-deficient glioblastoma. PLoS Med *5*, e8.

Colorado, P. C., Torre, A., Kamphaus, G., Maeshima, Y., Hopfer, H., Takahashi, K., Volk, R., Zamborsky, E. D., Herman, S., Sarkar, P. K., *et al.* (2000). Anti-angiogenic cues from vascular basement membrane collagen. Cancer Res *60*, 2520-2526.

Cooper, L. A., Gutman, D. A., Long, Q., Johnson, B. A., Cholleti, S. R., Kurc, T., Saltz, J. H., Brat, D. J., and Moreno, C. S. (2010). The proneural molecular signature is enriched in oligodendrogliomas and predicts improved survival among diffuse gliomas. PLoS One *5*, e12548.

Couvineau, A., Ceraudo, E., Tan, Y. V., and Laburthe, M. (2010). VPAC1 receptor binding site: contribution of photoaffinity labeling approach. Neuropeptides *44*, 127-132.

D'Adamo, D. R., Anderson, S. E., Albritton, K., Yamada, J., Riedel, E., Scheu, K., Schwartz, G. K., Chen, H., and Maki, R. G. (2005). Phase II study of doxorubicin and bevacizumab for patients with metastatic soft-tissue sarcomas. J Clin Oncol *23*, 7135-7142.

de Fraipont, F., Nicholson, A. C., Feige, J. J., and Van Meir, E. G. (2001). Thrombospondins and tumor angiogenesis. Trends Mol Med *7*, 401-407.

De Palma, M., Venneri, M. A., Galli, R., Sergi Sergi, L., Politi, L. S., Sampaolesi, M., and Naldini, L. (2005). Tie2 identifies a hematopoietic lineage of proangiogenic monocytes required for tumor vessel formation and a mesenchymal population of pericyte progenitors. Cancer Cell *8*, 211-226.

Deane, R., and Zlokovic, B. V. (2007). Role of the blood-brain barrier in the pathogenesis of Alzheimer's disease. Curr Alzheimer Res *4*, 191-197.

Dejana, E. (1996). Endothelial adherens junctions: implications in the control of vascular permeability and angiogenesis. J Clin Invest *98*, 1949-1953.

Dejana, E., Corada, M., and Lampugnani, M. G. (1995). Endothelial cell-to-cell junctions. Faseb J *9*, 910-918.

Dejana, E., and Del Maschio, A. (1995). Molecular organization and functional regulation of cell to cell junctions in the endothelium. Thromb Haemost *74*, 309-312.

DeRosse, P., Lencz, T., Burdick, K. E., Siris, S. G., Kane, J. M., and Malhotra, A. K. (2008). The genetics of symptom-based phenotypes: toward a molecular classification of schizophrenia. Schizophr Bull *34*, 1047-1053.

Deryugina, E. I., Ratnikov, B. I., Yu, Q., Baciu, P. C., Rozanov, D. V., and Strongin, A. Y. (2004). Prointegrin maturation follows rapid trafficking and processing of MT1-MMP in Furin-Negative Colon Carcinoma LoVo Cells. Traffic *5*, 627-641.

Desgrosellier, J. S., and Cheresh, D. A. (2010). Integrins in cancer: biological implications and therapeutic opportunities. Nat Rev Cancer *10*, 9-22.

Desjardins, A., Quinn, J. A., Vredenburgh, J. J., Sathornsumetee, S., Friedman, A. H., Herndon, J. E., McLendon, R. E., Provenzale, J. M., Rich, J. N., Sampson, J. H., *et al.* (2007). Phase II study of imatinib mesylate and hydroxyurea for recurrent grade III malignant gliomas. J Neurooncol *83*, 53-60.

Deyev, I. E., and Petrenko, A. G. (2010). Regulation of CIRL-1 proteolysis and trafficking. Biochimie *92*, 418-422.

Diedrich, U., Lucius, J., Baron, E., Behnke, J., Pabst, B., and Zoll, B. (1995). Distribution of epidermal growth factor receptor gene amplification in brain tumours and correlation to prognosis. J Neurol *242*, 683-688.

Doherty, L., Gigas, D. C., Kesari, S., Drappatz, J., Kim, R., Zimmerman, J., Ostrowsky, L., and Wen, P. Y. (2006). Pilot study of the combination of EGFR and mTOR inhibitors in recurrent malignant gliomas. Neurology *67*, 156-158.

Doonan, S. (1996). Protein Purification Protocols, Vol 59: Humana Press, Inc.).

Duckert, P., Brunak, S., and Blom, N. (2004). Prediction of proprotein convertase cleavage sites. Protein Eng Des Sel *17*, 107-112.

Duda, D. G., Sunamura, M., Lozonschi, L., Yokoyama, T., Yatsuoka, T., Motoi, F., Horii, A., Tani, K., Asano, S., Nakamura, Y., and Matsuno, S. (2002). Overexpression of the p53-inducible brain-specific angiogenesis inhibitor 1 suppresses efficiently tumour angiogenesis. Br J Cancer *86*, 490-496.

Duncan, C. G., Killela, P. J., Payne, C. A., Lampson, B., Chen, W. C., Liu, J., Solomon, D., Waldman, T., Towers, A. J., Gregory, S. G., *et al.* (2010). Integrated genomic analyses identify ERRFI1 and TACC3 as glioblastoma-targeted genes. Oncotarget *1*, 265-277.

Eliceiri, B. P., and Cheresh, D. A. (2000). Role of alpha v integrins during angiogenesis. Cancer J *6 Suppl 3*, S245-249.

Escudier, B., Pluzanska, A., Koralewski, P., Ravaud, A., Bracarda, S., Szczylik, C., Chevreau, C., Filipek, M., Melichar, B., Bajetta, E., *et al.* (2007). Bevacizumab plus interferon alfa-2a for treatment of metastatic renal cell carcinoma: a randomised, double-blind phase III trial. Lancet *370*, 2103-2111.

Eskens, F. A., and Verweij, J. (2006). The clinical toxicity profile of vascular endothelial growth factor (VEGF) and vascular endothelial growth factor receptor (VEGFR) targeting angiogenesis inhibitors; a review. Eur J Cancer *42*, 3127-3139.

Febbraio, M., Hajjar, D. P., and Silverstein, R. L. (2001). CD36: a class B scavenger receptor involved in angiogenesis, atherosclerosis, inflammation, and lipid metabolism. J Clin Invest *108*, 785-791.

Febbraio, M., and Silverstein, R. L. (2007). CD36: implications in cardiovascular disease. Int J Biochem Cell Biol *39*, 2012-2030.

Felbor, U., Dreier, L., Bryant, R. A., Ploegh, H. L., Olsen, B. R., and Mothes, W. (2000). Secreted cathepsin L generates endostatin from collagen XVIII. Embo J *19*, 1187-1194.

Fillmore, H. L., VanMeter, T. E., and Broaddus, W. C. (2001). Membrane-type matrix metalloproteinases (MT-MMPs): expression and function during glioma invasion. J Neurooncol *53*, 187-202.

Folkman, J. (1971). Tumor angiogenesis: therapeutic implications. N Engl J Med *285*, 1182-1186.

Folkman, J. (1995). Seminars in Medicine of the Beth Israel Hospital, Boston. Clinical applications of research on angiogenesis. N Engl J Med *333*, 1757-1763.

Folkman, J., Watson, K., Ingber, D., and Hanahan, D. (1989). Induction of angiogenesis during the transition from hyperplasia to neoplasia. Nature *339*, 58-61.

Fortin, J. P., Zhu, Y., Choi, C., Beinborn, M., Nitabach, M. N., and Kopin, A. S. (2009). Membrane-tethered ligands are effective probes for exploring class B1 G protein-coupled receptor function. Proc Natl Acad Sci U S A *106*, 8049-8054.

Franceschi, E., Cavallo, G., Lonardi, S., Magrini, E., Tosoni, A., Grosso, D., Scopece, L., Blatt, V., Urbini, B., Pession, A., *et al.* (2007). Gefitinib in patients with progressive high-grade gliomas: a multicentre phase II study by Gruppo Italiano Cooperativo di Neuro-Oncologia (GICNO). Br J Cancer *96*, 1047-1051.

Freire, P., Vilela, M., Deus, H., Kim, Y. W., Koul, D., Colman, H., Aldape, K. D., Bogler, O., Yung, W. K., Coombes, K., *et al.* (2008). Exploratory analysis of the copy number alterations in glioblastoma multiforme. PLoS One *3*, e4076.

Fujiwara, T., Mammoto, A., Kim, Y., and Takai, Y. (2000). Rho small G-protein-dependent binding of mDia to an Src homology 3 domain-containing IRSp53/BAIAP2. Biochem Biophys Res Commun *271*, 626-629.

Fukumura, D., Duda, D. G., Munn, L. L., and Jain, R. K. (2010). Tumor microvasculature and microenvironment: novel insights through intravital imaging in pre-clinical models. Microcirculation *17*, 206-225.

Fukumura, D., and Jain, R. K. (2007). Tumor microvasculature and microenvironment: targets for anti-angiogenesis and normalization. Microvasc Res *74*, 72-84.

Fukumura, D., and Jain, R. K. (2008). Imaging angiogenesis and the microenvironment. APMIS *116*, 695-715.

Fukushima, Y., Oshika, Y., Tsuchida, T., Tokunaga, T., Hatanaka, H., Kijima, H., Yamazaki, H., Ueyama, Y., Tamaoki, N., and Nakamura, M. (1998). Brain-specific angiogenesis inhibitor 1 expression is inversely correlated with vascularity and distant metastasis of colorectal cancer. Int J Oncol *13*, 967-970.

Fukuzawa, T., and Hirose, S. (2006). Multiple processing of Ig-Hepta/GPR116, a G protein-coupled receptor with immunoglobulin (Ig)-like repeats, and generation of EGF2-like fragment. J Biochem *140*, 445-452.

Gavard, J., and Gutkind, J. S. (2006). VEGF controls endothelial-cell permeability by promoting the beta-arrestin-dependent endocytosis of VE-cadherin. Nat Cell Biol *8*, 1223-1234.

Gelinas, D. S., Bernatchez, P. N., Rollin, S., Bazan, N. G., and Sirois, M. G. (2002). Immediate and delayed VEGF-mediated NO synthesis in endothelial cells: role of PI3K, PKC and PLC pathways. Br J Pharmacol *137*, 1021-1030.

Gerhardt, H., and Betsholtz, C. (2003). Endothelial-pericyte interactions in angiogenesis. Cell Tissue Res *314*, 15-23.

Gerstner, E. R., Duda, D. G., di Tomaso, E., Ryg, P. A., Loeffler, J. S., Sorensen, A. G., Ivy, P., Jain, R. K., and Batchelor, T. T. (2009). VEGF inhibitors in the treatment of cerebral edema in patients with brain cancer. Nat Rev Clin Oncol *6*, 229-236.

Gerstner, E. R., Sorensen, A. G., Jain, R. K., and Batchelor, T. T. (2008). Advances in neuroimaging techniques for the evaluation of tumor growth, vascular permeability, and angiogenesis in gliomas. Curr Opin Neurol *21*, 728-735.

Gomes, I., Gupta, A., Singh, S. P., and Sharma, S. K. (1999). Monoclonal antibody to the delta opioid receptor acts as an agonist in dual regulation of adenylate cyclase in NG108-15 cells. FEBS Lett *456*, 126-130.

Gottardi, C. J., Wong, E., and Gumbiner, B. M. (2001). E-cadherin suppresses cellular transformation by inhibiting beta-catenin signaling in an adhesion-independent manner. J Cell Biol *153*, 1049-1060.

Gray, J. X., Haino, M., Roth, M. J., Maguire, J. E., Jensen, P. N., Yarme, A., Stetler-Stevenson, M. A., Siebenlist, U., and Kelly, K. (1996). CD97 is a processed, seven-transmembrane, heterodimeric receptor associated with inflammation. J Immunol *157*, 5438-5447.

Greenberg, D. A., and Jin, K. (2005). From angiogenesis to neuropathology. Nature *438*, 954-959.

Guan, M., Pang, C. P., Yam, H. F., Cheung, K. F., Liu, W. W., and Lu, Y. (2004). Inhibition of glioma invasion by overexpression of pigment epithelium-derived factor. Cancer Gene Ther *11*, 325-332.

Guedez, L., Rivera, A. M., Salloum, R., Miller, M. L., Diegmueller, J. J., Bungay, P. M., and Stetler-Stevenson, W. G. (2003). Quantitative assessment of angiogenic responses by the directed in vivo angiogenesis assay. Am J Pathol *162*, 1431-1439.

Gupta, K., Gupta, P., Wild, R., Ramakrishnan, S., and Hebbel, R. P. (1999). Binding and displacement of vascular endothelial growth factor (VEGF) by thrombospondin: effect on human microvascular endothelial cell proliferation and angiogenesis. Angiogenesis *3*, 147-158.

Gutheil, J. C., Campbell, T. N., Pierce, P. R., Watkins, J. D., Huse, W. D., Bodkin, D. J., and Cheresh, D. A. (2000). Targeted antiangiogenic therapy for cancer using Vitaxin: a humanized monoclonal antibody to the integrin alphavbeta3. Clin Cancer Res *6*, 3056-3061.

Hamano, Y., Zeisberg, M., Sugimoto, H., Lively, J. C., Maeshima, Y., Yang, C., Hynes, R. O., Werb, Z., Sudhakar, A., and Kalluri, R. (2003). Physiological levels of tumstatin, a fragment of collagen IV alpha3 chain, are generated by MMP-9 proteolysis and suppress angiogenesis via alphaV beta3 integrin. Cancer Cell *3*, 589-601.

Hanahan, D., and Folkman, J. (1996). Patterns and emerging mechanisms of the angiogenic switch during tumorigenesis. Cell *86*, 353-364.

Handsley, M. M., and Edwards, D. R. (2005). Metalloproteinases and their inhibitors in tumor angiogenesis. Int J Cancer *115*, 849-860.

Harhaj, N. S., Felinski, E. A., Wolpert, E. B., Sundstrom, J. M., Gardner, T. W., and Antonetti, D. A. (2006). VEGF activation of protein kinase C stimulates occludin

phosphorylation and contributes to endothelial permeability. Invest Ophthalmol Vis Sci *47*, 5106-5115.

Hashizume, H., Baluk, P., Morikawa, S., McLean, J. W., Thurston, G., Roberge, S., Jain, R. K., and McDonald, D. M. (2000). Openings between defective endothelial cells explain tumor vessel leakiness. Am J Pathol *156*, 1363-1380.

Hatanaka, H., Oshika, Y., Abe, Y., Yoshida, Y., Hashimoto, T., Handa, A., Kijima, H., Yamazaki, H., Inoue, H., Ueyama, Y., and Nakamura, M. (2000). Vascularization is decreased in pulmonary adenocarcinoma expressing brain-specific angiogenesis inhibitor 1 (BAI1). Int J Mol Med *5*, 181-183.

Hayashi, T., Noshita, N., Sugawara, T., and Chan, P. H. (2003). Temporal profile of angiogenesis and expression of related genes in the brain after ischemia. J Cereb Blood Flow Metab *23*, 166-180.

Held-Feindt, J., Paredes, E. B., Blomer, U., Seidenbecher, C., Stark, A. M., Mehdorn, H. M., and Mentlein, R. (2006). Matrix-degrading proteases ADAMTS4 and ADAMTS5 (disintegrins and metalloproteinases with thrombospondin motifs 4 and 5) are expressed in human glioblastomas. Int J Cancer *118*, 55-61.

Herbst, R. S., Mullani, N. A., Davis, D. W., Hess, K. R., McConkey, D. J., Charnsangavej, C., O'Reilly, M. S., Kim, H. W., Baker, C., Roach, J., *et al.* (2002). Development of biologic markers of response and assessment of antiangiogenic activity in a clinical trial of human recombinant endostatin. J Clin Oncol *20*, 3804-3814.

Hoekstra, R., de Vos, F. Y., Eskens, F. A., Gietema, J. A., van der Gaast, A., Groen, H. J., Knight, R. A., Carr, R. A., Humerickhouse, R. A., Verweij, J., and de Vries, E. G. (2005). Phase I safety, pharmacokinetic, and pharmacodynamic study of the thrombospondin-1-

mimetic angiogenesis inhibitor ABT-510 in patients with advanced cancer. J Clin Oncol *23*, 5188-5197.

Hofmann, M., Schultz, M., Bernd, A., Bereiter-Hahn, J., Kaufmann, R., and Kippenberger, S. (2007). Long-term lowering of tumour interstitial fluid pressure reduces Ki-67 expression. J Biomech *40*, 2324-2329.

Holopainen, J. M., Moilanen, J. A., Sorsa, T., Kivela-Rajamaki, M., Tervahartiala, T., Vesaluoma, M. H., and Tervo, T. M. (2003). Activation of matrix metalloproteinase-8 by membrane type 1-MMP and their expression in human tears after photorefractive keratectomy. Invest Ophthalmol Vis Sci *44*, 2550-2556.

Hotary, K. B., Yana, I., Sabeh, F., Li, X. Y., Holmbeck, K., Birkedal-Hansen, H., Allen, E. D., Hiraoka, N., and Weiss, S. J. (2002). Matrix metalloproteinases (MMPs) regulate fibrin-invasive activity via MT1-MMP-dependent and -independent processes. J Exp Med *195*, 295-308.

Hsiao, C. C., Cheng, K. F., Chen, H. Y., Chou, Y. H., Stacey, M., Chang, G. W., and Lin, H. H. (2009). Site-specific N-glycosylation regulates the GPS auto-proteolysis of CD97. FEBS Lett *583*, 3285-3290.

Huang, Y., Fan, J., Yang, J., and Zhu, G. Z. (2008). Characterization of GPR56 protein and its suppressed expression in human pancreatic cancer cells. Mol Cell Biochem *308*, 133-139.

Ilan, N., Tucker, A., and Madri, J. A. (2003). Vascular endothelial growth factor expression, beta-catenin tyrosine phosphorylation, and endothelial proliferative behavior: a pathway for transformation? Lab Invest *83*, 1105-1115.

Ishii, N., Maier, D., Merlo, A., Tada, M., Sawamura, Y., Diserens, A. C., and Van Meir, E. G. (1999). Frequent co-alterations of TP53, p16/CDKN2A, p14ARF, PTEN tumor suppressor genes in human glioma cell lines. Brain Pathol *9*, 469-479.

Ito, J., Ito, M., Nambu, H., Fujikawa, T., Tanaka, K., Iwaasa, H., and Tokita, S. (2009). Anatomical and histological profiling of orphan G-protein-coupled receptor expression in gastrointestinal tract of C57BL/6J mice. Cell Tissue Res *338*, 257-269.

Itoh, Y. (2006). MT1-MMP: a key regulator of cell migration in tissue. IUBMB Life *58*, 589-596.

Itoh, Y., and Seiki, M. (2006). MT1-MMP: a potent modifier of pericellular microenvironment. J Cell Physiol *206*, 1-8.

Itoh, Y., Takamura, A., Ito, N., Maru, Y., Sato, H., Suenaga, N., Aoki, T., and Seiki, M. (2001). Homophilic complex formation of MT1-MMP facilitates proMMP-2 activation on the cell surface and promotes tumor cell invasion. EMBO J *20*, 4782-4793.

Jain, R. K. (2005). Normalization of tumor vasculature: an emerging concept in antiangiogenic therapy. Science *307*, 58-62.

Jain, R. K., and Baxter, L. T. (1988). Mechanisms of heterogeneous distribution of monoclonal antibodies and other macromolecules in tumors: significance of elevated interstitial pressure. Cancer Res *48*, 7022-7032.

Jain, R. K., Tong, R. T., and Munn, L. L. (2007). Effect of vascular normalization by antiangiogenic therapy on interstitial hypertension, peritumor edema, and lymphatic metastasis: insights from a mathematical model. Cancer Res *67*, 2729-2735.

Jeong, B. C., Kim, M. Y., Lee, J. H., Kee, H. J., Kho, D. H., Han, K. E., Qian, Y. R., Kim, J. K., and Kim, K. K. (2006). Brain-specific angiogenesis inhibitor 2 regulates VEGF through GABP that acts as a transcriptional repressor. FEBS Lett *580*, 669-676.

Jimenez, B., Volpert, O. V., Crawford, S. E., Febbraio, M., Silverstein, R. L., and Bouck, N. (2000). Signals leading to apoptosis-dependent inhibition of neovascularization by thrombospondin-1. Nat Med *6*, 41-48.

Jimenez, B., Volpert, O. V., Reiher, F., Chang, L., Munoz, A., Karin, M., and Bouck, N. (2001). c-Jun N-terminal kinase activation is required for the inhibition of neovascularization by thrombospondin-1. Oncogene *20*, 3443-3448.

Jin, Z., Tietjen, I., Bu, L., Liu-Yesucevitz, L., Gaur, S. K., Walsh, C. A., and Piao, X. (2007). Disease-associated mutations affect GPR56 protein trafficking and cell surface expression. Hum Mol Genet *16*, 1972-1985.

Kamphaus, G. D., Colorado, P. C., Panka, D. J., Hopfer, H., Ramchandran, R., Torre, A., Maeshima, Y., Mier, J. W., Sukhatme, V. P., and Kalluri, R. (2000). Canstatin, a novel matrix-derived inhibitor of angiogenesis and tumor growth. J Biol Chem *275*, 1209-1215.

Kan, Z., Jaiswal, B. S., Stinson, J., Janakiraman, V., Bhatt, D., Stern, H. M., Yue, P., Haverty, P. M., Bourgon, R., Zheng, J., *et al.* (2010). Diverse somatic mutation patterns and pathway alterations in human cancers. Nature *466*, 869-873.

Kaur, B., Brat, D. J., Calkins, C. C., and Van Meir, E. G. (2003). Brain angiogenesis inhibitor 1 is differentially expressed in normal brain and glioblastoma independently of p53 expression. Am J Pathol *162*, 19-27.

Kaur, B., Brat, D. J., Devi, N. S., and Van Meir, E. G. (2005). Vasculostatin, a proteolytic fragment of brain angiogenesis inhibitor 1, is an antiangiogenic and antitumorigenic factor. Oncogene *24*, 3632-3642.

Kaur, B., Cork, S. M., Sandberg, E. M., Devi, N. S., Zhang, Z., Klenotic, P. A., Febbraio, M., Shim, H., Mao, H., Tucker-Burden, C., *et al.* (2009). Vasculostatin inhibits intracranial glioma growth and negatively regulates in vivo angiogenesis through a CD36-dependent mechanism. Cancer Res *69*, 1212-1220.

Kee, H. J., Koh, J. T., Kim, M. Y., Ahn, K. Y., Kim, J. K., Bae, C. S., Park, S. S., and Kim, K. K. (2002). Expression of brain-specific angiogenesis inhibitor 2 (BAI2) in normal and

ischemic brain: involvement of BAI2 in the ischemia-induced brain angiogenesis. J Cereb Blood Flow Metab *22*, 1054-1067.

Kimmelman, J., and Nalbantoglu, J. (2007). Faithful companions: a proposal for neurooncology trials in pet dogs. Cancer Res *67*, 4541-4544.

Klenotic, P. A., Huang, P., Palomo, J., Kaur, B., Van Meir, E. G., Vogelbaum, M. A., Febbraio, M., Gladson, C. L., and Silverstein, R. L. (2010). Histidine-rich glycoprotein modulates the anti-angiogenic effects of vasculostatin. Am J Pathol *176*, 2039-2050.

Koh, J. T., Lee, Z. H., Ahn, K. Y., Kim, J. K., Bae, C. S., Kim, H. H., Kee, H. J., and Kim, K. K. (2001). Characterization of mouse brain-specific angiogenesis inhibitor 1 (BAI1) and phytanoyl-CoA alpha-hydroxylase-associated protein 1, a novel BAI1-binding protein. Brain Res Mol Brain Res *87*, 223-237.

Krasnoperov, V., Deyev, I. E., Serova, O. V., Xu, C., Lu, Y., Buryanovsky, L., Gabibov, A. G., Neubert, T. A., and Petrenko, A. G. (2009). Dissociation of the subunits of the calcium-independent receptor of alpha-latrotoxin as a result of two-step proteolysis. Biochemistry *48*, 3230-3238.

Krasnoperov, V., Lu, Y., Buryanovsky, L., Neubert, T. A., Ichtchenko, K., and Petrenko, A. G. (2002). Post-translational proteolytic processing of the calcium-independent receptor of alpha-latrotoxin (CIRL), a natural chimera of the cell adhesion protein and the G protein-coupled receptor. Role of the G protein-coupled receptor proteolysis site (GPS) motif. J Biol Chem *277*, 46518-46526.

Kudo, S., Konda, R., Obara, W., Kudo, D., Tani, K., Nakamura, Y., and Fujioka, T. (2007). Inhibition of tumor growth through suppression of angiogenesis by brain-specific angiogenesis inhibitor 1 gene transfer in murine renal cell carcinoma. Oncol Rep *18*, 785-791.

Kuwada, S. K., and Li, X. (2000). Integrin alpha5/beta1 mediates fibronectin-dependent epithelial cell proliferation through epidermal growth factor receptor activation. Mol Biol Cell *11*, 2485-2496.

Lambrechts, D., Lafuste, P., Carmeliet, P., and Conway, E. M. (2006). Another angiogenic gene linked to amyotrophic lateral sclerosis. Trends Mol Med *12*, 345-347.

Lampugnani, M. G., and Dejana, E. (2007). The control of endothelial cell functions by adherens junctions. Novartis Found Symp *283*, 4-13; discussion 13-17, 238-241.

Lee, J. H., Koh, J. T., Shin, B. A., Ahn, K. Y., Roh, J. H., Kim, Y. J., and Kim, K. K. (2001). Comparative study of angiostatic and anti-invasive gene expressions as prognostic factors in gastric cancer. Int J Oncol *18*, 355-361.

Lim, I. A., Hall, D. D., and Hell, J. W. (2002). Selectivity and promiscuity of the first and second PDZ domains of PSD-95 and synapse-associated protein 102. J Biol Chem *277*, 21697-21711.

Lin, H. H., Chang, G. W., Davies, J. Q., Stacey, M., Harris, J., and Gordon, S. (2004). Autocatalytic cleavage of the EMR2 receptor occurs at a conserved G protein-coupled receptor proteolytic site motif. J Biol Chem *279*, 31823-31832.

Lin, T. N., Kim, G. M., Chen, J. J., Cheung, W. M., He, Y. Y., and Hsu, C. Y. (2003). Differential regulation of thrombospondin-1 and thrombospondin-2 after focal cerebral ischemia/reperfusion. Stroke *34*, 177-186.

Lissitzky, J. C., Luis, J., Munzer, J. S., Benjannet, S., Parat, F., Chretien, M., Marvaldi, J., and Seidah, N. G. (2000). Endoproteolytic processing of integrin pro-alpha subunits involves the redundant function of furin and proprotein convertase (PC) 5A, but not paired basic amino acid converting enzyme (PACE) 4, PC5B or PC7. Biochem J *346 Pt 1*, 133-138.

Liu, W., James, C. D., Frederick, L., Alderete, B. E., and Jenkins, R. B. (1997). PTEN/MMAC1 mutations and EGFR amplification in glioblastomas. Cancer Res *57*, 5254-5257.

MacDonald, T. J., Taga, T., Shimada, H., Tabrizi, P., Zlokovic, B. V., Cheresh, D. A., and Laug, W. E. (2001). Preferential susceptibility of brain tumors to the antiangiogenic effects of an alpha(v) integrin antagonist. Neurosurgery *48*, 151-157.

Macfarlane, S. R., Seatter, M. J., Kanke, T., Hunter, G. D., and Plevin, R. (2001). Proteinase-activated receptors. Pharmacol Rev *53*, 245-282.

Machein, M. R., and Plate, K. H. (2000). VEGF in brain tumors. J Neurooncol *50*, 109-120.

Machein, M. R., and Plate, K. H. (2004). Role of VEGF in developmental angiogenesis and in tumor angiogenesis in the brain. Cancer Treat Res *117*, 191-218.

Madhavan, S., Zenklusen, J. C., Kotliarov, Y., Sahni, H., Fine, H. A., and Buetow, K. (2009). Rembrandt: helping personalized medicine become a reality through integrative translational research. Mol Cancer Res *7*, 157-167.

Maubant, S., Saint-Dizier, D., Boutillon, M., Perron-Sierra, F., Casara, P. J., Hickman, J. A., Tucker, G. C., and Van Obberghen-Schilling, E. (2006). Blockade of alpha v beta3 and alpha v beta5 integrins by RGD mimetics induces anoikis and not integrin-mediated death in human endothelial cells. Blood *108*, 3035-3044.

McCarty, M. F., Liu, W., Fan, F., Parikh, A., Reimuth, N., Stoeltzing, O., and Ellis, L. M. (2003). Promises and pitfalls of anti-angiogenic therapy in clinical trials. Trends Mol Med *9*, 53-58.

McLendon, R., and Network, T. C. G. A. R. (2008). Comprehensive genomic characterization defines human glioblastoma genes and core pathways. Nature *455*, 1061-1068.

McMahon, S., Grondin, F., McDonald, P. P., Richard, D. E., and Dubois, C. M. (2005). Hypoxia-enhanced expression of the proprotein convertase furin is mediated by hypoxia-inducible factor-1: impact on the bioactivation of proproteins. J Biol Chem *280*, 6561-6569.

Mercapide, J., Lopez De Cicco, R., Bassi, D. E., Castresana, J. S., Thomas, G., and Klein-Szanto, A. J. (2002). Inhibition of furin-mediated processing results in suppression of astrocytoma cell growth and invasiveness. Clin Cancer Res *8*, 1740-1746.

Mijares, A., Lebesgue, D., Wallukat, G., and Hoebeke, J. (2000). From agonist to antagonist: Fab fragments of an agonist-like monoclonal anti-beta(2)-adrenoceptor antibody behave as antagonists. Mol Pharmacol *58*, 373-379.

Miller, K., Wang, M., Gralow, J., Dickler, M., Cobleigh, M., Perez, E. A., Shenkier, T., Cella, D., and Davidson, N. E. (2007). Paclitaxel plus bevacizumab versus paclitaxel alone for metastatic breast cancer. N Engl J Med *357*, 2666-2676.

Mischel, P. S., Cloughesy, T. F., and Nelson, S. F. (2004). DNA-microarray analysis of brain cancer: molecular classification for therapy. Nat Rev Neurosci *5*, 782-792.

Miyamoto, N., Yamamoto, H., Taniguchi, H., Miyamoto, C., Oki, M., Adachi, Y., Imai, K., and Shinomura, Y. (2007). Differential expression of angiogenesis-related genes in human gastric cancers with and those without high-frequency microsatellite instability. Cancer Lett *254*, 42-53.

Mongiat, M., Sweeney, S. M., San Antonio, J. D., Fu, J., and Iozzo, R. V. (2003). Endorepellin, a novel inhibitor of angiogenesis derived from the C terminus of perlecan. J Biol Chem *278*, 4238-4249.

Mori, K., Kanemura, Y., Fujikawa, H., Nakano, A., Ikemoto, H., Ozaki, I., Matsumoto, T., Tamura, K., Yokota, M., and Arita, N. (2002). Brain-specific angiogenesis inhibitor 1 (BAI1) is expressed in human cerebral neuronal cells. Neurosci Res *43*, 69-74.

Moriguchi, T., Haraguchi, K., Ueda, N., Okada, M., Furuya, T., and Akiyama, T. (2004). DREG, a developmentally regulated G protein-coupled receptor containing two conserved proteolytic cleavage sites. Genes Cells *9*, 549-560.

Morikawa, W., Yamamoto, K., Ishikawa, S., Takemoto, S., Ono, M., Fukushi, J., Naito, S., Nozaki, C., Iwanaga, S., and Kuwano, M. (2000). Angiostatin generation by cathepsin D secreted by human prostate carcinoma cells. J Biol Chem *275*, 38912-38920.

Mullan, P. B., and Millikan, R. C. (2007). Molecular subtyping of breast cancer: opportunities for new therapeutic approaches. Cell Mol Life Sci *64*, 3219-3232.

Mundel, T. M., and Kalluri, R. (2007). Type IV collagen-derived angiogenesis inhibitors. Microvasc Res *74*, 85-89.

Nabors, L. B., Mikkelsen, T., Rosenfeld, S. S., Hochberg, F., Akella, N. S., Fisher, J. D., Cloud, G. A., Zhang, Y., Carson, K., Wittemer, S. M., *et al.* (2007). Phase I and correlative biology study of cilengitide in patients with recurrent malignant glioma. J Clin Oncol *25*, 1651-1657.

Nam, D. H., Park, K., Suh, Y. L., and Kim, J. H. (2004). Expression of VEGF and brain specific angiogenesis inhibitor-1 in glioblastoma: prognostic significance. Oncol Rep *11*, 863-869.

Nicholson, A. C., Malik, S. B., Logsdon, J. M., Jr., and Van Meir, E. G. (2005). Functional evolution of ADAMTS genes: evidence from analyses of phylogeny and gene organization. BMC Evol Biol *5*, 11.

Nishimori, H., Shiratsuchi, T., Urano, T., Kimura, Y., Kiyono, K., Tatsumi, K., Yoshida, S., Ono, M., Kuwano, M., Nakamura, Y., and Tokino, T. (1997). A novel brain-specific p53-target gene, BAI1, containing thrombospondin type 1 repeats inhibits experimental angiogenesis. Oncogene *15*, 2145-2150.

Nishizaki, M., Fujiwara, T., Tanida, T., Hizuta, A., Nishimori, H., Tokino, T., Nakamura, Y., Bouvet, M., Roth, J. A., and Tanaka, N. (1999). Recombinant adenovirus expressing wild-type p53 is antiangiogenic: a proposed mechanism for bystander effect. Clin Cancer Res *5*, 1015-1023.

Noushmehr, H., Weisenberger, D. J., Diefes, K., Phillips, H. S., Pujara, K., Berman, B. P., Pan, F., Pelloski, C. E., Sulman, E. P., Bhat, K. P., *et al.* (2010). Identification of a CpG island methylator phenotype that defines a distinct subgroup of glioma. Cancer Cell *17*, 510-522.

Obermann, H., Samalecos, A., Osterhoff, C., Schroder, B., Heller, R., and Kirchhoff, C. (2003). HE6, a two-subunit heptahelical receptor associated with apical membranes of efferent and epididymal duct epithelia. Mol Reprod Dev *64*, 13-26.

Oda, K., Shiratsuchi, T., Nishimori, H., Inazawa, J., Yoshikawa, H., Taketani, Y., Nakamura, Y., and Tokino, T. (1999). Identification of BAIAP2 (BAI-associated protein 2), a novel human homologue of hamster IRSp53, whose SH3 domain interacts with the cytoplasmic domain of BAI1. Cytogenet Cell Genet *84*, 75-82.

Ohnishi, Y., Shioda, T., Nakayama, K., Iwata, S., Gotoh, B., Hamaguchi, M., and Nagai, Y. (1994). A furin-defective cell line is able to process correctly the gp160 of human immunodeficiency virus type 1. J Virol *68*, 4075-4079.

Okajima, D., Kudo, G., and Yokota, H. (2010). Brain-specific angiogenesis inhibitor 2 (BAI2) may be activated by proteolytic processing. J Recept Signal Transduct Res *30*, 143-153.

Omuro, A. M., Faivre, S., and Raymond, E. (2007). Lessons learned in the development of targeted therapy for malignant gliomas. Mol Cancer Ther *6*, 1909-1919.

Ovaska, K., Laakso, M., Haapa-Paananen, S., Louhimo, R., Chen, P., Aittomaki, V., Valo, E., Nunez-Fontarnau, J., Rantanen, V., Karinen, S., *et al.* (2010). Large-scale data integration framework provides a comprehensive view on glioblastoma multiforme. Genome Med *2*, 65.

Paris, D., Ganey, N., Banasiak, M., Laporte, V., Patel, N., Mullan, M., Murphy, S. F., Yee, G. T., Bachmeier, C., Ganey, C., *et al.* (2010). Impaired orthotopic glioma growth and vascularization in transgenic mouse models of Alzheimer's disease. J Neurosci *30*, 11251-11258.

Park, D., Tosello-Trampont, A. C., Elliott, M. R., Lu, M., Haney, L. B., Ma, Z., Klibanov, A. L., Mandell, J. W., and Ravichandran, K. S. (2007). BAI1 is an engulfment receptor for apoptotic cells upstream of the ELMO/Dock180/Rac module. Nature *450*, 430-434.

Parsons, D. W., Jones, S., Zhang, X., Lin, J. C., Leary, R. J., Angenendt, P., Mankoo, P., Carter, H., Siu, I. M., Gallia, G. L., *et al.* (2008). An integrated genomic analysis of human glioblastoma multiforme. Science *321*, 1807-1812.

Perler, F. B. (1998). Breaking up is easy with esters. Nat Struct Biol *5*, 249-252.

Perler, F. B., Xu, M. Q., and Paulus, H. (1997). Protein splicing and autoproteolysis mechanisms. Curr Opin Chem Biol *1*, 292-299.

Pettersson, A., Nagy, J. A., Brown, L. F., Sundberg, C., Morgan, E., Jungles, S., Carter, R., Krieger, J. E., Manseau, E. J., Harvey, V. S., *et al.* (2000). Heterogeneity of the angiogenic response induced in different normal adult tissues by vascular permeability factor/vascular endothelial growth factor. Lab Invest *80*, 99-115.

Phillips, H. S., Kharbanda, S., Chen, R., Forrest, W. F., Soriano, R. H., Wu, T. D., Misra, A., Nigro, J. M., Colman, H., Soroceanu, L., *et al.* (2006). Molecular subclasses of high-grade glioma predict prognosis, delineate a pattern of disease progression, and resemble stages in neurogenesis. Cancer Cell *9*, 157-173.

Pioszak, A. A., Parker, N. R., Suino-Powell, K., and Xu, H. E. (2008). Molecular recognition of corticotropin-releasing factor by its G-protein-coupled receptor CRFR1. J Biol Chem *283*, 32900-32912.

Pioszak, A. A., and Xu, H. E. (2008). Molecular recognition of parathyroid hormone by its G protein-coupled receptor. Proc Natl Acad Sci U S A *105*, 5034-5039.

Plate, K. H. (1999). Mechanisms of angiogenesis in the brain. J Neuropathol Exp Neurol *58*, 313-320.

Plate, K. H., Breier, G., and Risau, W. (1994). Molecular mechanisms of developmental and tumor angiogenesis. Brain Pathol *4*, 207-218.

Prandini, M. H., Dreher, I., Bouillot, S., Benkerri, S., Moll, T., and Huber, P. (2005). The human VE-cadherin promoter is subjected to organ-specific regulation and is activated in tumour angiogenesis. Oncogene *24*, 2992-3001.

Preusser, M., Gelpi, E., Rottenfusser, A., Dieckmann, K., Widhalm, G., Dietrich, W., Bertalanffy, A., Prayer, D., Hainfellner, J. A., and Marosi, C. (2008). Epithelial Growth Factor Receptor Inhibitors for treatment of recurrent or progressive high grade glioma: an exploratory study. J Neurooncol *89*, 211-218.

Pumiglia, K., and Temple, S. (2006). PEDF: bridging neurovascular interactions in the stem cell niche. Nat Neurosci *9*, 299-300.

Purow, B., and Schiff, D. (2009). Advances in the genetics of glioblastoma: are we reaching critical mass? Nat Rev Neurol *5*, 419-426.

Raizer, J. J., Abrey, L. E., Lassman, A. B., Chang, S. M., Lamborn, K. R., Kuhn, J. G., Yung, W. K., Gilbert, M. R., Aldape, K. A., Wen, P. Y., *et al.* (2010). A phase II trial of erlotinib in patients with recurrent malignant gliomas and nonprogressive glioblastoma multiforme postradiation therapy. Neuro Oncol *12*, 95-103.

Ramjaun, A. R., and Hodivala-Dilke, K. (2009). The role of cell adhesion pathways in angiogenesis. Int J Biochem Cell Biol *41*, 521-530.

Rangarajan, A., and Weinberg, R. A. (2003). Opinion: Comparative biology of mouse versus human cells: modelling human cancer in mice. Nat Rev Cancer *3*, 952-959.

Rao, J. S. (2003). Molecular mechanisms of glioma invasiveness: the role of proteases. Nat Rev Cancer *3*, 489-501.

Rasheed, B. K., McLendon, R. E., Herndon, J. E., Friedman, H. S., Friedman, A. H., Bigner, D. D., and Bigner, S. H. (1994). Alterations of the TP53 gene in human gliomas. Cancer Res *54*, 1324-1330.

Rasheed, B. K., Stenzel, T. T., McLendon, R. E., Parsons, R., Friedman, A. H., Friedman, H. S., Bigner, D. D., and Bigner, S. H. (1997). PTEN gene mutations are seen in high-grade but not in low-grade gliomas. Cancer Res *57*, 4187-4190.

Raymond, E., Brandes, A. A., Dittrich, C., Fumoleau, P., Coudert, B., Clement, P. M., Frenay, M., Rampling, R., Stupp, R., Kros, J. M., *et al.* (2008). Phase II study of imatinib in patients with recurrent gliomas of various histologies: a European Organisation for Research and Treatment of Cancer Brain Tumor Group Study. J Clin Oncol *26*, 4659-4665.

Rege, T. A., Fears, C. Y., and Gladson, C. L. (2005). Endogenous inhibitors of angiogenesis in malignant gliomas: nature's antiangiogenic therapy. Neuro Oncol *7*, 106-121.

Reiss, K., Maretzky, T., Ludwig, A., Tousseyn, T., de Strooper, B., Hartmann, D., and Saftig, P. (2005). ADAM10 cleavage of N-cadherin and regulation of cell-cell adhesion and beta-catenin nuclear signalling. Embo J *24*, 742-752.

Ricci-Vitiani, L., Pallini, R., Biffoni, M., Todaro, M., Invernici, G., Cenci, T., Maira, G., Parati, E. A., Stassi, G., Larocca, L. M., and De Maria, R. (2010). Tumour vascularization via endothelial differentiation of glioblastoma stem-like cells. Nature *468*, 824-828.

Rockwell, N. C., Krysan, D. J., Komiyama, T., and Fuller, R. S. (2002). Precursor processing by kex2/furin proteases. Chem Rev *102*, 4525-4548.

Roebroek, A. J., Taylor, N. A., Louagie, E., Pauli, I., Smeijers, L., Snellinx, A., Lauwers, A., Van de Ven, W. J., Hartmann, D., and Creemers, J. W. (2004). Limited redundancy of the proprotein convertase furin in mouse liver. J Biol Chem *279*, 53442-53450.

Rozanov, D. V., and Strongin, A. Y. (2003). Membrane type-1 matrix metalloproteinase functions as a proprotein self-convertase. Expression of the latent zymogen in Pichia pastoris, autolytic activation, and the peptide sequence of the cleavage forms. J Biol Chem *278*, 8257-8260.

Rusk, A., McKeegan, E., Haviv, F., Majest, S., Henkin, J., and Khanna, C. (2006). Preclinical evaluation of antiangiogenic thrombospondin-1 peptide mimetics, ABT-526 and ABT-510, in companion dogs with naturally occurring cancers. Clin Cancer Res *12*, 7444-7455.

Rusnati, M., Camozzi, M., Moroni, E., Bottazzi, B., Peri, G., Indraccolo, S., Amadori, A., Mantovani, A., and Presta, M. (2004). Selective recognition of fibroblast growth factor-2 by the long pentraxin PTX3 inhibits angiogenesis. Blood *104*, 92-99.

Saba, M. T., and Magolan, J. M. (1991). Understanding cerebral edema: implications for oncology nurses. Oncol Nurs Forum *18*, 499-505.

Sandler, A., Gray, R., Perry, M. C., Brahmer, J., Schiller, J. H., Dowlati, A., Lilenbaum, R., and Johnson, D. H. (2006). Paclitaxel-carboplatin alone or with bevacizumab for non-small-cell lung cancer. N Engl J Med *355*, 2542-2550.

Sato, H., Kinoshita, T., Takino, T., Nakayama, K., and Seiki, M. (1996). Activation of a recombinant membrane type 1-matrix metalloproteinase (MT1-MMP) by furin and its interaction with tissue inhibitor of metalloproteinases (TIMP)-2. FEBS Lett *393*, 101-104.

Sato, H., Takino, T., Okada, Y., Cao, J., Shinagawa, A., Yamamoto, E., and Seiki, M. (1994). A matrix metalloproteinase expressed on the surface of invasive tumour cells. Nature *370*, 61-65.

Sato, Y., and Sonoda, H. (2007). The vasohibin family: a negative regulatory system of angiogenesis genetically programmed in endothelial cells. Arterioscler Thromb Vasc Biol *27*, 37-41.

Schober, R., Bilzer, T., Waha, A., Reifenberger, G., Wechsler, W., von Deimling, A., Wiestler, O. D., Westphal, M., Kemshead, J. T., Vega, F., and et al. (1995). The epidermal growth factor receptor in glioblastoma: genomic amplification, protein expression, and patient survival data in a therapeutic trial. Clin Neuropathol *14*, 169-174.

Shibuya, M., and Claesson-Welsh, L. (2006). Signal transduction by VEGF receptors in regulation of angiogenesis and lymphangiogenesis. Exp Cell Res *312*, 549-560.

Shiratsuchi, T., Futamura, M., Oda, K., Nishimori, H., Nakamura, Y., and Tokino, T. (1998a). Cloning and characterization of BAI-associated protein 1: a PDZ domain-containing protein that interacts with BAI1. Biochem Biophys Res Commun *247*, 597-604.

Shiratsuchi, T., Nishimori, H., Ichise, H., Nakamura, Y., and Tokino, T. (1997). Cloning and characterization of BAI2 and BAI3, novel genes homologous to brain-specific angiogenesis inhibitor 1 (BAI1). Cytogenet Cell Genet *79*, 103-108.

Shiratsuchi, T., Oda, K., Nishimori, H., Suzuki, M., Takahashi, E., Tokino, T., and Nakamura, Y. (1998b). Cloning and characterization of BAP3 (BAI-associated protein 3), a C2 domain-containing protein that interacts with BAI1. Biochem Biophys Res Commun *251*, 158-165.

Sidransky, D., Mikkelsen, T., Schwechheimer, K., Rosenblum, M. L., Cavanee, W., and Vogelstein, B. (1992). Clonal expansion of p53 mutant cells is associated with brain tumour progression. Nature *355*, 846-847.

Smith, J. S., Tachibana, I., Passe, S. M., Huntley, B. K., Borell, T. J., Iturria, N., O'Fallon, J. R., Schaefer, P. L., Scheithauer, B. W., James, C. D., *et al.* (2001). PTEN mutation, EGFR amplification, and outcome in patients with anaplastic astrocytoma and glioblastoma multiforme. J Natl Cancer Inst *93*, 1246-1256.

Somanath, P. R., Malinin, N. L., and Byzova, T. V. (2009). Cooperation between integrin alphavbeta3 and VEGFR2 in angiogenesis. Angiogenesis *12*, 177-185.

Stawowy, P., Meyborg, H., Stibenz, D., Borges Pereira Stawowy, N., Roser, M., Thanabalasingam, U., Veinot, J. P., Chretien, M., Seidah, N. G., Fleck, E., and Graf, K. (2005). Furin-like proprotein convertases are central regulators of the membrane type matrix metalloproteinase-pro-matrix metalloproteinase-2 proteolytic cascade in atherosclerosis. Circulation *111*, 2820-2827.

Steck, P. A., Pershouse, M. A., Jasser, S. A., Yung, W. K., Lin, H., Ligon, A. H., Langford, L. A., Baumgard, M. L., Hattier, T., Davis, T., *et al.* (1997). Identification of a candidate tumour suppressor gene, MMAC1, at chromosome 10q23.3 that is mutated in multiple advanced cancers. Nat Genet *15*, 356-362.

Stetler-Stevenson, W. G., and Seo, D. W. (2005). TIMP-2: an endogenous inhibitor of angiogenesis. Trends Mol Med *11*, 97-103.

Stromblad, S., and Cheresh, D. A. (1996). Cell adhesion and angiogenesis. Trends Cell Biol *6*, 462-468.

Stupack, D. G., and Cheresh, D. A. (2002). Get a ligand, get a life: integrins, signaling and cell survival. J Cell Sci *115*, 3729-3738.

Stupack, D. G., and Cheresh, D. A. (2003). Apoptotic cues from the extracellular matrix: regulators of angiogenesis. Oncogene *22*, 9022-9029.

Stupack, D. G., Puente, X. S., Boutsaboualoy, S., Storgard, C. M., and Cheresh, D. A. (2001). Apoptosis of adherent cells by recruitment of caspase-8 to unligated integrins. J Cell Biol *155*, 459-470.

Sudhakar, A., Sugimoto, H., Yang, C., Lively, J., Zeisberg, M., and Kalluri, R. (2003). Human tumstatin and human endostatin exhibit distinct antiangiogenic activities mediated by alpha v beta 3 and alpha 5 beta 1 integrins. Proc Natl Acad Sci U S A *100*, 4766-4771.

Sugita, S., Ichtchenko, K., Khvotchev, M., and Sudhof, T. C. (1998). alpha-Latrotoxin receptor CIRL/latrophilin 1 (CL1) defines an unusual family of ubiquitous G-protein-linked receptors. G-protein coupling not required for triggering exocytosis. J Biol Chem *273*, 32715-32724.

Sun, Y., Jin, K., Xie, L., Childs, J., Mao, X. O., Logvinova, A., and Greenberg, D. A. (2003). VEGF-induced neuroprotection, neurogenesis, and angiogenesis after focal cerebral ischemia. J Clin Invest *111*, 1843-1851.

Takahashi, S., Nakagawa, T., Kasai, K., Banno, T., Duguay, S. J., Van de Ven, W. J., Murakami, K., and Nakayama, K. (1995). A second mutant allele of furin in the processing-incompetent cell line, LoVo. Evidence for involvement of the homo B domain in autocatalytic activation. J Biol Chem *270*, 26565-26569.

Tarkowski, E., Issa, R., Sjogren, M., Wallin, A., Blennow, K., Tarkowski, A., and Kumar, P. (2002). Increased intrathecal levels of the angiogenic factors VEGF and TGF-beta in Alzheimer's disease and vascular dementia. Neurobiol Aging *23*, 237-243.

Thomas, G. (2002). Furin at the cutting edge: from protein traffic to embryogenesis and disease. Nat Rev Mol Cell Biol *3*, 753-766.

Tol, J., Koopman, M., Cats, A., Rodenburg, C. J., Creemers, G. J., Schrama, J. G., Erdkamp, F. L., Vos, A. H., van Groeningen, C. J., Sinnige, H. A., *et al.* (2009). Chemotherapy, bevacizumab, and cetuximab in metastatic colorectal cancer. N Engl J Med *360*, 563-572.

Tolsma, S. S., Volpert, O. V., Good, D. J., Frazier, W. A., Polverini, P. J., and Bouck, N. (1993). Peptides derived from two separate domains of the matrix protein thrombospondin-1 have anti-angiogenic activity. J Cell Biol *122*, 497-511.

Tong, R. T., Boucher, Y., Kozin, S. V., Winkler, F., Hicklin, D. J., and Jain, R. K. (2004). Vascular normalization by vascular endothelial growth factor receptor 2 blockade induces a pressure gradient across the vasculature and improves drug penetration in tumors. Cancer Res *64*, 3731-3736.

Turk, B. E., Huang, L. L., Piro, E. T., and Cantley, L. C. (2001). Determination of protease cleavage site motifs using mixture-based oriented peptide libraries. Nat Biotechnol *19*, 661-667.

Ueki, K., Ono, Y., Henson, J. W., Efird, J. T., von Deimling, A., and Louis, D. N. (1996). CDKN2/p16 or RB alterations occur in the majority of glioblastomas and are inversely correlated. Cancer Res *56*, 150-153.

Usui, T., Shima, Y., Shimada, Y., Hirano, S., Burgess, R. W., Schwarz, T. L., Takeichi, M., and Uemura, T. (1999). Flamingo, a seven-pass transmembrane cadherin, regulates planar cell polarity under the control of Frizzled. Cell *98*, 585-595.

Vagnucci, A. H., Jr., and Li, W. W. (2003). Alzheimer's disease and angiogenesis. Lancet *361*, 605-608.

Valen, E., Pascarella, G., Chalk, A., Maeda, N., Kojima, M., Kawazu, C., Murata, M., Nishiyori, H., Lazarevic, D., Motti, D., *et al.* (2009). Genome-wide detection and analysis of hippocampus core promoters using DeepCAGE. Genome Res *19*, 255-265.

Van Cutsem, E., Vervenne, W. L., Bennouna, J., Humblet, Y., Gill, S., Van Laethem, J. L., Verslype, C., Scheithauer, W., Shang, A., Cosaert, J., and Moore, M. J. (2009). Phase III trial of bevacizumab in combination with gemcitabine and erlotinib in patients with metastatic pancreatic cancer. J Clin Oncol *27*, 2231-2237.

Van Meir, E. G., Hadjipanayis, C. G., Norden, A. D., Shu, H. K., Wen, P. Y., and Olson, J. J. (2010). Exciting new advances in neuro-oncology: the avenue to a cure for malignant glioma. CA Cancer J Clin *60*, 166-193.

Van Meir, E. G., Polverini, P. J., Chazin, V. R., Su Huang, H. J., de Tribolet, N., and Cavenee, W. K. (1994). Release of an inhibitor of angiogenesis upon induction of wild type p53 expression in glioblastoma cells. Nat Genet *8*, 171-176.

Varner, J. A., and Cheresh, D. A. (1996a). Integrins and cancer. Curr Opin Cell Biol *8*, 724-730.

Varner, J. A., and Cheresh, D. A. (1996b). Tumor angiogenesis and the role of vascular cell integrin alphavbeta3. Important Adv Oncol, 69-87.

Verhaak, R. G., Hoadley, K. A., Purdom, E., Wang, V., Qi, Y., Wilkerson, M. D., Miller, C. R., Ding, L., Golub, T., Mesirov, J. P., *et al.* (2010). Integrated genomic analysis identifies clinically relevant subtypes of glioblastoma characterized by abnormalities in PDGFRA, IDH1, EGFR, and NF1. Cancer Cell *17*, 98-110.

Vichai, V., and Kirtikara, K. (2006). Sulforhodamine B colorimetric assay for cytotoxicity screening. Nat Protoc *1*, 1112-1116.

Vitucci, M., Hayes, D. N., and Miller, C. R. (2010). Gene expression profiling of gliomas: merging genomic and histopathological classification for personalised therapy. Br J Cancer.

Vogel, T., Guo, N. H., Krutzsch, H. C., Blake, D. A., Hartman, J., Mendelovitz, S., Panet, A., and Roberts, D. D. (1993). Modulation of endothelial cell proliferation, adhesion, and motility by recombinant heparin-binding domain and synthetic peptides from the type I repeats of thrombospondin. J Cell Biochem *53*, 74-84.

Volynski, K. E., Silva, J. P., Lelianova, V. G., Atiqur Rahman, M., Hopkins, C., and Ushkaryov, Y. A. (2004). Latrophilin fragments behave as independent proteins that associate and signal on binding of LTX(N4C). EMBO J *23*, 4423-4433.

Vu, T. K., Hung, D. T., Wheaton, V. I., and Coughlin, S. R. (1991). Molecular cloning of a functional thrombin receptor reveals a novel proteolytic mechanism of receptor activation. Cell *64*, 1057-1068.

Wang, R., Chadalavada, K., Wilshire, J., Kowalik, U., Hovinga, K. E., Geber, A., Fligelman, B., Leversha, M., Brennan, C., and Tabar, V. (2010). Glioblastoma stem-like cells give rise to tumour endothelium. Nature *468*, 829-833.

Wang, S. I., Puc, J., Li, J., Bruce, J. N., Cairns, P., Sidransky, D., and Parsons, R. (1997). Somatic mutations of PTEN in glioblastoma multiforme. Cancer Res *57*, 4183-4186.

Wang, Y., Jin, G., Miao, H., Li, J. Y., Usami, S., and Chien, S. (2006). Integrins regulate VE-cadherin and catenins: dependence of this regulation on Src, but not on Ras. Proc Natl Acad Sci U S A *103*, 1774-1779.

Watanabe, K., Hasegawa, Y., Yamashita, H., Shimizu, K., Ding, Y., Abe, M., Ohta, H., Imagawa, K., Hojo, K., Maki, H., *et al.* (2004). Vasohibin as an endothelium-derived negative feedback regulator of angiogenesis. J Clin Invest *114*, 898-907.

Webster, L. R., Lee, S. F., Ringland, C., Morey, A. L., Hanby, A. M., Morgan, G., Byth, K., Mote, P. A., Provan, P. J., Ellis, I. O., *et al.* (2008). Poor-prognosis estrogen receptor-positive breast cancer identified by histopathologic subclassification. Clin Cancer Res *14*, 6625-6633.

Wei, W., Hackmann, K., Xu, H., Germino, G., and Qian, F. (2007). Characterization of cis-autoproteolysis of polycystin-1, the product of human polycystic kidney disease 1 gene. J Biol Chem *282*, 21729-21737.

Weis, S. M., and Cheresh, D. A. (2005). Pathophysiological consequences of VEGF-induced vascular permeability. Nature *437*, 497-504.

Wikstrand, C. J., McLendon, R. E., Friedman, A. H., and Bigner, D. D. (1997). Cell surface localization and density of the tumor-associated variant of the epidermal growth factor receptor, EGFRvIII. Cancer Res *57*, 4130-4140.

Woessner, J. F., and Nagase, H. (2000). Matrix metalloproteinases and TIMPs, 2 edn: Oxford University Press).

Wrensch, M., Jenkins, R. B., Chang, J. S., Yeh, R. F., Xiao, Y., Decker, P. A., Ballman, K. V., Berger, M., Buckner, J. C., Chang, S., *et al.* (2009). Variants in the CDKN2B and RTEL1 regions are associated with high-grade glioma susceptibility. Nat Genet *41*, 905-908.

Xiao, X. R., Kang, X. X., and Zhao, J. Z. (2006). [Therapeutic effect of brain-specific angiogenesis inhibitor 1 on glioblastoma: an animal experiment]. Zhonghua Yi Xue Za Zhi *86*, 1342-1346.

Yamauchi, H., Cristofanilli, M., Nakamura, S., Hortobagyi, G. N., and Ueno, N. T. (2009). Molecular targets for treatment of inflammatory breast cancer. Nat Rev Clin Oncol *6*, 387-394.

Yan, H., Parsons, D. W., Jin, G., McLendon, R., Rasheed, B. A., Yuan, W., Kos, I., Batinic-Haberle, I., Jones, S., Riggins, G. J., *et al.* (2009). IDH1 and IDH2 mutations in gliomas. N Engl J Med *360*, 765-773.

Yana, I., and Weiss, S. J. (2000). Regulation of membrane type-1 matrix metalloproteinase activation by proprotein convertases. Mol Biol Cell *11*, 2387-2401.

Yang, H., and Kaelin, W. G., Jr. (2001). Molecular pathogenesis of the von Hippel-Lindau hereditary cancer syndrome: implications for oxygen sensing. Cell Growth Differ *12*, 447-455.

Yang, Q., Tian, Y., Liu, S., Zeine, R., Chlenski, A., Salwen, H. R., Henkin, J., and Cohn, S. L. (2007). Thrombospondin-1 peptide ABT-510 combined with valproic acid is an effective antiangiogenesis strategy in neuroblastoma. Cancer Res *67*, 1716-1724.

Yazdani, S., Hendi, K., Pakravan, M., Mahdavi, M., and Yaseri, M. (2009). Intravitreal bevacizumab for neovascular glaucoma: a randomized controlled trial. J Glaucoma *18*, 632-637.

Yi, M., and Ruoslahti, E. (2001). A fibronectin fragment inhibits tumor growth, angiogenesis, and metastasis. Proc Natl Acad Sci U S A *98*, 620-624.

Yoon, K. C., Ahn, K. Y., Lee, J. H., Chun, B. J., Park, S. W., Seo, M. S., Park, Y. G., and Kim, K. K. (2005). Lipid-mediated delivery of brain-specific angiogenesis inhibitor 1 gene reduces corneal neovascularization in an in vivo rabbit model. Gene Ther *12*, 617-624.

Yoshida, Y., Oshika, Y., Fukushima, Y., Tokunaga, T., Hatanaka, H., Kijima, H., Yamazaki, H., Ueyama, Y., Tamaoki, N., Miura, S., and Nakamura, M. (1999). Expression of angiostatic factors in colorectal cancer. Int J Oncol *15*, 1221-1225.

Yu, J. L., Rak, J. W., Coomber, B. L., Hicklin, D. J., and Kerbel, R. S. (2002). Effect of p53 status on tumor response to antiangiogenic therapy. Science *295*, 1526-1528.

Zania, P., Gourni, D., Aplin, A. C., Nicosia, R. F., Flordellis, C. S., Maragoudakis, M. E., and Tsopanoglou, N. E. (2009). Parstatin, the cleaved peptide on proteinase-activated receptor 1 activation, is a potent inhibitor of angiogenesis. J Pharmacol Exp Ther *328*, 378-389.

Zhang, X., and Lawler, J. (2007). Thrombospondin-based antiangiogenic therapy. Microvasc Res *74*, 90-99.

Zhao, S., Lin, Y., Xu, W., Jiang, W., Zha, Z., Wang, P., Yu, W., Li, Z., Gong, L., Peng, Y., *et al.* (2009). Glioma-derived mutations in IDH1 dominantly inhibit IDH1 catalytic activity and induce HIF-1alpha. Science *324*, 261-265.

Zhou, A. T., Bessalle, R., Bisello, A., Nakamoto, C., Rosenblatt, M., Suva, L. J., and Chorev, M. (1997). Direct mapping of an agonist-binding domain within the parathyroid hormone/parathyroid hormone-related protein receptor by photoaffinity crosslinking. Proc Natl Acad Sci U S A *94*, 3644-3649.

Zlokovic, B. V. (2008). The blood-brain barrier in health and chronic neurodegenerative disorders. Neuron *57*, 178-201.

Zohrabian, V. M., Nandu, H., Gulati, N., Khitrov, G., Zhao, C., Mohan, A., Demattia, J., Braun, A., Das, K., Murali, R., and Jhanwar-Uniyal, M. (2007). Gene expression profiling of metastatic brain cancer. Oncol Rep *18*, 321-328.

APPENDIX I

PROTOCOLS

Protocols used in experiments:

Protocol 1. Cell culture.

Tumor and immortalized cell culture. Culture immortalized cells in DMEM with 10% fetal bovine serum (FBS) and antibiotics and passage every 2-4 days. Treat cells with ciprofloxacin as necessary to prevent mycoplasma contamination.

Complete immortalized cell culture medium:

- DMEM (Mediatech, 10-013-CV) 400 mL
- Fetal bovine serum (Gibco) 45 mL
- Nonessential amino acids 5 mL
- Sodium pyruvate 5 mL
- Antibiotic/Antimycotic solution 5 mL

Immortalized cell types used in experiments:

Human glioma cell lines U87MG, LN229, U251-B12, and stably transfected derivatives.

Other cancer cell lines: LoVo (human colon adenocarcinoma).

Other: HEK 293, HFF-1 (immortalized human fibroblasts)

Refer to cell line information sheets for specific details regarding generation and selection maintenance.

Primary endothelial cell culture. Frozen stocks may be obtained from the Emory Dermatology Core. Culture endothelial growth medium supplemented with growth factors (Lonza, CC-4176). Treat with ciprofloxacin as necessary to prevent mycoplasma contamination.

Complete primary endothelial culture medium (all included inLonza):

- Endothelial growth medium 400 mL
- GA1000 (gentamycin/amphotericin) 0.5 mL
- Heparin 0.5 mL
- Hydrocortisone 0.2 mL
- Ascorbic acid 0.5 mL
- R3-IGF-1 0.5 mL
- hFGF-B 0.5 mL
- hEGF 0.5 mL
- VEGF 0.5 mL
- FBS 10 mL

Primary cell types used in experiments:

Human dermal microvascular endothelial cells (HDMECs) and human umbilical vein endothelial cells (HUVECs).

Special waste considerations: dispose of biological material into Biohazard containment receptacles.

Protocol 2. Transient transfection of cDNA and siRNA in mammalian cells.

The purpose of this experiment is to generate transient expression of desired genes in mammalian cells. This protocol is derived from the GenePorter (Genlantis) protocol for transfection. Please refer to the manufacturer's instructions. All experimental apparatus must be kept sterile during transfection.

Reagents and Equipment

Mammalian cells of interest

Culture media: both complete and serum-free

15 mL tubes (Corning) and culture plates (10-15 cm)

1x sterile PBS

GenePorter transfection reagent

Purified cDNA or siRNA

Protocol

- Grow cells of interest to 60-80% confluency in plates or wells of desired size for experiments. To generate large quantities of CM or generate stable clones, 100-150 mm dishes are preferable, while 6 or 12 well plates are preferable for siRNA transfection.
- Incubate GenePorter (20 μL/mL of serum-free transfection medium) and purified plasmid DNA (0.5-1 μg/mL) or siRNA separately in 15 mL tubes containing half the total transfection volume of serum-free medium for 10 minutes. Mix by inversion.

- Combine GenePorter and DNA mixtures and mix by inversion. Incubate for 10 minutes at room temperature and briefly centrifuge.
- Meanwhile, wash cells thoroughly with PBS 2x.
- Add transfection medium to plates or wells and swirl gently to cover.
- Allow transfection to proceed for 4-6 hours in cell incubator.
- Terminate transfection either by aspirating transfection medium and adding complete medium, or by adding medium containing 20% FBS in a 1:1 ratio.
- Allow transfected cells to recover overnight.
- Continue with experimentation or proceed to collection of CM by washing off all complete medium with PBS and incubating in serum-free medium.

Special waste considerations: Dispose of biological material in appropriate Biohazard box.

Protocol 3. Preparation of conditioned medium from mammalian cells.

The purpose of preparation of conditioned medium (CM) is to generate quantities of bioactive, biologically-generated secreted proteins for use in experiments. It should be noted that different cell types may endogenously express different levels of secreted proteins that may confound experimental findings. It may be desirable to screen the background CM of secretor cells with Coomassie or silver stain to determine if other proteins are expressed at high levels.

Reagents and Equipment

Mammalian cells of interest

Culture media: both complete and serum-free

15-50 mL tubes (Corning) and culture plates (10-15 cm)

1x sterile PBS

For concentrating: Amicon concentrators of desired volume (15 mL suggested)

Protocol

- Prior to CM collection, transfect cells to express the desired protein of interest. It is important that cells recover overnight in serum-containing medium prior to CM collection.
- Wash cells extensively with PBS to remove bovine serum albumin from cell surface.
- Incubate cells for 24-48 hours in serum-free medium for all CM collections. Do not use serum-containing medium. Incubation periods longer than 48 hours are not recommended as cells will begin to undergo apoptosis.

- Harvest CM by pipetting into 15 or 50 mL conical tubes. Keep tube contents sterile if they will be used in further biological experiments.
- Centrifuge CM at 6000xg for 15' to remove floating cells prior to analysis or concentration.

Precipitating CM: proceed to CM precipitation protocol to generate samples for Western blot analysis.

Concentrating CM for biological experiments:

- Transfer centrifuged CM to the top compartment of an Amicon Ultra concentrator (5 kDa MW cut-off), being careful to maintain sterile conditions.
- Centrifuge at no greater speed than 6000xg as faster speeds may compromise the filter membrane.
- The time of centrifugation may range depending on the temperature of the centrifuge (recommended: 4-9 degrees Celsius) and the volume of the sample to be concentrated. It is recommended to monitor centrifugation at regular intervals, such as every 20-30 minutes, to prevent overcentrifugation and sample loss.
- Concentrate sample to desired volume. For example, a 15 mL starting sample may be concentrated approximately 30x to a final volume of 500 μL. This concentrated sample may be diluted in appropriate medium to 1x (33 μL concentrate in 1 mL of medium).
- One may elect to save samples of CM prior to and after concentration to determine success of sample concentration or gain an understanding of levels of protein expression in the final sample(s).
- Store unused concentrate at -80 degrees Celsius.

- Alternatively, sample may be buffer-exchanged after concentration. Simply add 15 mL of reaction buffer to concentrated sample and invert to mix, then recentrifuge to desired reaction volume (100-500 μL).
- If desired, a Bradford assay may be performed to quantify protein in the sample. For identifying levels of specific proteins in a heterogenous CM mix, however, quantification using Western blot may prove more useful.

Special waste considerations: Dispose of biological material in appropriate Biohazard box.

Protocol 4. Protein precipitation by TCA or acetone.

The purpose of this experiment is to precipitate the secreted contents of conditioned medium from animal cells to ascertain levels of secreted proteins.

Recommended usage: TCA precipitation may be desirable for large samples, while acetone precipitation may be desirable for small samples.

Reagents and Equipment

Mammalian cells of interest

Culture media: both complete and serum-free for the preparation of CM described in Protocol 3.

15 mL tubes (Corning) and culture plates (10-15 cm)

1x sterile PBS for washing pellets

Acetone (chilled to -20 degrees C), or

50% TCA: diluted in dH2O and stored at 4 degrees C. Protect from light.

Vortexer

High-speed (15-20,000xg) centrifuge

Eppendorf tubes

1x Laemmli sample buffer

Protocol

- Harvest CM and centrifuge at 6000xg for 15 minutes at 4 degrees Celsius to remove floating cells.

TCA precipitation:

- Dilute trichloroacetic acid (TCA) to 50% with dH2O. Store at 4 degrees. Protect from light. Take extreme care when handling TCA as it is highly corrosive.
- Add 250 uL 50% TCA for every mL of CM. Invert or vortex to mix thoroughly.
- Place samples on ice for one hour.
- Following precipitation, centrifuge samples at maximum speed (15,000xg) for half an hour at 4 degrees.
- Remove samples from centrifuge immediately and decant supernatant.
- Wash step (at least one is important to remove residual TCA): wash cell pellet with acetone.
- Centrifuge as before. Decant supernatant. Allow to air-dry, inverted, over a paper towel, for 10-15 minutes.
- Resuspend samples in desired volume of 1x sample buffer (try 150 uL for a 5 mL starting sample) for Western blot analysis.

Acetone precipitation:

- Pre-chill acetone in -20 degrees Celsius.
- Add 4 volumes of ice-cold acetone to CM. Invert or vortex to mix thoroughly.
- Place samples at -20 degrees for at least 2 hours; overnight if possible.
- Following precipitation, centrifuge samples at maximum speed (15,000xg) for half an hour at 4 degrees.
- Remove samples from centrifuge immediately and decant supernatant.
- Allow samples to air-dry, inverted, over a paper towel for 10-15 minutes.

- Resuspend samples in desired volume of 1x sample buffer (try 150 uL for a 5 mL starting sample) for Western blot analysis.

Notes on CM precipitation

- There is not enough protein in typical CM collected in serum-free medium to yield a "pellet": precipitate will look like a fine white mist along one edge of the tube.
- If a pellet is present, it is likely due to too much BSA remaining in the CM from an incomplete wash of the cells prior to CM collection. Anticipate a distortion of the Western blot at approximately 60 kDa.
- When resuspending in sample buffer, make sure to generously wash the inside of the tube with buffer to make sure all precipitate is resuspended. It may be desirable to recentrifuge the tubes briefly to minimize sample loss.
- When working with TCA, take care that the sample buffer does not change color from blue to yellow (due to residual acid from the TCA). If so, add a small amount of dilute NaOH until buffer regains its color.

Special waste considerations: dispose of acetone and TCA in special containers. Dispose of biological material in appropriate Biohazard box.

Protocol 5. PAGE/Western blot analysis.

The purpose of this protocol is to analyze the expression of proteins in a sample of whole cell extract or conditioned medium.

Reagents and Equipment

Samples (CM or WCE) to be analyzed

Gel-loading pipet tips

Power supply for electrophoresis

BioRad precast Criterion gels of desired acrylamide concentration (18 well gel/10%: Catalog #345-0010)

BioRad electrophoresis (running) apparatus

BioRad electrophoresis (transfer) apparatus

BioRad sandwich cassette for transfer

Whatman paper

Nitrocellulose membrane

1x running and transfer buffers (below)

Ponceau staining solution

1x PBS-0.2% Tween20 detergent ("PBST"), or

1x Tris-buffered saline-0.1%Tween20 ("TBST")

Powdered milk, bovine serum albumin or other blocking agent

Primary and secondary antibodies

Chemoluminescence detection reagent (Pierce)

Protocol

SDS-polyacrylamide gel electrophoresis (SDS-PAGE):

- Electrophoresis ("running") buffer: (10x stock in 1L dH2O)
    - Tris-Cl 30.2 g
    - Glycine 144 g
    - SDS 10 g

- Running buffer and stock do not need to be pHed, and may be stored at room temperature. For best results, make 1x running buffer fresh each time.
- Preferably premade gels should be used to minimize gel imperfections and make most efficient use of time.
- Plan sample loading in gel. A little diagram of what lanes contain what samples will be helpful when analyzing blot later.
- Select a gel (BioRad Criterion preferred) based on size of protein of interest. 10% acrylamide works well when visualizing proteins in the 30-70 kDa range.
- Rinse gel with dH2O and remove protective strip at bottom.
- Add samples (20-35 uL/well, depending on well size) to gel carefully, to avoid sample loss or spillage. Do not keep samples on ice prior to loading as some sample components may start to accumulate due to the cold, making equal pipetting difficult.
- Reserve at least one lane for protein size marker (15-20 uL).
- Electrophoresis: 80V for 15 minutes, until the samples contact the resolving gel. After this, voltage can be increased to 110V. Monitor sample progress through the gel to prevent sample loss. Electrophoresis should last 2-2.5 hours.

- Turn off power supply and remove gel from PAGE cassette.
- Prepare transfer "sandwich" as shown in figure by preparing plastic casing, 4 pieces Whatman paper and two sponges in transfer buffer as shown. Prepare a piece of nitrocellulose membrane by cutting it to gel dimensions and soaking it in electrophoretic transfer buffer. Be careful when handling membrane as it is fragile and may pick up skin proteins.

Transfer setup

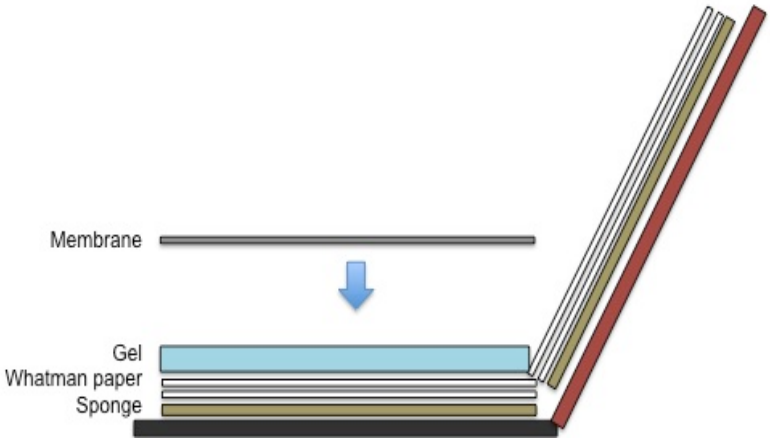

Electrophoretic transfer:

- Transfer buffer (10x stock in 1L dH20)
    - Tris-Cl 30.2 g
    - Glycine 144 g
    - SDS 1 g

- Transfer buffer stock does not need to be pHed and may be stored at RT.

- Transfer buffer, 1x working dilution (1x in 1.5 L):
    - 10x Transfer buffer 150 mL
    - Methanol 300 mL
    - dH2O 1050 mL

- 1x transfer buffer should be stored at 4 degrees C.
- Open gel casing using specially designed top of PAGE cassette. Carefully exise top (wells) and bottom (thick 'foot' of gel) with a razor blade and discard.
- Gently lift gel and place on top of Whatman paper in transfer buffer.
- Cover gel with prewet transfer membrane and roll a glass pipette tube over the membrane to remove bubbles between membrane and gel. Cover with remaining Whatman paper and sponge and close transfer sandwich.
- Place cooling pack and stir bar in clean transfer cassette.
- Place transfer sandwich in transfer cassette and cover with 1x transfer buffer.
- Transfer: 87 V for 1.5 hours or 50 V for 3 hours. Transfer should be done at 4 degrees. Incubate transfer cassette in ice bucket if necessary.
- Stop transfer and determine that lane marker has transferred to membrane. Wash membrane with PBS.
- If desired, incubate membrane with ponceau stain prior to antibody treatment to determine levels of protein and verify that there are no bubbles interfering with signal.
- Remove ponceau by washing with 0.2% PBS-Tween20.

Antibody incubation: refer to manufacturers' protocols for specific wash buffers to be used for particular antibodies (Cell Signaling: use TBST-BSA instead of PBST-milk).

- Block membrane in fresh 5% PBST-milk for 1 hour.
- Incubate with primary antibody (BNT: 1:1000) in PBST-milk overnight at 4 degrees on the rocker.
- Wash 3x 5 minutes with PBST at RT.
- Incubate 5-7 hours at RT on rocker with respective secondary antibody (rabbit 1:1000, Dako preferred) in PBST-milk.
- Wash 3x 5 minutes with PBST. An additional quick wash step with PBS may be desired.
- Prepare chemiluminscence detection agents. Cover the membrane thoroughly with ECL agents, seal under plastic flap in ECL cassette, and visualize with film in the darkroom.

Special waste considerations: 1x transfer buffer may be stored and reused once. Methanol-containing liquids should be properly disposed of.

Protocol 6: Sulforhodamine B (SRB) or crystal violet cell growth assay.

These simple staining procedures are useful to analyze cell number increase over time (ie, net growth). SRB staining protocol is derived from (Vichai and Kirtikara, 2006).

Reagents and Equipment

Mammalian cells of interest

Culture media: both complete and serum-free

Culture plates (Corning; 10-15 cm)

1x sterile PBS

Spectrophotometer

TCA, chilled

Sulforhodamine B

Acetic acid

10 mM Tris buffer, or

Crystal violet

Methanol

Protocol

- Trypsinize cells under study and plate in a 24-well plate at a density of 2.5 x10^4 cells per well in complete medium.
- If administering an inducing agent, such as doxycycline (2 μg/mL), wash cells and add in fresh complete medium after each 24 hour period.

- Fix cells at 4 degrees with cold 10% TCA in PBS after the desired time intervals (0 hr, 24 hr, 48 hr, 72 hr, 96 hr).
- Wash fixed cells 3x with dH2O and air-dry prior to staining.
- SRB staining: prepare 0.4% SRB in 1% acetic acid solution
- After staining 1 hr, wash cells 5x with 1% acetic acid and air-dry.
- Solubilize SRB dye with 10 mM Tris buffer and quantify absorbance using a spectrophotometer at 564 nm.

- Crystal violet staining:
- Wash cells with PBS and fix for 10 minutes on ice using ice-cold methanol.
- Aspirate methanol and cover cells with crystal violet stain (0.5% crystal violet in 25% methanol) for 10 minutes at room temperature.
- Wash cells thoroughly with dH2O to remove excess dye. Allow to air-dry.
- Cells may be counted or the dye solubilized in 100% methanol for quantification.
- Quantify absorbance at OD540.

Special waste considerations: solutions containing methanol or TCA should be disposed of in appropriate containers.

Protocol 7. Modified Boyden chamber cell migration assay

The purpose of this assay is to quantify the migration of cells in response to a stimulus and/or the presence of an inhibitor.

Reagents and Equipment

Mammalian cells of interest (endothelial between passages 2-5)

Endothelial culture media: both complete and serum-free

Culture plates (10-15 cm; Corning)

Transwell chambers (Becton Dickinson labware #353097, with a pore size of 8 μm.)

Migration-stimulating or inhibiting agents of interest

Hemocytometer/microscope

Q-tips

Diff-Quik staining kit (Dade Behring)

Aspirator

Trypsin-EDTA

Microscope slides, coverslips, razor blades, tweezers and clear nail polish

Protocol

- Grow cells of interest to generate a desired quantity of cells. Serum-starve cells overnight prior to performing assay. Maintain sterile conditions and reagents during experiment.
- Hydrate Transwell chambers with 200 uL serum-free culture medium prior to plating.

- If using a migration-inhibiting agent, suspend agent in serum-free culture medium at desired concentration (concentrated CM should be used at 1x). Otherwise, use plain serum-free culture medium to resuspend counted cells (next step).
- Wash, trypsinize and count cells with a hemocytometer. Resuspend cells in serum-free culture medium at a desirable density for plating (eg, $5x10^4$ cells /100-200uL).
- If using a migration-stimulating agent, suspend at desired concentration in serum-containing or serum-free culture medium for use in the bottom chamber. Otherwise, use serum-containing culture medium.
- Add 500 uL (migration-stimulating) serum-containing culture medium to bottom well of Transwell chambers, making sure that the chamber insert rests in the migration stimulating medium.
- Plate in triplicate at a density of $5x10^4$ cells per chamber in the top well of Transwell chambers.
- Incubate cells in cell culture incubator for 8-12 hours.
- Remove cells from top side of membrane using a Q-tip. Wash membrane with PBS to remove dislodged cells, and remove wash buffer with an aspirating pipet. **Be careful not to touch tip of aspirator to fragile membrane during washes.
- Fix and stain cells using the Diff-Quik staining kit (Dade Behring), according to the manufacturer's instructions. Air-dry stained membranes overnight.
- Gently excise membranes from inserts using a razor blade and tweezers.
- Place membranes on a microscope slide. Take care to verify that membranes are lying as flat as possible on slide. Cover with a clean coverslip. Attach coverslip using very small drops of clear nail polish. **If nail polish bleeds to membranes and leaches out

the dye, there is still a very good chance that the cells themselves will still be stained and can be counted.

- Visualize and count cells per view field using 10x magnification.

Special waste considerations: none.

Protocol 8. Scratch wound cell migration assay.

The purpose of this experiment is to quantify rate (speed and distance) of cell migration in the presence of stimulators or inhibitors. It is critical to verify that cells are confluent prior to experiment and that the precise region of migration measurement can be found again after migration (8-12 hours later).

Reagents and Equipment

Mammalian cells of interest (endothelial between passages 2-5)

Endothelial culture media: both complete and serum-free

Culture plates (10-15 cm; Corning)

Migration-stimulating or inhibiting agents of interest

Microscope with camera/imaging software

Sharpie, 10 uL pipet tips

Protocol

- Grow cells of interest to complete confluency in 6 well plates. Serum-starve cells overnight prior to performing assay. Maintain sterile conditions and reagents during experiment.
- Reserve microscope for assay start and endpoints as imaging is critical and will take a long time.
- Prepare control and experimental media (budget 0.5-1mL medium per well). Serum-free medium may be used as a negative control; other conditions should contain migration-stimulating serum.

- Mix agents in experimental medium thoroughly and centrifuge prior to use.
- Draw two perpendicular lines on the bottom of each well using a straight edge and Sharpie (may be easier to do this prior to plating cells).
- Maintaining sterile conditions, use a 10 uL pipet tip to draw 2-4 straight parallel lines in each well (dotted in diagram).
- Wash cells 2x with 1 mL PBS to remove dislodged cells.

Representative image of scratch wound assay setup.

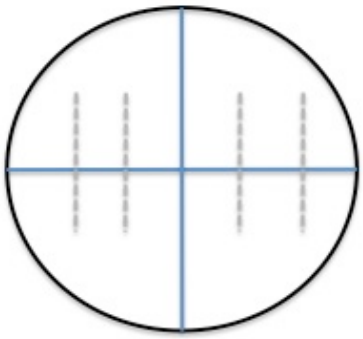

- Cover cells with desired medium. If pretreating cells, incubate with agents of interest mixed with serum-free medium for 30 minutes, then mix with 20% serum-containing medium to promote migration.
- **First image**: take cells to microscope immediately as imaging will take some time (depending on how many wells/scratches, 1-2 hours). Assign a number to each well. Use grid on well to locate scratches, using 20x magnification. Take measurements using computer software (if available – otherwise be sure to include scale bar on image). Select scratches with clean parallel borders for ease of measurement. Take a picture for each measurement and save it with the well number and notation concerning the scratch. Keep a physical record of what scratch is being imaged in what well, and note the relationship to the grid.
- Incubate in cell culture incubator for 8-12 hours depending on speed of migration/cell type.

- **Second image**: for best results, cells should not be fixed for the second image as this may interfere with cell shape. Repeat imaging as previously described, generating images/measurements for each observable scratch.
- Calculating wound closure: if measurements of wound width were not available from the computer software, use a straight edge to measure the width of the wound to the length of the scale bar.

  (initial wound width – final wound width)/(initial wound width)*100 = %closure

Special waste considerations: dispose of biological material in appropriate Biohazard box.

Protocol 9. Matrigel endothelial cord formation assay.

The purpose of this experiment is to observe elements of the recapitulation of endothelial cord formation *in vivo*.

Reagents and Equipment

Mammalian cells of interest (endothelial between passages 2-5)

Complete endothelial cell culture medium (Lonza)

Trypsin-EDTA

1x sterile PBS

6-well culture dishes (Corning)

Cell-stimulating or inhibiting agents of interest

Microscope with camera/imaging software to take pictures of cords, if desired

Matrigel (Becton Dickinson: store at -20 degrees C)

Protocol

- Grow primary cultures of endothelial cells (HDMEC, HUVEC) at passage 2-4 to generate a desired quantity of cells. Serum-starve cells overnight (1% serum) prior to performing assay. Maintain sterile conditions and reagents during experiment.
- Thaw matrigel at 4 degrees for several hours or overnight before experiment. (Matrigel should be stored at -20 degrees.)
- Precoat wells of a 24-well plate with 250 uL of matrigel. Keep matrigel on ice, and use chilled tips if possible. Allow matrigel to solidify in a 37 degree incubator for at least an hour prior to experiment.

- Trypsinize and count endothelial cells, and resuspend in serum-containing endothelial culture medium.
- Seed cells into wells at a density of 50,000 cells/well. Each condition should be performed in triplicate.
- Prepare treatment medium, if desired: combine agents of interest with serum-containing culture medium at desired concentration (accounting for presence of medium in wells), and add to wells. Add equivalent volumes of culture medium to control wells. Minimize use of medium: total volume not to exceed 500 uL. Swirl to mix.
- Allow cells to recover in culture incubator overnight (12-18 hours, depending on cell type: HUVEC recover more quickly than HDMEC).
- Image using 10x microscopy.
- Notes: Endothelial cells will arrange themselves into 'nodes' which may connect to other nodes. Single node-node connections may be scored as 'cords', whereas connections of cords that arrange themselves into a ring-like structure (recapitulating the formation of the endothelial lumen) may be scored as enclosed structures.
- Quantify vascular structure formation with three views per well and calculate using statistical software.

Special waste considerations: dispose of biological material into Biohazard boxes.

Protocol 10. Quantitative directed *in vivo* angiogenesis assay (DIVAA).

The purpose of this experiment is to quantify physiological angiogenesis *in vivo* in the presence of stimulators or inhibitors. This protocol is derived from that of the kit manufacturer (Trevigen, Catalog # 3450-048-K).

Reagents and Equipment

Tube preparation:

DIVAA kit (Trevigen, Catalog # 3450-048-K): contains tubes, growth factors, matrigel, FITC stock solution, CellSperse solution

Angiorack (Trevigen): sold separately, but essential for holding tubes upright

Agents of interest to be added to tubes

Fine-tipped forceps to handle tubes

Sterile eppendorf tubes

Surgery:

Sterile sutures

Sterile ketamine/xylazine solution

Sterile scalpels

Sterile forceps

Sterile surgery scissors to make initial cut

Ethanol/alcohol prep pads to sterilize equipment during surgery

Warming pad

Scale to weigh animals

Notes on preparation for DIVAA:

- This protocol is optimized for use in nude mice. Plan to implant two tubes per side of each mouse; however, three per side is possible. If more than one treatment condition is being used, tattoo the mice of each treatment group for ease of identification.
- **Make sure to have the AngioRack (Trevigen, 3450-048-09) on hand. Otherwise it will be impossible to hold the tiny tubes upright and in place while filling them.
- **Preparation of tubes**. Store reagents at their respective temperatures prior to use.
- Plan experiment with the assumption that animals may be able to remove several tubes and thus extras may be desirable. Ideally, 8-10 reactors should be used per condition to achieve statistical significance, but pilot experiments may require fewer.

- Thaw matrigel at 4 degrees. Keep all reagents on ice. Prior to adding agents of interest, prepare matrigel by combining with provided VEGF (0.5 ng/ mL), bFGF (1.5 ng/mL) and heparin (100 ng/mL) according to the manufacturer's instructions.
- Divide prepared matrigel into chilled 1.5 mL microfuge tubes into portions as required for the experiment. Budget 20 uL matrigel mix per tube, so that one 250 uL tube of matrigel may fill 12 reactors.
- Add agents of interest to respective tubes. **Do not let volume of added agents exceed 10% of volume as this may compromise matrigel solidification. Pipet thoroughly to mix. Avoid air bubbles in mix.
- Add matrigel mix to tubes. To avoid air bubbles in mix, bend reactor slightly and begin pipetting mix at bottom of tube, drawing tip out as tube fills. Fill completely with matrigel mix, avoiding formation of a meniscus at the top of the tube.

- Remove tube from AngioRack with tweezers and place, inverted, into a labeled sterile microfuge tube and cap.
- When all tubes are prepared and in microfuge tubes, place tubes at 37 degrees for at least an hour to allow gel to solidify.
- **Implantation of tubes**. Anesthetize mice using intraperitoneal injection of ketamine/xylazine. Do not anesthetize all at once as surgery may take some time.
- Make a small surgical incision above the flank of the anesthetized mouse. Avoid the musculature and body cavity. Keep the incision as small as possible to prevent the subject from removing the tubes when it wakes up. Refer to the Trevigen protocol for images of how surgery should look. Insert scissors into the incision to gently cut away connective tissue between skin and body wall to facilitate tube insertion.
- Implant the control tubes on one side of each mouse (for example, all control tubes implanted above the left flank) and the treatment tubes on the other.
- Use tweezers to insert tube into incision, with the open end of the tube facing into the wound. Be careful not to squeeze the tube so that the gel is dislodged. Push first tube in, so that there is room for a second tube next to it. Insert the second tube in the same manner.
- Close the incision site using sterile sutures close together (without severing the connection between sutures – this will prevent the mouse from opening up a hole in the surgery site to remove the tubes).
- Repeat procedure for opposite flank.
- Allow subjects to recover on heating pad until awake.
- Monitor subjects for health and tube removal for 10-15 days after implantation.

- **Tube excision and FITC quantification**. After desired period, humanely sacrifice subjects with CO2.
- Cut a fairly wide swath of skin around reactors to prevent gel being dislodged. **Carefully remove excess skin from tubes. Be aware that vessels growing into the tube are still attached to the skin and do not pull on the skin at the tube opening as this will dislodge vessels/clots.
- After excision, photograph the tubes or image with microscopy to obtain preliminary images of vascularization.
- To remove gel from tubes, first excise closed end with a razor and discard. Aiming end of reactor into an microfuge tube, insert pipette tip in other end and pipet 300 uL of CellSperse wash buffer (from kit components) to flush gel into microfuge tube. **Use a separate microfuge tube for each reactor.
- Recap tube and incubate at 37 degrees for 1-3 hours.
- Prepare 1x DIVAA wash buffer from 10x stock.
- Centrifuge cell suspensions at 250xg for 10 minutes at room temperature to generate cell pellet. Wash with 500 uL 1x wash buffer and re-centrifuge.
- Dilute 25x FITC dilution buffer (provided in kit) to 1x. Add 1 uL 200x FITC-lectin per 200 uL FITC dilution buffer. Protect FITC solutions from light.
- Add 200 uL diluted FITC solution to each cell pellet. Invert to suspend and briefly centrifuge.
- Incubate pellets at 4 degrees C overnight in darkness.
- Wash pellet 3x with wash buffer, centrifuging at 250xg for 5 minutes.

- Suspend each pellet in 100 uL of wash buffer and place in well of 96 well plate. Perform fluorimetric analysis at 485 nm excitation, 510 nm emission. Use wash buffer as a control.

Protocol 11. *In vitro* vascular permeability assay.

The purpose of this assay is to determine whether agents of interest may interfere with or promote vascular permeability. This protocol is derived from the Chemicon *In Vitro* vascular permeability assay (Catalog #ECM640).

Reagents and Equipment

Chemicon *In Vitro* vascular permeability assay kit (Catalog #ECM640): contains culture wells and FITC-dextran solution

rhVEGF165 (Cell Signaling)

Endothelial cells (HDMEC or HUVEC, p. 2-4)

Permeability-modulating agents

1x sterile PBS

Endothelial culture media: both serum-free and complete

- Culture endothelial cells of interest at low passage (2-3) to generate sufficient cells for assay (to be performed in triplicate).
- On day of assay start, trypsinize cells and count. Resuspend in complete endothelial culture medium at a concentration of $1x10^6$ cells/mL.
- Keep forceps in ethanol and handle inserts with forceps.
- Add 200 uL collagen coating solution to bottom of inserts. Incubate at room temperature for 1 hour, maintaining sterile conditions.
- Shake out residual solution into a waste container (do not aspirate).
- Hydrate inserts with 250 uL of provided Cell Growth medium at RT for 15 minutes.

- Remove growth medium. Seed cells into wells (200 uL/well = $2x10^5$ cells/well).
- Cover with 500 uL culture medium.
- Allow to recover several days until confluent monolayer is formed.
- Serum-starve cells overnight.
- Pretreatment: combine agents of interest with endothelial culture medium (final volume: 500 uL per well). Carefully aspirate medium from cells and pretreat for 30 minutes.
- Add rhVEGF165 to a final concentration of 10 ng/mL.
- Incubate in cell incubator for 18 hours.
- Visualization: remove medium from cells carefully. Transfer inserts to detection plate.
- Add 500 uL medium to the bottom chamber of each well. Dilute FITC-dextran solution (250 uL) in 1.75 mL culture medium. Protect FITC from light.
- Add 150 uL of diluted FITC-dextran solution to each insert. Incubate at RT for 5 minutes.
- Remove inserts from detection plate. Gently rock plate to mix.
- Remove aliquots of solution from each well and pipet into a 96well plate.
- Read plate with a fluorimeter at excitation 485 nm and emission 530 nm.

Special waste considerations: dispose of biological material in a Biohazard container.

Protocol 12. Vector cloning.

The purpose of cloning vectors is to insert DNA encoding genes of interest into vectors designed to express them under certain conditions, such as doxycycline inducibility described below.

Reagents and Equipment

PCR:

Commercially available expression vector (Invitrogen)

Desired cDNA of interest to serve as PCR template

PCR primers to generate insert

PCR mix (Invitrogen Platinum Taq SuperMix)

DMSO (for GC-rich templates such as BAI1)

PCR thermal cycler

PCR tubes

Digestion and ligation:

Restriction enzymes (New England Biolabs)

Restriction enzyme digestion buffer (New England Biolabs)

Bovine serum albumin (New England Biolabs)

Eppendorf tubes

Gel purification kit (QiaGen Catalog # 28104)

T4 Ligase (Invitrogen Catalog #15224-041)

Ligase buffer (Invitrogen)

Plating:

Luria-Bertani (LB) powder

Agar

Ampicillin

Untreated plastic dishes to make bacterial plates

Glass spreaders, sterilizing Bunsen burner and EtOH

Protocol

Making LB-amp plates:

- Make 1L LB stock by mixing 25 g LB powder in dH2O on stir plate.
- pH LB stock to approximately 7.4 using NaOH.
- Make 1000x ampicillin stock (100 mg/mL). Store at -20 degrees C.
- Divide LB stock into two 500 mL solutions. Add 7.5 g agar to one beaker. Cover with aluminum foil and autoclave tape. Autoclave (liquid cycle) for 15-30 minutes.
- Allow to cool. Monitor LB-agar to make sure it doesn't solidify. When warm but still liquid, add 500 uL 1000x ampicillin stock and swirl gently (no bubbles!) to mix.
- Pour onto plates and allow to dry (15-20 min) on benchtop. Do not overdry. Store in the dark at 4 degrees.
- LB stock can be kept on benchtop if sterile; add amp stock to grow colonies.

PCR:

- Use PCR to generate Vstat40 encoding insert (comprising BAI1 amino acids 1-328) flanked at the 5' end by a HindIII site and at the 3' end by an XbaI restriction site.
- Inducible vector: pTRE2 (Invitrogen). Does not contain a selection marker for geneticin selection.

- Primers ordered from IDTDna and resuspended in dH2O at a concentration of 500 ng/uL.
- PCR setup protocol for BAI1 cDNA (GC-rich, requires 5% DMSO): follow specific manufacturer's protocol for individual polymerases.

▪ DNA (5-10 ng)	2-4 uL
▪ 10x PCR buffer	2 uL
▪ DMSO	2 uL
▪ Forward primer	0.5 uL
▪ Reverse primer	0.5 uL
▪ Polymerase (Taq, Pfu)	0.4 uL
▪ Clean dH2O	to final volume
▪ Total reaction volume: 20 uL	

- PCR reaction protocol:

  - 2 minutes, 94 degrees C
  - 30 seconds, 94 degrees C
  - 30 seconds, 57 degrees C
  - 1 minute 45 seconds, 72 degrees C
  - Repeat steps 2-4 34 times.
  - 10 minutes, 72 degrees C
  - Until retrieval, 4 degrees C

- Purify insert using a Qiagen gel purification kit. Digest insert and vector in preparation for ligation.
- Typical digest protocol, to be altered as desired:

▪ DNA	3-7 uL
▪ 10x buffer (NE Biolabs)	2 uL
▪ 10 BSA (NE Biolabs)	2 uL
▪ HindIII	0.8 uL
▪ XbaI	0.8 uL
▪ dH2O	to final volume
▪ Total digest volume: 20 uL	

- Purify digested insert and vector in preparation for ligation. Quantify purified DNA to determine relative concentrations.

- Ligate purified insert and vector (approximate ratio of 3:1). Take vector size into account (if 3x larger than insert, use equivalent amounts of DNA).
- Ligation protocol (from protocol for T4 ligase, Invitrogen, Catalog #15224-041):

▪ Vector (35 ng)	1 uL
▪ Insert (35 ng)	1 uL
▪ 5x reaction buffer	4 uL
▪ T4 ligase (2.5 U)	0.5 uL
▪ Fresh dH2O	to final volume
▪ Total reaction volume: 20 uL	

- Proceed with transformation and plating on fresh LB-ampicillin plates.

Transformation:

- Thaw 50 uL competent TOP10 E.coli on ice on benchtop for 10 minutes.
- Add 1-3 uL desired cDNA (0.1 ug – 0.5 ug) to bacteria and keep on ice for 15-20 minutes.
- Heat-shock bacteria for 30 seconds at 42 degrees C.
- Immediately return to ice for 2 minutes.
- Plate desired amount in 200 uL LB-amp puddle on fresh plates (prewarmed at 37 degrees C). Spread with sterilized, cooled glass spreader.
- Incubate inverted at 37 degrees C overnight to obtain colonies.

Special waste considerations: dispose of biological material in a biohazard container.

Protocol 13. Preparation of stable inducible clones for tumorigenesis studies.

The purpose of this experiment is to generate tumor cell line clones stably expressing a gene of interest (Vstat40).

Reagents and Equipment

Tumor cells of interest

Complete cell culture medium

Trypsin-EDTA

1x sterile PBS

Vectors containing DNA of interest

Selection reagents (G418: Clontech Catalog # 631308)

Cell culture dishes (15 cm)

Cloning disks (Sigma, Z374431)

6-well plates (Corning)

Forceps, alcohol prep pads

Protocol

- Culture tumor cells stably expressing the tet-on plasmid, such as LN229-L16 glioma cells. Maintain selection using appropriate antibiotic (puromycin (0.5 ug/mL) for lN229-L16 cells).
- Transform TOP10 E.coli with inducible plasmid or select a colony from a plate. If necessary, grow up additional plasmid containing selection marker of interest, such as

pEGFP-N2 (Invitrogen, Catalog # 6081-1), which contains the neomycin resistance marker for geneticin selection. Grow in LB/ampicillin overnight.

- Purify DNA using a Qiagen midiprep kit according to manufacturer's instructions. Run an aliquot on gel to verify plasmid of correct size.
- Verify plasmid composition with combinations of restriction enzymes as desired.
- Quantify inducible vector and selection marker vector.
- Vectors may be linearized prior to transfection if desired.
- Transfect cells according to the GenePorter transfection protocol. Combine inducible and selection marker (cDNA to be at a ratio of 10:1 to ensure selected colonies will express gene of interest.
- After 24 hours recovery from transfection, passage cells to very low density in 15 mL plates (use 5-10 plates), in complete medium containing 800 μg/mL G418 (Invitrogen) and 0.5 μg /mL puromycin.
- Maintain selection, changing medium every other day. Wash away dead cells.
- Within 2 weeks, most cells should be dead (a control plate containing non-transfected cells may be used to verify) and drug-resistant colonies should be developing.
- Selecting colonies using cloning disks:
- Keep cloning disks sterile. Place 25-50 disks in small dish of trypsin to soak.
- Wash remaining cells with PBS and aspirate medium.
- Keeping cells sterile, circle colonies on bottom of plate with sharpie to indicate presence of colonies.
- Allow plate to dry somewhat to prevent trypsin spreading to other colonies.
- Use sterile forceps to place cloning disks on desired colonies. Wipe forceps with alcohol prep pads between colony selections.

- After 3-5 minutes, gently remove cloning disks, taking care not to touch other clones, and place in 6 well dishes containing 1-2 mL complete medium with selection drug (geneticin) as before. Gently tap plate to encourage cells to detach from disks.
- Allow cells to recover and expand for several days.
- To determine inducibility, passage each colony into two wells. After recovery, cover cells with serum-free medium and treat one well with doxycycline (2 ug/mL).
- **Doxycyline should always be made fresh and filtered prior to use. Do not freeze doxycycline. Harvest CM for Western blot to determine inducibility and leakiness of clone.
- Select clones with good inducibility and no background for use in experiments.
- Switch drug concentration in medium to half selection concentration for maintenance.

Special waste considerations: dispose of biological material in a Biohazard container.

Protocol 14. *In vivo* vascular permeability with Evans blue dye in intracranial tumors.

The purpose of this experiment is to demonstrate vascular permeability in tumors in the presence or absence of permeability-modulating agents. Small molecules such as EBD leach through fenestrations in irregulat tumor vasculature, permitting detection of tumor and approximate size (principle of MRI detection).

Reagents and Equipment

Evans blue dye powder (Sigma Catalog # E2129)

Syringe (25 bore)

Mice bearing intracranial tumors (also can be performed with nude mice injected subdermally with permeability-inducing agents such as VEGF)

Scale

Ketamine-xylazine anesthesia solution

Heating pad

Brain dissection tools: scissors, forceps

Protocol

- Implant mice intracranially with tumor cells. Do not wait until subjects have reached endpoint of tumor burden as it is likely that all tumors will be quite vascularized by this time.
- Weigh subjects of control and treatment conditions to assure that animals of equivalent weight and health status are being assayed.

- Weigh animals prior to tail vein injection.

Tail vein injection protocol:

- Anesthetize subjects intraperitoneally with ketamine/xylazine. The TVI injection procedure is approved by IACUC either for awake or anesthetized subjects, but may be practiced upon anesthetized subjects only.
- Immobilize tail proximally and distally.
- Begin injections in the distal tail and move towards the animal. One cannot inject behind a punctured vein. Either vein may be used.
- Hold syringe with bevel facing up, in such a way to maintain outward pressure against the plunger. The plunger must be held this way in a gentle, constant manner in order to aspirate blood from the tail vein. The needle is not in the vein until the blood is aspirated. Make sure no bubbles are in the solution prior to injection; however, the mouse tolerance for injected air is much better than humans'.
- If there is resistance to injection, the needle is not in the vein. The injected substance should go in smoothly and the blood in the vein should disappear briefly after injection.

- Evans blue dye: administer 30 mg/kg.
- Allow subjects to recover on heating pad. Return to cage for 24 hours.
- Humanely sacrifice subjects using CO2. Dissect out brain and image any observable dye on brain surface.
- Homogenize brain tissue with a douncer and suspend in 1 mL dimethylformamide to extract the dye overnight.

- Centrifuge extracts at 5000xg for 10 minutes. Aliquot supernatant into 96 well plate. Use DMF as a negative control.
- Analyze fluorescence of supernatant using a fluorometer at 540 nm excitation and 680 nm emission.

Special waste considerations: dispose of biological material in Biohazard boxes. Store carcasses in appropriate DAR refrigerator.

Protocol 15: Production of GST-tagged peptides and inclusion body solubilization.

Inclusion bodies containing the GST-Vstats may be solubilized using 8M Urea buffer. A washing protocol was developed to solubilize the protein, consisting of four steps with associated buffers, based on the protocol described in Chapter 4 of Protein Purification Protocols (D. Margaret Worrall) (Doonan, 1996).

Reagents and Equipment

Competent E.coli (BL21.DE, Invitrogen – preferred)

LB-amp

Bacterial shaker (able to perform 250 rpm at 37 degrees C)

Spectrophotometer

IPTG (Sigma, Catalog # I6758)

Buffers: composition for lysis, wash and solubilization buffers described below.

Rocker/ice

Protocol

Induction:

- Transform bacteria with IPTG-inducible construct of interest.
- Resuspend bacteria in LB-amp (regular LB may be used, if kept sterile) so that 50 uL of bacterial prep grows in 4 mL LB-amp.
- Grow at 37 degrees C/250 rpm on shaker until an OD600 value of approximately 0.6 (range 0.5-0.7) is reached. Begin testing OD values after 1 hour on shaker as this value may be reached between 1.5 and 3 hours.

- Once the optimal OD value is achieved, add IPTG to the prep at desired concentration (1 mM starting concentation).
- Grow induced bacteria on shaker another 1.5-3 hours on shaker at same conditions.
- Remove bacteria and pellet 8000xg/15 min/4 degrees to obtain pellet for analysis.

Lysis:

- Resuspend bacterial pellets in lysis buffer (below) and incubate for 30 minutes on ice on the rocker.

Lysis buffer: 100 mM Tris-Cl, 50 mM EDTA, 50 mM PMSF, lysozyme (300 μg/mL), sodium deoxycholate (1 mg/mL) and DNAse (10 mg/mL).

Wash 1:

- Centrifuge bacterial slurry for 15 minutes at 15,000xg at 4 degrees.
- Store supernatant fraction for precipitation and analysis.
- Resuspend insoluble fraction in Wash 1 buffer and incubate for 4 hours at room temperature on the rocker.

Wash 1 buffer: Lysis buffer, 2M urea, 0.5% Triton X-100.

Wash 2:

- Centrifuge bacterial slurry for 15 minutes at 15,000xg at 4 degrees.
- Store supernatant fraction for precipitation and analysis.
- Resuspend insoluble fraction in Wash 2 buffer and incubate for 2 hours at room temperature on the rocker.

Wash 2 buffer: Lysis buffer, 4M urea, 0.5% Triton X-100.

Solubilization:

- Centrifuge bacterial slurry for 15 minutes at 15,000xg at 4 degrees.
- Store supernatant fraction for precipitation and analysis.

- Resuspend insoluble fraction in Solubilization buffer and incubate overnight at room temperature on the rocker. This will dissolve inclusion bodies and the resulting slurry can be dialyzed to remove urea.

Solubilization buffer: 8M urea, 50 mM Tris, 1 mM DTT.

Special waste considerations: none.

Protocol 16. Dialysis and thrombin purification of GST-tagged peptides.

The purpose of these experiments is to remove urea from solubilization buffers used to solubilize inclusion bodies containing GST-tagged peptides. Dialysis removes urea in a stepwise fashion, while glutathione beads specifically bind to the GST tag for a pulldown procedure. Purified recombinant peptide may be obtained by cleaving the GST tag off the peptide using thrombin enzyme.

Reagents and Equipment

Solubilized inclusion body fraction (from Protocol 15)

Slide-A-Lyzer G2 dialysis cassettes (15 mL, 10 kDa MW cut-off: ThermoScientific Catalog # 87731)

Dialysis buffers (composition described below)

Stir bar and magnetic plate

15 mL centrifuge tubes

Chilled acetone

Glutathione resin ("beads") (Clontech Catalog # 635607)

Eppendorf tubes

1x PBS

Thrombin (GE Life Sciences, Catalog # 27-0846-01)

Protocol

Dialysis.

- Obtain 15 mL Slide-A-Lyzer G2 dialysis cassettes (ThermoScientific).

- Hydrate cassette in dialysis buffer for 2 minutes prior to adding substance to be dialyzed.
- Remove and tap dry (do not blot membrane).
- Twist cap carefully until open. Use a 10 mL pipette to add substance to be dialyzed into cassette.
- Suspend cassette (autoclave tape works well) so that it is immersed in dialysis buffer in large (2L) glass beaker.
- Add stir bar and place on magnetic stir plate. Agitate gently.
- Keep an eye on cassette to verify that it does not overswell.
- Change dialysis buffer as desired (after 12-24 hour intervals). Use decreasing concentrations of urea in 50 mM Tris buffer. Recommended starting point: two-fold dilution per step. Start with 4M urea dialysis buffer, then progress to 2M urea, then 1M urea, then 0.5M urea, and so forth until desired concentration is obtained.
- Take aliquots of dialysate during dialysis to monitor sample loss. Precipitate with chilled acetone for analysis by Western blot.

GST pulldown.

- Following dialysis, recover the dialysate from the inside of the cassette using a 10 mL pipette. For best results, immediately proceed to GST pulldown. However, it may be desired to precipitate aliquots of dialysate to verify levels of protein prior to pulldown.
- Prepare glutathione resin for pulldown by washing with 1 volume of PBS and centrifuging at 1500xg for 10 minutes.
- Add dialysate to glutathione resin in clean eppendorf tubes. Starting ratio: combine 300 uL resin per 1 mL dialysate.

- Seal tubes with parafilm. Incubate at 4 degrees C on the rocker overnight.
- Centrifuge tubes at 1500xg at 4 degrees C for 15 minutes to collect pellet.
- Retain and precipitate supernatant with 4 volumes of chilled acetone to determine how much sample is not bound to glutathione.
- Wash pellet containing GST-tagged proteins gently with PBS and centrifuge.

Thrombin purification.

- Resuspend pellet in 300 uL fresh PBS.
- Add 1 U catalytically active thrombin to bead slurry.
- Incubate at RT on the rocker as desired (overnight).
- Centrifuge pellet at 1500xg for 15 minutes to collect supernatant fraction (containing cleaved protein) and pellet fraction.
- Precipitate supernatant fraction with acetone and analyze with Western blot. It is a good idea to also analyze the pellet fraction to determine the levels of GST-tagged protein retained on the beads. To do so, suspend the pellet fraction in 1 volume sample buffer and boil for 3 minutes to dissolve resin prior to loading on electrophoresis gel.

Special waste considerations: none. Take care when handling urea.

APPENDIX II

PLASMID CONSTRUCTS

Constructs developed:

Probe records:

Record Number	8-048
gene name	BAI1
plasmid/probe/vector name	Vstat40-Q2-5, R323A
Keywords	BAI1, Vasculostatin, Vstat
species and origin	human
HGM symbol	BAI1
chrom. location	8q24
copy number	1
GenBank #	
Source	S Cork, NB1 p186-222
References	Nishimori, et al., Oncogene 15:2145-2150 (1997). Cork SM et al. (2011) Oncogene, submitted.
user and date	S Cork, November 2007
Comments	The (tagged) insert is the BAI1 N terminal domain up to amino acid 329 with a point mutation R323A, which does not appear to abrogate Vstat40 process ing.

Description:

vector	pcDNA 3.1/V5-His-TOPO (Invitrogen) 5.5 kb
cloning site	no digestion; PCR-generated inserts ligate directly with linear vector
insert kb	1 kb
total size	6.5 kb
resist.	amp
Bacteria	TOP10
Freezer Location	B 8a-48,49

Polymorphisms:

enzyme	allele size (Kb)	frequency

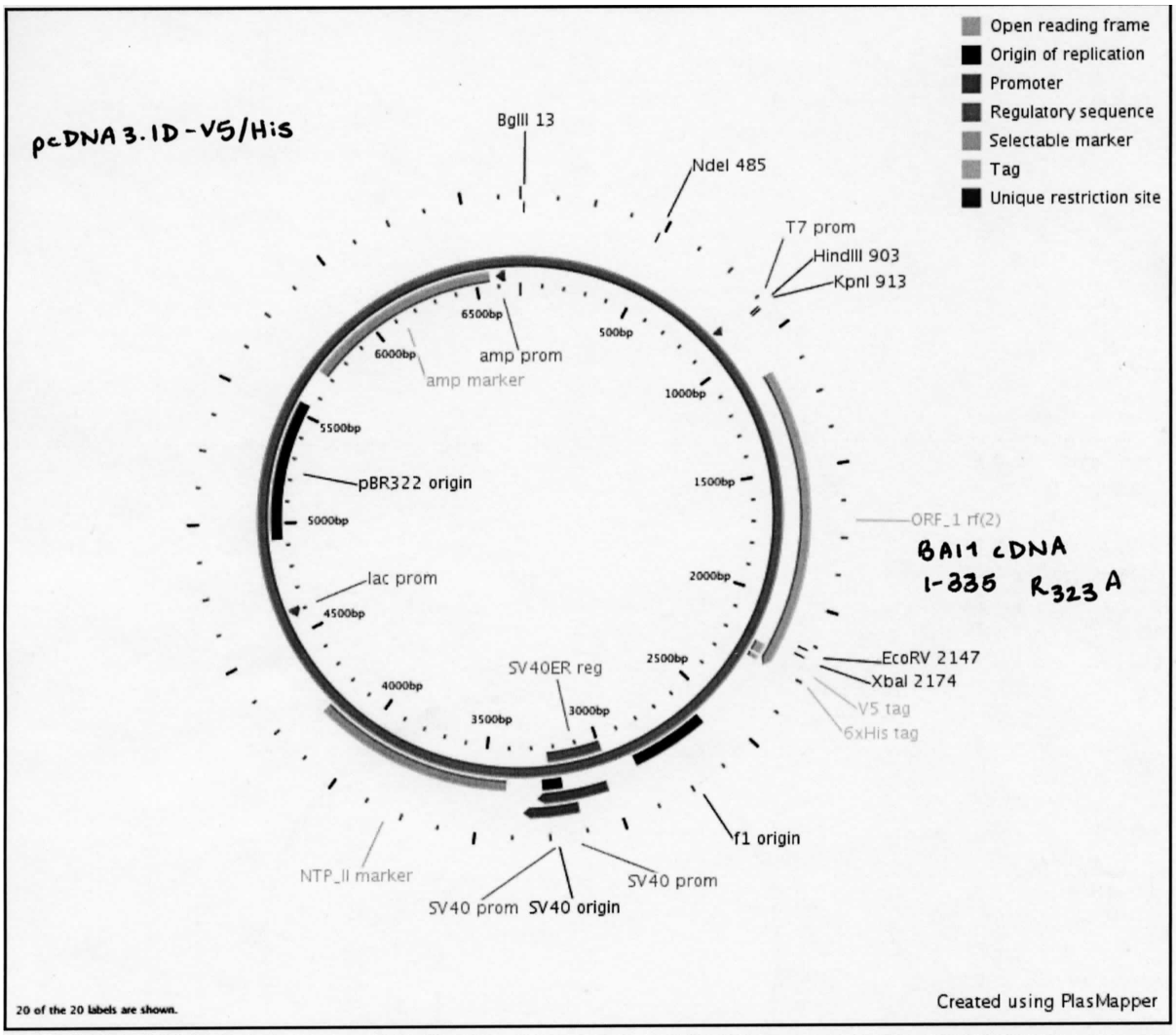
pcDNA 3.1D-V5/His
Open reading frame
Origin of replication
Promoter
Regulatory sequence
Selectable marker
Tag
Unique restriction site
BglII 13
NdeI 485
T7 prom
HindIII 903
KpnI 913
6500bp
500bp
6000bp
amp prom
amp marker
1000bp
5500bp
pBR322 origin
1500bp
5000bp
ORF_1 rf(2)
BAI1 cDNA
1-335 R323A
lac prom
2000bp
4500bp
EcoRV 2147
XbaI 2174
2500bp
SV40ER reg
4000bp
V5 tag
3000bp
3500bp
6xHis tag
f1 origin
NTP_II marker
SV40 prom
SV40 prom
SV40 origin
20 of the 20 labels are shown.
Created using PlasMapper

Probe records:

Record Number	8-050
gene name	BAI1
plasmid/probe/vector name	Vstat40-Q2-6, Q325A
Keywords	BAI1, Vasculostatin, Vstat
species and origin	human
HGM symbol	BAI1
chrom. location	8q24
copy number	1
GenBank #	
Source	S Cork, NB1 p186-222
References	Nishimori, et al., Oncogene 15:2145-2150 (1997). Cork SM et al. (2011) Oncogene, submitted.
user and date	S Cork, November 2007
Comments	The (tagged) insert is the BAI1 N terminal domain up to amino acid 331 with a point mutation Q325A, which does not appear to abrogate Vstat40 processing. Insert is cloned into pcDNA3.1/V5-His.

Description:

vector	pcDNA 3.1/V5-His-TOPO (Invitrogen) 5.5 kb
cloning site	no digestion; PCR-generated inserts ligate directly with linear vector
insert kb	1 kb
total size	6.5 kb
resist.	amp
Bacteria	TOP-10
Freezer Location	B 8a-50,51

Polymorphisms:

enzyme	allele size (Kb)	frequency

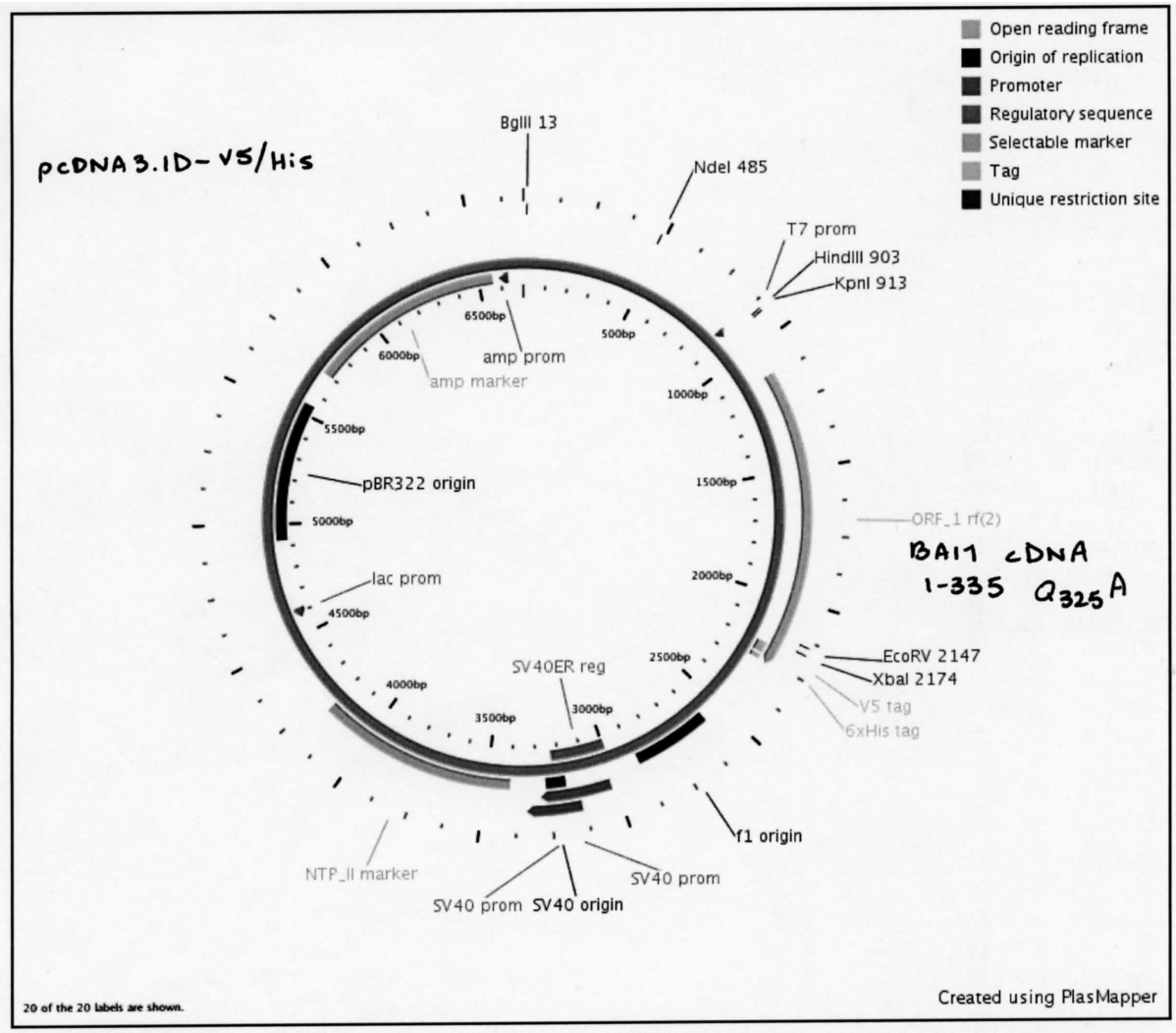
pcDNA 3.1D-V5/His
Open reading frame
Origin of replication
Promoter
Regulatory sequence
Selectable marker
Tag
Unique restriction site
BglII 13
NdeI 485
T7 prom
HindIII 903
KpnI 913
6500bp
500bp
6000bp
amp prom
amp marker
1000bp
5500bp
pBR322 origin
1500bp
5000bp
ORF_1 rf(2)
BA11 cDNA
1-335 Q325A
lac prom
2000bp
4500bp
EcoRV 2147
SV40ER reg
2500bp
XbaI 2174
4000bp
V5 tag
3000bp
3500bp
6xHis tag
f1 origin
NTP_II marker
SV40 prom
SV40 prom
SV40 origin
20 of the 20 labels are shown.
Created using PlasMapper

Probe records:

Record Number	8-052
gene name	BAI1
plasmid/probe/vector name	Vstat40-Q2-7, S326A
Keywords	BAI1, Vasculostatin, Vstat
species and origin	human
HGM symbol	BAI1
chrom. location	8q24
copy number	1
GenBank #	
Source	S Cork, NB1 p186-222
References	Nishimori, et al., Oncogene 15:2145-2150 (1997). Cork SM et al. (2011) Oncogene, submitted.
user and date	S Cork, November 2007
Comments	The (tagged) insert is the BAI1 N terminal domain up to amino acid 332 with a point mutation S326A, which does not appear to abrogate Vstat40 process ing.

Description:

vector	pcDNA 3.1/V5-His-TOPO (Invitrogen) 5.5 kb
cloning site	no digestion; PCR-generated inserts ligate directly with linear vector
insert kb	1 kb
total size	6.5 kb
resist.	amp
Bacteria	TOP10
Freezer Location	B 8a-52,53

Polymorphisms:

enzyme	allele size (Kb)	frequency

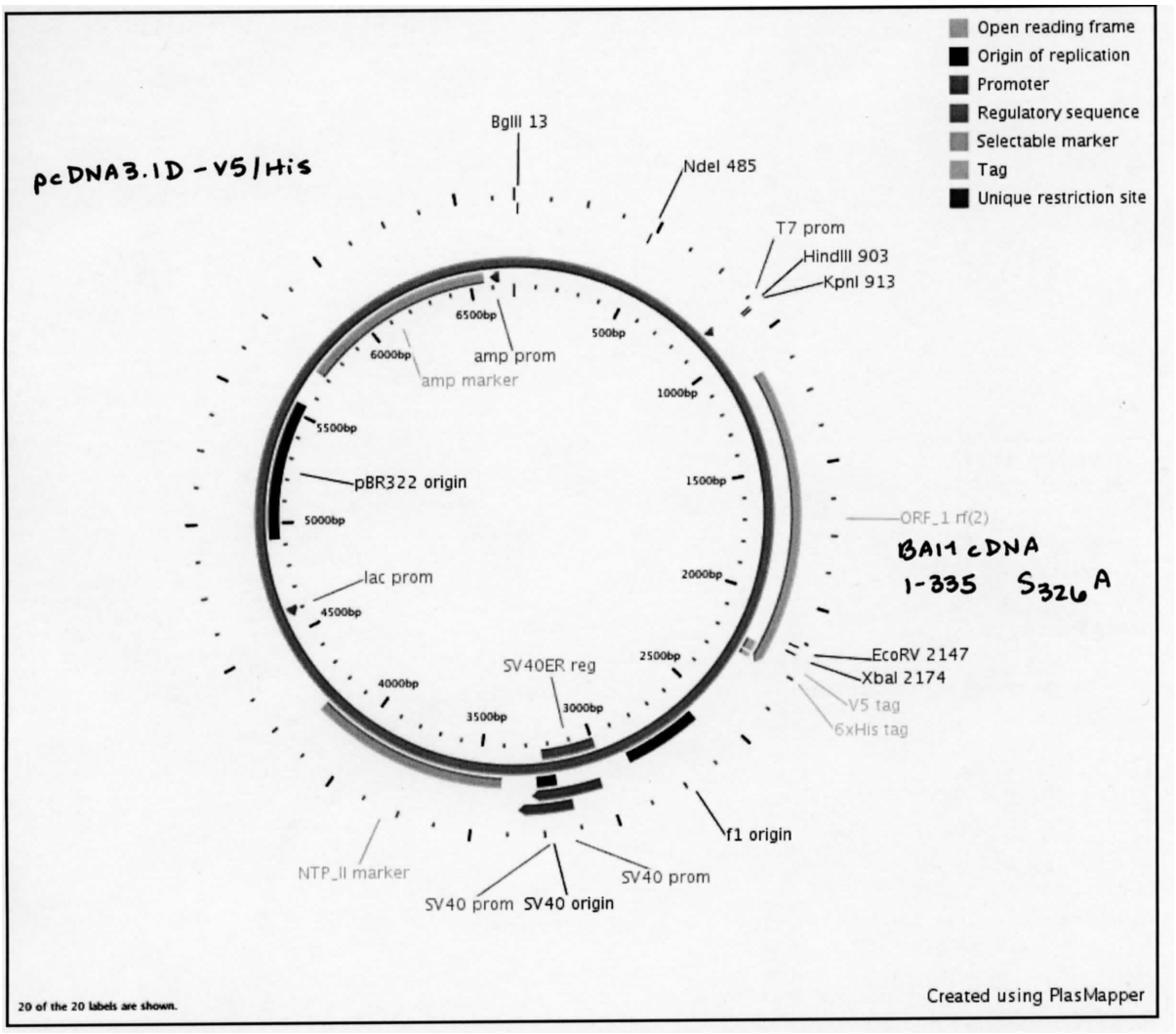
pcDNA3.1D-V5/His
Open reading frame
Origin of replication
Promoter
Regulatory sequence
Selectable marker
Tag
Unique restriction site
BglII 13
NdeI 485
T7 prom
HindIII 903
KpnI 913
amp prom
amp marker
pBR322 origin
ORF_1 rf(2)
BA11 cDNA
1-335 S326A
lac prom
EcoRV 2147
XbaI 2174
V5 tag
6xHis tag
SV40ER reg
f1 origin
NTP_II marker
SV40 prom
SV40 prom
SV40 origin
500bp
1000bp
1500bp
2000bp
2500bp
3000bp
3500bp
4000bp
4500bp
5000bp
5500bp
6000bp
6500bp
20 of the 20 labels are shown.
Created using PlasMapper

Probe records:

Record Number	8-046
gene name	BAI1
plasmid/probe/vector name	Vstat40-Q9, R328A
Keywords	BAI1, Vasculostatin, Vstat
species and origin	human
HGM symbol	BAI1
chrom. location	8q24
copy number	1
GenBank #	
Source	S Cork, NB1 p186-222
References	Nishimori, et al., Oncogene 15:2145-2150 (1997). Cork SM et al. (2011) Oncogene, submitted.
user and date	S Cork, November 2007
Comments	The insert is the BAI1 N terminal domain up to amino acid 334, with a point mutation (R328A) at the arginine believed to be the final amino acid in Vstat 40, in a predicted furin cleavage site. This mutation is observed to abrogate Vstat40 processing.

Description:

vector	pcDNA 3.1/V5-His-TOPO (Invitrogen) 5.5 kb
cloning site	no digestion; PCR-generated inserts ligate directly with linear vector
insert kb	1 kb
total size	6.5 kb
resist.	amp
Bacteria	TOP10
Freezer Location	B 8a-46,47

Polymorphisms:

enzyme	allele size (Kb)	frequency

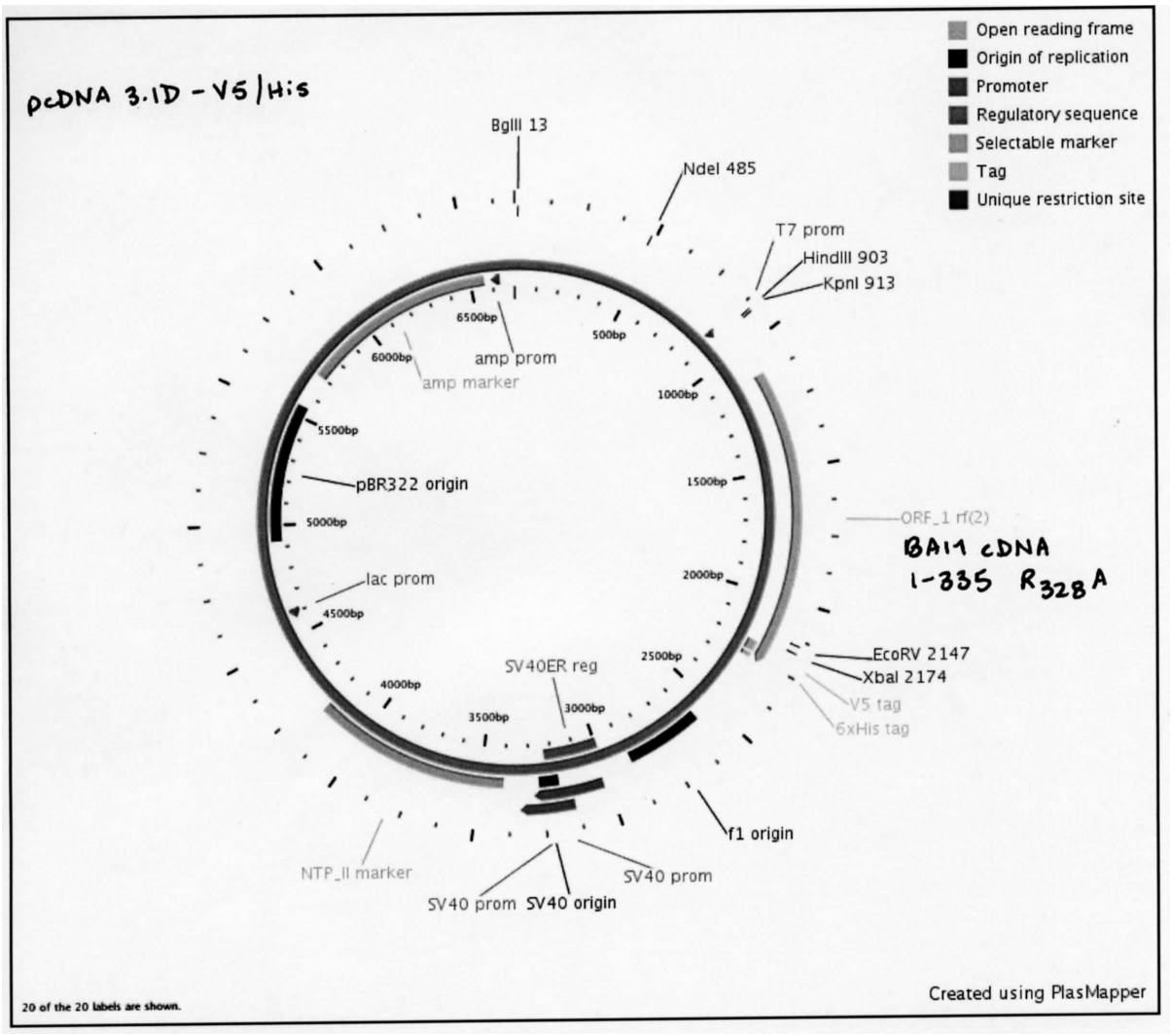
pcDNA 3.1D - V5/His
Open reading frame
Origin of replication
Promoter
Regulatory sequence
Selectable marker
Tag
Unique restriction site
BglII 13
NdeI 485
T7 prom
HindIII 903
KpnI 913
500bp
1000bp
1500bp
2000bp
2500bp
3000bp
3500bp
4000bp
4500bp
5000bp
5500bp
6000bp
6500bp
amp prom
amp marker
pBR322 origin
lac prom
SV40ER reg
ORF_1 rf(2)
BAI1 cDNA
1-335 R328A
EcoRV 2147
XbaI 2174
V5 tag
6xHis tag
f1 origin
SV40 prom
SV40 prom
SV40 origin
NTP_II marker
20 of the 20 labels are shown.
Created using PlasMapper

Probe records:

Record Number	8-044
gene name	BAI1
plasmid/probe/vector name	Vstat40-Q8, S329A
Keywords	BAI1, Vasculostatin, Vstat
species and origin	human
HGM symbol	BAI1
chrom. location	8q24
copy number	1
GenBank #	602682
Source	S Cork, NB1 p186-222
References	Nishimori, et al., Oncogene 15:2145-2150 (1997). Cork SM et al. (2011) Oncogene, submitted.
user and date	S Cork November 2007
Comments	Tagged insert is BAI1 N terminal domain until a.a. 344 amplified by PCR, wit h point mutation S329A. This mutation does not prevent Vstat40 processing.

Description:

vector	pcDNA 3.1D/V5-His-TOPO (5.5kb vector)
cloning site	no digestion; PCR-generated inserts ligate directly with linear vector
insert kb	1kb
total size	6.5
resist.	amp
Bacteria	TOP10 (Invitrogen supercompetent)
Freezer Location	B 8a-44,45

Polymorphisms:

enzyme	allele size (Kb)	frequency

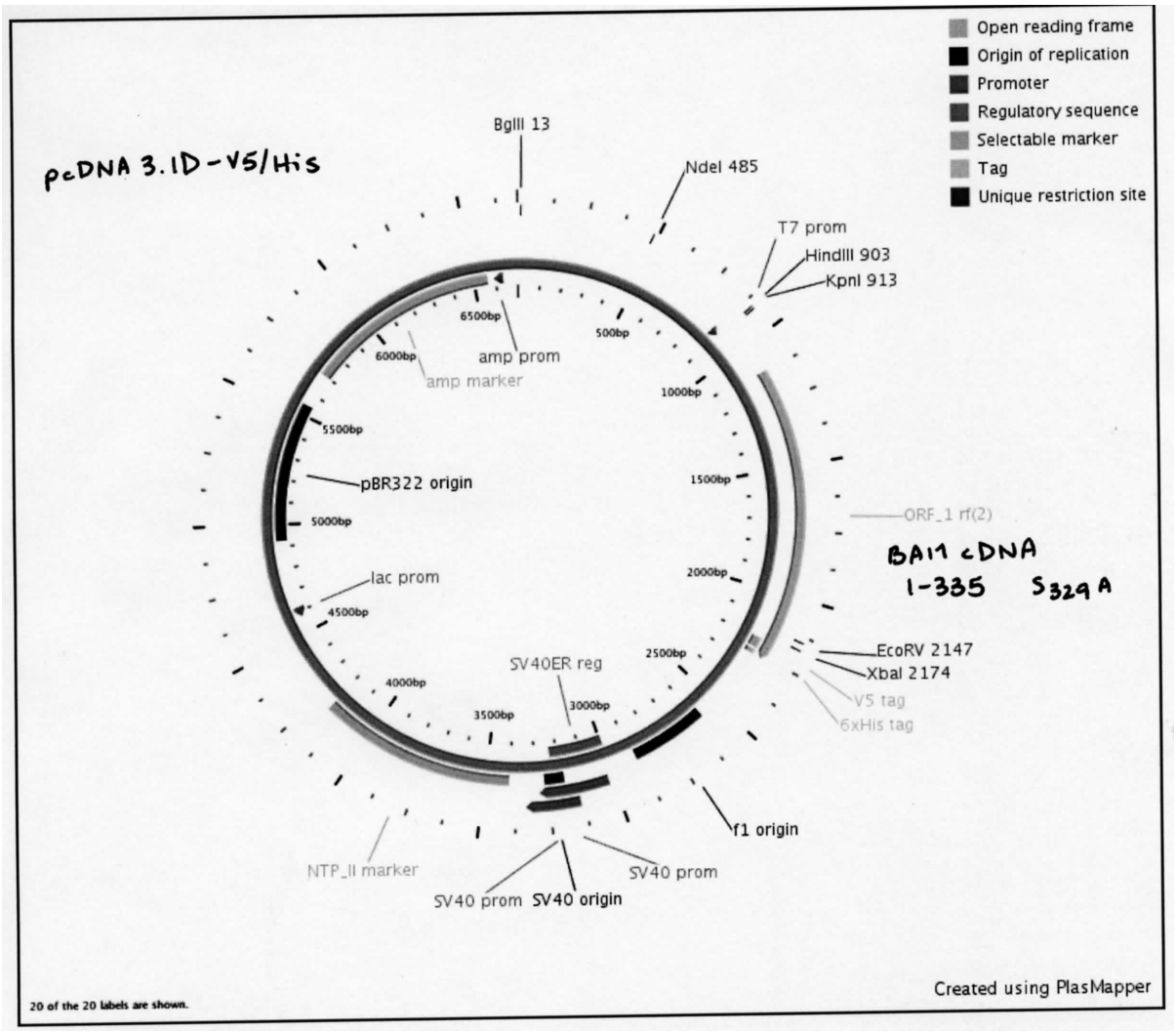
pcDNA 3.1D-V5/His
Open reading frame
Origin of replication
Promoter
Regulatory sequence
Selectable marker
Tag
Unique restriction site
BglII 13
NdeI 485
T7 prom
HindIII 903
KpnI 913
6500bp
500bp
6000bp
amp prom
amp marker
1000bp
5500bp
pBR322 origin
1500bp
ORF_1 rf(2)
BAI1 cDNA
1-335 S329A
5000bp
lac prom
2000bp
4500bp
EcoRV 2147
2500bp
SV40ER reg
XbaI 2174
4000bp
3000bp
V5 tag
3500bp
6xHis tag
f1 origin
NTP_II marker
SV40 prom
SV40 prom
SV40 origin
Created using PlasMapper
20 of the 20 labels are shown.

Probe records:

Record Number	8-042
gene name	BAI1
plasmid/probe/vector name	Vstat40-R3
Keywords	BAI1, Vasculostatin, Vstat
species and origin	human
HGM symbol	BAI1
chrom. location	8q24
copy number	1
GenBank #	
Source	S Cork, NB1 p186-222
References	Nishimori, et al., Oncogene 15:2145-2150 (1997). Cork SM et al. (2011) Oncogene, submitted.
user and date	S Cork, November 2007
Comments	The insert is the BAI1 N terminal domain up to amino acid 322. Vstat40 isob served to be not processed from this slightly smaller (tagged) fragment.

Description:

vector	pcDNA 3.1/V5-His-TOPO (Invitrogen) 5.5 kb
cloning site	no digestion; PCR-generated inserts ligate directly with linear vector
insert kb	1 kb
total size	6.5 kb
resist.	amp
Bacteria	TOP10
Freezer Location	B 8a-42,43

Polymorphisms:

enzyme	allele size (Kb)	frequency

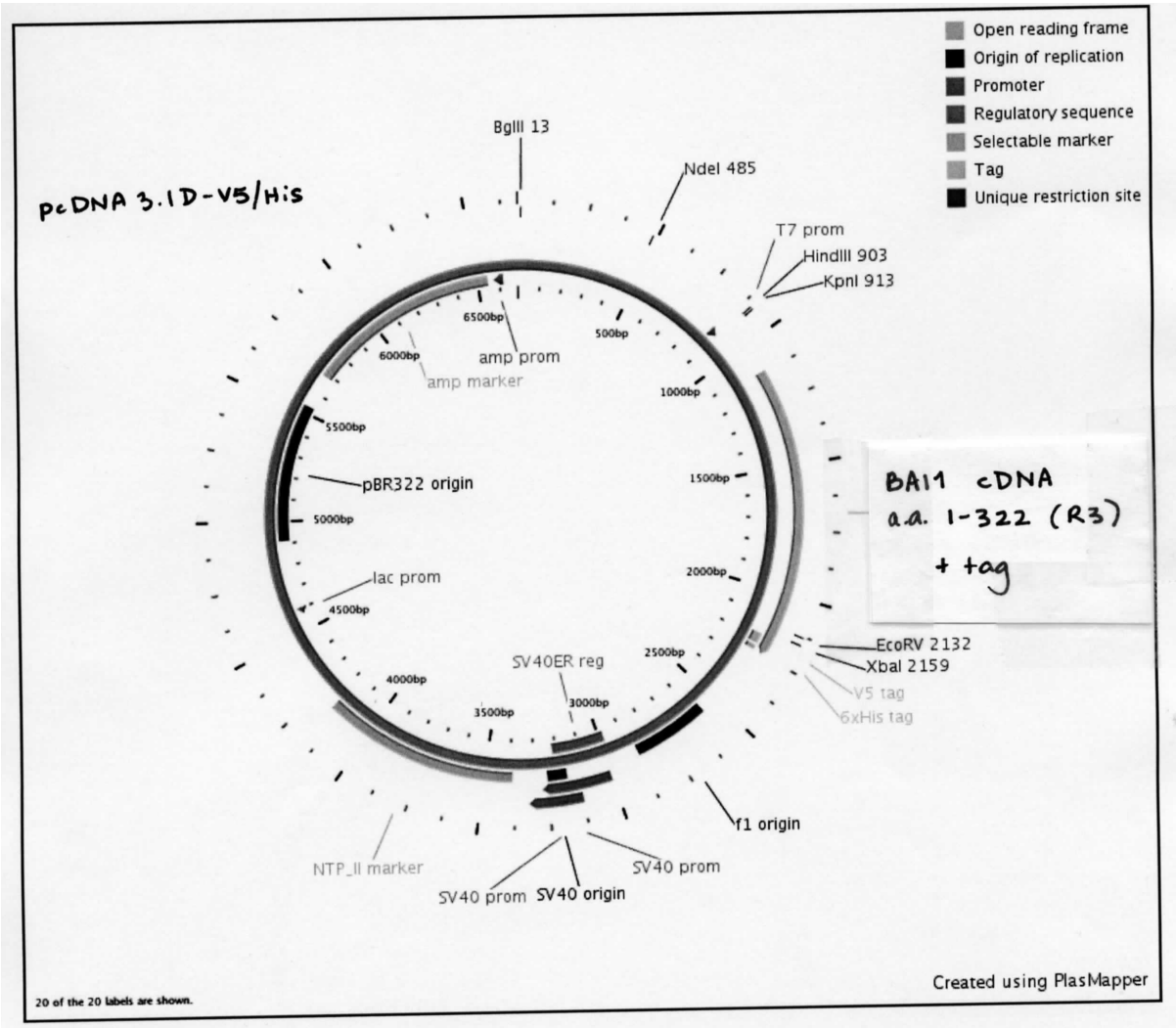
pcDNA 3.1D-V5/His
Open reading frame
Origin of replication
Promoter
Regulatory sequence
Selectable marker
Tag
Unique restriction site
BglII 13
NdeI 485
T7 prom
HindIII 903
KpnI 913
6500bp
500bp
6000bp
amp prom
amp marker
1000bp
5500bp
pBR322 origin
1500bp
5000bp
lac prom
2000bp
4500bp
SV40ER reg
2500bp
4000bp
3000bp
3500bp
BA11 cDNA
a.a. 1-322 (R3)
+ tag
EcoRV 2132
XbaI 2159
V5 tag
6xHis tag
f1 origin
NTP_II marker
SV40 prom
SV40 prom
SV40 origin
Created using PlasMapper
20 of the 20 labels are shown.

Probe records:

Record Number	8-054
gene name	BAI1
plasmid/probe/vector name	Vstat40-Q3
Keywords	BAI1, Vasculostatin, Vstat
species and origin	human
HGM symbol	BAI1
chrom. location	8q24
copy number	1
GenBank #	
Source	S Cork, NB1 p186-222
References	Nishimori, et al., Oncogene 15:2145-2150 (1997). Cork SM et al. (2011) Oncogene, submitted.
user and date	S Cork, November 2007
Comments	The insert is the BAI1 N terminal domain up to amino acid 330. Vstat40 is ob served to be processed from this slightly larger (tagged) fragment.

Description:

vector	pcDNA 3.1/V5-His-TOPO (Invitrogen) 5.5 kb
cloning site	no digestion; PCR-generated inserts ligate directly with linear vector
insert kb	1 kb
total size	6.5 kb
resist.	amp
Bacteria	TOP10
Freezer Location	B 8a-54,55

Polymorphisms:

enzyme	allele size (Kb)	frequency

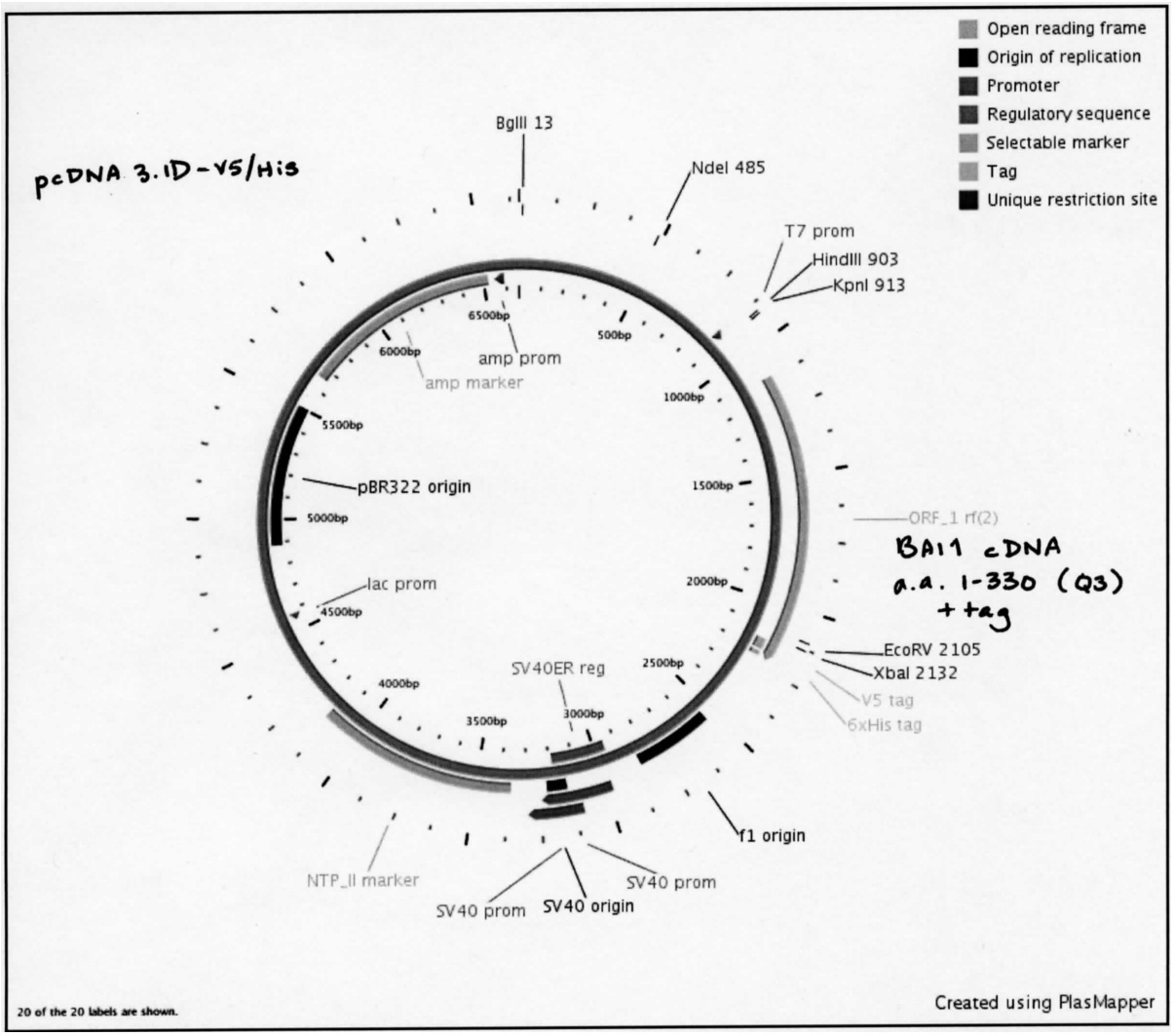
pcDNA 3.1D-V5/His
Open reading frame
Origin of replication
Promoter
Regulatory sequence
Selectable marker
Tag
Unique restriction site
BglII 13
NdeI 485
T7 prom
HindIII 903
KpnI 913
500bp
1000bp
1500bp
2000bp
2500bp
3000bp
3500bp
4000bp
4500bp
5000bp
5500bp
6000bp
6500bp
amp prom
amp marker
pBR322 origin
lac prom
SV40ER reg
ORF_1 rf(2)
BAI1 cDNA
a.a. 1-330 (Q3)
+tag
EcoRV 2105
XbaI 2132
V5 tag
6xHis tag
f1 origin
SV40 prom
SV40 origin
SV40 prom
NTP_II marker
20 of the 20 labels are shown.
Created using PlasMapper

Probe records:

Record Number	8-056
gene name	BAI1
plasmid/probe/vector name	Vstat40-R1
Keywords	BAI1, Vasculostatin, Vstat
species and origin	human
HGM symbol	BAI1
chrom. location	8q24
copy number	1
GenBank #	
Source	S Cork, NB1 p186-222
References	Nishimori, et al., Oncogene 15:2145-2150 (1997). Cork SM et al. (2011) Oncogene, submitted.
user and date	S Cork, October 2007
Comments	This insert contains N-terminal BAI1 cDNA up to amino acid 277 cloned into pcDNA3.1/V5-His. Vstat40 is not processed from this smaller untagged fragment.

Description:

vector	pcDNA 3.1/V5-His-TOPO (Invitrogen) 5.5 kb
cloning site	no digestion; PCR-generated inserts ligate directly with linear vector
insert kb	1 kb
total size	6.5 kb
resist.	amp
Bacteria	TOP10
Freezer Location	B-8a-76

Polymorphisms:

enzyme	allele size (Kb)	frequency

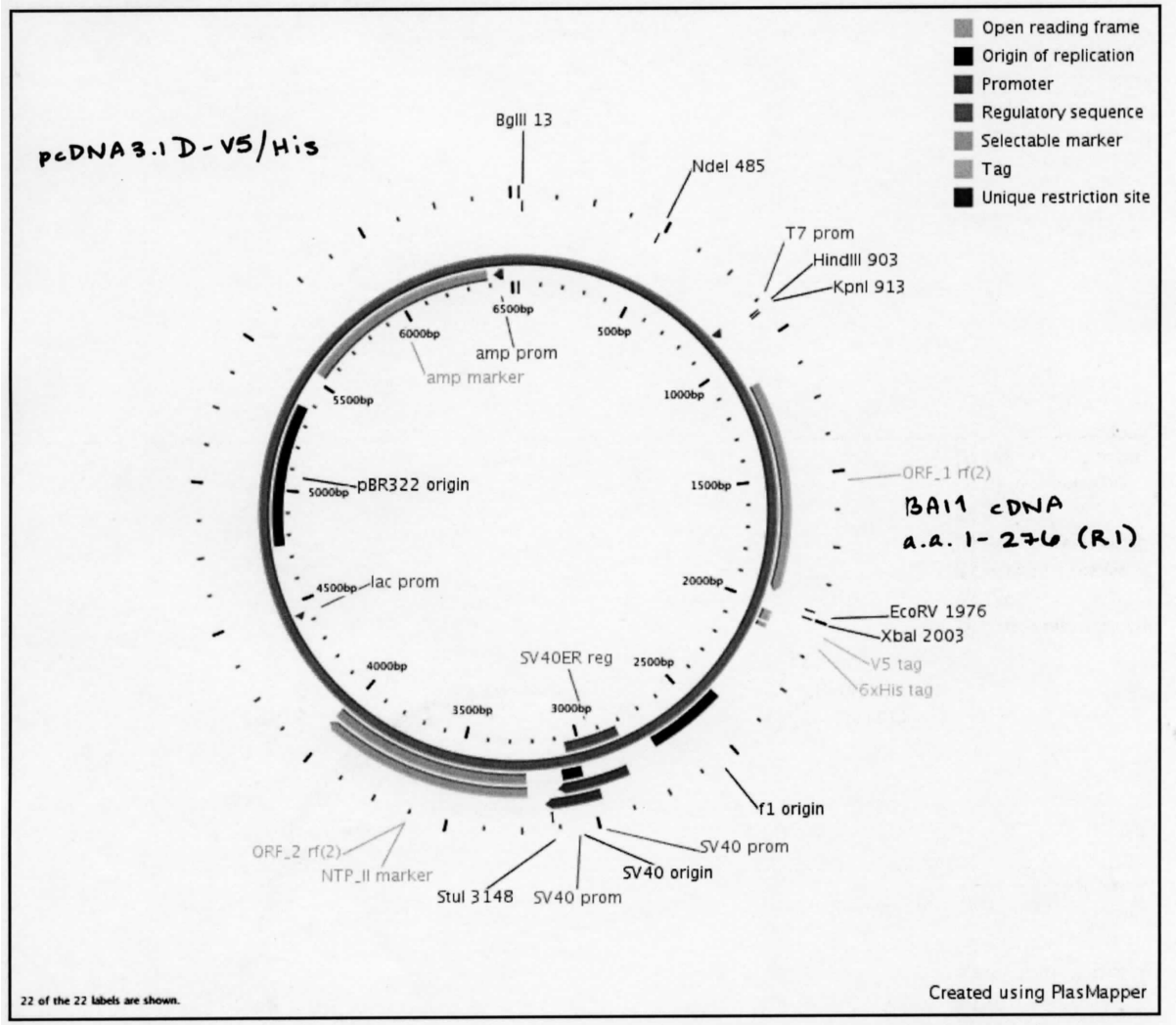
pcDNA3.1D-V5/His
Open reading frame
Origin of replication
Promoter
Regulatory sequence
Selectable marker
Tag
Unique restriction site
BglII 13
NdeI 485
T7 prom
HindIII 903
KpnI 913
6500bp
500bp
6000bp
amp prom
amp marker
5500bp
1000bp
5000bp
pBR322 origin
1500bp
ORF_1 rf(2)
BA11 cDNA
a.a. 1-276 (R1)
4500bp
lac prom
2000bp
EcoRV 1976
XbaI 2003
V5 tag
6xHis tag
4000bp
SV40ER reg
2500bp
3500bp
3000bp
f1 origin
ORF_2 rf(2)
NTP_II marker
SV40 prom
SV40 origin
StuI 3148
SV40 prom
22 of the 22 labels are shown.
Created using PlasMapper

Probe records:

Record Number	8-058
gene name	BAI1
plasmid/probe/vector name	Vstat40-R2
Keywords	BAI1, Vasculostatin, Vstat
species and origin	human
HGM symbol	BAI1
chrom. location	8q24
copy number	1
GenBank #	
Source	S Cork, NB1 p186-222
References	Nishimori, et al., Oncogene 15:2145-2150 (1997). Cork SM et al. (2011) Oncogene, submitted.
user and date	S Cork, October 2007
Comments	This insert contains N-terminal BAI1 cDNA up to amino acid 298 cloned into pcDNA3.1/V5-His.. Vstat40 is not processed from this smaller untagged fragment.

Description:

vector	pcDNA 3.1/V5-His-TOPO (Invitrogen) 5.5 kb
cloning site	no digestion; PCR-generated inserts ligate directly with linear vector
insert kb	1 kb
total size	6.5 kb
resist.	amp
Bacteria	TOP10
Freezer Location	B-8a-70

Polymorphisms:

enzyme	allele size (Kb)	frequency

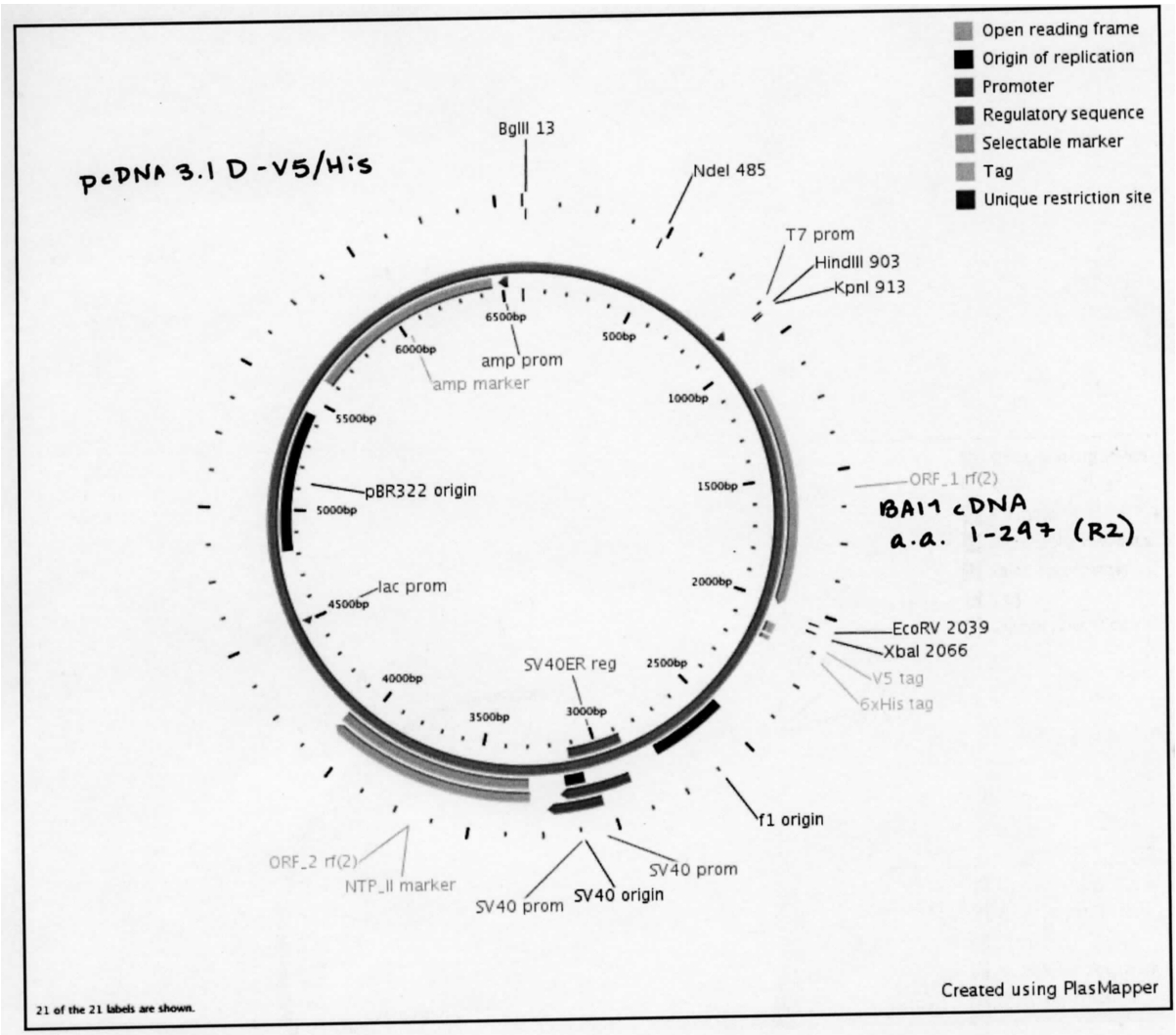
pcDNA 3.1 D-V5/His
Open reading frame
Origin of replication
Promoter
Regulatory sequence
Selectable marker
Tag
Unique restriction site
BglII 13
NdeI 485
T7 prom
HindIII 903
KpnI 913
6500bp
500bp
6000bp
amp prom
amp marker
1000bp
5500bp
pBR322 origin
1500bp
5000bp
ORF_1 rf(2)
BA11 cDNA
a.a. 1-297 (R2)
lac prom
2000bp
4500bp
EcoRV 2039
XbaI 2066
SV40ER reg
2500bp
V5 tag
4000bp
6xHis tag
3500bp
3000bp
f1 origin
ORF_2 rf(2)
SV40 prom
NTP_II marker
SV40 prom
SV40 origin
Created using PlasMapper
21 of the 21 labels are shown.

Probe records:

Record Number	8-060
gene name	BAI1
plasmid/probe/vector name	Vstat40-R5
Keywords	BAI1, Vasculostatin, Vstat
species and origin	human
HGM symbol	BAI1
chrom. location	8q24
copy number	1
GenBank #	
Source	S Cork, NB1 p186-222
References	Nishimori, et al., Oncogene 15:2145-2150 (1997). Cork SM et al. (2011) Oncogene, submitted.
user and date	S Cork, October 2007
Comments	This untagged construct contains N-terminal BAI1 cDNA up until amino acid 351 cloned into pcDNA3.1/V5-His. Vstat40 is processed from this larger fragment.

Description:

vector	pcDNA 3.1/V5-His-TOPO (Invitrogen) 5.5 kb
cloning site	no digestion; PCR-generated inserts ligate directly with linear vector
insert kb	1 kb
total size	6.5kb
resist.	amp
Bacteria	TOP10
Freezer Location	B-8a-71

Polymorphisms:

enzyme	allele size (Kb)	frequency

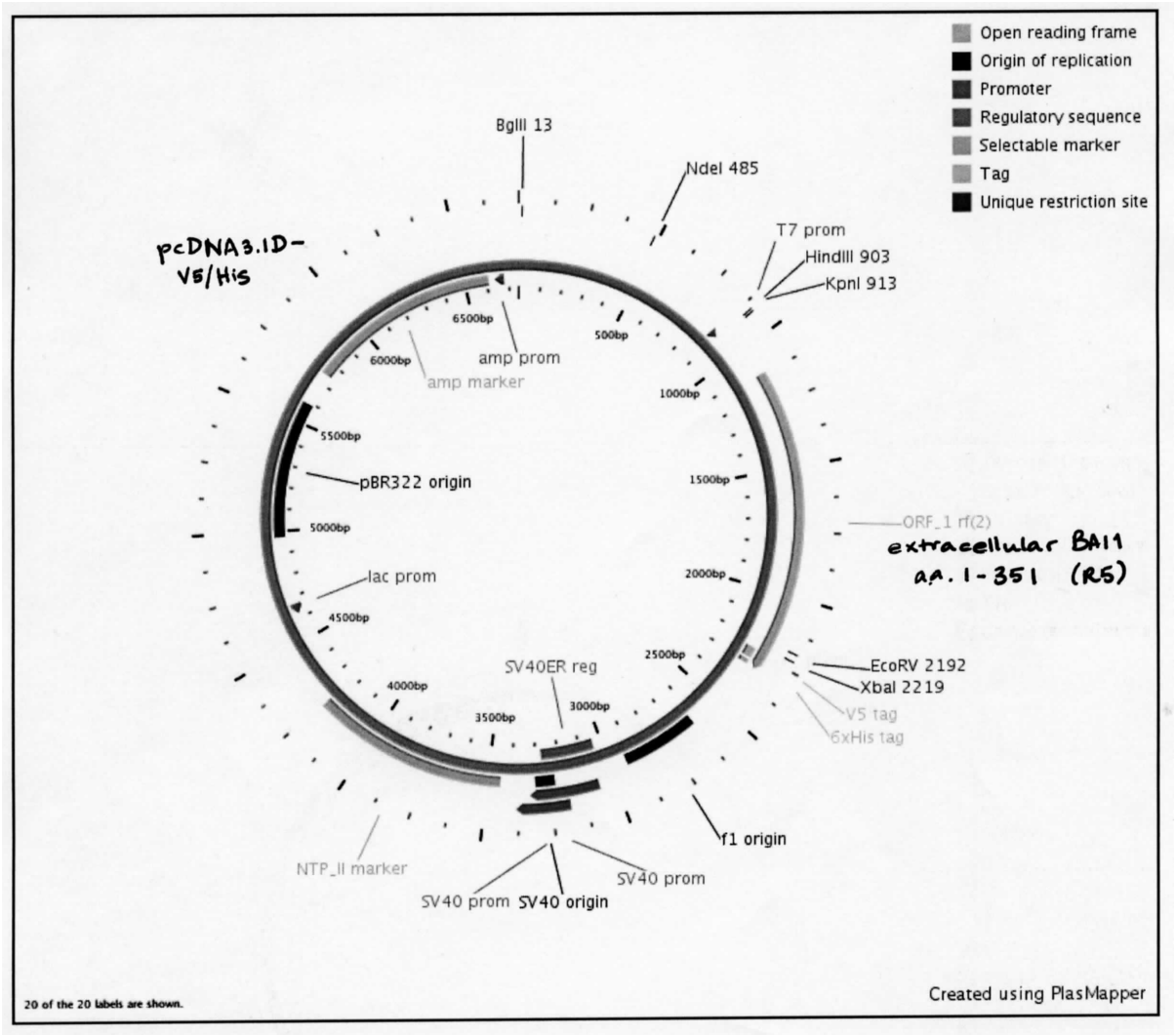
Open reading frame
Origin of replication
Promoter
Regulatory sequence
Selectable marker
Tag
Unique restriction site
pcDNA3.1D-
V5/His
BglII 13
NdeI 485
T7 prom
HindIII 903
KpnI 913
6500bp
500bp
6000bp
amp prom
amp marker
1000bp
5500bp
pBR322 origin
1500bp
ORF_1 rf(2)
extracellular BAI1
aa. 1-351 (R5)
5000bp
lac prom
2000bp
4500bp
2500bp
SV40ER reg
EcoRV 2192
4000bp
XbaI 2219
3500bp
3000bp
V5 tag
6xHis tag
f1 origin
NTP_II marker
SV40 prom
SV40 prom
SV40 origin
20 of the 20 labels are shown.
Created using PlasMapper

Probe records:

Record Number	8-062
gene name	BAI1
plasmid/probe/vector name	Vstat40-R6
Keywords	BAI1, Vasculostatin, Vstat
species and origin	human
HGM symbol	BAI1
chrom. location	8q24
copy number	1
GenBank #	
Source	S Cork, NB1 p186-222
References	Nishimori, et al., Oncogene 15:2145-2150 (1997). Cork SM et al. (2011) Oncogene, submitted.
user and date	S Cork, October 2007
Comments	This construct contains N-terminal BAI1 cDNA up until amino acid 375 cloned into pcDNA3.1/V5-His.. Vstat40 is processed from this larger untagged fragment.

Description:

vector	pcDNA 3.1/V5-His-TOPO (Invitrogen) 5.5 kb
cloning site	no digestion; PCR-generated inserts ligate directly with linear vector
insert kb	1 kb
total size	6.5kb
resist.	amp
Bacteria	TOP10
Freezer Location	B-8a-72

Polymorphisms:

enzyme	allele size (Kb)	frequency

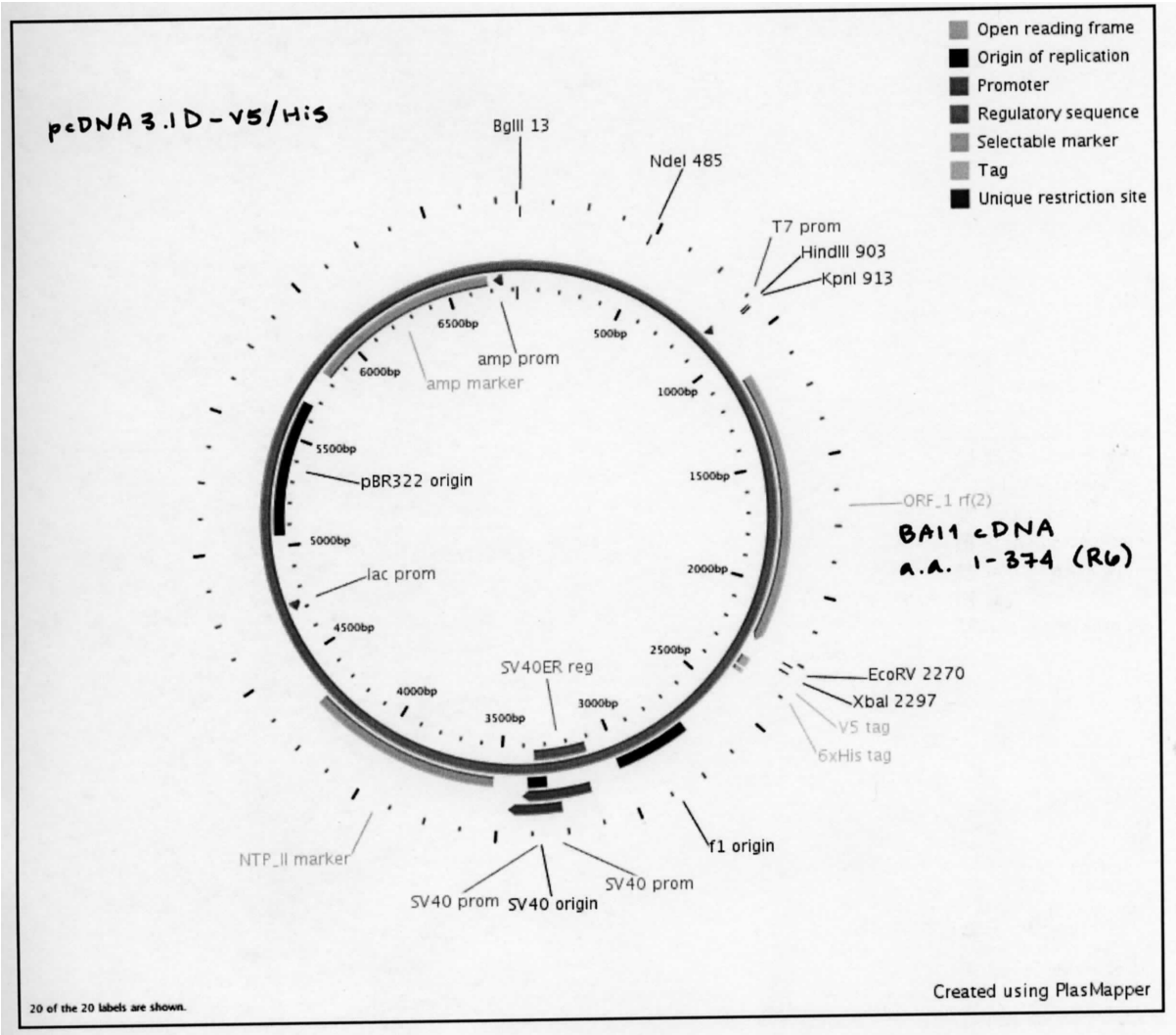
pcDNA 3.1D-V5/HiS
Open reading frame
Origin of replication
Promoter
Regulatory sequence
Selectable marker
Tag
Unique restriction site
BglII 13
NdeI 485
T7 prom
HindIII 903
KpnI 913
500bp
1000bp
1500bp
2000bp
2500bp
3000bp
3500bp
4000bp
4500bp
5000bp
5500bp
6000bp
6500bp
amp prom
amp marker
pBR322 origin
lac prom
SV40ER reg
ORF_1 rf(2)
BA11 cDNA
a.a. 1-374 (R6)
EcoRV 2270
XbaI 2297
V5 tag
6xHis tag
f1 origin
SV40 prom
SV40 origin
SV40 prom
NTP_II marker
20 of the 20 labels are shown.
Created using PlasMapper

Probe records:

Record Number	8-040
gene name	BAI1
plasmid/probe/vector name	Vstat40-Q1
Keywords	BAI1, Vasculostatin, Vstat
species and origin	human
HGM symbol	BAI1
chrom. location	8q24
copy number	1
GenBank #	
Source	S Cork, NB1 p186-222
References	Nishimori, et al., Oncogene 15:2145-2150 (1997). Cork SM et al. (2011) Oncogene, submitted.
user and date	S Cork, November 2007
Comments	The insert is the BAI1 N terminal domain up to amino acid 328 cloned into p cDNA3.1/V5-His, generating the predicted Vstat40 (untagged).

Description:

vector	pcDNA 3.1/V5-His-TOPO (Invitrogen) 5.5 kb
cloning site	no digestion; PCR-generated inserts ligate directly with linear vector
insert kb	1 kb
total size	6.5 kb
resist.	amp
Bacteria	TOP10
Freezer Location	B 8a-40,41

Polymorphisms:

enzyme	allele size (Kb)	frequency

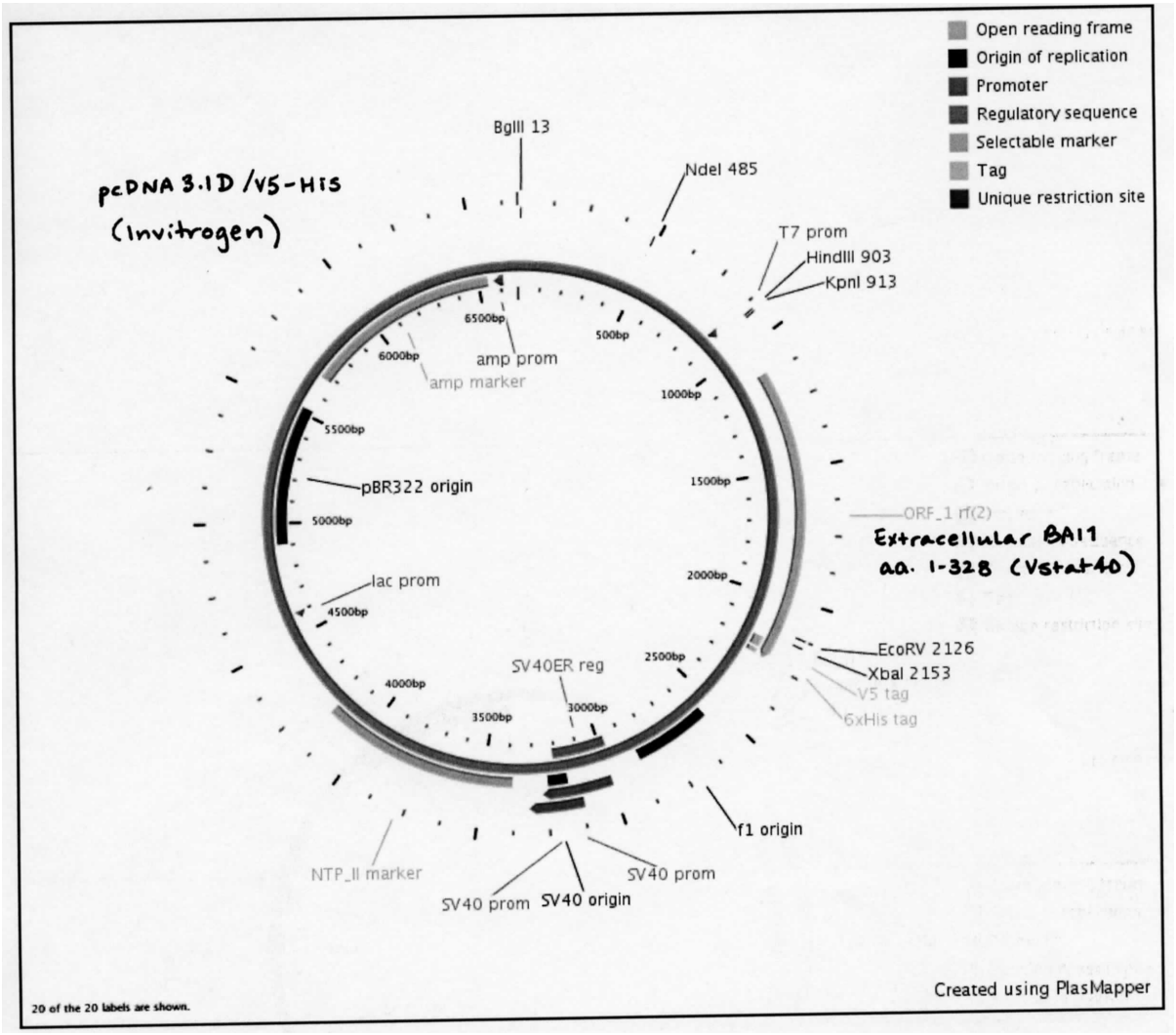
pcDNA 3.1D /V5-HIS
(Invitrogen)
Open reading frame
Origin of replication
Promoter
Regulatory sequence
Selectable marker
Tag
Unique restriction site
BglII 13
NdeI 485
T7 prom
HindIII 903
KpnI 913
6500bp
500bp
6000bp
amp prom
amp marker
1000bp
5500bp
pBR322 origin
1500bp
5000bp
ORF_1 rf(2)
Extracellular BAI1
aa. 1-328 (VStat40)
lac prom
2000bp
4500bp
EcoRV 2126
2500bp
SV40ER reg
XbaI 2153
4000bp
V5 tag
3000bp
3500bp
6xHis tag
f1 origin
NTP_II marker
SV40 prom
SV40 prom
SV40 origin
Created using PlasMapper
20 of the 20 labels are shown.

Probe records:

Record Number	8-064
gene name	BAI1
plasmid/probe/vector name	pTRE2-Vstat40
Keywords	BAI1, vasculostatin, Vstat40
species and origin	human
HGM symbol	BAI1
chrom. location	8q24
copy number	1
GenBank #	
Source	S Cork NB2 p264-298, NB3 p11-31
References	Nishimori, et al., Oncogene 15:2145-2150 (1997). Cork SM et al. (2011) Oncogene, submitted.
user and date	S Cork, August 2009
Comments	This vector expresses Vstat40 (BAI1 aa 1-328) in response to doxycycline (1 -2 ug/mL). This vector was used to generate inducible Vstat40-expressing L 16 cells for tumor experiments.

Description:

vector	pTRE2 (Clontech)
cloning site	HindIII/XbaI
insert kb	1 kB
total size	5 kB
resist.	amp
Bacteria	TOP10
Freezer Location	B-8a-73

Polymorphisms:

enzyme	allele size (Kb)	frequency

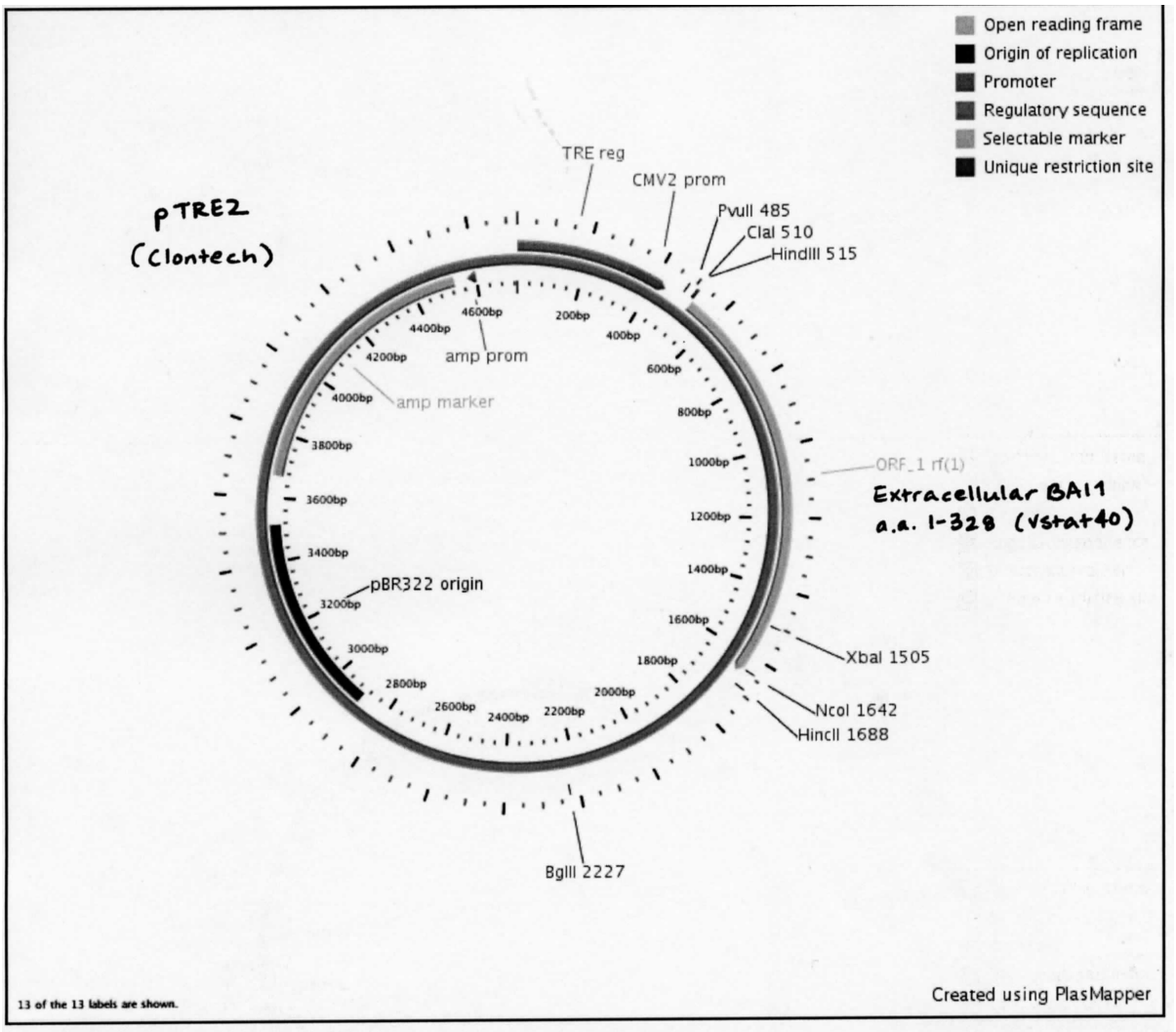
Open reading frame
Origin of replication
Promoter
Regulatory sequence
Selectable marker
Unique restriction site
pTRE2
(Clontech)
TRE reg
CMV2 prom
PvuII 485
ClaI 510
HindIII 515
amp prom
amp marker
pBR322 origin
ORF_1 rf(1)
Extracellular BAI1
a.a. 1-328 (vstat40)
XbaI 1505
NcoI 1642
HincII 1688
BglII 2227
1bp
200bp
400bp
600bp
800bp
1000bp
1200bp
1400bp
1600bp
1800bp
2000bp
2200bp
2400bp
2600bp
2800bp
3000bp
3200bp
3400bp
3600bp
3800bp
4000bp
4200bp
4400bp
4600bp
13 of the 13 labels are shown.
Created using PlasMapper

Probe records:

Record Number	8-066
gene name	BAI1
plasmid/probe/vector name	pGEX2T-Vstat40
Keywords	BAI1, vasculostatin, Vstat40
species and origin	human
HGM symbol	BAI1
chrom. location	8q24
copy number	1
GenBank #	
Source	S Cork NB2 p290-298, NB3 p62-90
References	Nishimori, et al., Oncogene 15:2145-2150 (1997).
user and date	S Cork, January 2010
Comments	This vector expresses GST-tagged Vstat40 (BAI1 aa 10-340) in response to IPTG (1 mM) administration. Created using primers designed by D Zhu.

Description:

vector	pGEX-2T (Amersham)
cloning site	BamHI/EcoRI
insert kb	1 kB
total size	6 kB
resist.	amp
Bacteria	TOP10
Freezer Location	B-8a-74

Polymorphisms:

enzyme	allele size (Kb)	frequency

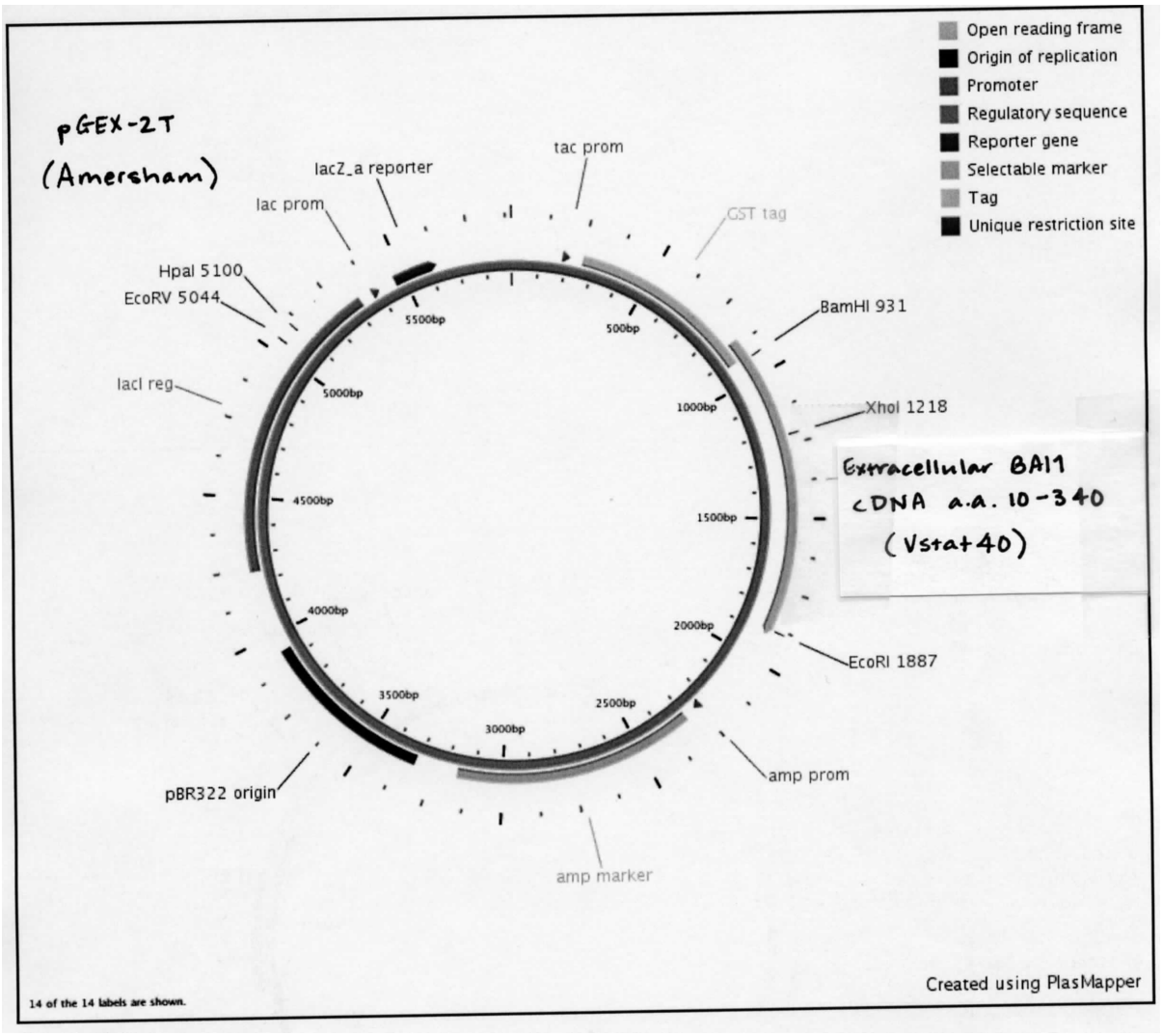
pGEX-2T
(Amersham)
Open reading frame
Origin of replication
Promoter
Regulatory sequence
Reporter gene
Selectable marker
Tag
Unique restriction site
tac prom
lacZ_a reporter
lac prom
GST tag
HpaI 5100
EcoRV 5044
BamHI 931
lacI reg
XhoI 1218
Extracellular BAI1
cDNA a.a. 10-340
(Vstat40)
EcoRI 1887
amp prom
pBR322 origin
amp marker
500bp
1000bp
1500bp
2000bp
2500bp
3000bp
3500bp
4000bp
4500bp
5000bp
5500bp
Created using PlasMapper
14 of the 14 labels are shown.

Probe records:

Record Number	8-068
gene name	BAI1
plasmid/probe/vector name	pGEX2T-Vstat120
Keywords	BAI1, vasculostatin, Vstat
species and origin	human
HGM symbol	BAI1
chrom. location	8q24
copy number	1
GenBank #	
Source	S Cork NB2 p290-298, NB3 p62-125
References	Nishimori, et al., Oncogene 15:2145-2150 (1997).
user and date	S Cork, January 2010
Comments	This vector expresses GST-tagged Vstat120 (BAI1 aa 10-927) in response t o IPTG (0.1-1 mM) administration. Created using primers designed by D Zhu .

Description:

vector	pGEX2T (Amersham)
cloning site	BamHI/EcoRI
insert kb	3 kB
total size	8 kB
resist.	ampicillin
Bacteria	TOP10
Freezer Location	B-8a-75

Polymorphisms:

enzyme	allele size (Kb)	frequency

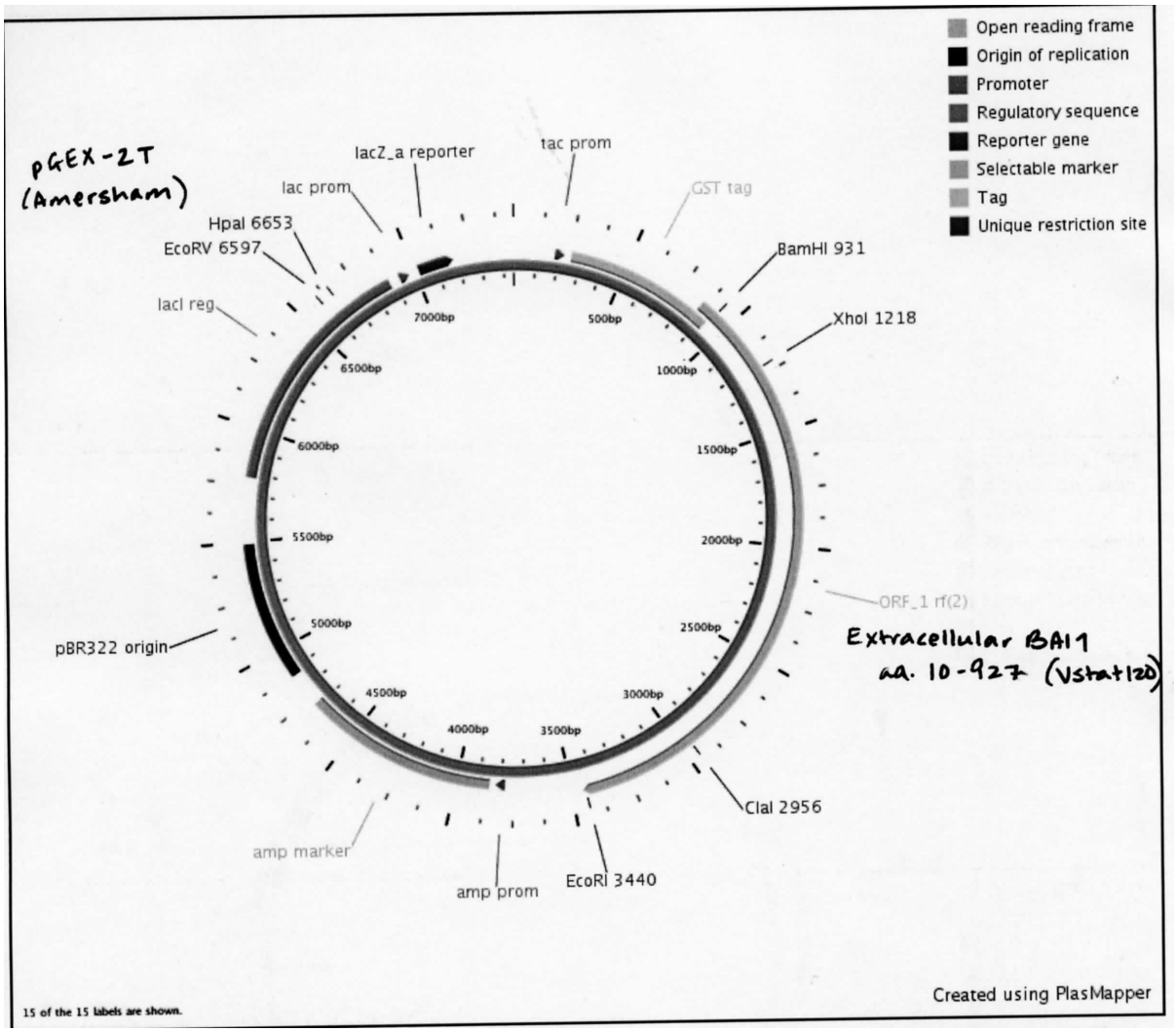
pGEX-2T
(Amersham)
Open reading frame
Origin of replication
Promoter
Regulatory sequence
Reporter gene
Selectable marker
Tag
Unique restriction site
lacZ_a reporter
tac prom
lac prom
GST tag
HpaI 6653
EcoRV 6597
BamHI 931
lacI reg
XhoI 1218
7000bp
500bp
6500bp
1000bp
6000bp
1500bp
5500bp
2000bp
ORF_1 rf(2)
5000bp
2500bp
pBR322 origin
Extracellular BAI1
aa. 10-927 (Vstat120)
4500bp
3000bp
4000bp
3500bp
ClaI 2956
amp marker
amp prom
EcoRI 3440
Created using PlasMapper
15 of the 15 labels are shown.

Probe records:

Record Number	8-070
gene name	BAI1
plasmid/probe/vector name	Vstat40-RAD
Keywords	BAI1, vasculostatin, Vstat40
species and origin	human
HGM symbol	BAI1
chrom. location	8q24
copy number	1
GenBank #	
Source	S Cork NB4 p12-69
References	Nishimori, et al., Oncogene 15:2145-2150 (1997).
user and date	S. Cork, July 2010
Comments	This construct contains the RAD mutant at the RGD motif (in Vstat40 in pcDNA3.1 vector). Introduced by primer overlap extension using Xho fwd and rev primers and RAD fwd and rev mutant primers.

Description:

vector	pcDNA3.1-Vstat40 (Q1)
cloning site	XhoI (between Vstat40 XhoI site and pcDNA MCS XhoI site)
insert kb	1 kb
total size	5 kb
resist.	ampicillin
Bacteria	TOP10
Freezer Location	B-8a-76

Polymorphisms:

enzyme	allele size (Kb)	frequency

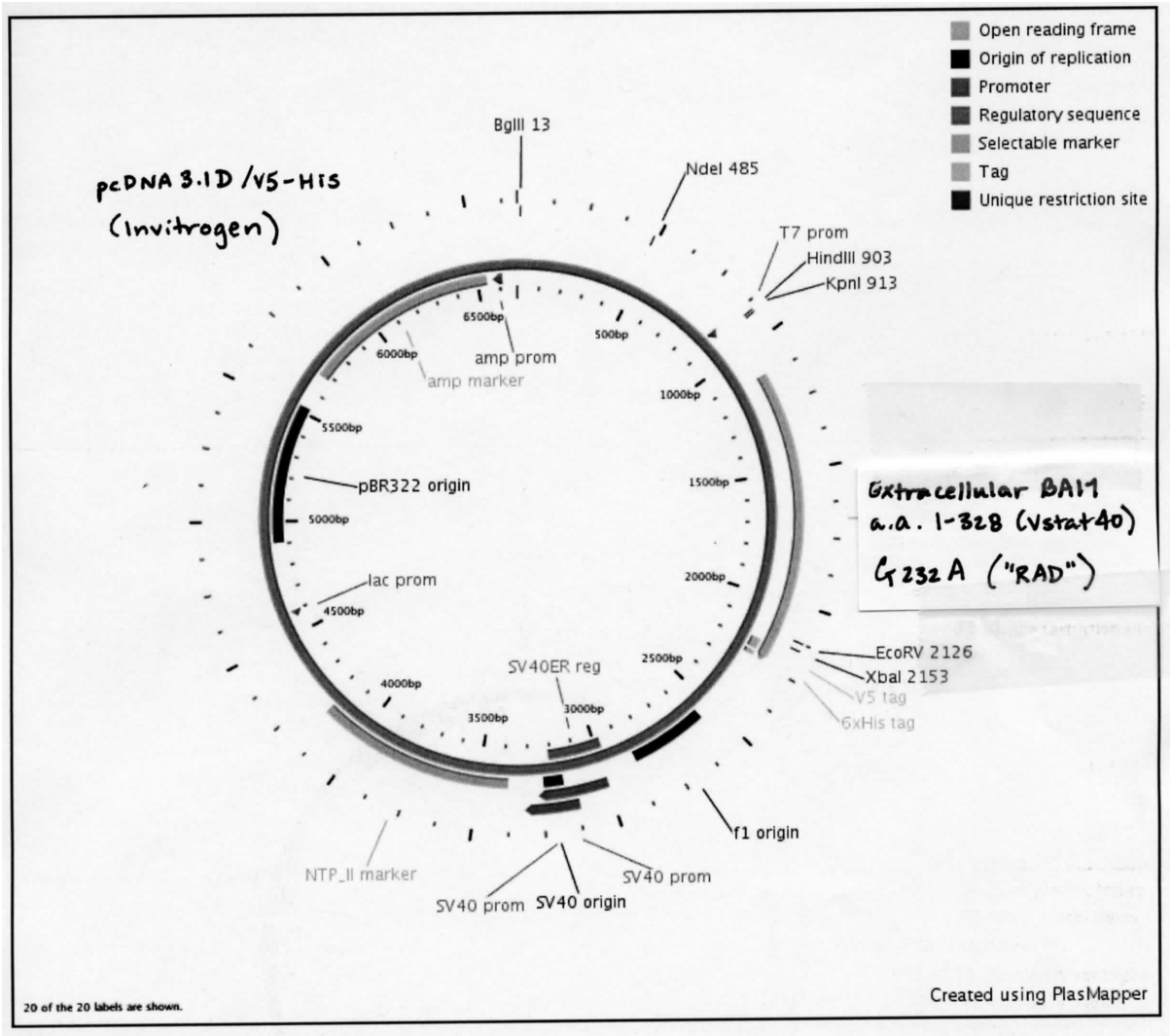
pcDNA 3.1D /V5-HIS
(Invitrogen)
Open reading frame
Origin of replication
Promoter
Regulatory sequence
Selectable marker
Tag
Unique restriction site
BglII 13
NdeI 485
T7 prom
HindIII 903
KpnI 913
6500bp
500bp
6000bp
amp prom
amp marker
1000bp
5500bp
pBR322 origin
1500bp
5000bp
lac prom
2000bp
4500bp
SV40ER reg
2500bp
4000bp
3000bp
3500bp
Extracellular BAI1
a.a. 1-328 (vstat40)
G232A ("RAD")
EcoRV 2126
XbaI 2153
V5 tag
6xHis tag
f1 origin
NTP_II marker
SV40 prom
SV40 prom
SV40 origin
20 of the 20 labels are shown.
Created using PlasMapper

Probe records:

Record Number	8-072
gene name	BAI1
plasmid/probe/vector name	BAI1-L1
Keywords	BAI1, vasculostatin, vstat
species and origin	human
HGM symbol	BAI1
chrom. location	8q24
copy number	1
GenBank #	
Source	S Cork NB4 p85-103
References	Nishimori, et al., Oncogene 15:2145-2150 (1997). Cork SM et al. (2011) Oncogene, submitted.
user and date	S Cork, July 2011
Comments	This vector contains alterations in the MCS of the vector containing full-length BAI1 cDNA cloned into pcDNA3.1D+, with the result that this vector contains only a single XhoI site (in the BAI1 gene). Following double digest with EcoRV and XbaI to remove the XhoI site in the MCS, the vector was treated with the Klenow fragment and religated.

Description:

vector	pcDNA3.1
cloning site	EcoRV/XbaI digest to remove XhoI site
insert kb	none
total size	10 kB
resist.	amp
Bacteria	TOP10
Freezer Location	B-8a-77

Polymorphisms:

enzyme	allele size (Kb)	frequency

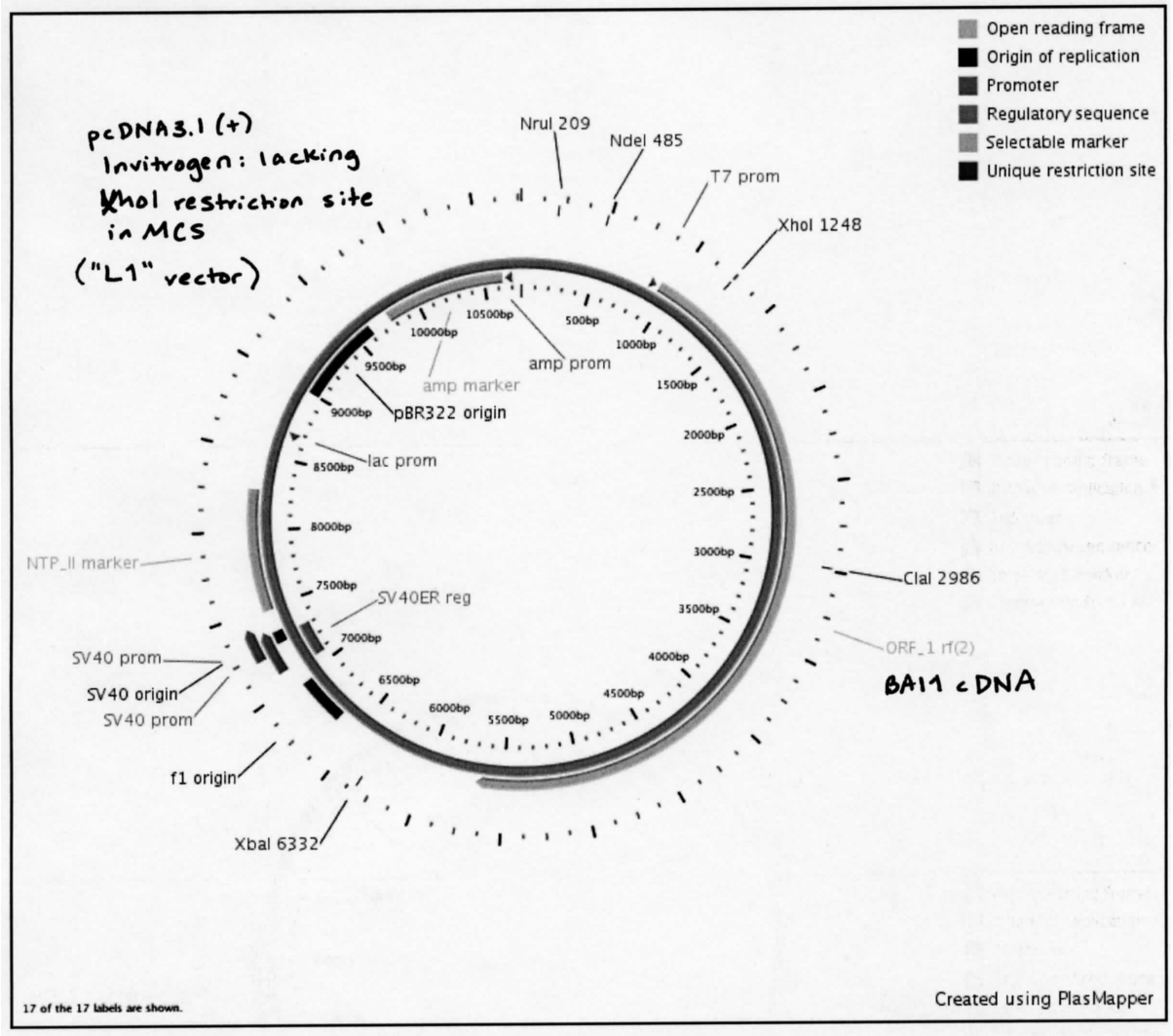
pcDNA3.1 (+)
Invitrogen: lacking
XhoI restriction site
in MCS
("L1" vector)
Open reading frame
Origin of replication
Promoter
Regulatory sequence
Selectable marker
Unique restriction site
NruI 209
NdeI 485
T7 prom
XhoI 1248
ClaI 2986
ORF_1 rf(2)
BA11 cDNA
amp prom
amp marker
pBR322 origin
lac prom
SV40ER reg
NTP_II marker
SV40 prom
SV40 origin
SV40 prom
f1 origin
XbaI 6332
500bp
1000bp
1500bp
2000bp
2500bp
3000bp
3500bp
4000bp
4500bp
5000bp
5500bp
6000bp
6500bp
7000bp
7500bp
8000bp
8500bp
9000bp
9500bp
10000bp
10500bp
17 of the 17 labels are shown.
Created using PlasMapper

Probe records:

Record Number	8-074
gene name	BAI1
plasmid/probe/vector name	BAI1-RSQ
Keywords	BAI1, vasculostatin, Vstat
species and origin	human
HGM symbol	BAI1
chrom. location	8q24
copy number	1
GenBank #	
Source	S Cork NB4 p85-140
References	Nishimori, et al., Oncogene 15:2145-2150 (1997). Cork SM et al. (2011) Oncogene, submitted.
user and date	S Cork, July 2011
Comments	This vector contains a point mutant in the BAI1 gene cloned into the L1 vect or, changing RSQ in the Vstat40 cleavage site to AAA using primer overlap extension.

Description:

vector	BAI1-L1 (pcDNA3.1+)
cloning site	between AgeI and XhoI sites
insert kb	1 kB
total size	10 kB
resist.	amp
Bacteria	TOP10
Freezer Location	B-8a-78

Polymorphisms:

enzyme	allele size (Kb)	frequency

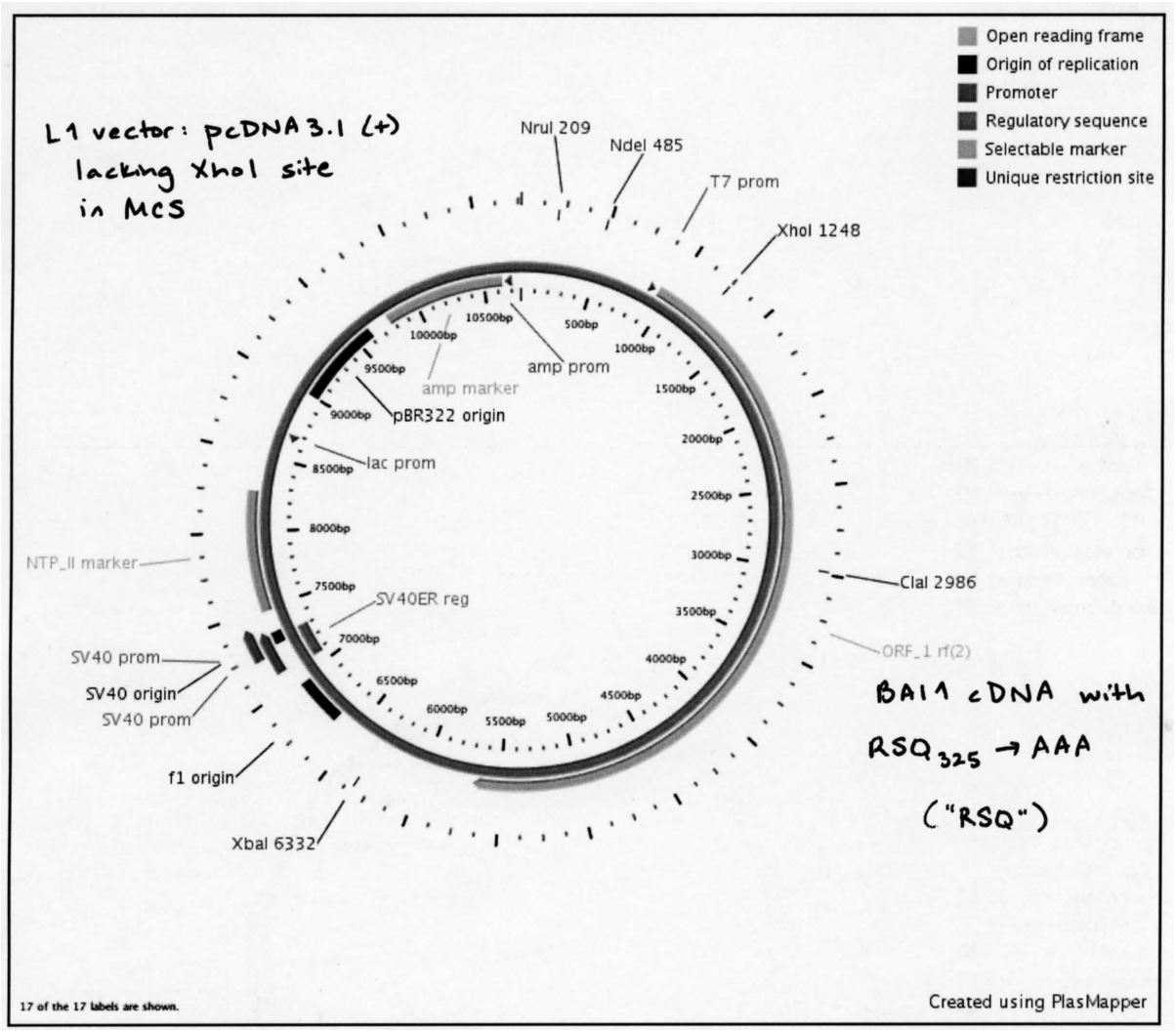
L1 vector: pcDNA 3.1 (+) lacking XhoI site in MCS
Open reading frame
Origin of replication
Promoter
Regulatory sequence
Selectable marker
Unique restriction site
NruI 209
NdeI 485
T7 prom
XhoI 1248
amp prom
amp marker
pBR322 origin
lac prom
SV40ER reg
ClaI 2986
ORF_1 rf(2)
NTP_II marker
SV40 prom
SV40 origin
SV40 prom
f1 origin
XbaI 6332
BA11 cDNA with RSQ325 → AAA ("RSQ")
17 of the 17 labels are shown.
Created using PlasMapper

Probe records:

Record Number	8-076
gene name	BAI1
plasmid/probe/vector name	BAI1-QSL
Keywords	BAI1, vasculostatin, Vstat
species and origin	human
HGM symbol	BAI1
chrom. location	8q24
copy number	1
GenBank #	
Source	S Cork NB4 p85-140
References	Nishimori, et al., Oncogene 15:2145-2150 (1997). Cork SM et al. (2011) Oncogene, submitted.
user and date	S Cork, July 2011
Comments	This vector contains a point mutant in the BAI1 gene cloned into the L1 vect or, changing QSL in the Vstat40 cleavage site to AAA using primer overlap e xtension.

Description:

vector	BAI1-L1 (pcDNA3.1+)
cloning site	between AgeI and XhoI sites
insert kb	1 kB
total size	10 kB
resist.	amp
Bacteria	TOP10
Freezer Location	B-8a-79

Polymorphisms:

enzyme	allele size (Kb)	frequency

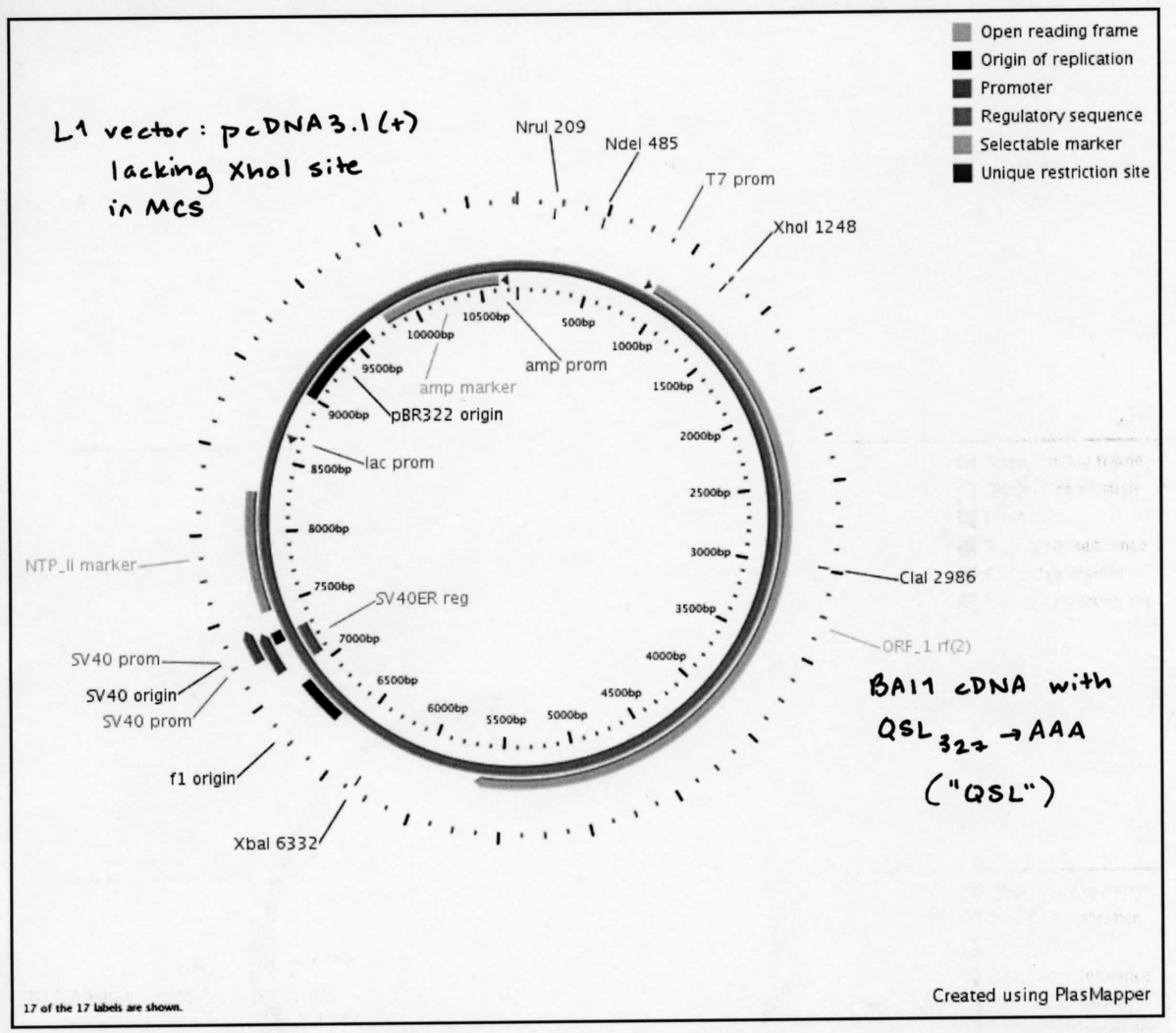
L1 vector: pcDNA3.1(+)
lacking XhoI site
in MCS
Open reading frame
Origin of replication
Promoter
Regulatory sequence
Selectable marker
Unique restriction site
NruI 209
NdeI 485
T7 prom
XhoI 1248
500bp
1000bp
1500bp
2000bp
2500bp
3000bp
3500bp
4000bp
4500bp
5000bp
5500bp
6000bp
6500bp
7000bp
7500bp
8000bp
8500bp
9000bp
9500bp
10000bp
10500bp
amp prom
amp marker
pBR322 origin
lac prom
SV40ER reg
ClaI 2986
ORF_1 rf(2)
BA11 cDNA with
QSL327 → AAA
("QSL")
NTP_II marker
SV40 prom
SV40 origin
SV40 prom
f1 origin
XbaI 6332
17 of the 17 labels are shown.
Created using PlasMapper

APPENDIX III

CELL LINES

Cell lines developed:

1	Record #	E11
	Cell Line names	LN229-L16-5
	Date received	25/7/2011
	at Passage #	2
	Species	human
	Cell type	glioma (tet-inducible)
	key word search	BAI1, vasculostatin, Vstat40, L16, LN229
	Source address	S Cork NB3, p45-74
	published reference	none
	Description/purpose	These cells were created for the purpose of studying Vstat40 anti-tumor activity in vivo. They were created by co-transfecting pTRE2-Vstat40 vector (no selection marker) with pEGFP-N2 vector (G4 18 resistance) into LN229-L16 cells at 10:1 ratio to ensure that virtually all G48-resistant colonies would contain the inducible Vstat40 vector. Clones were screened (-/+ dox) to verify selective indu cibility in the presence of doxycycline.
	Media Requirements	Complete growth medium (10% FBS in DMEM) with appropriate antibiotics (see b elow).
	Growth conditions	
	drug sensitivity	Cells must be cultured in 0.5 ug/mL puromycin to maintain rtTA vector selection/ind ucibility. Further culturing in 400 ug/mL G418 (Invitrogen) maintains clonal selection . Doxycycline (2 ug/ml) may be used to selectively induce Vstat40 expression.
	transfection	
	AdenoLacZ infection	none
	nude tumorig. dose	Growth similar to parental LN229 cells (tumor burden reached at 2-3 months post-implantation).
	Phenotype	Immunotype
	Chrom. abnormal.	
	Karyotype	
	patient name	
	sex/age	birth date
	Neuropathology #	
	Pedigree	
	Member number	
	Location	2J40-41
	Vials	
	Passages Frozen	mycotest Date frozen
	DAR certif	

1 Record #	E12
Cell Line names	LN229-L16-14
Date received	25/7/2011
at Passage #	2
Species	human
Cell type	glioma (tet-inducible)
key word search	BAI1, vasculostatin, Vstat40, L16, LN229
Source address	S Cork NB3, p45-74
published reference	none
Description/purpose	These cells were created for the purpose of studying Vstat40 anti-tumor activity in vivo. They were created by co-transfecting pTRE2-Vstat40 vector (no selection marker) with pEGFP-N2 vector (G4 18 resistance) into LN229-L16 cells at 10:1 ratio to ensure that virtually all G48-resistant colonies would contain the inducible Vstat40 vector. Clones were screened (-/+ dox) to verify selective indu cibility in the presence of doxycycline.
Media Requirements	Complete growth medium (10% FBS in DMEM) with appropriate antibiotics (see b elow).
Growth conditions	
drug sensitivity	Cells must be cultured in 0.5 ug/mL puromycin to maintain rtTA vector selection/ind ucibility. Further culturing in 400 ug/mL G418 (Invitrogen) maintains clonal selection . Doxycycline (2 ug/ml) may be used to selectively induce Vstat40 expression.
transfection	
AdenoLacZ infection	none
nude tumorig. dose	Growth similar to parental LN229 cells (tumor burden reached at 2-3 months post-implantation).
Phenotype	Immunotype
Chrom. abnormal.	
Karyotype	
patient name	
sex/age	birth date
Neuropathology #	
Pedigree	
Member number	
Location	2J42-43
Vials	
Passages Frozen	mycotest Date frozen
DAR certif	

1 Record #	E13
Cell Line names	LN229-L16-17
Date received	25/7/2011
at Passage #	2
Species	human
Cell type	glioma (tet-inducible)
key word search	BAI1, vasculostatin, Vstat40, L16, LN229
Source address	S Cork NB3, p45-74
published reference	none
Description/purpose	These cells were created for the purpose of studying Vstat40 anti-tumor activity in vivo. They were created by co-transfecting pTRE2-Vstat40 vector (no selection marker) with pEGFP-N2 vector (G418 resistance) into LN229-L16 cells at 10:1 ratio to ensure that virtually all G48-resistant colonies would contain the inducible Vstat40 vector. Clones were screened (-/+ dox) to verify selective inducibility in the presence of doxycycline.
Media Requirements	Complete growth medium (10% FBS in DMEM) with appropriate antibiotics (see below).
Growth conditions	
drug sensitivity	Cells must be cultured in 0.5 ug/mL puromycin to maintain rtTA vector selection/inducibility. Further culturing in 400 ug/mL G418 (Invitrogen) maintains clonal selection. Doxycycline (2 ug/ml) may be used to selectively induce Vstat40 expression.
transfection	
AdenoLacZ infection	none
nude tumorig. dose	Growth similar to parental LN229 cells (tumor burden reached at 2-3 months post-implantation).
Phenotype	Immunotype
Chrom. abnormal.	
Karyotype	
patient name	
sex/age	birth date
Neuropathology #	
Pedigree	
Member number	
Location	2J44-45
Vials	
Passages Frozen	mycotest Date frozen
DAR certif	